IDO - 16570

EXPERIMENTAL ORGANIC COOLED REACTOR CONCEPTUAL DESIGN

W. E. Nyer
J. H. Rainwater

December 1, 1959

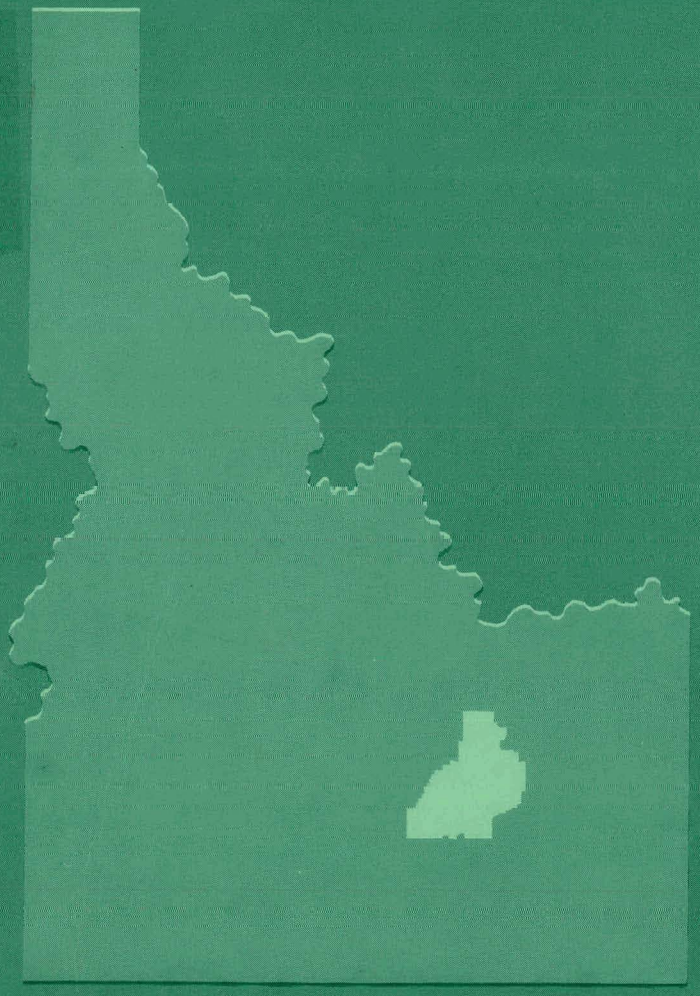

PHILLIPS PETROLEUM COMPANY

ATOMIC ENERGY DIVISION

NATIONAL REACTOR TESTING STATION
US ATOMIC ENERGY COMMISSION

DISCLAIMER

PRICE $2.50

Available from the
Office of Technical Services
U. S. Department of Commerce
Washington 25, D. C.

LEGAL NOTICE

This report was prepared as an account of Government sponsored work. Neither the United States, nor the Commission, nor any person acting on behalf of the Commission:

A. Makes any warranty or representation, express or implied, with respect to the accuracy, completeness, or usefulness of the information contained in this report, or that the use of any information, apparatus, method, or process disclosed in this report may not infringe privately owned rights; or

B. Assumes any liabilities with respect to the use of, or for damages resulting from the use of any information, apparatus, method, or process disclosed in this report.

As used in the above, "person acting on behalf of the Commission" includes any employee or contractor of the Commission, or employee of such contractor, to the extent that such employee or contractor of the Commission, or employee of such contractor prepares, disseminates, or provides access to, any information pursuant to his employment or contract with the Commission, or his employment with such contractor.

Printed in USA

IDO-16570
AEC Research and Development Report
Reactor Technology
TID-4500 (16th Ed.)

EXPERIMENTAL ORGANIC COOLED REACTOR CONCEPTUAL DESIGN

December 1, 1959

J. R. Huffman
Assistant Manager, Technical

W. E. Nyer
Manager, Reactor Projects

J. H. Rainwater
Supervisor, Plant Engineering

PHILLIPS
PETROLEUM
COMPANY

Atomic Energy Division

Contract AT(10-1)-205
Idaho Operations Office
U. S. ATOMIC ENERGY COMMISSION

EOCR CONCEPTUAL DESIGN STAFF

Overall Supervision - W. E. Nyer and J. H. Rainwater

Editors - G. H. Hanson, R. G. Beck and R. S. Marsden

M. H. Bartz
R. G. Beck
J. M. Beeston
A. W. Brown
E. S. Brown
W. J. Byron
S. Cohen
R. S. Fisher
R. W. Goin
R. A. Grimesey
F. C. Haas
O. M. Hauge
W. M. Hawkins
J. C. Hillyer
B. D. Johnson
R. D. Johnson
F. R. Keller
R. S. Kern
W. C. King
R. B. Lemon
J. L. Liebenthal
K. A. McCollom
R. S. McPherson
R. S. Marsden
D. R. Metcalf
E. C. Newman
E. F. Peterson
D. L. Reid
B. D. Tackett
J. L. Taylor
F. R. Vanderwiele
R. B. Van Sice
R. J. Wagner
V. A. Walker
J. A. Yeates

EXPERIMENTAL ORGANIC COOLED REACTOR

CONCEPTUAL DESIGN

S U M M A R Y

At the request of the Idaho Operations Office of the United States Atomic Energy Commission, the Atomic Energy Division of Phillips Petroleum Company has prepared the conceptual design for an Experimental Organic-Cooled Reactor which will provide a flexible facility for experimentation to speed the advancement of the organic-cooled power reactor toward its goal of economic nuclear power. Basically, this calls for a facility capable of irradiating simultaneously a number of different types of fuel structures and moderators under environmental conditions approximating or exceeding those in organic power reactors.

These requirements are provided by an organic-cooled and -moderated reactor designed for operation at 40 Mw at 500°F inlet temperature. This reactor, as designed, can also be operated at 20 Mw and 700°F or intermediate conditions to provide desired test environments for the program. Plate-type fuel elements with stainless steel cladding over a UO_2-stainless steel alloy will be used. The reactor will operate at a pressure of 150 psi and a flow rate of 25,000 gpm. The system is designed to operate at pressures up to 300 psig and temperatures as high as 850°F. The reactor tank, thermal shields and biological shielding are designed for power levels up to 220 Mw.

The design incorporates provision for installation of several experimental loops up to 7.5 in. in diameter. Of these, two loops about 6.5 in. in diameter and three loops 2.5 in. in diameter are recommended as part of initial construction. The core lattice spacing is such that driver (stainless steel) elements can be replaced by large-cross-section power reactor elements for experimental purposes. Fuel and coolant studies can also be carried out in larger scale by utilizing the entire core and coolant system. Removable grids and tank internals will permit core rearrangement for testing any core array not accommodated by the original grids.

The estimated cost for the reactor constructed at the National Reactor Testing Station (excluding loops) is $6,310,000 and the operating costs, not including the experimental program, are $1,510,000 annually for a staff of 59. The estimated cost of one 6.5-in. OD loop is $484,000, and the total cost of the five loops which constitutes the recommended initial installation of experimental facilities is $1,800,000.

Section 1.000 discusses the general needs of the organic program and presents the principal design features of the EOCR. The research program and design objectives are given in detail in Sections 2.000 and 3.000, respectively. Sections 4.000 through 9.000 present the EOCR design. Supporting information and design details may be found in Sections 11.000 through 20.000.

EXPERIMENTAL ORGANIC COOLED REACTOR

CONTENTS

CONTENTS

CONTENTS

1.000 INTRODUCTION AND PRINCIPAL DESIGN FEATURES

The Organic Cooled Reactor is generally conceded to offer one of the more promising avenues to economic nuclear power. The OMRE at the National Reactor Testing Station has, within its rather limited experimental capability, demonstrated that the concept is technically feasible. However, much remains to be done in the area of research and development on both the moderator and the fuel elements before it can be determined with certainty whether the economic potential believed to be inherent in the organic reactor concept can be realized in practice. In this respect the organic reactor is substantially behind either the pressurized water reactor or the boiling water reactor at the present time.

Before stating the major problems in the application of organic systems to nuclear reactors, a recapitulation of the present state of the art is in order. Examination of the properties of organics, theoretical studies on the expected characteristics of organic reactors, and the successful operation of an organic-cooled and -moderated reactor, OMRE, have been carried out by Atomics International. The essential accomplishment of the program has been to demonstrate the technical feasibility of the concept. The major problems in applying the concept can now be more clearly defined. However, it cannot be said that there exists a proven technology upon which the design of reasonably successful organic power reactors can be based. Considerable additional developmental work is required to advance the present form of the organic concept to that stage and to explore alternative forms that may more fully develop the potential advantages of the concept. In a large measure the outstanding problems, although technical in nature, are really related to the economic feasibility of the concept and this aspect must be borne in mind in the planning of an effective program with the objectives stated above.

It is also useful to review the reasons why organic substances are considered for use in reactors. The principal advantages of organics over water are their low vapor pressure and low corrosion effects. Other advantages can be given but they are peripheral. Moreover, expressing the advantages in this way emphasizes that the essential properties of organics do not require their use as a moderator. Hence, it is necessary to consider in the long-range picture the possibility of two classes of organic systems. On the one hand there will be the organic-cooled and -moderated reactors and, on the other hand, organic-cooled reactors moderated by substances other than organic materials.

For either of these approaches, the major problem areas are the usual ones common to any reactor system; namely fuel, coolants, technology, and physics. For the present purpose, the following list gives a representative aspect of each problem area which is unique to organic systems or which requires the use of organics in its study and which is a problem of major importance in the effective application of the organic concept:

Problem Area	Outstanding Problem
Fuel	Materials and Heat Transfer
Coolant	Radiolysis
Technology	Waste Disposal
Physics	Long-Term Reactivity

These are approximately in the order of decreasing importance, although fuel and coolant problems are very nearly equal. In the long-run the problem of waste disposal may also be of equal importance but certainly at present it is not as pressing even though the current way of coping with this problem may not be satisfactory on an industrial scale.

The specific studies believed necessary to advance the organic concept fall into two groups. First are those which could contribute most quickly to the resolution of problems in the organic power reactor designs presently under consideration. Thus, the first phase of the program proposed herein is slanted toward providing the remaining information needed to permit effective scaleup of present knowledge and experience to power reactor conditions. Three major problems exist in the proposed power designs and they may be regarded as equally essential to alternative designs that may arise in the future. The investigation of two of these, the development of low-cost fuel assemblies such as the proposed sintered aluminum powder design, and the uncertainty in the organic decomposition rates under power reactor conditions, are expected to occupy a prominent part of the early program for the EOCR. Because it appears to be crucial as well as relatively least developed, the fuel problem was placed first in the above list. The investigation of the third problem, the use of nucleate boiling, is not so strongly dependent, in its early stages, on the test environment to be provided by the EOCR but will be in its later stages and thus will also be a part of the program.

The longer-range group have the objective of more fully exploiting all the promising possibilities of organic systems. Thus the second phase emphasizes the development of new and modified organics and includes the possibility of studying other moderator-coolant combinations.

On the basis of this program of studies the design objectives of the proposed organic reactor have been established in terms of the conditions which must be provided in order to carry out the proposed fuel and coolant research. These test conditions will exceed those of proposed power reactors and are significantly beyond those provided by tests to date. (See tables and discussions in Section 2.000 for details). For example, heat fluxes of 27,000 Btu/hr-ft^2 in power reactor fuel elements have been obtained in OMRE experiments, whereas fluxes as high as 165,000 are planned for organic-cooled and -moderated power reactors with a possibility of 500,000 being required for an organic-cooled deuterium-moderated power reactor. It is planned that values greater than 500,000 can be provided in the EOCR test positions. Similarly, the required total radiation intensity for power reactor conditions is 2.6 w/g, which is higher than OMRE by a

factor of 2, and the required ratio of neutron-to-gamma intensity is higher by a factor of 4. A final example of conditions to be provided is the possibility of performing full-core tests under power reactor conditions.

In turn, the experimental conditions fix the specific requirements on neutron flux, heat flux, and dosage rates. These considerations are discussed in Section 3.000. For the usual reasons, an additional condition is imposed that the design and construction of the reactor entail a minimum of development. A final limitation, which is essentially an economic one, is that of the power. All of these design requirements set forth a problem which might not be solvable and could only be settled by detailed calculation of the properties of various core designs. For these purposes, several core designs were examined. The results of the study show that it is feasible to design the reactor with the properties and within the limitations stated above. Solely for reasons of simplicity and cost these initial cores were organic-moderated as well as organic-cooled.

Alternative possibilities, such as D_2O-moderated systems or H_2O-moderated systems and the like, could satisfy some of the objectives. All of these have been ruled out because they add complexity and limit the flexibility for testing fuel elements. It should be noted that the proposed organic reactor will operate under conditions well beyond those of the OMRE and will thus, in itself, be a significant advance in the operating experience and technology of organic reactors.

D_2O-moderated systems for power reactors may have some long-range potentials, but the use of D_2O in the EOCR would introduce an additional complexity that it would be desirable to avoid initially. Even if no other factors were involved, the D_2O inventory would add the order of a million dollars to the cost. The use of organics as a coolant only should be explored at a later stage in the development of the program.

Some comments should be made in regard to the reliability of the studies which have been made for this report. For a conceptual design it is necessary to accept a limited degree of accuracy in order to use methods which are fast and relatively inexpensive. The reactor physics studies have been made with these requirements in mind. Calculated values, as determined by EOCR methods, of k_{eff} for the OMRE over a range of temperatures were compared with measurements by Atomics International and the results used to determine an experimental correction for EOCR work. The calculated values are always higher but at no temperature do they differ by more than three per cent from the measured values. This agreement is sufficient to establish that the reliability of the methods is adequate for the purposes of this project. It should be generally realized that a very limited amount of information exists on experiments or on comparison of theory and calculation. Thus, at present, it is difficult to make more than an approximate evaluation of computational methods. In addition, there is considerable uncertainty in the values

of the cross sections and other constants required for the computations. Therefore, it is doubtful if use of more exact methods can be justified. Developmental work to obtain a consistent set of constants and computational techniques is currently under way by Atomics International and will undoubtedly improve this situation. The detailed optimization of the final design can incorporate the results of this work and can be made on the basis of intensive studies for which more exact methods will be feasible.

The principal features and design specifications of the final concept for the EOCR are presented in Table 1.0A. The loop sizes available are dependent on final mechanical design of the system and, hence, cannot be precisely defined at this time; however, the maximum size for the standard core, with one driver element displaced, is 7.5 in. in diameter. The top and bottom heads are provided with holes which match the grid plate holes at every location in order to permit the installation of a loop of some size in any position or to completely isolate sections of the core by installing a very large loop with coolant routed to this section via the holes in the bottom grid. All variations are not described in this report. The loops tabulated in the table are only those needed for the initial phase of the program. Proven components were selected to avoid the need for a comprehensive research and development program to support the EOCR design. The replaceable grids, top-head and bottom-head permit testing major variations in core design, including organic cooling with heavy-water moderation.

Table 1.0A

EOCR CHARACTERISTICS

Reactor Core

Design Operating Power	40 Mw ($500^{\circ}F$); 20 Mw ($700^{\circ}F$)
Lattice Spacing, Square Array	5.75 in.
Number of Positions in Core	37
Number of Positions in Reflector	20
Fuel Elements	20
Control Rods	12
Loop Positions (in Core)*	
6.5" OD	2
2.5" OD	3
Capsule Positions (1.0" to 1.5")	25
Rabbit Facilities	2

Fuel Elements (Ref. to Fig. 4.2A)

Number of Assemblies	20
Active Core Length	35.5 in.
Length of Assembly	13 ft
Size of Assemblies	4 in. sq.
Fuel Plates per Assembly	46
Fuel Plate Thickness	0.030 in.
Core Alloy Thickness	0.020 in.
Core Alloy Material	UO_2-SS
Cladding Thickness	0.005 in.
Box and Rib Thickness	0.050 in.
Coolant Channel Thickness	0.125 in. to 0.255 in.
Nominal Spacing Between Elements	1.75 in.
U^{235} per Element	1.6 kg

Control Rods (Refer to Fig. 4.3A)

Number	12
Type	Fuel Follower
Size Fuel Section	4 in. sq.
Size Poison Section	4 in. sq.
Clad Poison Material	B^{10}-SS or B_4C

*Includes initially installed loops only. Space is provided for more loops if required.

Table 1.0A (Continued)

EOCR CHARACTERISTICS

Reactor Physics

Active Core Volume, liters	615
Vertical Max/Ave Power Ratio in Fuel	1.4
Horizontal Max/Ave Power Ratio in Fuel	3.3
Core Max/Ave Power Ratio in Fuel	4.6
Average Specific Power, kw/kg U	770
Total U_{235} in Core	52 kg
Initial Core Effective Reactivity	1.16
Control Rod Worth, all 12 Rods	31% Δk eff

Reactor Heat Transfer

Coolant	Santowax R or OMP
Flow in Fuel Elements and Control Rods	20,500 gpm
Reactor Inlet Temperature	500°F (40 Mw); 700°F (20 Mw)
Reactor Outlet Temperature	525°F (40Mw); 715°F (20 Mw)
Maximum Coolant Velocity in Fuel	37.5 ft/sec
Minimum Coolant Velocity in Fuel	9.0 ft/sec
Core Pressure Drop	40 psi
Average Heat Flux, Btu/hr-ft^2 (40 Mw)	
Start of Cycle	144,000
End of Cycle	108,000
Maximum Heat Flux (40 Mw)	660,000
Maximum Fuel Element Surface Temperature	850°F
Burnout Heat Flux, Btu/hr-ft^2	2,140,000

Reactor Vessel

Height	18 ft 9 in.
Inside Diameter	7 ft
Design Pressure	300 psi
Design Temperature	850°F
Design Maximum Power	220 Mw
Wall Thickness	1.25 in.
Number and Size of Nozzles	8 : 8 in. OD
Material	347 SS

Process System

Number of Pumps	1
Coolant Flow	25,000 gpm
Total System Pressure Drop	75 psi
Heat Removal Capacity	45 Mw (500°F)
Purification System	2000 lb/hr
Degasification System	200 gpm
Design Temperature	850°F
Design Pressure	300 psi

Table 1.0A (Continued)

EOCR CHARACTERISTICS

Experimental Fuel Power Density * in Central Loop at 40 Mw (w/cc)	Average	Maximum
2.5% Enriched Fuel	135	260
7.5% Enriched Fuel	257	495
13.5% Enriched Fuel	320	620
Experimental Fuel Power Density * in Central Core Position (no loops) at 20 Mw		
2.5% Enriched Fuel	101	195
7.5% Enriched Fuel	192	372
13.5% Enriched Fuel	240	465

* The maximum power density in proposed organic-cooled and -moderated reactors is about 200 w/cc.

2.000 RESEARCH PROGRAMS TO BE PERFORMED IN EOCR

In formulating the following research and development programs consideration was first given to the status of the organic reactor program as indicated by a survey of the pertinent experimental work; secondly, to proposed organic-cooled power reactors which are either organic- or D_2O-moderated; and finally, to recommendations of Atomics International[1] which were supplied at the request of Phillips Petroleum Company.

Based on these considerations, the immediate program for the EOCR is to verify, in the test facilities and core positions provided for that purpose, the performance of fuel elements of proposed power reactors[2,3,4] so that proven technology is available to permit actual construction of the reactors. The longer-range needs include several other areas of research to be undertaken in EOCR. These are tabulated below and discussed in the following sub-sections.

1. Develop new fuel elements for organic-cooled power reactors.

2. Develop new or modified coolant materials for use in organic-cooled reactors moderated by D_2O, graphite or organics.

3. Develop improved methods of fuel and moderator separation for organic-cooled, solid-moderated reactors.

4. Conduct heat transfer tests with fuel elements cooled by organics.

5. Conduct physics tests with different core configurations.

6. Conduct tests with core arrangements and fuel elements proposed for power reactors at their design power densities.

7. Test auxiliary processing equipment.

---

1. J. E. Stewart, "Suggested Experimental Facilities for the Experimental Organic Cooled Reactor (EOCR)", Report NAA-SR-MEMO-4319, September 29, 1959.

2. Bechtel Corporation and Atomics International, "Organic Cooled Power Reactor Study - Summary of Study", Report TID-8501 (Part 1), July 1959.

3. Bechtel Corporation and Atomics International, "Organic Cooled Power Reactor Study - Reactor Concept Evaluation", Report TID-8501 (Part 3), July 1959.

4. Bechtel Corporation and Atomics International, "Organic Cooled Power Reactor Study - 300 Mw Power Plant Conceptual Design", Supplement No. 2, Report BCPI-I, June 26, 1959.

2.100 Fuel Testing

The minimum fuel element environmental conditions that are needed in the EOCR are shown in Table 2.1A which lists the maximum design power density and heat flux for fuel elements in the proposed organic power reactors and also shows the values which have been attained in OMRE tests. The design objectives for EOCR fuel tests are given in Section 3.000.

Table 2.1A

FUEL ELEMENT ENVIRONMENT IN PROPOSED POWER REACTORS AND TEST ENVIRONMENT TO DATE IN OMRE

Reactor Fuel Elements	Size of Fuel Elements	Power Density, watts/cc *		Heat Flux, Btu/hr-ft^2	
		Ave	Max	Ave	Max
Piqua OMR[1]	5.25" OD	30	117	34,000	132,000
300 Mwe[2] (Forced Convection)	5.16" OD	65	197	54,000	164,000
300 Mwe[2] (Nucleate Boiling)	5.375" x 5.375"	44	165	37,000	139,000
D_2O-Moderated Organic-Cooled	2.760" OD	100[3]	300[3]	150,000[3]	450,000[3]
Test of Piqua[4] Prototypes in OMRE	2.965" OD	--	19	------	27,000

1. "Preliminary Safeguards Report for the Piqua Organic Moderated Reactor (Revised)", Report NAA-SR-3575, April 13, 1959.
2. Bechtel Corporation and Atomics International, "Organic Cooled Power Reactor Study - 300 Mw Power Plant Conceptual Design", Supplement No. 2, Report BCPI-I, June 26, 1959.
3. Estimated from "Proceedings of the OCDR Symposium "at Atomic Energy of Canada Limited, Chalk River, Ontaria, June 15, 1959, Civilian Atomic Power Department, Canadian General Electric Company Limited.
4. Personal communication with Mr. J. E. Stewart and Mr. M. A. Perlow of Atomics International.

* Volume ≅ volume of fuel and organic in the core.

The initial test program on fuel elements in the EOCR will be directed at evaluating fuel elements similar to those proposed for the 300 Mwe OCR.[1] These fuel elements are made with sintered UO_2 pellets clad with finned tubes of aluminum powdered metal (APM). Tests in the EOCR will be designed to:

1. Evaluate structural integrity of APM and the closures of the fuel tubes at OCR maximum design operating conditions.

2. Determine fouling rate on finned surfaces of APM cladding.

3. Determine rate of fission product release through APM cladding.

4. Determine creep strength and other strength properties of APM after exposure to irradiation at elevated temperatures.

5. Determine maximum permissible operating velocities and temperatures suitable for APM use.

In addition to tests related to development of APM clad fuel elements, fuel element tests will also be conducted in the EOCR to:

1. Evaluate cladding materials for uranium metal, oxide, and carbide fuels.

2. Evaluate structural stability of fuel materials at different temperatures, burnup, and heat generation rates.

3. Determine maximum heat generation rates of organic cooled fuel elements as a function of fuel element size, geometry, and cladding.

4. Evaluate new fabrication techniques for fuel elements proposed for use in organic reactors.

5. Prove production type fuel elements by testing statistical quantities of fuel elements.

6. Test unclad uranium metal, plated uranium metal, and carbon clad uranium metal exposed to organic coolant.

7. Evaluate new fuel types such as uranium impregnated graphite or others which may be proposed for organic cooled power reactors.

2.200 Organic Testing

The organic test program proposed for the EOCR will study the pyrolysis and radiolysis of many possible organic reactor coolants under power reactor

---

1. Bechtel Corporation and Atomics International, "Organic Cooled Power Reactor Study - 300 Mw Power Plant Conceptual Design", Supplement No. 2, Report BCPI-1, June 26, 1959.

conditions and evaluate new coolant materials and additives that may result in lower radiolytic damage, improved heat transfer and lower pumping costs.

The objective of the first tests in the EOCR is to verify the predicted radiolysis of organic coolants, such as Santowax R and Santowax OMP, under conditions duplicating those to be encountered in proposed organic cooled power reactors. These conditions, which are listed in Table 2.2B with previous test conditions, show that most organic tests performed to date have been in environments at much lower intensities than those proposed for the power reactors; also, damage to organic materials may be dependent on the ratio of fast neutron intensity to gamma intensity and temperature. At the present time there is no suitable facility to study the effects of different ratios of neutron-to-gamma radiation on organic decomposition rates.

Table 2.2B

ORGANIC RADIATION ENVIRONMENTS IN TESTS TO DATE AND IN PROPOSED POWER REACTORS

Environment	Total Intensity, watts/gram	Neutron Intensity, watts/gram	Gamma Intensity, watts/gram	Ratio of Neutron-to-Gamma Intensity
Test Facilities[1]				
OMRE (6 Mw)	1.2	0.34	0.86	0.4
BEPO	0.008	0.0043	0.0037	1.2
MTR Canal	0.046	-----	0.046	0
MTR In-Pile	0.33	0.04	0.29	0.14
Van de Graff (1 Mev Electrons)	0.6 to 7.3	-----	-----	----
Power Reactors				
Piqua OMR[2]				
Average	1.3	0.8	0.5	1.6
Maximum	5.2	3.2	2.0	1.6
300 Mwe OCR[3] (Forced Convection)				
Average	2.6	1.6	1.0	1.6
Maximum	7.8	4.9	2.9	1.6

1. R. H. J. Gercke, C. A. Trilling, "A Survey of the Decomposition Rates of Organic Reactor Coolants", Report NAA-SR-3835, June 10, 1959.

2. Personal communication with Mr. J. E. Stewart of Atomics International.

3. Bechtel Corporation and Atomics International, "Organic Cooled Power Reactor Study - 300 Mw Power Plant Conceptual Design", Supplement No. 2, Report BCPI-I, June 26, 1959.

The general area of investigation for all organics will be aimed at collecting sufficient data to predict radiolysis in any reactor system (such as organic-cooled and -moderated, organic-cooled and D_2O-moderated, organic-cooled and graphite-moderated, and organic-cooled and zirconium-hydride-moderated) and to explore possibilities for improving power reactor economics by modifying coolants or operating conditions. Some of the areas to be studied are:

1. Effect of temperature and pressure on radiolysis.

2. Effect of ratio of neutron-to-gamma dose rate on radiolysis.

3. Effect of radiation intensity on radiolysis.

4. Testing of certain very cheap petroleum fractions which are rich in the radiation resistant aromatics and substantially free of less resistant napthenes and paraffins.

5. Testing of synthetic coolants made especially for nuclear reactor cooling. One area considered promising which has not been studied is nitrogen containing analogues of the polyphenyls such as pyridine ring types. Another group of compounds not fully investigated are the alkyl phenanthrenes; for example, retene.

6. Effect of additives on radiolytic damage. Considerable promise for additives has already been shown. Specifically, several condensed ring nitrogen compounds and some sulfur compounds related to thianthrene[1] are being considered. Another approach suggested by previous work is the use of compounds absorbing and emitting fluorescent energy. The use of condensed ring aromatics will also be studied.

7. Modification of the coolant to reduce viscosity at operating temperatures. The use of additives for viscosity control, as is done in lubricating oil technology, seems a definite possibility. Since it is desired to reduce viscosity at high temperatures, with not too much interest in the viscosity at low temperatures, an additive with a negative viscosity index is indicated. Such additives are found among the perfluorinated oils. These were developed in connection with isotope separations at Oak Ridge and are reputed to be very stable chemically.

8. Modification of the organic coolant to stabilize the liquid state at temperatures below the normal solidification point. This has been carried out on some other aromatic liquids, using certain classes of surfactant organic compounds.

---

1. California Research Corporation, AEC Contract No. AT(11-1)-174, Report No. 13, "The Radiolysis of Prospective Dynamic Reactor Coolants," p.27, Compiled by W. W. West, August 13, 1959.

9. Effect of "in-pile" catalysis. Additions of trace amounts of metals or metal complexes to catalyze the back reaction or to change the end product composition appears to be a possibility since similar effects have been observed in petroleum processing as well as radiolysis in in-pile aqueous solutions.

10. Fouling characteristics of all proposed coolants.

11. Effect of water content on radiolysis and fouling.

2.300 Heat Transfer Tests

The power densities that are presently being considered for organic-cooled reactors are relatively low because of poor heat transfer characteristics of organic coolants. An important part of the organic reactor program is that of evaluating the heat transfer performance of fuel elements and organic coolants and developing methods of improving the heat transfer to increase reactor power densities. The initial heat transfer test program will be directed toward determining whether finned APM fuel proposed for organic cooled power reactors can be operated at the conditions assumed for the design. Concurrent tests will duplicate conditions proposed for the forced convection cooled power reactor and the nucleate boiling power reactor.[1] If loop tests demonstrate that nucleate boiling presents no problems, an early solution of flow stability considerations will be sought by operating an entire core of power reactor elements under nucleate boiling conditions.

The general areas of heat transfer research should be the following:

1. Evaluate methods of improving heat transfer, such as varying fuel element geometry and using coolant additives such as viscosity improvers.

2. Determine maximum operating limits of fuel elements and organic coolants without surface fouling or fuel element burnout.

3. Compare heat transfer by forced convection, nucleate boiling and bulk boiling.

4. Study flow stability with forced-convection nucleate boiling and natural-convection nucleate boiling.

5. Study fouling with fuel elements cooled by natural-convection, forced-convection, and nucleate-boiling heat transfer.

2.400 Auxiliary Tests

A reactor facility capable of operating at a range of power levels and accommodating different core configurations of fuel elements and moderator can yield many results significant in predicting performance of other

---

1. Bechtel Corporation and Atomics International, "Organic Cooled Power Reactor Study - 300 Mw Power Plant Conceptual Design", Supplement No. 2, Report BCPI-1, June 26, 1959.

reactors in the field of physics, organic technology and general operational information pertaining to maintenance and instrumentation. Some of these tests are mentioned in the following paragraphs.

2.410 Low Power Physics Tests. Much of the physics of organic reactors is based on theory with very little attempt to experimentally verify calculations. Some of the areas which can be explored in EOCR are power flattening, statics and dynamics of full cores, moderator control studies and D_2O-moderator systems.

2.411 Power Flattening Studies. The organic reactor designs which have been proposed have very high maximum to average heat flux which results in an economic disadvantage caused by increased reactor size and pumping cost since the thermal design must be based on the hottest point in the reactor. Several methods of flattening the heat flux are considered feasible. Some of these are variation of moderator radially in the core, variation of fuel density both radially and vertically, or a combination of these. The EOCR can be used to test various methods proposed for power flattening.

2.412 Static and Dynamic Physics of Cores. The EOCR can be used to obtain experimental information concerning the statics and dynamics of the reactor cores being studied. These data, as well as being valuable per se, permit evaluation of calculational methods. The following topics are illustrative: variation of reactivity with temperature, void coefficients and local flux variations due to control rod perturbations. Zero-power reactor frequency response studies provide valuable safeguards information. The EOCR can also be used to establish some of the reactor physics constants for the cores being studied, e.g., τ, L^2, ε, ρ, f, B^2, β_{eff}, and ℓ_{eff}.

2.413 Moderator Control Studies. It is theoretically possible to control an organic power reactor by the use of moderator with varying hydrogen density or by the use of hydrocarbons having poison additives, e.g., borated hydrocarbons. The benefits of this type of control are the elimination of complicated mechanical control rods with a resultant increase in average power density and a decrease in size of the reactor for a given power output. Reactor size is further reduced by utilization of the space normally used by control rods for power producing elements. The EOCR can be used for this type of study if the grids and internal components are removable so as to allow testing of cores designed specifically for these tests.

2.414 D_2O Moderation Systems. The use of D_2O as a moderator and organic as a coolant offers some possibility for improvement in power reactor economics because of the possibility of reduced fuel cost and higher operating coolant temperatures. It will be desirable to mock-up a section of the core which is moderated by D_2O and cooled by organic to determine the actual organic damage rates. This mockup can also be used to determine certain physics parameters for the D_2O system;

however, a full scale or near full scale mockup is needed for final results on D_2O systems. The EOCR reactor vessel is designed in such a manner that a D_2O calandria can be installed at some future date.

2.420 Core Tests at High Power Levels. Since very little experience has been developed with operation of organic-cooled reactors, EOCR can make significant contributions by operation of test cores to obtain the following information: (1) change in flux with time in operating cores, (2) effect of core layout on radiolysis, and (3) stability of an organic-cooled reactor operating with nucleate boiling.

2.421 Burnup Effects on Reactivity and Heat Flux. The change in reactivity and heat distribution with time is important in predicting the performance of power reactor cores. It would be extremely valuable to have actual operating data on a large core to check calculated values; however, useful data for checking calculations can be obtained from medium-sized cores. For this purpose it would be desirable to operate EOCR with a simulated power reactor core and monitors to determine power shifts and reactivity changes as a function of burnup.

2.422 Effect of Core Composition on Radiolysis. Very low radiolytic damage rates are predicted from the available data for systems having a high metal-to-organic ratio and particularly for systems employing graphite or heavy water moderation. The predicted rates can be verified for the most promising systems by operating one core with characteristics similar to power reactor cores. This testing will be preceded by loop tests to define the areas of importance.

2.423 Stability of Organic Cooled Reactor Operating with Nucleate Boiling. Loop tests, out-of-pile heat transfer tests, and analytical calculations can be performed to predict the problems involved in operation of a reactor with nucleate boiling heat transfer. However, actual operation of a core in nucleate boiling is recommended to finally demonstrate the problems to be encountered due to flow instability and fouling. The EOCR can be used to test the operation of an organic reactor at high power density with nucleate boiling.

2.430 Process Studies. A number of different methods of maintenance of the coolant in organic reactors should be tested because of the economic importance generated by the cost of replenishing the organic and the cost of disposal of the waste organic. In a large power reactor such as a 300 Mwe organic cooled reactor the volume of makeup is estimated to be about 5000 gallons per day. Since all the radioactive wastes eventually end up in the decomposition products, the problems of waste disposal may be extremely severe. The EOCR offers an ideal facility for exploring the problems of proposed systems such as burning of the HB, degasification systems, purification systems, and fission gas removal and holdup systems. Of more economic importance to the organic reactor program are the possibilities of (1) reconstitution of the HB* by thermal or catalytic cracking, (2) decreasing the production of the HB by addition of hydrogen donor

* HB is defined as polymerization products which are less volatile than para-terphenyl.

materials to the circulating stream, and (3) changing the decomposition rates and/or end products by "in-pile" catalysis. The EOCR is readily adaptable to studies of the latter type on a large scale after promising techniques are developed in small scale loop systems

3.000 DESIGN OBJECTIVES

The design objectives for the EOCR are defined by the test program discussed in Section 2.000. The design specifications for test facilities are developed from available information on proposed organic-cooled and -moderated power reactors, proposed organic-cooled D_2O-moderated power reactors, and the projected needs of the organic-cooled reactor program. Despite the advances in technology required for these proposals to be successful, prudent design practices suggest that they may be conservative if used as the basis for planning a developmental program. Therefore, test conditions in excess of those for proposed power reactors are necessary to check the limits of extension of the technology. For this reason the design objectives for environmental conditions of organic tests, fuel tests and heat transfer tests given in Tables 3.1A, 3.2A, and 3.3A are in excess of similar conditions in power reactor proposals.

Tests will be conducted in the EOCR in loops of several sizes, in fuel element positions in the EOCR core by partially or totally replacing the EOCR core driver elements with power-reactor fuel elements and in small static test positions cooled by EOCR coolant. It will be possible to utilize each loop for fuel, heat transfer, and organic tests, although not necessarily at the same time, and as many loop positions as economically feasible should be provided in the design. Table 3.0A summarizes the size and number of in-pile loops proposed for initial installation. Design objectives for other research programs are satisfied

Table 3.0A

SUMMARY OF TEST POSITIONS REQUIRED FOR FUEL, ORGANIC AND HEAT TRANSFER TESTS IN EOCR

Type of Facility	Capsule or Lead Type*	Small Loops	Large Loops	In-Core Positions
Number of Fuel Tests	4	2	1	10
Number of Organic Tests	6	---	1	---
Number of Heat Transfer Tests	4	1	1**	4
Total	14	3	2	14
External Facilities	Minor	Complete loop facility except for purification system.	Complete loop facility***	Flow and temperature monitoring.

* These facilities are cooled by reactor coolant.
** The large loop required for heat transfer tests will be shared with the fuel and organic test program.
*** Refer to Section 8.000 for detailed loop design.

by removable grids, replaceable top and bottom heads, design of the tank and shields for high power levels, and design of the primary system for 850°F and 300 psig.

3.100 Fuel Testing

The program outlined for fuel testing in the EOCR requires reactor facilities to: (1) test small fuel capsules, (2) test prototype fuel elements in loop positions, and (3) test statistical quantities of fuel elements in core positions. The number, size and test conditions for fuel testing are summarized in Table 3.1A.

Table 3.1A

REQUIREMENTS FOR INITIAL FUEL TESTS IN EOCR

Type of Facility	Small	Large	In-Core
Number of Facilities	6	1	10
Size of Loop, Capsule, or Test Position, inches	1.0 to 2.5 dia	6.5 dia	5.5 dia or 5.5 square
Power Density, watts/cc	50 to 300	50 to 300	50 to 300
Heat Flux, Btu/hr/ft^2	30,000 to 450,000	100,000 to 300,000	100,000 to 450,000
Maximum Coolant Velocity, ft/sec	30	25	30
Maximum Coolant Temperature, °F	850	850	850
Maximum Pressure, psig	600	300	300
External Facilities Required	Two entire loop facilities except for purification system. Minor out-of-pile equipment for other tests.	Entire loop facility, i.e. pumps, heat exchangers, purification system, etc.	Monitors to determine power production in each element

3.110 Small Test Facilities. These facilities are provided for evaluation of individual segments of elements in the areas discussed in Section 2.100. Out-of-pile loop facilities are provided for two 2.5-in. OD loops. One other 2.5-in. loop is provided for the heat transfer program which may be used for fuel tests when available. Additional capsule or lead-type experiments may be cooled by reactor primary coolant. Many spaces for this type of test are provided.

3.120 Large Test Facility. This loop test facility for testing of full-scale power reactor elements includes out-of-pile equipment such as pumps, heat exchangers, flow control equipment, temperature control equipment, purification and degassing equipment for maintenance of coolant, and reactor interlocks. Since this type of test facility is quite expensive, only one facility is recommended in the initial phases of the program. Another facility of identical size is proposed for the organic test program which may also be used for the fuel test program. A typical design of this facility is described in Section 8.000. Five suitable positions for this type of facility are provided in the core; however, it is proposed that three of these positions will initially be occupied by smaller loops as shown in Fig. 4.1A.

3.130 In-Core Tests. The lattice spacing of the EOCR has been chosen such that power reactor elements as large as 5.5 in. square may be used to replace any driver fuel element not adjacent to a large loop. This makes it possible to test several power reactor elements or an entire core. In order to achieve the temperature conditions desired for most tests it will be necessary to raise the bulk coolant temperature of EOCR which in turn causes a reduction in the allowable power level; however, the permissible power at higher temperatures is sufficient to provide power densities in excess of those proposed for power reactors. These in-core tests result in a requirement of a high bulk coolant design temperature for EOCR. No additional flow is provided for these tests since these fuel elements will normally require less flow than the displaced driver elements.

3.200 Organic Testing

In order to carry out the organic-coolant test program as outlined in 2.200, the design includes facilities for testing organic materials at temperatures, pressures, flux densities and neutron-to-gamma ratios in excess of those proposed for power reactors and past test conditions. This should culminate in testing of the organic by use as the primary coolant for the EOCR. Laboratory facilities for determination of the resulting alterations in coolant properties and decomposition products formed are an essential requirement in accomplishing these objectives. The design should provide means for testing organics in three general categories: (1) simple, brief tests for rapidly screening numbers of new and modified coolants; (2) more intensive small scale tests under a variety of radiation and temperature conditions; (3) dynamic loop tests in contact with full size fuel elements. The number and size for each of these categories are summarized in Table 3.2A.

Table 3.2A

REQUIREMENTS FOR INITIAL ORGANIC TESTS IN EOCR

Type of Facility	Small Short Term	Small Long Term	Large
Number of Facilities	2	4	1
Diameter of Facility, inches	1.5	1.5	6.5
Radiation Intensity Total, w/g Ratio Neutron to Gamma	2.0 to 12 0.5 to 3.0	2.0 to 12 0.5 to 3.0	2.0 to 12 0.5 to 3.0
Temperature, ^{o}F	---	500 to 850^{o}	500 to 850^{o}
Pressure, psig	---	10 to 300	10 to 300
External Facilities Required	Equipment to insert and remove capsules during reactor operation.	Sample tube, fill tube, pressurizing tube, and temperature control.	Entire loop facility, i.e. pumps, heaters, coolers, purification system, etc.

3.210 Small Short-Term Facilities. Provisions are required for screening small samples of new coolant compositions in tests of a few hours to a few days duration, in relatively large numbers on a continuing basis. Out-of-pile equipment can be designed to provide for insertion and removal of samples without reactor shutdown. Sample size will approximate 100 cc in most cases. Capsule tests of this type could be done in a rabbit facility, for instance. Provisions to test at two flux densities are provided. One of these facilities is provided in the reflector and the other in the core. Temperature control is not stated as a requirement; however, operation at reactor coolant temperature or above is desirable.

3.220 Small Long-Term Facilities. In the next category, tests are required in which small to moderate size samples are subjected to a variety of temperatures, pressures, and flux densities. Such conditions are provided, for example, in capsules with limited out-of-pile equipment such as sample tubes, fill tubes, temperature and pressure control. Facilities of this type are in the core as shown in Fig. 4.1A. Other positions are available for these tests in the space between fuel elements and in the reflector.

3.230 Dynamic Loop Tests. One large loop should be provided in which coolants are tested in contact with full size fuel elements. Because of the complexity and cost of such loops this test work may use the same loop as, and be integrated with, fuel element and heat transfer testing. It would therefore need to be large enough to test a typical power reactor element. It should have its own independent purification system. Five possible positions are provided for this loop. Two positions are initially provided as shown in Fig. 4.1A. Out-of-pile equipment is identical with that shown for the fuel test loop. Small scale dynamic tests may also utilize one of the three fuel element test loops.

3.300 Heat Transfer Studies

Some of the heat transfer tests proposed in Section 2.300 require higher heat fluxes and more extreme temperatures than required for fuel element tests. These can be conducted in the central loop. One 2.5 in. loop is also provided in the core for heat transfer tests. Other facilities for long-term tests are provided in the reflector or between driver elements. Finally, nucleate boiling tests may be performed in the core. The same loops proposed for fuel and organic tests can be used for heat transfer tests to some extent.

The facilities provided to conduct heat transfer tests fall into three catagories:

1. Small test facilities up to 2.5 in. in diameter are provided in the core or in the reflector. Out-of-pile loop facilities are provided for one 2.5 in. diameter loop. Other tests will be cooled by reactor coolant and will have a minimum out-of-pile equipment.

2. One large facility located in the highest flux region of the reactor will be used for heat transfer tests of power elements or burnout tests of small elements. The large facility is shared with the fuel and organic programs.

3. In-core positions will accommodate power reactor fuel elements and will be used for nucleate boiling tests or long-term fouling tests. No out-of-pile equipment is required except for instrumentation.

Table 3.3A summarizes the number, size, and test conditions of loops required for heat transfer tests.

Table 3.3A

REQUIREMENTS FOR HEAT TRANSFER TESTS IN EOCR

Type of Facility	Small	Large*	In-Core
Number	5	1	4
Size, inches	1.0 to 2.5 dia	6.5 dia	5.5 square
Maximum Power Density, watts/cc	500	300	300
Heat Flux, Btu/hr-ft^2	100,000 to 500,000	200,000 to 1,000,000	500,000
Maximum Coolant Velocity, ft/sec	30	25	30
Maximum Coolant Temperature, ^{o}F	850	850	850
Maximum Pressure, psig	300	300	300
External Facilities Required	One complete loop facility except for purification system.	Complete loop facilities.	Flow and temperature monitoring.

* A separate facility is not proposed for heat transfer tests. For economic reasons this facility is shared with the fuel or organic program.

3.400 Reactor Physics

In order to carry out the EOCR-startup physics investigations and the physics research program outlined in Section 2.410, the EOCR is as flexible and accessible as practical. For example, many of these measurements involve the irradiation of flux wires and foils; therefore, it is desirable that facilities be provided for the convenient introduction and removal of these wires and foils. In order to conduct investigations at various temperatures during initial operation with each type of core, it is desirable to have a non-nuclear source of heating for the organic; the friction energy developed in the circulating organic coolant can produce temperature levels up to 700^{o}F The EOCR is designed to permit investigations with other moderators; for example, provisions for introduction of a calandria to provide D_2O moderation. There are other design objectives, important to the reactor

physics tests, which are discussed in the following section under "Tests of Power Reactor Cores".

3.500 Test of Power Reactor Cores

Tests are proposed for the EOCR to study the engineering performance and physics of power reactor cores. These tests require that the EOCR be designed so that the reactor core configuration can be completely changed and any desired core layout studied by operating at the maximum power level permitted by the capacity of the EOCR heat removal system. Removable fuel element grids are needed in order to study cores with various combinations of fuel element size and core lattice spacing. Removable top and bottom reactor heads are provided for future use, i.e., to make possible the use of various control rod systems, the monitoring of individual fuel assemblies of different core arrangements, and special measurements.

3.510 Core Layouts. The size and description of the cores proposed for organic-cooled power reactors are given in Table 3.5A. It is not an objective to design the EOCR to accommodate the full-size power reactor cores; however, portions of the larger cores and possibly a full-size Piqua core can be accommodated. The reactor is designed to test fuel elements of the power reactor design in lengths up to at least 4.5 ft without modification of grids or other internal components with lattice spacings as shown in Table 3.5A and other variations by replacement of grids and, if necessary, the top and bottom heads.

Table 3.5A

DESCRIPTION OF PROPOSED ORGANIC-COOLED POWER REACTOR CORES

Reactor	Fuel Element Cross Section, inches	Lattice Spacing, inches	Length of Core, inches	Diameter of Core, inches	Number of Fuel Elements
Piqua[1]	5.25 OD	6.00 Triangular	54	60	78
300 Mwe[2] Forced Convection	5.16 OD	6.30 Triangular	144	132	396
300 Mwe[2] Nucleate Boiling	5.38 square	5.88 square	144	153	310

1. J. Jacobson, "Preliminary Safeguards Report for the Piqua Organic Moderated Reactor (Revised)", Report NAA-SR-3575, April 13, 1959.
2. Bechtel Corporation and Atomics International, "Organic Cooled Power Reactor Study - 300 Mw Power Plant Conceptual Design", Supplement No. 2, Report BCPI-1, June 26, 1959.

3.520 Permissible Power Levels. Power flattening over a 4-ft-diameter by 4.5-ft high core operating at a power density of 200 w/cc results in a power level of about 220 Mw. The primary coolant system flow rate is adequate to remove 220 Mw when extended surface fuel elements are used. To accommodate power levels of this magnitude the reactor tank, thermal shields, and biological shielding are designed for 220 Mw. These features do not add significantly to the overall cost. The fin-fan heat exchangers are designed to allow additional units to be added to bring the heat removal capacity up to 220 Mw.

4.000 EOCR CORE

Several possible cores were studied prior to selection of the final configuration that best suited the design objectives. The cores studied and the basis of selection of the final core are described in Section 11.000. The preferred EOCR core design is presented in this section. This core is referred to as the "standard" core throughout the remainder of the report. Physics calculations were made on the standard core with several different experiment and fuel arrangements. These variations are described in Section 5.000.

4.100 Core Arrangement

The standard core, shown in Fig. 4.1A, is made up of 4-in. square fuel assemblies and control rods equally spaced on 5.75-in. square centers. Of the 37 major core positions, 20 are occupied by fuel assemblies, 12 by control rods with fuel followers, and 5 by experiments. Fuel element orientation is required throughout the core as shown to locate high-velocity channels in the high flux region of each position. The 5.75-in. square lattice is continued into the reflector region to provide additional experimental space. For illustrative purposes eight typical power reactor elements are shown. Fission chamber thimbles and the neutron source are also located in the reflector region. The core height is 36 in. with provisions to ultimately accommodate core heights up to 4.5 feet. It is recommended that, initially, two 6.5-in. OD loops, three 2.5-in. OD loops, two rabbit facilities and positions for several capsule or lead-type experiments be provided.

The core is cooled, moderated and reflected with Santowax R at 500°F. The power is 40 Mw (500°F inlet temperature) or 20 Mw (700°F inlet temperature).

4.200 Fuel Elements

A conceptual drawing of an EOCR fuel element is shown in Fig. 4.2A. The design is based on proven fabrication technology and very little development and test work is foreseen in adapting this fuel element for use. These fuel elements are referred to as "driver" assemblies or "driver" fuel elements throughout this report to distinguish them from the power reactor fuel elements which are tested in the core.

The fuel element is 4 in. square and is made of 23 flat fuel-plates in each of two 4-in.-by-2-in. sections. The 0.030-in. thick fuel plates, which have a fully enriched UO_2-SS fuel core clad with 0.005-in. thick stainless steel, are contained with a 0.050-in. thick stainless steel box so that coolant flow to the fuel element can be orificed and isolated from the moderator flow between fuel elements. Cooling of the fuel plates is optimized by non-uniform flow distribution throughout the element. This will provide high velocities in areas where neutron flux peaking causes high heat flux, as described in detail in Section 6.000. The fuel assembly is fabricated by attaching the fuel plates to the fuel

element box by some mechanical means such as used in the OMRE fuel element,[1] if necessary, to relieve thermal stresses that develop because the operating temperature of the fuel plates is about 300°F higher than the temperature of the containing box.

4.300 Control Rods

A conceptual drawing of a control rod assembly is shown in Fig. 4.3A. The control rods that will be used are the fuel-follower type with the fuel section similar to the fuel element. A 0.25-in. thick hollow square box is to be used for the poison section. The poison, which is either B^{10} in the form of boron stainless or boron carbide powder, is clad with stainless steel.

4.400 Regulating Rods

Two of the control rods, which are to be used as regulating rods, are provided with automatic control instrumentation.

4.500 Experimental Positions

The core is designed to accommodate many experiments both in loop positions and core positions. Loops as large as 7.5 in. can be installed in any fuel element position by removal of a fuel assembly. Any or all of the driver fuel assemblies can be replaced by test elements as large as 5.5 in. square, except in core positions adjacent to large loops.

Fig. 4.1A shows a typical core layout with two 6.5-in. diameter loops, three 2.5-in. diameter loops and twenty-six 1.5-in. diameter positions for capsule- and lead-type tests. In addition, the core shows eight experimental fuel assemblies in the reflector. Additional experimental space is available in the reflector for tests up to 5.5 in. square.

Sufficient space exists in the core to allow considerable freedom in locating loops or test capsules, providing this is considered in the final design of grids, bottom head and support or hold-down grids.

4.600 Reflector

The core will use the organic moderator as the reflector. A maximum reflector thickness of about 12 in. of organic will be provided between the core driver fuel elements and reactor inner tank. The reflector will change in thickness if experimental fuel assemblies are loaded into this area.

---

1. C. T. Armenoff and M. H. Binstock, "Fuel Elements for the Organic Moderated Reactor Experiment", Report NAA-SR-1934, December 15, 1957.

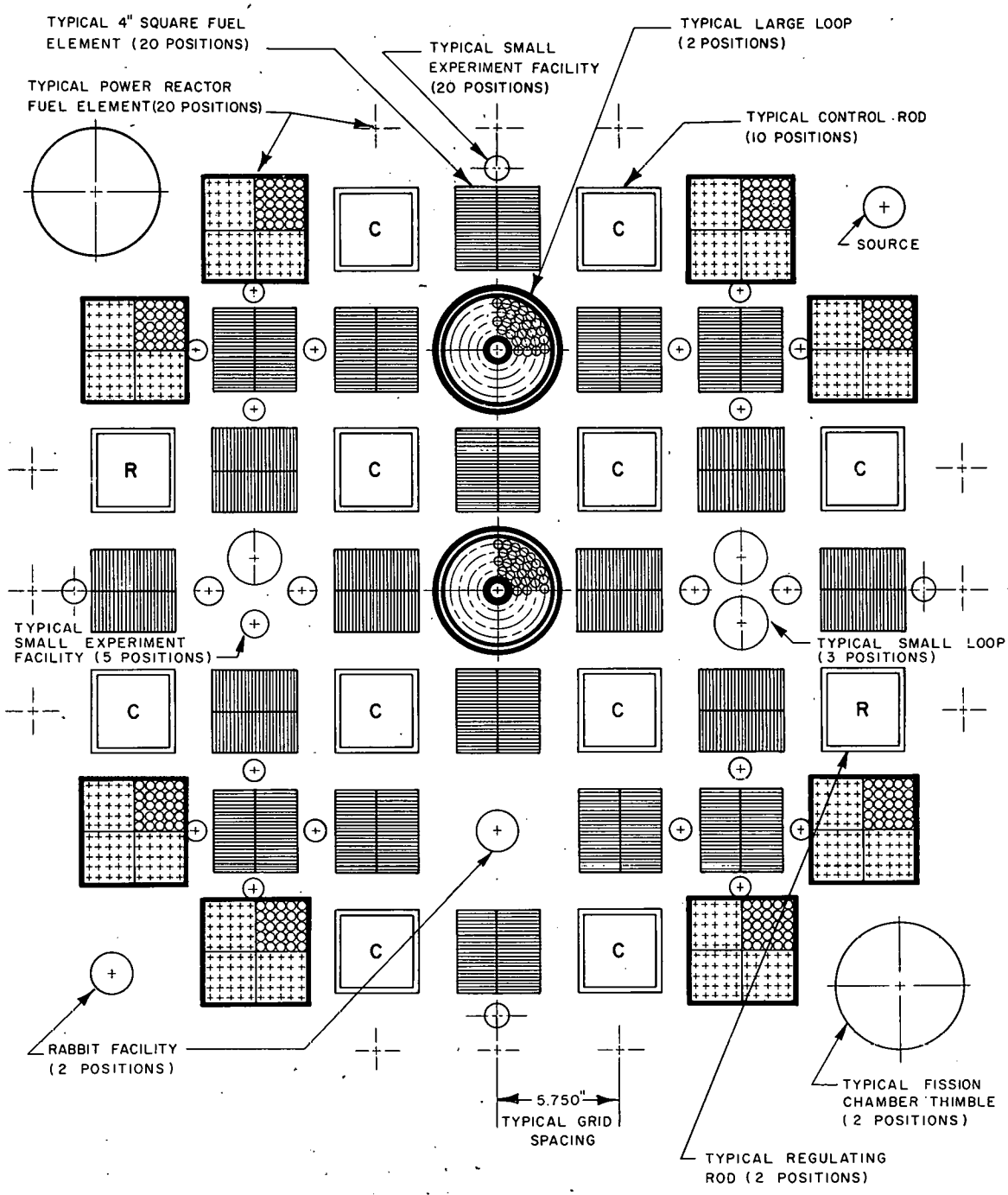

FIG. 4.1A
STANDARD EOCR CORE

P.P. CO. - C - 2500

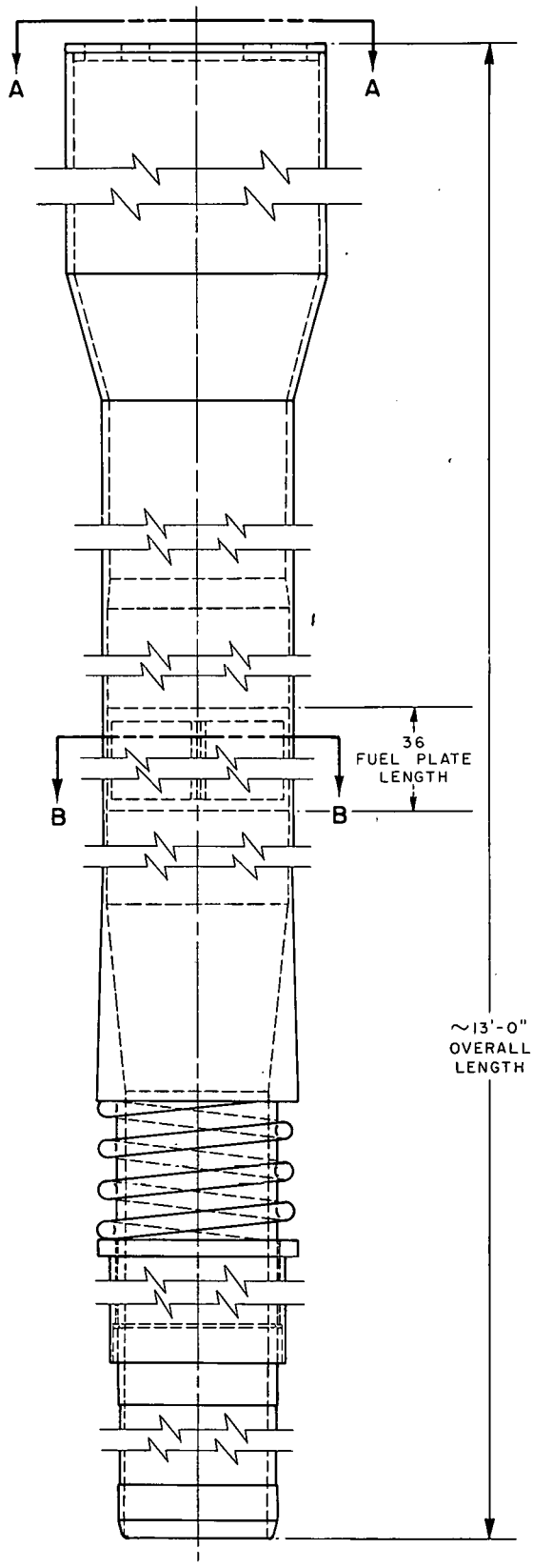

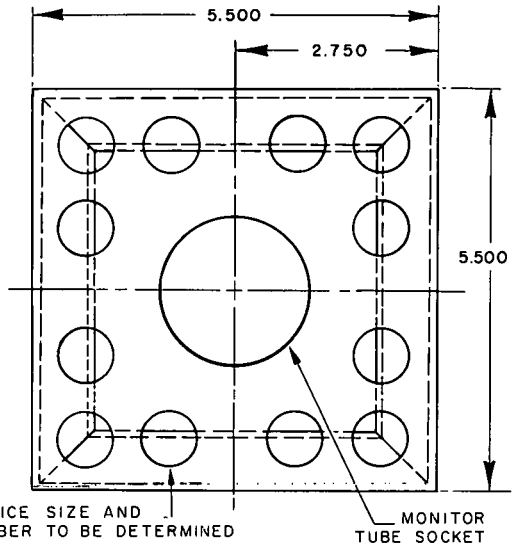

VIEW A-A

CHANNEL NUMBER	CHANNEL THICKNESS
1	.255
2	.180
3	.150
4	.125
5	.125
6	.125
7	.125
8	.125
9	.125
10	.125
11	.125
12	.125
13	.125
14	.125
15	.125
16	.125
17	.125
18	.125
19	.125
20	.125
21	.125
22	.125
23	.125
24	.125

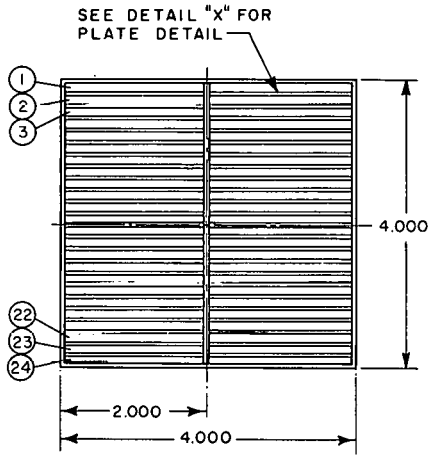

SECTION B-B

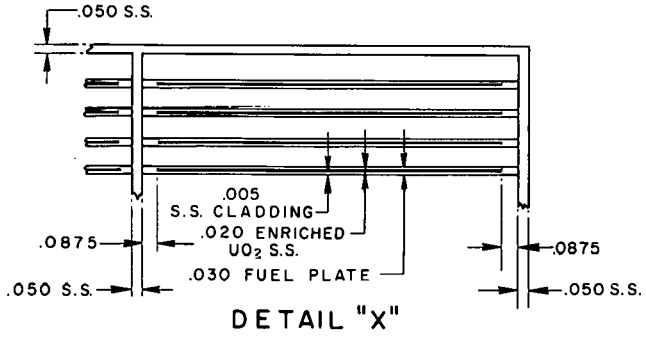

DETAIL "X"

FIG. 4.2 A

EOCR DRIVER FUEL ELEMENT

P.P. CO. - C - 2501

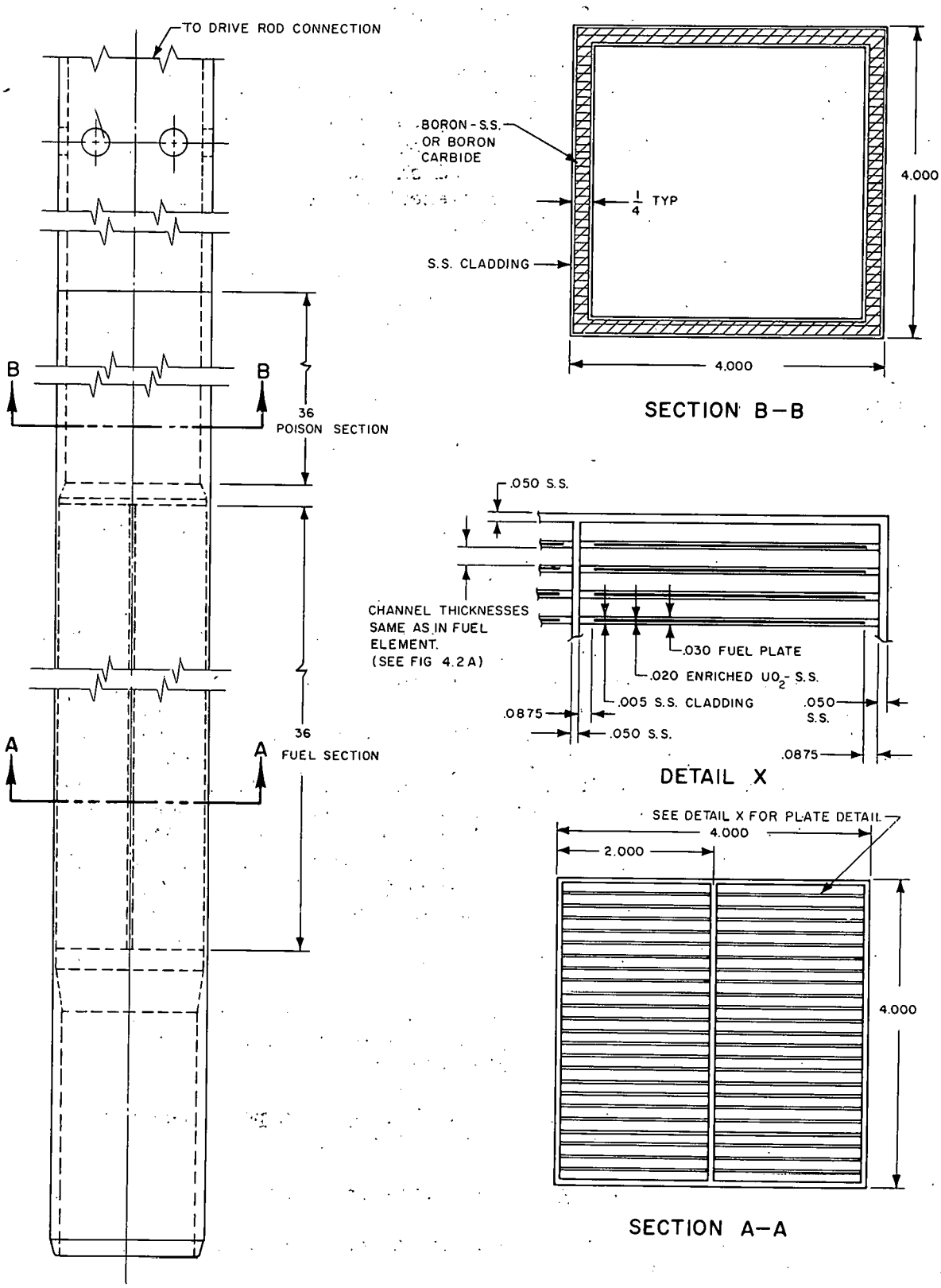

FIG. 4.3 A

EOCR CONTROL ROD

P.P. CO. - C - 2502

5.000 REACTOR PHYSICS

The reactor physics studies described in this section have been made to provide information required for a conceptual proposal. It is expected that further calculations and perhaps some experimental work will be needed to finalize the design. However, the studies are sufficiently complete that changes required should be minor and limited to items such as fuel-plate and fuel-element spacing, fuel loading, and placement and number of control rods.

The calculational methods have been selected on the basis of their acceptability for a conceptual proposal, i.e., a limited degree of accuracy is acceptable in order to provide the rapid and relatively inexpensive results needed. The flux and power distributions are determined by two-dimensional diffusion theory. Reactivity effects are calculated using one-dimensional diffusion theory with transport-theory corrections to account for the flux depression in the fuel resulting from the heterogeneous structure of the core. Two neutron groups are used in all of the EOCR calculations.

Two general types of core arrangements are considered. The reference core, the first type, has 37 driver elements and contains no experimental facilities. The standard core, the second type, has 32 driver elements (20 fuel elements and 12 control rods with fuel followers) and a number of test facilities in the core. Flux and power distributions and the effective multiplication factor have been found for the standard core with two different experimental loadings. Neither of these is identical with the proposed initial experimental loading as described in Section 4.000. The differences in the loadings are not great but these differences combined with uncertainties in the calculations may require slight adjustments in the fuel loading or number of fuel elements to achieve the desired reactivity. The core arrangements used as a basis for the calculations are described in Section 5.200. The results of the reactor physics studies are summarized in Section 5.100 and the flux and power distributions given in Section 5.300. Several alternate designs have been considered, and these are discussed in Section 11.000. Supplementary information on the reactor physics methods and on the proposed design is included in Section 14.000.

The design of the core is determined to a large extent by the following constraints which are imposed by the design objectives or by heat removal and mechanical considerations:

(1) the requirement that a 6.5-in. OD loop or a power reactor fuel element can be placed in any lattice location;

(2) the limit of 25,000 gpm on the organic flow;

(3) the desire to maximize the flux in the test facilities rather than in the driver elements; and,

(4) the restriction to stainless steel for the structural material in the core.

The requirement that a large loop or power reactor element can be placed in any lattice location has led to the selection of a square lattice on 5.75-in. centers. With the lattice size fixed the fuel element design is then influenced by the other three factors.

The limit on the organic flow and the use of stainless steel make it necessary to partially separate the coolant and moderator functions of the organic. In order to minimize the fuel loading and thus maximize the thermal neutron flux in the driver elements it is desirable to keep the metal-organic ratio in the core low. With a low metal-organic ratio and uniform distribution of fuel plates throughout the core the pumping requirement becomes excessive. By use of 4-in. square fuel elements on 5.75-in. centers and by controlling the flow of the organic outside of the fuel element with an orifice the organic flow is reduced to the desired limit while maintaining an acceptable metal-organic ratio.

For fuel elements of the EOCR type there is a spacing that minimizes the fuel requirement and maximizes the thermal flux in the driver elements. This spacing is somewhat smaller than that used in the EOCR as is discussed in Section 14.300. The lattice spacing which minimizes the fuel loading is not optimum for the EOCR because of the desire to maximize thermal flux in the tests rather than in the drivers. As is shown in Section 14.300 a substantial increase in flux can be obtained by having an adequate moderator channel around a test. In addition to the increase in fuel requirement, the spacing of the elements cannot be arbitrarily increased because of the positive component of the temperature coefficient that results. The choice of fuel element size and spacing is seen to be the result of compromises among a number of factors. Some further considerations are included in Section 14.300.

The replacement of all or a substantial portion of the stainless steel in the core by aluminum would make possible a number of improvements in the EOCR. If aluminum were simply substituted into the present design the fuel requirement would be lowered to an extent that would significantly increase the thermal flux and increase the fuel burnup. With aluminum, more fuel plates could be used to reduce the organic flow rate or increase the core power. The reduced neutron absorption with aluminum and the lower fuel loading would reduce the maximum-to-average flux ratio in the core. While aluminum is not considered feasible for initial use in the proposed design, it is expected that development of power reactor elements will eventually make the use of some form of aluminum practical for the EOCR.

5.100 Selected Design

A number of properties of the EOCR are listed in Table 5.1A. In general, this table applies to the standard core with the small central loop as shown in Fig. 5.2B. The fluxes in the core are for

the 45 kg loading used in the calculations. With the operational loading of 52 kg (see Section 5.600) the thermal fluxes in the core will be about 15% lower at the start of the cycle. The reactivity requirement and temperature coefficient are given for the reference core of Fig. 5.2A. For the purposes of a conceptual design, Table 5.1A is applicable to the standard core with the proposed initial loading as described in Section 4.000.

Table 5.1A

EOCR SUMMARY

Power, Drivers Only	Mw	40
Cycle Time	Mwd	3360
Epithermal Fissions	%	13
Excess Multiplication Requirements		
Equilibrium Xenon and Samarium	% Δk_{eff}	3.7
Other Fission Products	% Δk_{eff}	2.9
Burnup	% Δk_{eff}	3.8
Xenon Override	% Δk_{eff}	5.0
Total	% Δk_{eff}	15.4
Control Rod Worths		
Inner 4 Rods	% Δk_{eff}	12.4
Outer 8 Rods	% Δk_{eff}	10.2
All 12 Rods	% Δk_{eff}	30.7
Temperature Coefficient	% $\frac{\Delta k_{eff}}{k_{eff}}$ per ^{o}F	-1.5×10^{-5}
Thermal Flux in Drivers, Standard Core		
All Rods Out		
Average	$n/sec\text{-}cm^2$	0.37×10^{14}
Maximum	$n/sec\text{-}cm^2$	1.32×10^{14}
Outer Rods In		
Average	$n/sec\text{-}cm^2$	$.50 \times 10^{14}$
Maximum	$n/sec\text{-}cm^2$	2.27×10^{14}
Fast Flux in Drivers, Standard Core		
All Rods Out		
Average	$n/sec\text{-}cm^2$	1.73×10^{14}
Maximum	$n/sec\text{-}cm^2$	3.11×10^{14}
Outer Rods In		
Average	$n/sec\text{-}cm^2$	2.43×10^{14}
Maximum	$n/sec\text{-}cm^2$	5.31×10^{14}

NOTES: Values are for $500^{o}F$
Fluxes in drivers are for core of Fig. 5.2B with fuel loading of 45 kg.
With 20-Mw operation at $700^{o}F$ the flux values in the drivers are approximately half of those reported above.

Table 5.1A (Continued)

EOCR SUMMARY

Volume		
Unit Cell	cu in.	1,157
	liters	18.96
Fuel Element	cu in.	568
	liters	9.31
Reference Core, 37 Cells	cu in.	43,430
	liters	711.6
Standard Core, 32 Cells	cu in.	37,560
	liters	615.5
Active Height		
Core and Fuel Element	in.	35.5
	cm	90.17
Total Axial Reflector Savings	cm	14
Fuel Loading for Calculations		
Fuel Element	kg of U-235	1.406
Reference Core	kg of U-235	52
Standard Core	kg of U-235	45
Operational Fuel Loading		
Fuel Element	kg of U-235	1.625
Standard Core	kg of U-235	52
Fuel Enrichment	atom % of U-235	93.5
Organic Coolant-Moderator		Santowax R
Metal-Organic Ratio		
Fuel Element Region		0.295
Homogenized Core		0.124

NOTES: Values are for 500°F.
Fluxes in drivers are for core of Fig. 5.2B with fuel loading of 45 kg.
With 20-Mw operation at 700°F the flux values in the drivers are approximately half of those reported above.

5.200 EOCR Core Layouts

Fig. 5.2A shows the reference core used in calculations of reactivity effects and the correlation of one- and two-dimensional calculations. The standard core is shown with two different experimental loadings in Figs. 5.2B and 5.2C. The standard core with the proposed initial loading is discussed in Section 4.000. The PDQ problem numbers shown on the figures are the identification numbers for the two-dimensional calculations. The core arrangements, PDQ problem numbers, and control rod positions are tabulated in Table 5.2A. All control rod worths are determined for the core of Fig. 5.2B. When a control rod is withdrawn, it is equivalent to a driver fuel element and when inserted is black to thermal neutrons. Except as noted in Table 5.2A all control rods are withdrawn.

Table 5.2A

EOCR CORE ARRANGEMENTS

Core Arrangement	Figure Number	PDQ Problem Number	Control Rods Inserted
Reference	5.2A	11-1	None
Standard, small loop	5.2B	12-1	None
Standard, small loop	5.2B	12-2	4 Inner Rods
Standard, small loop	5.2B	12-3	8 Outer Rods
Standard, small loop	5.2B	12-4	All 12 Rods
Standard, large loop*	5.2C	14-1	None
Standard, large loop	5.2C	14-2	None

*4 Elements marked R in Figure 5.2C removed.

The experimental loadings used for the calculations must be considered as only typical. To make these loadings realistic the fuel tests and the power-reactor-type fuel elements are similar to those proposed for power reactors.[1] In all cases the fuel enrichment has been changed to 7.5% for the EOCR calculations. The stainless steel surrounding the test experiments was similar to the loop description given in Section 8.000.

5.300 Flux and Power Distributions

5.310 Distributions in Driver Fuel Elements

5.311 Overall Core Distributions. The neutron flux distributions have been obtained for a number of cores from the two-dimensional PDQ calculations and are shown in Figs. 5.3A through 5.3F.

---

1. Bechtel Corporation and Atomics International, "Organic Cooled Power Reactor Study - 300 Mw Power Plant Conceptual Design", Report TID-8501 (Part 2), July 1959.

The flux values are for the horizontal midplane and for a power of 40 Mw with a fuel loading of 45 kg of U-235 in the drivers. The cores for which the flux distributions are determined are shown in Figs. 5.2A, -B, and -C.

All of the flux plots are for the thermal-neutron group except that of Fig. 5.3F which shows the fast-group flux. The flux plots are taken along the center line except in Figs. 5.3C, -D, and -F, which are taken along a diagonal. Fig. 5.3D concerns the case in which the outer eight control rods are inserted, and the high thermal flux peaking in the center can be seen in the flux plot.

5.312 Flux Distribution Within an EOCR Cell. The one-dimensional thermal-flux distribution across a single cylindrical cell is used to make the corrections in the thermal-group constants, described in Section 14.100, because the driver assemblies are not in a close-packed array. A cylindrical P_3 transport-theory code is used to obtain this distribution in one dimension. Fig. 5.3G shows this flux plot along with one obtained using one-dimensional diffusion theory. These are both normalized to unity at the fuel region boundary. From these curves one can see how much more the P_3 transport theory accounts for the flux dipping in the fuel region and peaking in the moderator region. A further illustration of this is the maximum-to-average flux ratios in the fuel region, which for the P_3 flux is 1.92 whereas for the diffusion theory is only 1.58. A thermal-flux contour map for the cell has been obtained from the two-dimensional PDQ reference core, shown in Fig. 5.2A problem No. 11-1. The driver assembly chosen is located on the diagonal, one element off center. This map is shown in Fig. 5.3H. The fluxes shown are mid-plane values, with the power normalized to 40 Mw in the driver assemblies.

5.320 Power-Density Distribution in Fuel Test Positions. The power densities have been obtained for the loop positions from the two-dimensional PDQ problems and are shown in Table 5.3A. These power densities are given for all core arrangements studied which contained loops. This table also gives the power densities in the peripheral power-reactor elements which were in the control rod study problems 12-1, 12-2 and 12-3. Table 5.3B lists the fission power generated in the loops. The maximum powers and power densities given include both the vertical and horizontal peaking factors.

All of the above information applies to experiments with a fuel enrichment of 7.5%. The effect on the power generation of varying the enrichment has been studied for a large loop in the center of a one-dimensional cylindrical representation of the EOCR core. Except for enrichment the loop is identical with that described in Section 4.000. The power density in the test versus fuel enrichment is shown in Fig. 5.3I.

Table 5.3A

POWER DENSITY IN LOOPS WITH 40-MW OPERATION
(watts/cc)

PDQ Problem Number*		12-1	12-2	12-3	14-1	14-2
Small Center Loop	Avg.	245	123	430	----	----
	Max.	425	207	740	----	----
Large Center Loop	Avg.	----	----	----	178	146
	Max.	----	----	----	341	281
Large Off-Center Loop	Avg.	113	114	143	137	119
	Max.	300	270	385	330	284
Small Off-Center Loop	Avg.	138	118	182	168	137
	Max.	211	218	300	361	220
Peripheral Power Reactor Assembly	Avg.	83	108	62	----	----
	Max.	281	417	231	----	----

*See Table 5.2A for core arrangements corresponding to PDQ problem numbers.

Table 5.3B

TOTAL MEGAWATTS OF POWER GENERATED IN LOOPS
WITH 40-MW OPERATION

PDQ Problem Number*	12-1	12-2	12-3	14-1	14-2
Small Center Loop	.46	.23	.81	----	----
Large Center Loop	----	----	----	2.26	1.85
Large Off-Center Loop	1.44	1.45	1.82	1.74	1.51
Small Off-Center Loop	.26	.22	.34	.32	.26
Peripheral Power Reactor Assembly	1.42	1.84	1.06	----	----

*See Table 5.2A for core arrangements corresponding to PDQ problem numbers.

The power generation increases monotonically with enrichment, but the rate of increase rapidly becomes smaller. The power density can be increased by about 25% by increasing the enrichment from 7.5% to about 13.5%. Further increase in enrichment produces only a small increase in power density.

Some of the calculations on alternate cores described in Section 11.000 used 2.5%-enriched fuel, and these power densities should be multiplied by 1.9 for comparison with the values of Table 5.3A.

Table 5.3C gives the power densities attainable in a large central loop with three different enrichments and with the four central control rods withdrawn and eight peripheral control rods inserted, i.e., corresponding to PDQ problem 12-3. These power densities were developed by adjustment of values obtained in PDQ problem 14-2 with appropriate factors obtained from problems 12-1 and 12-3 and from Fig. 5.3I.

Table 5.3C

POWER DENSITY IN LARGE CENTER LOOP AT 40 MW

Fuel Enrichment	Power Density, watts/cc	
	Average	Maximum
2.5%	135	260
7.5	257	495
13.5	320	620

Table 5.3D presents estimates of the power densities obtainable in power-reactor-type fuel elements not in a loop at a reactor power of 20 Mw. Removal of the stainless steel in the loop from around the test element increases thermal flux in the test per megawatt of core power by about 50%.

Table 5.3D

POWER DENSITY IN CENTER POSITION (NO LOOP) AT 20 MW

Fuel Enrichment	Power Density, watts/cc	
	Average	Maximum
2.5%	101	195
7.5	192	372
13.5	240	465

5.330 Neutron and Gamma Fluxes in Organic Test Positions. The neutron fluxes in the organic test positions, shown in Figs. 5.2B and -C, have been obtained from two-dimensional PDQ calculations. These are presented in Table 5.3E where the maximum-to-average ratios include both the horizontal and vertical peaking factors.

Table 5.3E

NEUTRON FLUXES IN ORGANIC TEST LOOPS

		Neutron Fluxes x 10^{-14}				
PDQ Problem Number*		12-1	12-2	12-3	14-1	14-2
Fast	Avg.	1.88	.81	3.19	2.78	2.31
	Max./Avg.	1.50	1.67	1.48	1.46	1.46
Thermal	Avg.	.82	.31	1.38	1.00	.83
	Max./Avg.	1.85	2.23	1.89	1.62	1.62

*See Table 5.2A for core arrangements corresponding to PDQ problem numbers.

Local gamma-heating varies considerably depending upon control rod configuration and experiments in the core; however, detailed calculations are not necessary for the conceptual design. The values obtained from the limited calculations performed indicate that design objectives can be met. They also provide a basis for the design of experiment-loop pressure tubes. The rate of energy transfer to the organic by fast neutrons is found by taking the product of the fast flux at a point and the removal cross section and assuming that each neutron loses 2 Mev on being transferred from the fast to the slow group. Table 5.3F presents midplane gamma and neutron heating in the organic in test loops at three locations in the core of Fig. 5.2C.

Table 5.3F

HEATING RATES IN ORGANIC

Location	Neutron Heating Rate w/g	Gamma Heating Rate w/g	Total Heating Rate w/g	Ratio Neutron-Gamma
Center	2.9	8.6	11.5	0.34
4 In. Off Center	2.6	10.0	12.6	0.26
Core Boundary	0.2	3	3.2	0.07

For investigations on the mechanisms of radiation damage to organics it is desirable to vary the ratio of neutron-to-gamma power density over a wider range than shown by Table 5.3F. This variation can be achieved by placement of the organic test in a region where the composition of the surrounding medium can be controlled. If the test is surrounded by a moderator, the fast neutron flux is drastically reduced, whereas the effect on the gamma flux is small, and the ratio of neutron-to-gamma power density in the test is low. Placement of a metal of relatively high atomic number around the test will keep the fast-neutron flux high while attenuating the gamma flux more severely and thus yield a higher neutron-to-gamma power density ratio.

5.340 Gamma Heating in the Reactor Structure, Vessels, Thermal and Biological Shielding. The basic objective of this section is to provide gamma-heating data for the design of the reactor structure, vessels, thermal shields, and biological shielding. Since it is proposed that the EOCR will be used for the experimental operation of low enrichment power reactor cores, the design premises used to determine gamma heating in this section are that a low-enrichment core operates at 220 Mw with 1.85% uranium as fuel; the core is 4.5-ft.high and 4-ft in diameter; the organic moderator temperature is 600°F; and the critical mass is 118 kg of U-235. Since the average power density of this core is approximately twice that of the standard core, it is evident that if the neutron and gamma shielding are to be adequate for both cores, it must be designed to meet the requirements of the power reactor core. Since neutron flux distributions have not yet been calculated for the power reactor core, upper-limit estimates of the required neutron and gamma shielding are considered satisfactory for the conceptual design. Several important factors contribute to the "approximate nature" of the shielding requirements as they are considered here.

1. The critical mass and flux levels of the power reactor core have been estimated by elementary considerations. The general properties of the core, such as metal-organic ratio, were based on the Piqua OMR.

2. Since detailed multigroup fluxes are not available for the reflector and shield regions, simple models have been used to determine the capture-gamma production levels in the reflector and thermal shields.

3. Energy-dependent buildup factors for the complex mixtures of core materials and heterogeneous shielding have been estimated because little data are available concerning organic-metal mixtures, and time would not permit separate studies of this nature.

As stated previously the approximations made were governed by a desire to predict the maximum gamma heating levels to be expected at various points in the reactor structure vessel, thermal shields, and biological concrete. Fig. 7.1C indicates the geometry of the reactor structure vessels and thermal shields in relation to the core and biological shielding. It was determined that three one-inch-thick steel thermal shields would reduce the gamma and neutron heating in the reactor pressure vessel to permissible levels. Furthermore, it was determined that a three-inch-thick lead shield exterior to the pressure vessel would be necessary to reduce the gamma heating in the concrete biological shield to a permissible limit. The calculated heating levels in the various structural members are given in Table 5.3G.

Table 5.3G

HEATING LEVELS IN STRUCTURAL MEMBERS

Structural Member	Heating Level, w/g
Inner Reactor Tank	0.37
Reactor Pressure Vessel	0.025
Lead Shielding	0.03
Biological Concrete	0.00014

Table 5.3H lists the heating which was determined in the structural members listed above for 220-Mw operations. The table gives the contribution to the gamma heating in the various structural members from the gamma flux arising in three separate regions of the reactor: (1) flux from the core proper, (2) flux originating in the reflector, and (3) flux originating in the shielding region. Four discrete average energies were chosen as representative of all of the gamma rays arising in the reactor. This division is also indicated in Table 5.3H. No fast-neutron heating in the structure vessels and concrete is indicated because it was determined that this is negligible in comparison with the gamma heating rates.

A general discussion of the gamma-heating calculations and the approximations used is given in Section 14.400.

Table 5.3H

BREAKDOWN OF GAMMA HEATING IN STRUCTURAL MEMBERS AND SHIELDS

Energy Group Mev	Gamma Flux from Indicated Source w/cm^2				Total Gamma Heat, w/g
	Core	Reflector	Shield	Total	
	0.5-in. Inner Reactor Tank				
1	4.2			4.2	0.109
2.2		3.6	0.075	3.7	0.078
3	3.8			3.8	0.080
7	0.43		4.0	4.4	0.105
Total					0.372
	1.25-in. Steel Reactor Pressure Vessel				
1	0.12	0.25	0.0018	0.37	0.0096
2.2					
3	0.31			0.31	0.0065
7	0.08		0.30	0.38	0.0091
Total					0.0252
	Concrete Beyond 3-in. Lead Shield				
1					
2.2		0.0025		0.0025	0.000053
3	0.002			0.002	0.00004
7	0.0002		0.0017	0.0019	0.000046
Total					0.00014

5.400 Temperature Coefficient

The EOCR temperature coefficient of reactivity for the reference core, Fig. 5.2A, has been calculated by finding k_{eff} at a number of temperatures and plotting the results as shown in Fig. 5.4A. The temperature coefficient is defined as $(1/k_{eff})\ (dk_{eff}/dT)$ and is shown as a function of temperature in Fig. 5.4B. The derivatives have been determined graphically from Fig. 5.4A. The calculations of k_{eff} have been made for an equal-area cylindrical model using two-neutron-group diffusion theory. Corrections have been made at each temperature for flux depression effects in the heterogeneous core as described in Section 14.111.

The temperature coefficient calculated is that for a slowly varying isothermal change in temperature throughout the core and reflector. The expansion of the core and the change of the axial reflector savings with temperature were neglected. The calculation was made for Santowax R without high boiler residue.

Core arrangements which substantially increase the amount of moderator in the core above that for the reference core have a temperature coefficient more positive than shown by the calculations. Placement of a number of power reactor elements on the periphery of the core introduces a positive component because of the reduced leakage, but if these elements are close-packed there is a compensating negative effect.

The positive component of the temperature coefficient in the spaced lattice of the EOCR arises largely from the presence of moderator between the fuel elements. In a rapid transient the heating is confined mainly to the fuel element region, and the transient temperature coefficient is negative. No calculations have been made for this effect for the EOCR. Studies on the AETR in which the temperature is changed only in the region occupied by the fuel element give a value of -1.3×10^{-4} $(\Delta k_{eff}/k_{eff})/^{\circ}F$ as compared with $+3.3 \times 10^{-5}$ for the isothermal coefficient.[1] Thus, the temperature coefficient can be expected to give more protection against transient power increases in the EOCR than indicated by the isothermal value.

Since the temperature coefficient is the result of the difference between positive and negative effects, a satisfactory calculation is quite difficult. Until the variations with temperature of the age and other constants are better known, it is doubtful if consideration of the neglected effects and the use of more exact methods can be justified in the sense that significantly more confidence can be placed in results that have not been verified experimentally.

The calculated value of the temperature coefficient meets the requirement of being negative at the operating temperature of $500^{\circ}F$. However, the calculated magnitude of about 1.5×10^{-5} $(\Delta k_{eff}/k_{eff})/^{\circ}F$ is not sufficient to assure that the actual temperature coefficient in the EOCR will be negative. The most practical method of making the

---

1. D. R. deBoisblanc, "An Advanced Engineering Test Reactor Complex", Report IDO-16555, September 30, 1959.

coefficient more negative is probably to decrease the spacing between fuel elements by decreasing the center-to-center distance of the lattice. Holding the lattice constant and increasing the size of the fuel element is not quite as effective. Some further discussion of the effect of the lattice structure on the temperature coefficient is given in Section 14.300.

5.500 Excess Multiplication Requirements

5.510 Effective Multiplication Factors. The effective multiplication factors, k_{eff}, of a number of EOCR cores are tabulated in Table 5.5A. All values are for a temperature of 500°F. The designations 1D and 2D indicate whether the calculations were made with a one- or with a two-dimensional model. The terms P_3 and P_1 corrections refer to the corrections described in Section 14.111 and are applicable only to one-dimensional calculations. S.L. indicates a small central loop, L.L. a large central loop. Except as indicated for the cases with a small central loop all control rods are completely withdrawn.

Table 5.5A

EOCR EFFECTIVE MULTIPLICATION FACTORS

Core	Figure Number	PDQ Number	Remarks	k_{eff}
Reference	5.2A	11-1	2D	1.225
Reference	5.2A	----	1D, P_1 and P_3 Corrections	1.188
Reference	5.2A	----	1D, P_3 Correction Only	1.192
Standard, S.L.	5.2B	12-1	2D, All Rods Out	1.173
Standard, S.L.	5.2B	12-2	2D, 4 Inner Rods In	1.049
Standard, S.L.	5.2B	12-3	2D, 8 Outer Rods In	1.071
Standard, S.L.	5.2B	12-4	2D, 12 Rods In	0.866
Standard, L.L.	5.2C	14-1	2D, 4 Elements Removed	1.112
Standard, L.L.	5.2C	14-2	2D	1.142

NOTES: S.L. indicates a small central loop in the core.
L.L. indicates a large central loop in the core.

5.520 Addition of Thermal Neutron Absorber. The change in k_{eff} produced by addition of a thermal neutron absorber is found by changing the value of Σ_{2a}, the thermal absorption cross section, in the calculation of reactivity of the homogenized EOCR reference core. The results are shown in Fig. 5.5A. This procedure gives the effect of adding a poison uniformly throughout the core. This makes the poison about twice as effective on a cross section basis as if it were distributed uniformly in the fuel elements only. The curve of Fig. 5.5A is used to find the reactivity effects produced by the formation of fission products. The

effects of added poison are found by subtracting k_{eff} for the poisoned core from that for the clean core and are given in terms of Δk_{eff} or excess multiplication rather than in reactivity.

5.530 Equilibrium Xenon and Samarium. The excess multiplication requirement for xenon and samarium is estimated to be 3.7%. This value is found by computing the equilibrium concentration of xenon and samarium atoms in a medium having the same U-235 atom concentration as the EOCR driver elements and a uniform thermal flux equal to the average flux in the EOCR reference core operating at 40 Mw. The thermal cross section resulting from the formation of xenon and samarium is found and the reactivity loss obtained from Fig. 5.5A. The reactivity loss to equilibrium xenon and samarium varies slowly with the thermal flux level and is quite well known for operating reactors. As the loss in the MTR is 4.9% at 30 Mw, the value quoted for the EOCR can hardly be in error by more than 1% of excess multiplication.

5.540 Other Fission Products. The amount of poisoning from fission products other than xenon and samarium is obtained from a report by J. W. Webster.[1] While the exact value depends on the flux in the core, this dependence is sufficiently small to be neglected as can be seen by comparing the values for the same number of megawatt-days at 30- and 300-Mw core power in the Webster report. Approximately 480 cm^2 of poison from low-cross-section fission products is formed in the EOCR core during a cycle. Assuming this to be homogenized throughout the fuel elements the added cross section is 0.0014 cm^{-1}, and the excess multiplication requirement is 2.9%.

The formation of the low-cross-section fission products is based on a uniform flux in the core, and this procedure is known to underestimate the reactivity effect. However, taking the change in k_{eff} from Fig. 5.5A with the assumption of a uniform distribution of poison throughout the core while assuming that the fission products are confined to the fuel elements provides a correction that should prevent the final estimate from being seriously in error.

5.550 Xenon Override. The excess multiplication requirement above equilibrium for xenon override is shown as a function of time in Fig. 5.5B. The xenon cross section is calculated assuming a uniform flux distribution in the EOCR after operation at 40 Mw until xenon equilibrium is obtained and neglecting the effect of fuel burnup. Standard differential equations are used to obtain the xenon concentration as a function of time after shutdown.[2] The xenon cross section includes the non 1/v contribution at 500°F. The excess multiplication requirement is then found in Fig. 5.5A. The assumption of a uniform flux is known to substantially underestimate the reactivity loss during the xenon transient. The xenon atom concentration was calculated for a

1. J. W. Webster, "The Low Cross Section Fission Product Poisons", Report IDO-16100, (1953).
2. S. Glasstone and M. C. Edlund, "The Elements of Nuclear Reactor Theory", Ch. XI, D. Van Nostrand, New York, (1952).

homogeneous core, and Fig. 5.5A does not provide a correction. Comparison of calculated and measured xenon transients in the MTR indicates the peak loss to xenon in the EOCR may be about 10% instead of 5.6% as shown in Fig. 5.5B. Provision of 5% excess multiplication for xenon override should permit two hours for startup at any time during the cycle even allowing for effects of non-uniform xenon formation.

5.560 Burnup Requirement and Cycle Time. The cycle time is selected on the basis of using three cores a year while operating at a power of 40 Mw with a 70% duty cycle. Thus, there are 3360 Mwd per cycle. It is assumed that 1.25 g of U-235 are consumed per Mwd. This value is compatible with MTR experience and is satisfactory for the purposes of estimating EOCR fuel burnup. The burnup of fuel is 4.2 kg of U-235 per cycle and this value can be considered quite reliable. The burnup of fuel is greater in positions of high statistical weight than in those of low weight. As a result considerably more fuel must be added to yield the desired fuel cycle than is consumed. Experience with the MTR indicates that a factor of 1.7 should be applied. This is of course only approximate but should make the estimates of fuel and excess multiplication requirements realistic. Thus, 7.1 kg is the estimated fuel to be added for burnup. Fig. 5.5C shows the variation of k_{eff} with fuel content. From this a value of 3.8% is found for the excess multiplication requirement for burnup. A precise calculation of the cycle time for a given fuel loading is quite difficult and must consider the effect of the experimental loading. However, neither the uranium concentration in the fuel meat nor the reactivity requirement limits a substantial increase in the fuel loading, and there should be no serious problem in obtaining an adequate cycle.

The amount of the fuel loading that is burned in a cycle is approximately 8%. This is quite low, and it may eventually be desirable to use a mixed loading of new and used fuel elements in a manner similar to the MTR to increase the burnup. The development of fuel elements in which a substantial amount of the stainless steel is replaced with aluminum will permit a significant increase in the per cent of fuel burnup per cycle.

5.570 Effect of Water Flooding. The organic in the EOCR is replaced with water when changes are made in the core, and the change in k_{eff} produced by the substitution must be considered. This effect has been investigated for the alternate design using circular fuel elements on a hexagonal lattice, described in Section 11.000. On changing from Santowax R at 500°F to water at 70°F the effective multiplication factor decreased from 1.189 to 1.164. This occurs because of the increased absorption in hydrogen resulting from the increased hydrogen atom density and flux peaking between elements. It is expected that at some intermediate hydrogen density, at the 350°F temperature of the water-flooding operation, with a mixture of organic and water the value of k_{eff} may be higher than with either material alone. However, the shutdown k is so great that the calculation of reactivities for the system at 350°F with various mixtures of Santowax R and water is not necessary for the conceptual design.

5.580 Control Rod Worths. The EOCR has 12 control rods. When a rod is completely withdrawn, it has a section in the core that is equivalent to a driver fuel element. When a rod is completely inserted, it has a section in the core that is black to thermal neutrons. The control rod worths have been determined for the core of Fig. 5.2B. The worth of a group of rods is expressed as the difference in k_{eff} with all rods withdrawn and with the designated rods inserted. The values of k_{eff} are determined by two-dimensional calculations. The poison sections of the inserted rods are represented by imposing a boundary condition that makes the slope of the thermal flux equal to that produced by a black rod.

The worths are summarized in Table 5.5B.

Table 5.5B

CONTROL ROD WORTHS

Inserted Rods	Worth $\% \Delta k_{eff}$	Worth Per Rod $\% \Delta k_{eff}$
Inner 4	12.4	3.10
Outer 8	10.2	1.28
All 12	30.7	2.56

5.590 Summary, Excess Multiplication. The excess multiplication requirements at 500°F are tabulated in Table 5.5C.

Table 5.5C

EXCESS MULTIPLICATION REQUIREMENTS FOR THE EOCR AT 500°F

Source of Reactivity Loss	$\% \Delta k_{eff}$
Equilibrium Xenon and Samarium	3.7
Other Fission Products	2.9
Fuel Burnup	3.8
Xenon Override	5.0
Total	15.4

Since the required available excess multiplication of the core at 500°F is 15.4%, the total worth of the control rods of 30.7% is ample for control and provides an adequate shutdown capability. The standard core with the small loop in the center has a value of 17.3% for the excess multiplication as computed for a two-dimensional model. Two

corrections are made to this value to bring the predicted k_{eff} into better agreement with experiment as determined by Atomics-International measurements on OMRE. Comparison of the k_{eff} for the reference core as computed by one- and by two-dimensional methods indicate that about 3.7% should be subtracted from the two-dimensional value. Comparison of calculated and measured values for the OMRE, as described in Section 14.200, show that 1.8% should be subtracted as an additional correction. The available excess reactivity of the standard core is 11.8% after these corrections are made. The addition of fuel to increase this value to 15.4% as required is discussed in Section 5.600.

5.600 Fuel Loading

In order to reduce the number of computations all investigations have been made with a fuel loading equivalent to 45 kg of U-235 in 32 fuel elements, and a correction is necessary to increase the fuel loading to bring k_{eff} to the value required for an operational loading. The reference core with 37 fuel elements contains approximately 52 kg of U-235. The required k_{eff} at 500°F is calculated as 1.154 while the standard core of Fig. 5.2B had a k_{eff} of 1.118 after the corrections described in Section 5.590 are made. From Fig. 5.5C an increase of 7 kg of U-235 is found to be necessary to bring k_{eff} to the desired value. This increase makes the fuel loading of the standard core 52 kg of U-235. The correction is, of course, only approximate but should make a significant improvement in the estimate of the required fuel.

The initial fuel loadings can be adjusted by the addition or removal of fuel elements in the core. Subsequent loadings can be altered by varying the amount of fuel in an element. The fuel loading of a test reactor is dependent upon the experimental loading, and even a very accurate calculation will probably not determine the loading that is eventually used. Operating experience is usually required to determine the most satisfactory loading as has been the case with both the MTR and ETR.

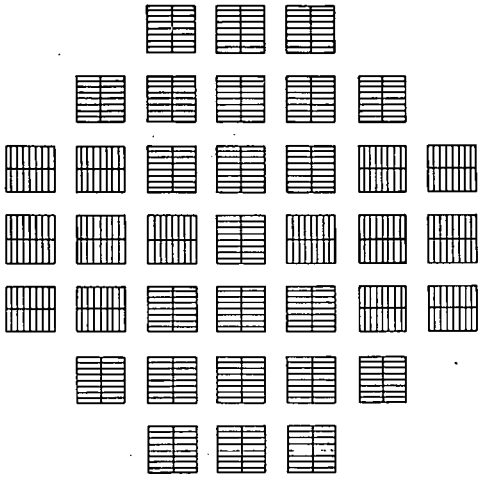

PDQ PROBLEM NUMBER 11-1

FIG. 5.2 A
REFERENCE CORE

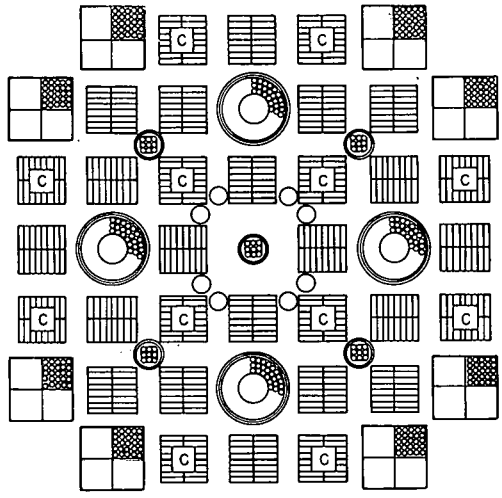

PDQ PROBLEM NUMBERS 12-1, 12-2, 12-3, 12-4

FIG. 5.2B
STANDARD CORE SMALL CENTRAL LOOP

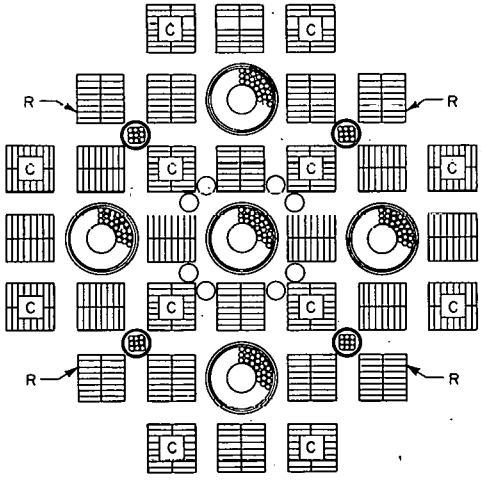

PDQ PROBLEM NUMBERS 14-1, 14-2

FIG. 5.2C
STANDARD CORE LARGE CENTRAL LOOP

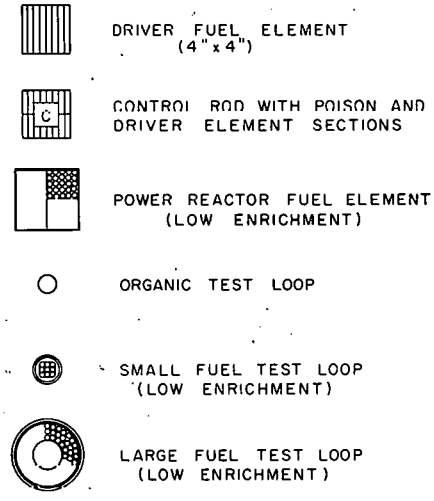

LEGEND

PPCo.-C-2503

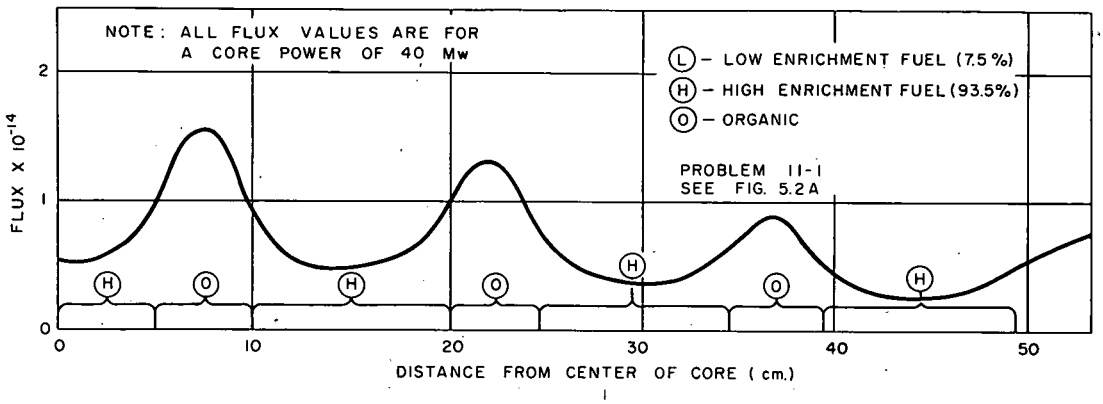

FIG. 5.3 A

MIDPLANE THERMAL FLUX ALONG CENTERLINE
EOCR REFERENCE CORE

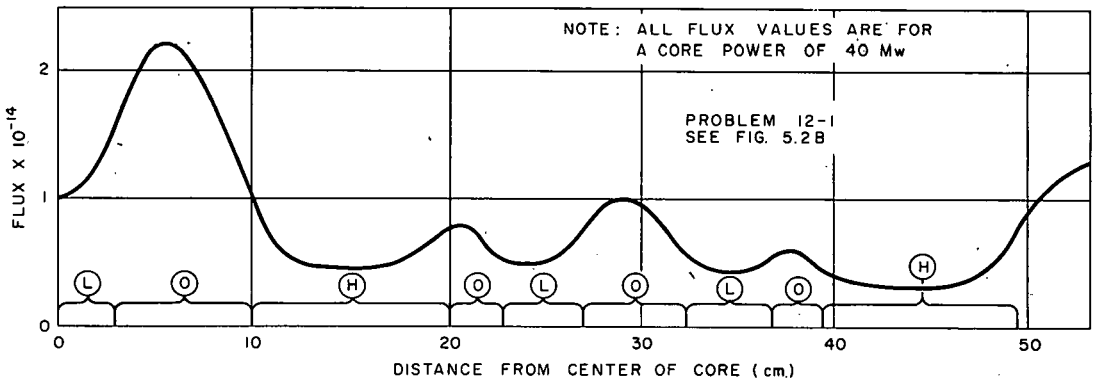

FIG. 5.3 B

MIDPLANE THERMAL FLUX ALONG CENTERLINE
EOCR STANDARD CORE WITH SMALL LOOP
ALL RODS WITHDRAWN

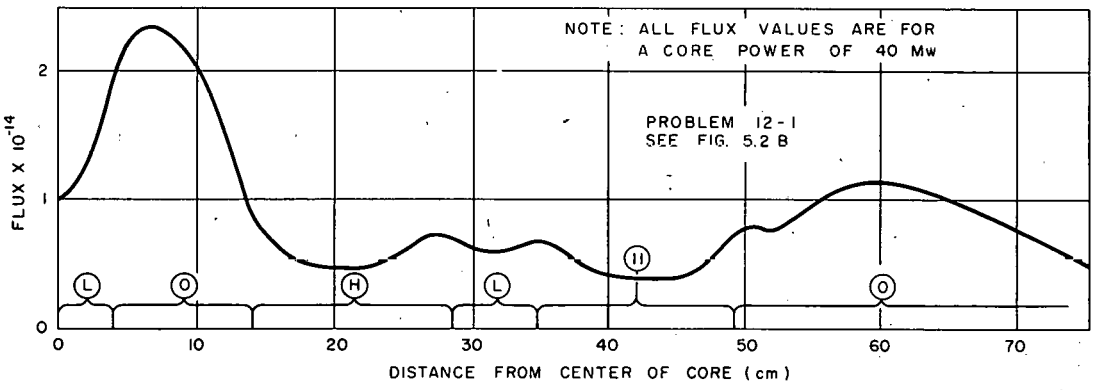

FIG. 5.3 C

MIDPLANE THERMAL FLUX ALONG DIAGONAL
EOCR STANDARD CORE WITH SMALL LOOP
ALL RODS WITHDRAWN

PPCo.-C-2504

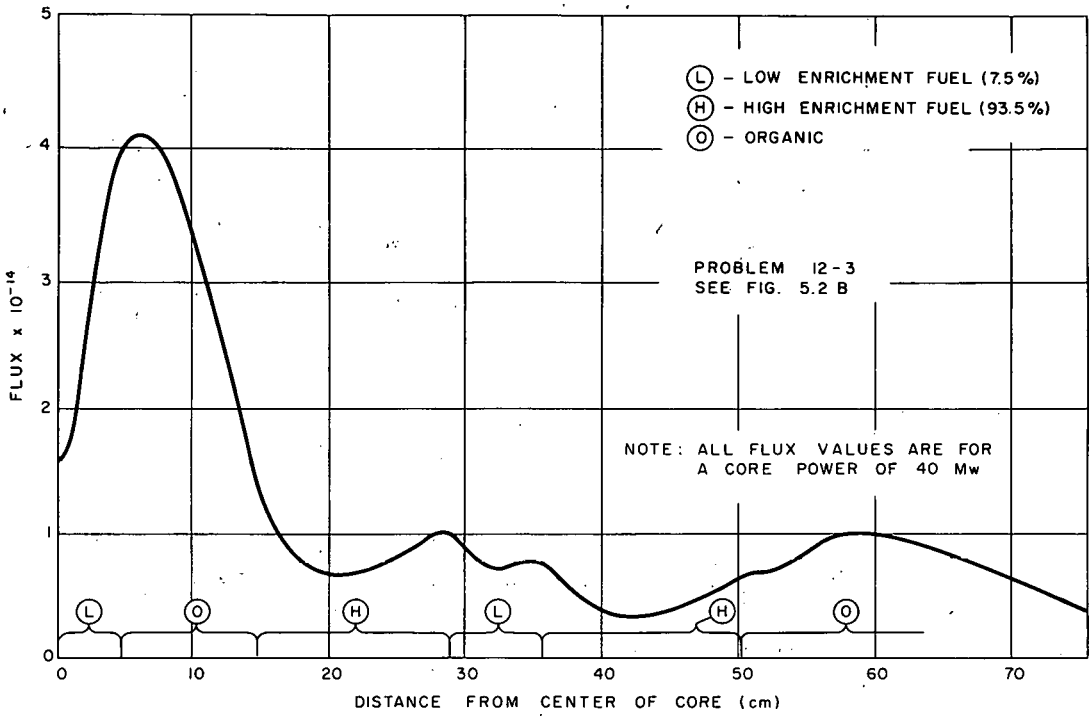

FIG. 5.3 D

MIDPLANE THERMAL FLUX ALONG DIAGONAL
EOCR STANDARD CORE WITH SMALL LOOP
8 OUTER RODS INSERTED

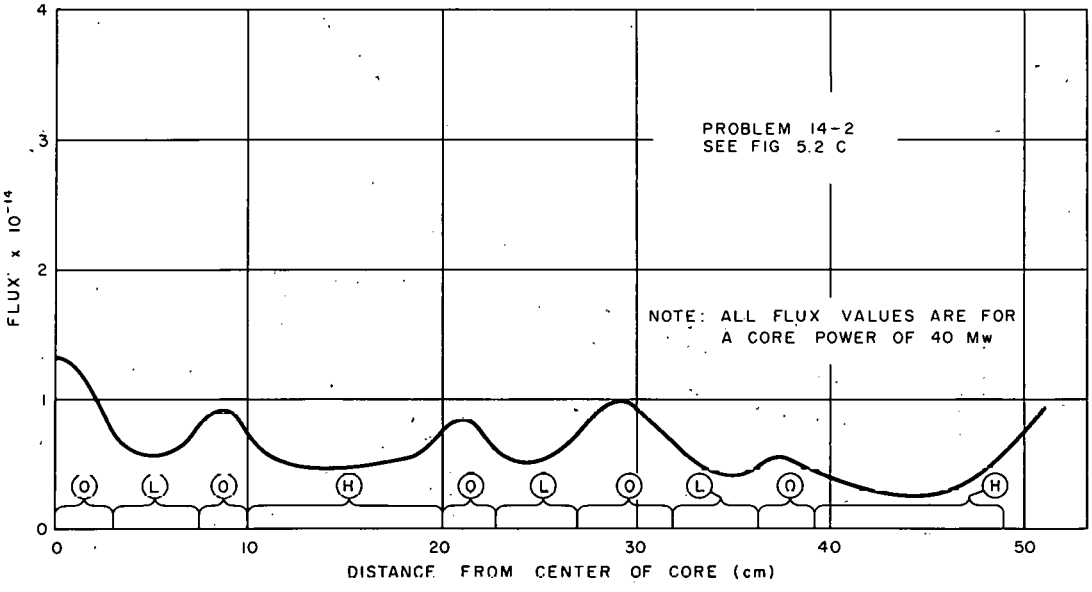

FIG. 5.3 E

MIDPLANE THERMAL FLUX ALONG CENTERLINE
EOCR STANDARD CORE WITH LARGE LOOP

PPCo.-C-2505

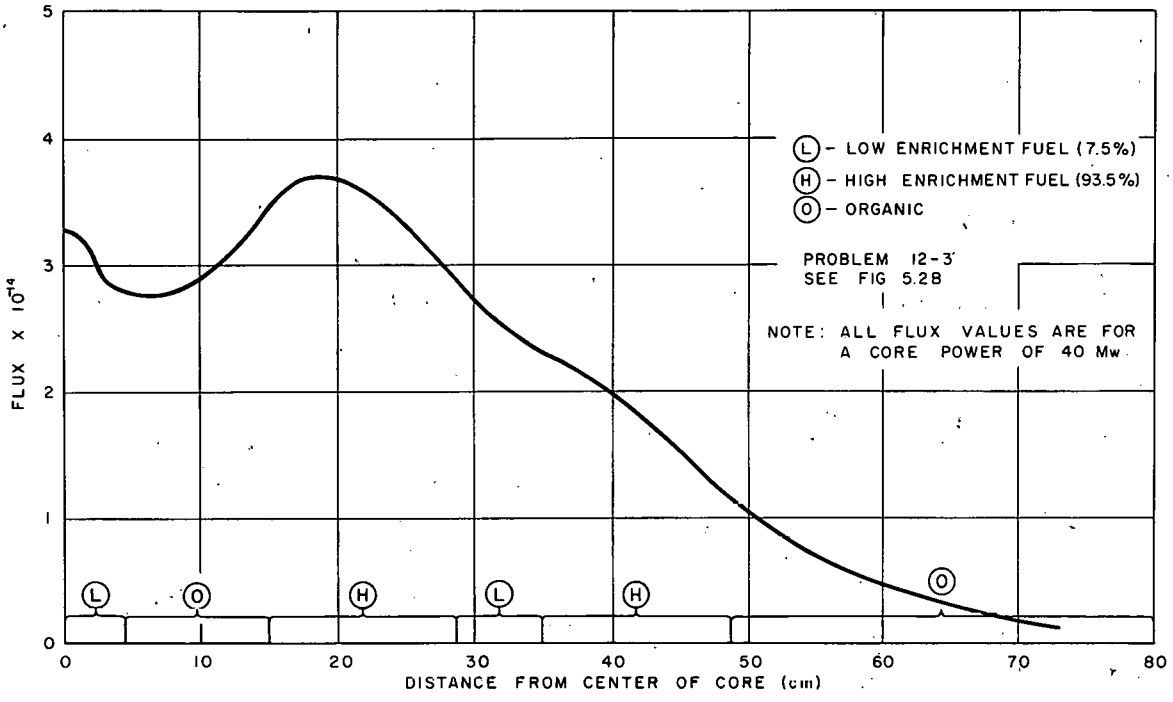

FIG. 5.3 F

MIDPLANE FAST FLUX ALONG DIAGONAL EOCR STANDARD CORE WITH SMALL LOOP, 8 OUTER RODS INSERTED

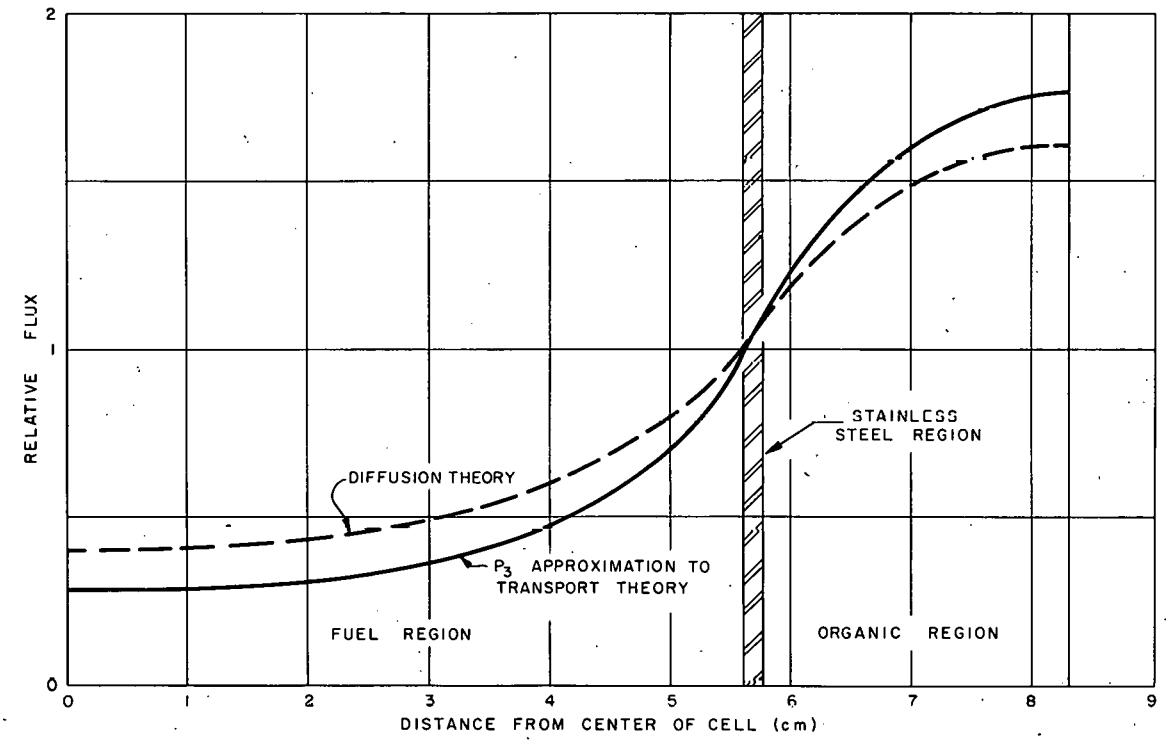

FIG. 5.3 G

THERMAL FLUX ACROSS AN EOCR CELL, COMPARISON OF DIFFUSION AND TRANSPORT THEORY

PPCo.-C-2506

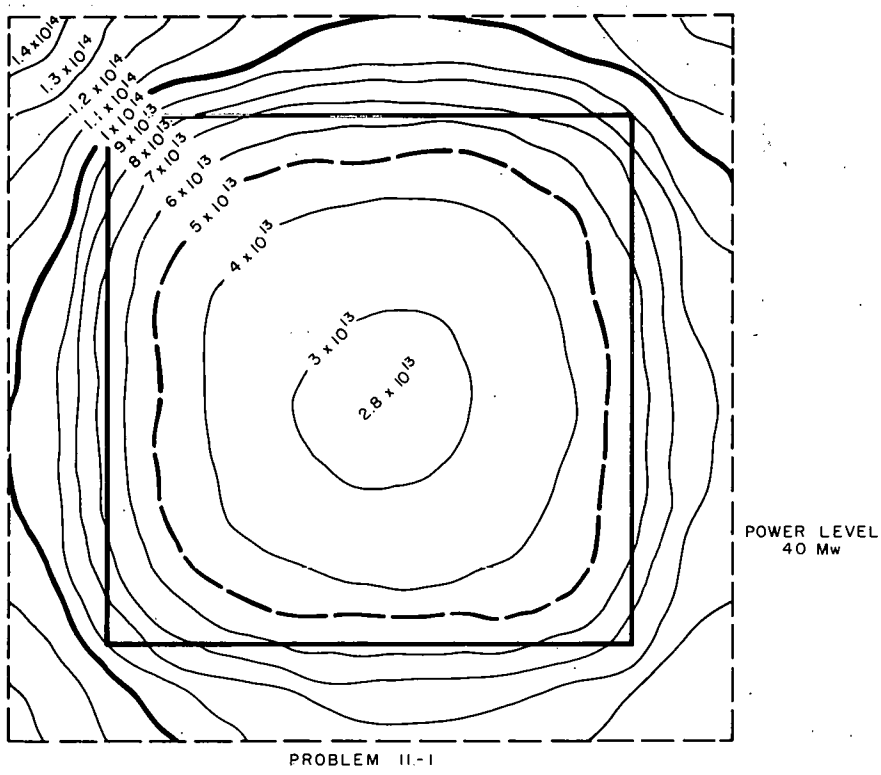

FIG. 5.3 H

THERMAL-FLUX CONTOUR MAP FOR AN OFF-CENTER, ON-DIAGONAL FUEL ELEMENT IN THE EOCR REFERENCE CORE

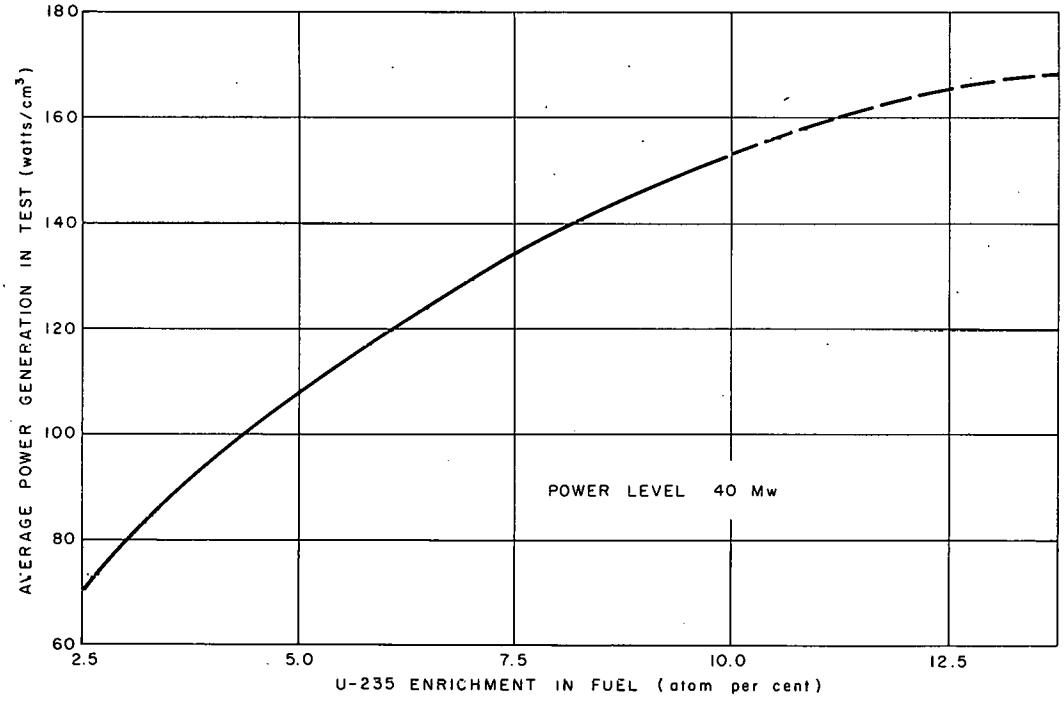

FIG. 5.3 I

FISSION POWER DENSITY VS. U-235 ENRICHMENT IN EOCR LARGE FUEL TEST LOOP

PPCo.-C-2507

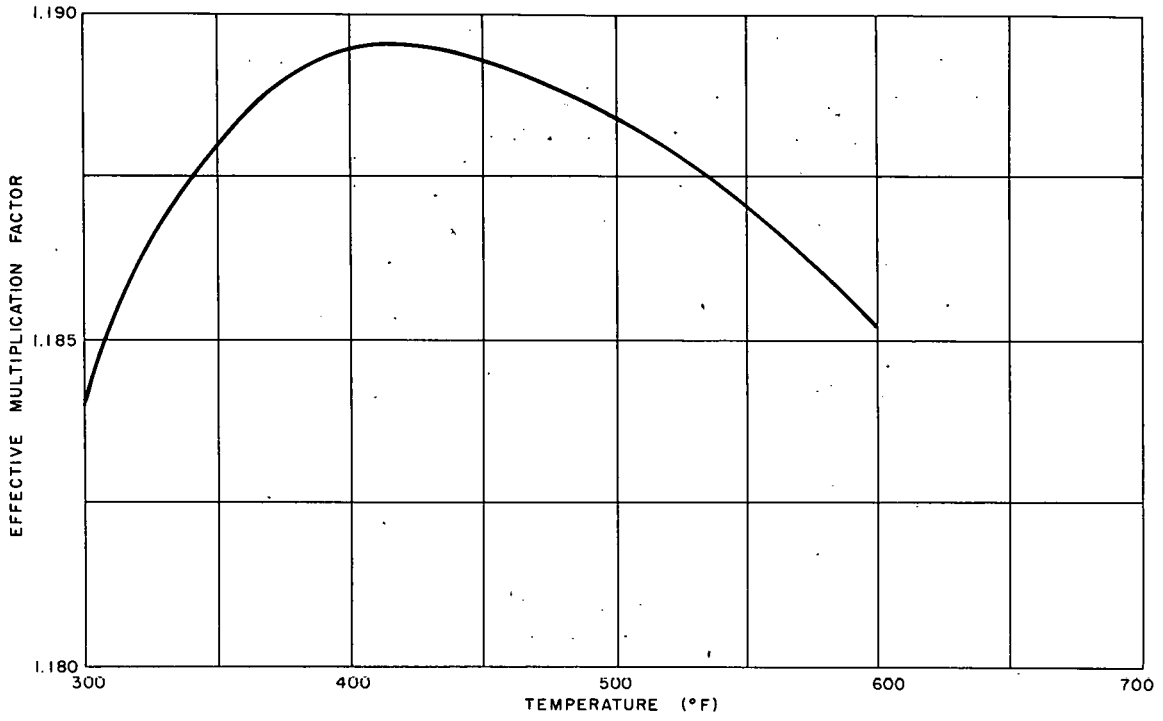

FIG. 5.4 A

EFFECTIVE MULTIPLICATION FACTOR VERSUS TEMPERATURE
EOCR REFERENCE CORE

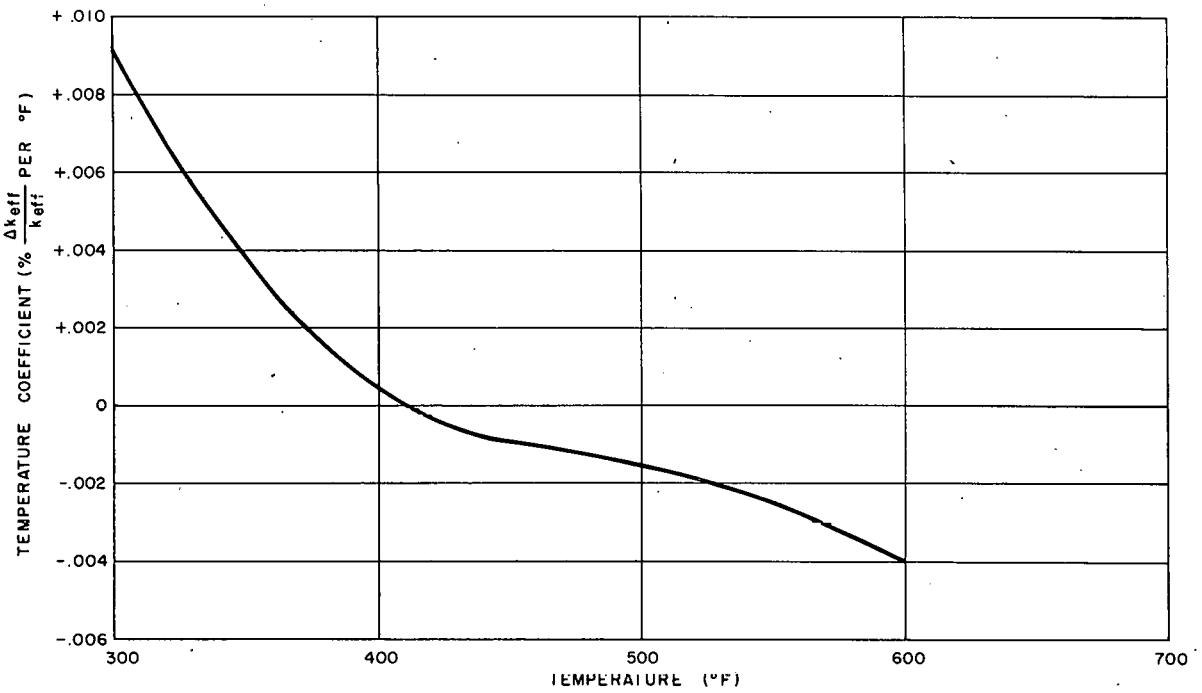

FIG. 5.4 B

TEMPERATURE COEFFICIENT
EOCR REFERENCE CORE

PPCo.-C-2508

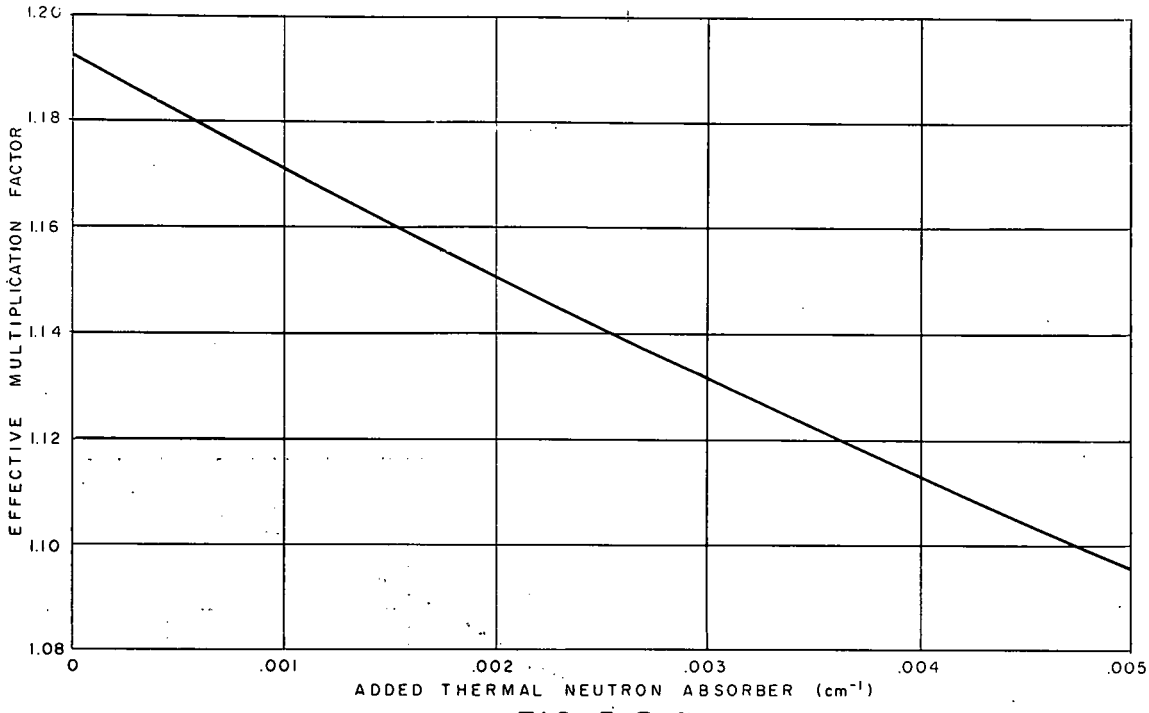

FIG. 5.5 A

EFFECTIVE MULTIPLICATION FACTOR VERSUS ADDED THERMAL NEUTRON ABSORBER E O C R REFERENCE CORE

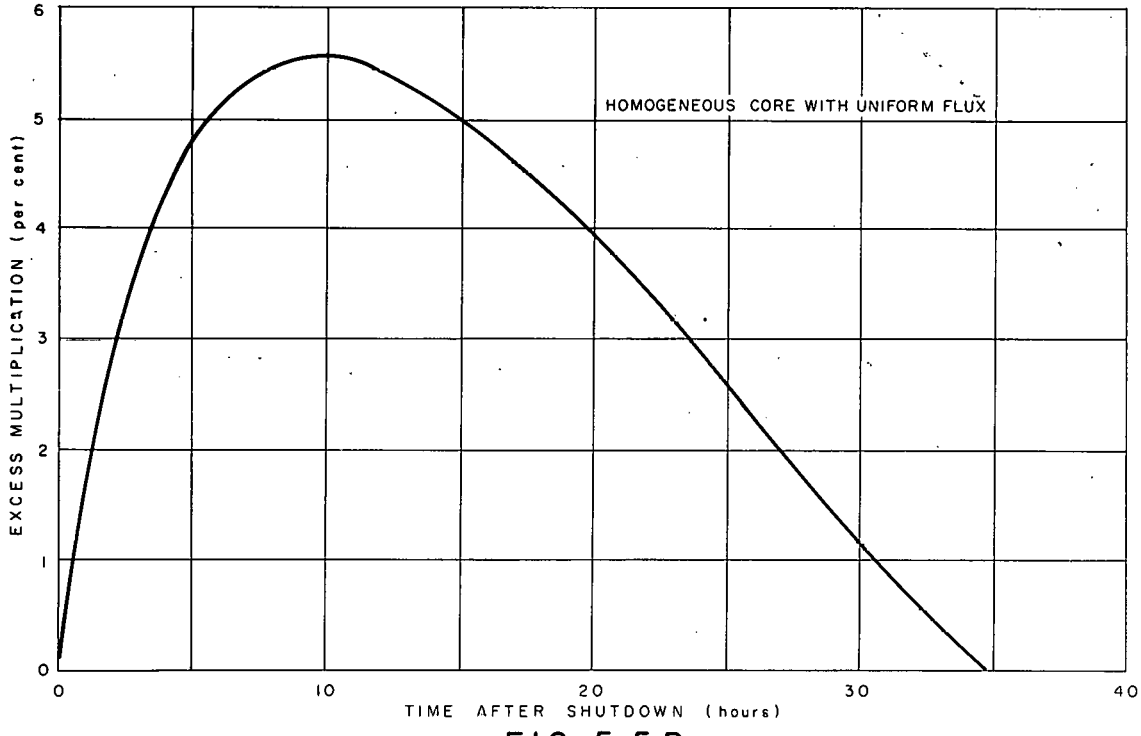

FIG. 5.5 B

EXCESS MULTIPLICATION REQUIREMENT ABOVE EQUILIBRIUM FOR XENON OVERRIDE AFTER SHUTDOWN FROM 40 MW IN E O C R

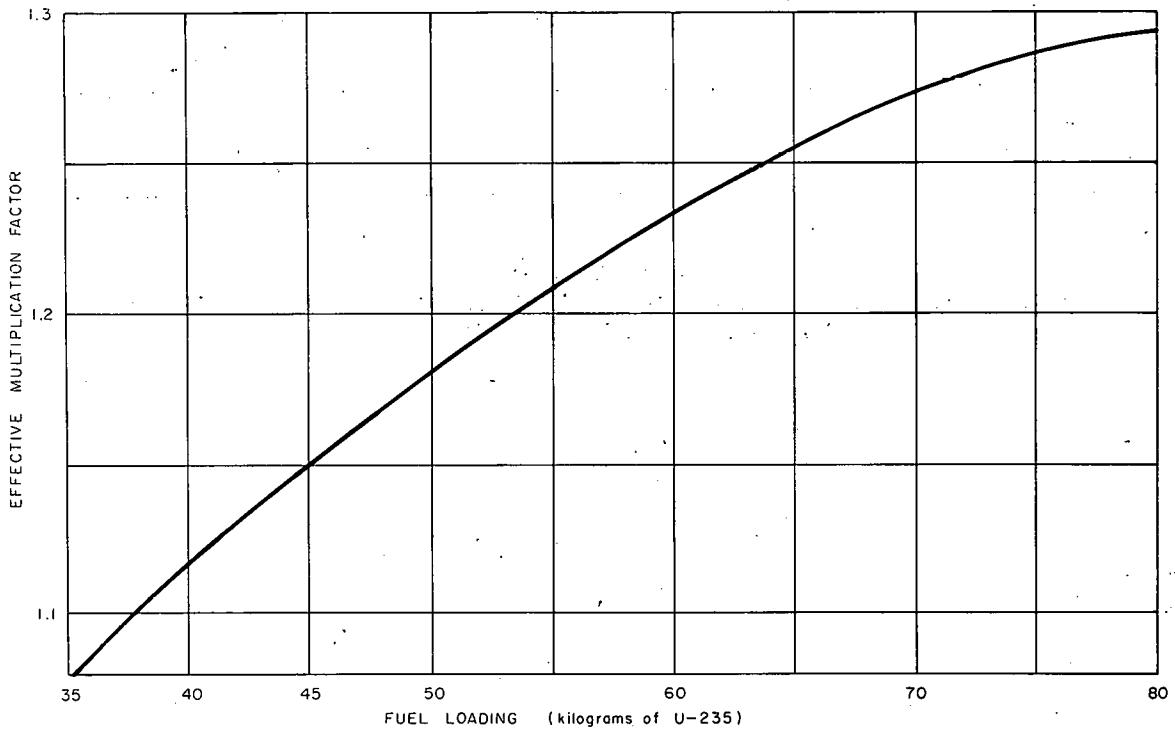

FIG. 5.5 C

EFFECTIVE MULTIPLICATION FACTOR VERSUS FUEL LOADING

EOCR REFERENCE CORE

PPCo.-C-2510

6.000 HEAT TRANSFER

Heat transfer studies described in this section show that cooling of the standard core can be accomplished within the limitations of allowable fuel plate surface area, available coolant flow, and required power level. Limitations on fuel plate surface area and coolant flow are determined by physics and economic considerations, respectively, and the power level requirements are set by power density requirements in experiments. Power densities in loop experiments in excess of design objectives are provided by operating the reactor at 40 Mw with a coolant inlet temperature of 500°F and the objective of in-core testing of power reactor fuel elements at their design temperatures and power density is met by operating at increased primary coolant temperature and lower reactor powers, e.g., 20 Mw is permissible at a bulk temperature of 700°F. Optimization of coolant flow has been provided by (1) non-uniform channel spacing within the fuel element to adjust flow to that required by local heat fluxes and (2) orificing of the fuel elements to reduce total flow in fuel elements in the low flux regions of the core. Thermal conditions upon loss of coolant pumping power have been determined in addition to normal operating conditions. The design premises upon which the calculations are based follow.

1. Fuel plate surface temperature and coolant velocity are chosen to prevent significant fouling,[1] i.e., less than 850°F scale-fluid interface temperature and greater than 8 ft/sec coolant velocity;

2. Limited fouling of fuel plate surfaces is tolerable because significant increase in the stainless steel fuel plate temperature can be tolerated without undue loss of plate strength;

3. Operating pressure is greater than that required to prevent nucleate boiling;

4. Burnout heat flux is at least twice the hot-spot heat flux.

Table 6.0A summarizes the results of the calculations and supplementary studies are given in Section 15.000. Discussion of the heat flux, shutdown conditions, coolant velocity, etc., are given in the following sub-sections.

6.100 Heat Flux

The local heat flux at any point on the fuel plates is determined by the power level, the heat transfer area, and the ratio of local to average neutron flux. The local to average neutron flux ratio is obtained from physics calculations described in Section 5.000.

---

1. W. R. Martini, "Summary of Organic Coolant Heat Transfer", Report NAA-SR-MEMO-4183, July 23, 1959.

Table 6.0A

CORE AND COOLANT OPERATING CONDITIONS

Reactor Power	20 to 40 Mw
Max/Avg Heat Flux in Driver Assemblies	4.6
Average Heat Flux (Dependent on Number of Control Rods Withdrawn)	1.08 to 1.44 x 10^5 Btu/hr-ft^2
Maximum Heat Flux at 40 Mw	6.6 x 10^5 Btu/hr-ft^2
Burnout Heat Flux at Hot Spot at 40 Mw	2,140,000 Btu/hr-ft^2
Maximum Nominal T_{wall} at Hot Spot	850°F
Saturation Temperature at Hot Spot	1000°F
Inlet Coolant Temperature	500°F
Outlet Coolant Temperature	525°F
Operating Pressure (Inlet)	150 psi
Maximum Coolant Velocity in Fuel Element Channel	37.5 ft/sec
Minimum Coolant Velocity in Fuel Element Channel	9 ft/sec
Coolant Flow Rate Through Driver Fuel Elements and Control Rods	20,500 gpm
Total Flow Through Reactor	25,000 gpm
Maximum Pressure Drop Through Unorificed Element	30 psi
Core Pressure Drop	40 psi
Heat Transfer Area per Element	39.5 ft^2
Total Core Heat Transfer Area (32 Element Core)	1260 ft^2

For purposes of determining heat transfer, flux has been averaged only over the fuel elements. Two cases (PDQ problems 12-3 and 12-1) which correspond to the start and end of the cycle were considered. PDQ problem 12-3 (four center rods withdrawn and the eight outer rods inserted[1])which is representative of the start of the cycle results in flux peaking in the center fuel elements. Problem 12-1 (with all rods withdrawn) results in flux peaking in the fuel elements near the reflector, typical of the end of the cycle. These two rod configurations include the most severe conditions throughout the cycle for all elements. The flow through each element is designed to provide cooling for the highest heat flux existing in either case. The peak heat flux is obtained in any element by determining the average heat flux over the core (power in Btu/hr divided by fuel area) and multiplying by the ratio of the maximum neutron flux in the element to the average neutron flux in the core fuel volume. For simplicity the core was divided into symmetrical quadrants and the fuel elements numbered as shown in Fig. 6.2A. The peak heat flux at 40 Mw for each element for the two cases described above is given in Table 6.1A. The maximum relative flux across the fuel element used for flow optimization, discussed in the next section, is shown in Fig. 6.1A.

Table 6.1A

MAXIMUM HEAT FLUX AT 40 MW AND MAX/AVG NEUTRON FLUX

Element	*PDQ Problem 12-1		**PDQ Problem 12-3		(Q/A) Max for Higher Case Btu/hr-ft^2 x 10^{-5}
	$\frac{\phi max}{\phi avg}$	$(Q/A)_{max}$ Btu/hr-ft^2 x 10^{-5}	$\frac{\phi max}{\phi avg}$	$(Q/A)_{max}$ Btu/hr-ft^2 x 10^{-5}	
1	3.53	3.81	4.58	6.60	6.60
2	3.58	3.87	4.14	5.96	5.96
3	3.11	3.36	3.40	4.90	4.90
4	2.37	2.56	1.30	1.93	2.56
5	2.70	2.92	Rod In	Rod In	2.92
6	2.55	2.75	1.82	2.62	2.75

* All control rods withdrawn. See Section 5.000.
** Four center control rods withdrawn. See Section 5.000.

1 The proposed control rod program is to pull the four center rods, followed by one control-regulating rod, followed by gang withdrawal of the remainder of the rods. This program results in highest flux for the central test hole.

6.200 Coolant Velocity Optimization

The fuel plates are cooled by forced convection, and the local wall temperature can be determined by the normal relationship

$$t_{wall} = t_{inlet} + \Delta t_{bulk} + \frac{Q}{Ah}$$

where

t_{wall} = scale-fluid interface temperature (^{o}F)

Δt_{bulk} = temperature increase of coolant from the inlet of the channel to the point in question (^{o}F)

Q/A = local or maximum heat flux ($Btu/hr\text{-}ft^2$)

h = local heat transfer coefficient ($Btu/hr\text{-}ft^2\text{-}^{o}F$)

The heat transfer coefficient is dependent upon the hydraulic diameter of the coolant channel, coolant velocity, and properties of the coolant. The heat transfer coefficient correlation[1] used in this study is reproduced in Section 15.000. This correlation is for Santowax R with 30% HB.

The coolant flow required by each element is kept to a minimum by providing wider channels in the region within the element where flux peaking occurs. The choice of channel thickness is based on the highest flux elements in the core, position 1 in Fig. 6.2A. The maximum flux for each channel of position 1 is shown in Fig. 6.1A. The channels nearest the center of the core are wider than those in lower flux regions to provide high coolant velocity in the high flux region and reduced velocity in the low flux region. The velocity in the widest channel is selected to limit the wall temperature of the fuel plate to $850^{o}F$. Table 6.2A gives the channel thickness, coolant velocity, and maximum plate temperature of each channel.

Table 6.2A

OPERATING CONDITIONS OF VARIED CHANNEL ELEMENT IN POSITION 1

Channel Number	Channel Thickness, Inches	Coolant Velocity, fps	Maximum Wall Temperature, ^{o}F
1	0.255	37.5	850
2	0.180	32.5	845
3	0.150	29.5	843
4 to 24	0.125	26.0	797 to 850

1 W. R. Martini, "Summary of Organic Coolant Heat Transfer", NAA-SR-MEMO-4183, July 23, 1959.

The same fuel element design is used in all core positions. Each fuel element is orificed to provide the flow necessary to maintain the hottest fuel plate at 850°F. Flow requirements for the various core positions are given in Fig. 6.2A. The total flow through all driver fuel elements and control rods is 20,500 gal/min.

An alternate method by which flow requirements may be minimized is to space fuel plates equally and to reduce the fuel content of plates in high flux regions. This possibility may be more attractive than the spaced plate element; however, it was not proposed for the conceptual design because it would have required re-evaluation of core physics. This alternate method should be evaluated before final design of the fuel element.

6.300 Operating Power as a Function of Bulk Coolant Temperature

Santowax R with 30% HB is most efficient as a heat transfer fluid at about 500°F, as shown in Section 15.000. An inlet coolant temperature of 500°F was therefore chosen to give the highest permissible operating power. For some tests in the EOCR it is desired to use inlet coolant temperatures above 500°F. If the same reactor flow rate and surface temperatures are maintained as specified in Section 6.200, the allowable reactor power would decrease as shown in Fig. 6.3A, to about 22 Mw at 700°F inlet temperature

6.400 Burnout

The heat-transfer criterion for safe reactor operation is based upon a comparison between predicted heat flux and burnout heat flux. The correlation used to calculate the burnout heat flux is that developed by Core and Sato[1] for Santowax OMP (see Section 15.220). To maintain a high burnout heat flux and to keep the possibility of boiling in the core to a minimum with a maximum scale-fluid-interface temperature of 850°F, an operating pressure of 150 psig was chosen. At this pressure the saturation temperature of Santowax R is about 1000°F. Because of uncertainties in the predicted heat flux, a hot-spot heat flux was determined for each position as described in Section 15.000.

Table 6.4A gives the maximum nominal heat flux, the hot-spot heat flux, the burnout heat flux, and ratios of the burnout to nominal and hot-spot heat flux at the hottest point in each element. This is the point at which the minimum ratio of burnout to nominal or hot spot heat flux occurs. The minimum ratio of burnout heat flux to maximum nominal heat flux is 3.2. The minimum ratio of burnout to hot-spot heat flux is 2.2. This is believed to be an adequate margin of safety, especially since OMRE experience has shown that even extensive burnout produces no serious reactor operating problems.

---

1 K. Sato and T. C. Core, "Determination of Burnout Limits of Santowax OMP", Space Technology Division, Aerojet General Corporation, Azusa, California, September 15, 1959.

Table 6.4A

COMPARISON BETWEEN MAXIMUM OPERATING HEAT FLUXES AND BURNOUT HEAT FLUX

Core Position	Maximum Nominal Heat Flux at 850° Point Btu/hr-ft^2 x 10^{-5}	Hot Spot Heat Flux at 850° Point Btu/hr-ft^2 x 10^{-5}	Burnout Heat Flux at 850° Point Btu/hr-ft^2 x 10^{-5}	Ratio of Burnout Q/A to Nominal Q/A	Ratio of Burnout Q/A to Hot Spot Q/A
1	6.60	9.44	21.4	3.24	2.26
2	5.96	8.53	19.9	3.34	2.33
3	4.90	7.00	16.5	3.37	2.36
4	2.32*	3.32	10.5	4.52	3.16
5	2.39*	3.42	10.7	4.48	3.13
6	2.49*	3.56	10.9	4.38	3.06

* Location of 850°F surface temperature not at point of maximum heat flux.

6.500 Shutdown Cooling

The shutdown cooling of the EOCR depends upon natural circulation of the coolant. The exact conditions at short shutdown times are difficult to predict because of redistribution of flow in the core at low flows, uncertainties as to resistances in the primary system, and lack of knowledge of low flow heat transfer properties of Santowax. An estimate of the effectiveness of thermal circulation shutdown cooling was made with the assumption that no changes in core flow distribution took place upon failure of the pump. The estimate is conservative in the sense that with upflow through the core, thermal convection in the separate channels should increase the flow of the hotter channels relative to the average when total flow becomes small. A pressure loss of 5 velocity heads through the pump was assumed in the calculation of the thermal circulation rate. The validity of this assumption should be evaluated when the pump is selected and its characteristics are known. Table 6.5A summarizes the results of shutdown cooling calculations and indicates that the maximum fuel surface temperature in the driver fuel elements after shutdown from 40 Mw operation with 500°F coolant inlet temperature will be 680°F.

Table 6.5A

SHUTDOWN COOLING

Time After Pump or Power Failure	ΔT Between Vertical Pipes in Primary Coolant Loop, °F	ΔP, ft of Liquid	Flow Rate, gpm	Assumed Inlet Temperature °F	Maximum Nominal Fuel Element Temperature, °F
1 minute	25	0.60	1100	500	680
10 minutes (Steady State Flow Obtained)	16	0.40	800	480	600
1 hour (Core in Laminar Flow)	12	0.29	680	400	550

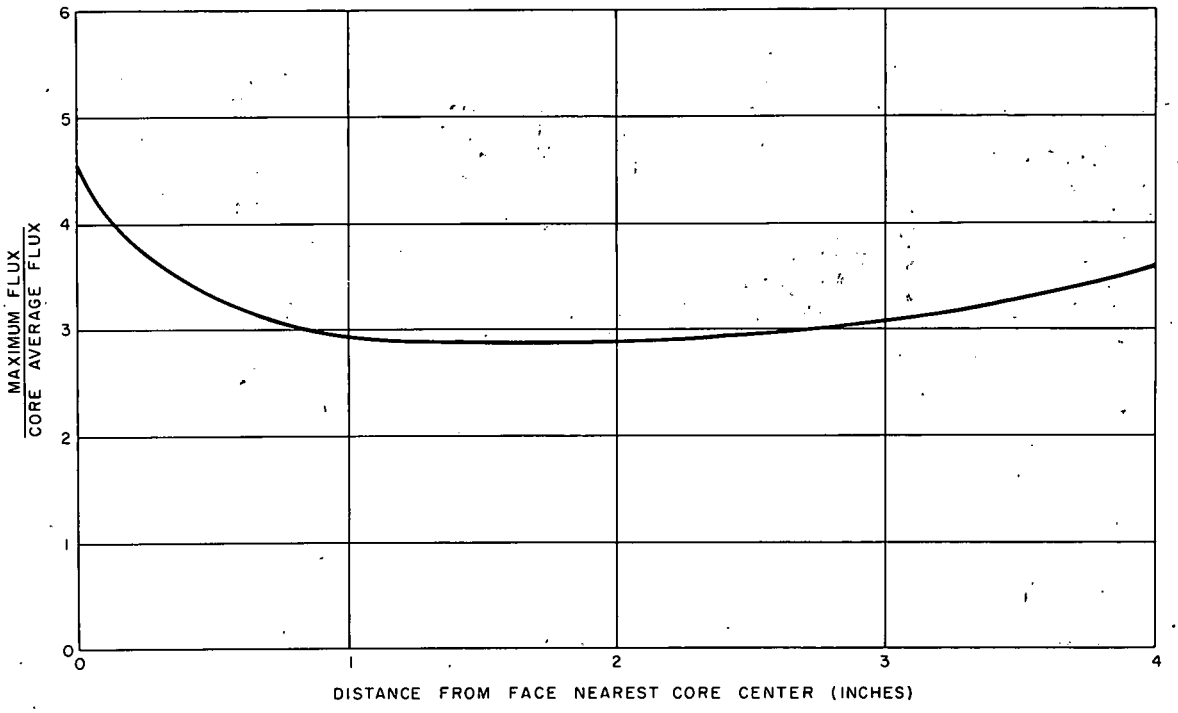

FIG. 6.1 A

RELATIVE FLUX IN POSITION I

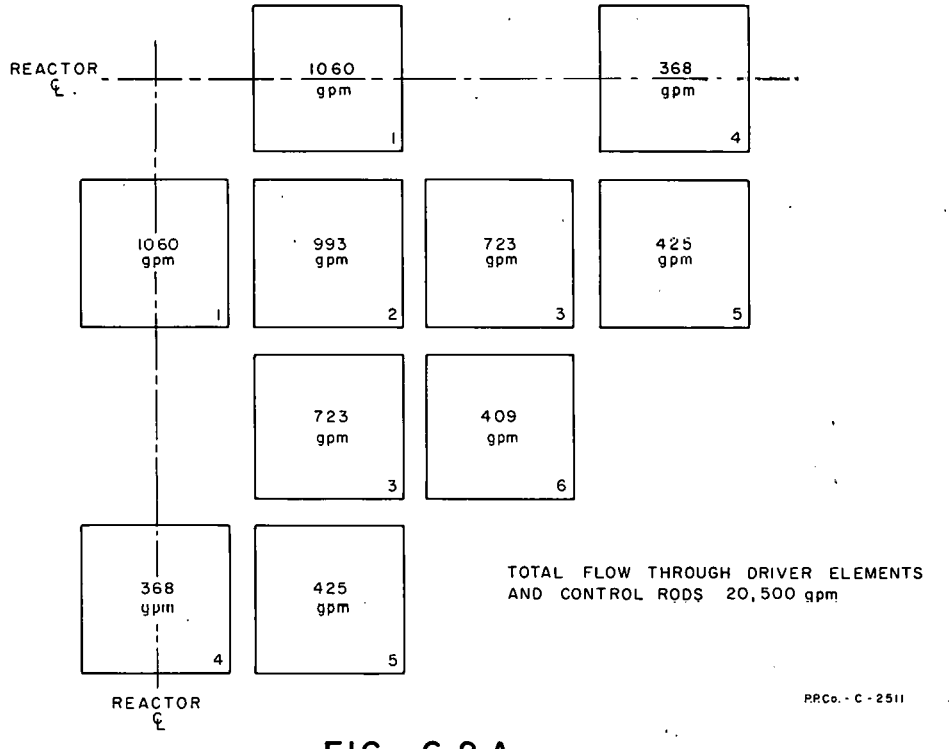

FIG. 6.2 A

FLOW RATES IN VARIED CHANNEL ELEMENTS

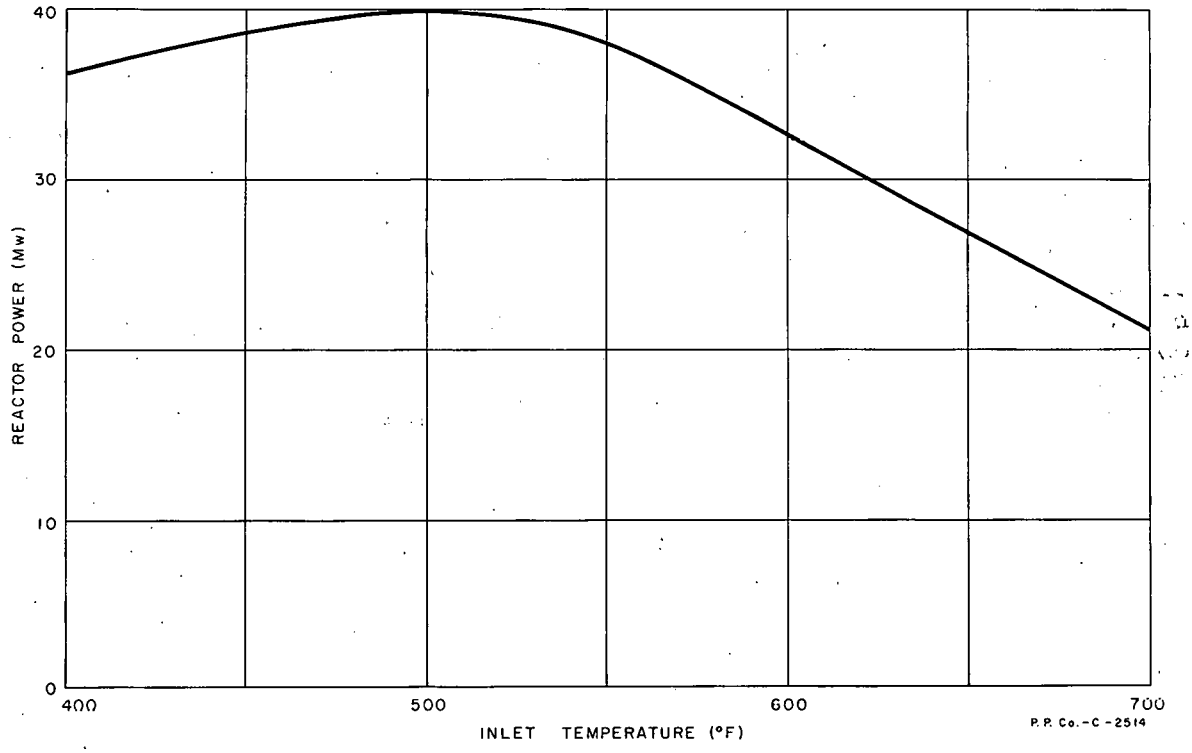

FIG. 6.3 A

INLET TEMPERATURE EFFECT ON REACTOR POWER

7.000 ENGINEERING DESCRIPTION

This section describes the reactor internals, reactor structure, buildings, process equipment, and site for the EOCR. Since this is a conceptual design, many of the mechanical features of the reactor are not detailed but do give a proposed method to meet the design objective in question. Sufficient layout of the site and buildings has been provided to form the basis for a preliminary cost estimate. The process system and utilities are based on calculated usage and experience with other similar reactor facilities and are sufficient to form the basis for the final design.

7.100 Reactor and Reactor Structure

The fullest utilization of EOCR requires insertion and removal of components of many shapes and sizes such as fuel elements, test loops, reactor inner tank, and grid plates. For this reason a handling system which is more versatile than the cask handling in use at OMRE and proposed for the Piqua power reactor is used. Investigation and limited experimental data indicate that it will be possible to handle the EOCR components and experimental equipment through cold demineralized water by use of the "water flooding" technique. Basically, "water flooding" consists of purging hot (approximately 350°F) organic from the reactor with hot demineralized water and then removing the hot water with high-pressure cold demineralized water. (See Section 7.470 for description of Water Flooding). Certain design and operating features peculiar to this reactor naturally arise from water flooding and are included in the design criteria, plant systems, and structures in this proposal:

1. All reactor internals, reactor vessel and heads, and primary coolant lines to and including the main block valves are fabricated from stainless steel, although more detailed study and tests may indicate the feasibility of using carbon steel.[1] These components should be designed to eliminate pockets or dead spots where organic or water may be difficult to displace during the water flooding operation or during the time the reactor is being refilled with organic coolant.

2. Some organic and water mixing will occur in the water flooding process, and it will be necessary to remove this water from organic coolant before re-using it as reactor primary coolant.

3. It appears there will be some scum formation in the canal and in the reactor pit as a result of water flooding. The canal and reactor pit are to be equipped with scum drains.

Another novel feature of the EOCR is the elimination of the reactor discharge chute by placing the reactor vessel at the bottom of the reactor pit which is directly connected to the canal, but is separated from that canal by a removable bulkhead with inflatable seals. During

---

1. See Sections 17.000 and 20.000.

reactor operation, the reactor pit is dry, and the reactor top head with the control and regulating rod drives is located there. After reactor shutdown and water flooding of the reactor vessel, the reactor top head is removed and the reactor pit is filled with demineralized water. This permits handling operations directly between the reactor and the canal.

Other factors which must be carefully considered in EOCR reactor and process design, but which are not the direct result of water flooding include: differential expansion between reactor components as a result of the moderately high operating temperatures; galling problems associated with all stainless steel reactor internals; expansion stresses in process piping; thermal stresses due to gamma heating in the reactor grid or other reactor components; arrangement of steam tracing network on all process lines containing organic; fire hazards naturally inherent with the use of hot organics; heat removal from main process line pipe trench; and other factors.

The following sections describe the reactor vessel, reactor internals, and reactor structure as shown in the following figures. (An alternate reactor arrangement is described in Section 16.000).

Fig. 7.1A	EOCR Reactor Structure Cross Sectional Elevation
Fig. 7.1B	EOCR Reactor Structure Horizontal Section through Nozzles
Fig. 7.1C	EOCR Reactor Structure Horizontal Section through Core Centerline

7.110 Pressure Vessel. The reactor vessel is to be constructed as specified in the ASME Unfired Pressure Vessel Code, and is to be fabricated of AISI Type 347 stainless steel. (See Sections 17.000 and 18.000 for Materials of Construction and pressure vessel design data). The design bulk coolant temperature is 850°F; the design pressure is 330 psig; and the design reactor power is 220 Mw thermal. The vessel ID is 7 ft 0 in. with a flange-to-flange length of 18 ft 9 in. and a wall thickness of 1.25 inches. The entire vessel, including the top and bottom heads, is covered with approximately 4.5 in. of high temperature insulation. Two 24-in. pipes provide coolant inlet and outlet passages, and are permanently welded to the vessel. Eight 8-in. nozzles arranged radially below the top flange (see Fig. 7.1B) are provided for use in conjunction with the experimental loops. Sufficient thermocouples are attached to the vessel external wall to give comprehensive operating temperature data. A definite air flow pattern around the vessel is to be designed to carry off heat lost through the vessel insulation.

The vessel is closed at each end with flat heads of code design. The top flat head is made up of two parts, an inner sealing head, and an outer shielding head which will remain cool during reactor operation. The inner head will have insulation applied to it and an air space will be maintained between this insulation and the shielding head. The top head will be fitted with replaceable seals for ten control rod drive rods and two regulating rod drive rods. Drive rod seals should be as leakproof as possible, and may be pressurized with nitrogen to prevent

leakage of organic vapors to the reactor building. Non-pressurized seals, if used, should vent any escaping organic vapors to a suitable freeze pot which is vented to the EOCR stack. Replaceable monitor tube assemblies for each fuel element position and five plugs to allow the full-size penetration of any of the major experimental loops are also located in the top head. These loop positions are the four spaced equally about the core center on an 11.5-in. radius plus the center loop position.

Since the monitor tubes are mounted in the top head and the tips of these tubes extend approximately 6 in. into the fuel element upper extension and may also extend through a removable orifice plate located at the top of this extension, dowels or other guides are utilized to guide the top head into position over its last 12 in. of downward travel.

The vessel bottom head has the same general configuration as the top head. Penetrations in this lower head include those for all loops and experimental positions shown in Fig. 4.1A, the two fission chamber tubes, the rabbit facility tubes, and the vessel drain piping. In addition, penetrations are to be provided under all core fuel element locations and reflector positions wherever possible. These penetrations should approach the size of the EOCR fuel element bottom end-box, if possible. Bottom head penetrations are provided with seal glands, valves, or other devices as necessary to seal the loops or experimental in-pile assemblies in the bottom head. In-pile assemblies are installed and removed from above the reactor when the vessel is filled with cold water. Shielding plugs with sufficient thickness to approximate the two lower heads will be placed in these pentrations when they are not occupied by loops.

In-pile experimental tubes are generally considered to be of the re-entrant type from the reactor subpile room, although through loops could be installed in certain locations. Instrumentation leads from in-pile experiments may be brought out through the piping penetrating the bottom head, out through top head penetrations, or out through the reactor vessel nozzles. Top head experimental penetrations should be avoided wherever possible, and must be of a nature which can be broken when the reactor is shut down for in-tank work.

7.120 Reactor Vessel Internals. The nuclear properties of the organic coolant used in this reactor have allowed a core configuration well-suited to a research-type reactor. Spacing between elements, as shown in Figs. 4.1A and 7.1C is such that various sizes and shapes of elements, experimental loops, or experimental facilities may be installed without driver element repositioning. A vertical section of the reactor structure is shown on Fig. 7.1A.

The basic functions of the reactor vessel internals, excluding the inner thermal shields, are to provide support and to position the driver and test elements and the experimental loops and facilities, and to channel the coolant flow where desired. In this reactor these

primary functions are handled by three core components: a grid with its support base; a spider located at the top of the inner tank; and the inner tank.

Coolant flow enters the reactor vessel through the lower 24-in. inlet pipe located above the inner thermal shields, flows down through the shield annuli, passes horizontally through perforations in the grid support base, and proceeds up through fuel elements and the large loop cooling-jacket annuli, emerges above the spider, and flows horizontally to the exit or upper 24-in. outlet pipe. The coolant flow requirement in the space between the grid and spider is 2000 - 4000 gpm. Less than 2000 gpm results in excessive organic heating; more than 4000 gpm results in excessive pumping requirements.

7.121 Grid. The grid is made of a heavy austenitic stainless steel plate, and has holes for the fuel element lower end-boxes, for the various experiment loops and facilities, and for the rabbit tubes and fission chamber tubes. Preliminary design data indicate that the two large loop experimental positions will have an approximate 6-in. diameter penetration in the reactor bottom head and an approximate 6.4-in. diameter penetration in the grid. The other three basic loop positions will have approximately 5.5-in. diameter penetrations at these locations. Control- and regulating-rod guide tubes are mounted on the grid and project below the grid and above the grid up to a position just below the lower boundary of the core fuel. This grid may also be fitted with a valve which will allow rapid liquid passage in the space between the grid and spider during the water flooding operation or when refilling the vessel with organic. This valve may be operated from the subpile room.

The grid supports the fuel elements and provides lateral support for the experiment loops and facilities and for the rabbit and fission chamber tubes. The grid is mounted on a support base, which in turn may be mounted on the lower head. The inner tank is fastened to the grid in a manner which will minimize coolant leakage and which will allow easy remote removal when the vessel is filled with cold water. Since the coolant flow in the space between the grid and spider is severely restricted, seals are provided where the fuel elements and loops penetrate this grid. Plugs or adapters are provided for positions occupied by loops or facilities and for the twenty power reactor element positions shown in the reflector. The grid must withstand a differential pressure of 50 psi over its gross area during reactor operation.

7.122 Spider. The spider provides lateral support for the tops of the fuel elements and for the large experimental loops. A plan view of this component is shown on Fig. 7.1B. Approximately 5.5-in. square holes are furnished over all grid basic element locations. The control rod and fuel element positions immediately surrounding the two large loop positions are furnished with approximately 4-in. square holes.

Circular holes approximately 6.4 in. in diameter are furnished over the two large loop positions, and holes approximately 5.5 in. in diameter are furnished over the three remaining basic loop locations. This spider is to be fabricated of an austenitic stainless steel, and fastened to the top of the inner tank in a manner that will allow easy removal. The spider is not removed for normal reactor operations, including fuel and control rod removal or insertion, in-pile experimental tube insertion or removal, etc.

7.123 Monitor Tubes. Mounted in the reactor vessel top sealing head are fuel element monitor tubes. These tubes monitor individual element coolant temperature and flow. They are also used to draw off samples of organic coolant during reactor operation. The monitor tube assemblies extend down to the top of the spider and hold the fuel elements in position vertically. Provision is to be made in the top head for mounting monitor tubes over all fuel element locations. The tubes are to be strong enough to withstand the upward force on the fuel elements, and the lateral force of the coolant moving horizontally to the exit pipe. Upward force on the fuel element occurs as a result of spring-loading on the fuel element and the pressure drop (50 psi) across the fuel element cross-sectional area. (For further discussion on fuel monitoring, see Section 7.172).

7.124 Experimental Facilities. The core includes the following experimental facilities, as shown on Figs. 4.1A and 7.1C:

1. Two Large Loops. These two are the major large re-entry or through loop positions. The pressure tube OD is approximately 6 in. and the cooling jacket OD is about 6.4 inches. A detailed discussion of these facilities is found in Section 8.000.

2. Three Other Basic Loops. These three loops occupy the core loop positions not used by the two loops described above, and may be used for single experiment facilities or for multiple facility applications that do not require a large tube. A rabbit facility is installed in one of these positions. Discussion of small loops is included in Section 8.000. A description of a rabbit facility is found in Item 4 of this list.

3. Twenty Small Facilities. These positions are included for future irradiation use. The size is about 1.5-in. OD, or as large as feasible, dependent upon final reactor design. Penetrations in the grid and bottom head only (none in the spider) are required. Insertion of samples is accomplished from the subpile room.

4. Rabbit Facility. Two rabbit facilities are planned for this reactor, one is incorporated in a 5-in. loop position, and the other in the outer reflector position. These facilities are about 1.5-in. OD. They are used for irradiation of capsules, and may be driven pneumatically, hydraulically, or mechanically. Provision is made to allow piping to the rabbit positions to be installed from either the subpile room or through the vessel 8-in. nozzles located below the top flange.

5. Power Reactor Element Positions. Power reactor elements undergoing tests may be placed in all core element positions except those immediately surrounding the two large loops. This requires that the overall length and end-box configurations be the same as the standard 4-in. square driver elements. In addition, there are twenty power element positions included in the spider and grid immediately surrounding the driver element core.

6. Alternate Loop Positions. The reactor vessel bottom head includes provisions for the installation of a loop facility in any feasible fuel element position, including the twenty power reactor test element positions outside the core. The feasibility of incorporating the necessary penetration and seal devices in the bottom head is to be determined by the space available after design of the other loop positions and equipment incorporated in the bottom head. The size of the penetration should be as large as the fuel element end-box hole in the grid, if possible.

Since the flow velocity in the space between the spider and grid is very low, the experiment loops, facilities, rabbit tubes, or fission chamber thimbles may be positioned in the core area without requiring support at the upper ends of the tubes. Thus, they can enter the vessel through seal devices in the lower head, pass through minimum leakage seals in the grid, and project in a cantilever manner into the core zone. Penetrations are not provided in the spider for the twenty small facilities or for the fission chamber thimbles. Only those loops or facilities requiring top access need project through the spider. Access to top closures in the loop facilities may be accomplished by dropping the water level below the loop closure. In rare cases, the fuel elements, control rod, and regulating rods may have to be removed from the core to reduce background radiation.

Installation of loops or facilities in the reactor is accomplished with the reactor vessel filled with cold demineralized water. Generally, installation and removal of these in-pile components will be done from the top of the reactor vessel.

7.125 Fuel Elements. The fuel plate section of the fuel elements is described in detail in Section 4.200 and is shown on Fig. 4.2A.

The spacing between the grid and spider requires a relatively long fuel element structure. The lower end-box, which incorporates a spring, is approximately three feet long. This end-box is circular in cross section, and is as large as is compatible with the design of the remainder of the core components. A transition section is employed in joining the end-box to the square fuel section.

The fuel element upper extension is 4-in. square in cross section. The top of this extension is enlarged to approximately 5.5-in. square to fit securely in the square holes in the spider, and

extends above the spider approximately 1 in. in the non-loaded (top head off) position. View A-A on Fig. 4.2A shows a removable orifice plate which is attached to the enlarged section of the upper extension, and the monitor tube tip is inserted in the center hole of this plate, nominally sealing the center hole by means of a flat or cupped plate mounted on the monitor tube body. The monitor tube and the center hole in the removable orifice plate should be sized for maximum clearance between the tip and the edge of the hole since the monitor tubes are mounted in the reactor top head, and it is anticipated that the head will be subject to minor misalignments due to tolerances of manufacture, clearances on dowels or other guides, etc. The orifice plate might also be attached to the monitor tube in such a manner that the orifice plate contacts the flat top surface of the fuel element upper extension as the top head is lowered into position. In this instance, the orifice plate must be readily removable. This arrangement gives more clearance between the monitor tube tip and the fuel element upper extension, but leakage between the orifice plate and fuel element will probably be greater.

The spring on the element lower end-box is preloaded upon manufacture. This preload supports the weight of the element when it rests on the grid. When the top head is put in place, the monitor tubes press the elements down approximately .25 to .50 in., which is enough to allow for element and vessel fabrication tolerances. This configuration provides a firm support for the fuel elements, but does not allow element movement during loss of coolant flow in reactor operation. The spring on the element lower end-box must be long enough to compensate for any growth in the fuel element due to increase in temperature.

Any experimental fuel elements tested in the core positions will have upper and lower end-boxes similar to the standard driver elements.

7.126 Control and Regulating Rods. The control and regulating rods are of similar design, the only difference being perhaps in the fuel loading. The control rod is shown on Fig. 4.3A. This rod incorporates a 4-in. by 4-in. poison section approximately 36-in. long, and a 4-in. by 4-in. fuel plate section of the same length. The construction of the control rod is such that there is minimum vertical spacing (0.125 to 0.25 in.) between the bottom of the nuclear poison and the top of the fuel. Appreciable space at this point might result in unstable control characteristics due to flux peaking between the fuel and poison sections. The control and regulating rods are connected to their drive rods by some device that will allow remote disconnection and connection with the top head in place. This internal connection eliminates the necessity of passing the drive rod completely through its seal in the top head when the head is removed or replaced.

The lower ends of the control and regulating rods are fitted with end-boxes that travel in the guide tubes fastened to the grid. These end-boxes have hard-faced rubbing bosses to guide the rod and provide low friction movement. The lower end of the guide tube has a stop that will prevent the rods from dropping down on the reactor bottom head when the drive rods are disconnected.

7.127 Source. A neutron source is provided for use in reactor startup and operation. It will be inserted through the spider into its receptacle adjacent to the core fuel elements when the vessel top head is removed. The source is located directly opposite the reflector rabbit facility, and at right angles to the two fission chamber thimbles.

7.130 Inner Tank. The reactor vessel incorporates an inner tank which contains the inlet coolant flow and directs it downward through the annuli formed by the inner tank, reactor vessel, and internal thermal shields. The flow then turns upward in the plenum above the reactor bottom head and passes through the core components. The inner tank is made of AISI Type 347 stainless steel and is designed for 50 psi external pressure at 850°F maximum bulk coolant temperature and a reactor core power of 220 Mw thermal. This tank must be secured to the vessel wall between the inlet and outlet 24-in. pipes by a method which will allow its remote removal under water and also one which will minimize coolant leakage past this connection. The bottom end of the inner tank must also be fastened to the grid in a manner which will minimize leakage and which will allow remote disassembly. A valve is mounted in the horizontal top section of the inner tank to allow liquid passage during water flooding or organic filling. This valve may be self-acting or, for more positive action, may be operated from outside the reactor vessel.

7.140 Thermal Shields. Thermal shields are provided for placement both inside and outside the reactor vessel to reduce thermal stress in the vessel wall and in the concrete biological shield to safe values. These shields are calculated on the basis of a reactor core power of 220 Mw thermal.

7.141 Internal Thermal Shields. Three 1-in. thick concentric internal thermal shields are placed inside of the reactor vessel wall and outside of the inner tank. These shields are fabricated of AISI Type 347 stainless steel, and are designed for highest coolant velocity in the annulus adjacent to the inner tank. Coolant flow enters the reactor vessel through the inlet pipe located just above these shields and flows downward in the four annuli, then turns upward to pass through the reactor core. Shields should be designed for easy insertion or removal.

7.142 External Thermal Shield. An external steel-jacketed lead thermal shield is provided for the protection of the concrete biological shield. This shield is approximately 3-in. thick, and is placed outside the reactor vessel thermal insulation. Cooling-water coils are embedded in the lead to carry off radiation-induced heating. This shield is separated from the vessel insulation and the concrete biological shield by air spaces.

7.150 Control Rod Drives. The reactor core includes ten positions for control rods and two positions for regulating rods. Control and regulating rods are described in Section 7.126.

The control and regulating rod drives are mounted on the reactor vessel top head and make connection with their respective rods by means of drive rods which penetrate the top head through replaceable seals. The control rod drive must be a reliable unit fully meeting all operating requirements while functioning in its environment. Adequate factors of safety are to be incorporated in the design. The drives must be capable of scramming the control rods with full upward coolant flow and maximum system operating pressures, and must lock the rods in the full down position. After remotely breaking the drive rod connections to the control and regulating rods, it must be possible to remove the reactor top head without passing the drive rods through the top head seals. Hydraulic, pneumatic-mechanical, or purely mechanical drives may be considered for these drives, but the performance of these units should be proved prior to actual use on the reactor.

7.160 Regulating Rod Drives. Two regulating rod drives are used in this reactor. These drives are of a design similar to the control rod drives, and are mounted adjacent to the control rod drives on the reactor top head. Their chief functional difference is that they will be capable of approximately twice the motor-driven speed as that of the control rod drives. While the function of the control rod drives is primarily to raise and hold the control rods to operating position, the function of the regulating rod drives is to continuously vary the regulating rod position in a manner which tends to level out the reactor power. Conventional regulating rod drives incorporate electric servo motors which are driven by reactor control circuits. Thus, the regulating rod drives will, of necessity, be more rugged and will be capable of continuous long term use. Again, as with the control rod drives, various systems may be considered for this application. These drives must be capable of driving the rods in at full-rated velocity against full coolant flow and system operating pressure, and must lock the rods in the down position. When removing the top head, requirements similar to those specified for the control rod drives must also be met. Only one of these drives will be utilized at any one time. The spare rod functions as a normal control rod when not in use.

7.170 Reactor Instrument Facilities. Facilities are necessary to provide accommodations for instrumentation such as the neutron sensitive chambers, resistance thermometers for measurement of inlet and outlet coolant temperatures from which the reactor power is calculated, and the temperature and pressure sensors at the outlet of each individual fuel element.

7.171 Neutron Sensing Chamber Facilities. The fission chamber facilities used for starting up the reactor from complete shutdown are located in the reflector region of the core as shown in Fig. 7.1C. This location is required to allow the proper sensitivity to neutrons present during reactor startup. These tubes are 6-in. inside diameter and are inserted from the bottom of the reactor through the

bottom head. The maximum operating temperature rating of commercially available chambers is 175°C. Since such chambers have an outside diameter of approximately 2 in., this allows a 2-in. annular space around the outside of the chamber for insulation and cooling. The design of the insulation and the determination of either air or water cooling will be a part of detailed design.

It is necessary to have a drive system which can remotely position the two fission chambers at any desired location within limits in the two tubes, since these are withdrawn during full power operation to lengthen the life of the chambers. This drive system is operated by a motor located on the bottom plug of the reactor tank. The control system for the motor is then tied into the reactor control system and is actuated from the reactor console.

There are five other neutron-sensing ionization chamber positions located around the perimeter of the lead shield of the reactor tank. The chamber tubes extend from a trench around the reactor pit parapet and into the lead outer thermal shield to a point approximately 1 ft below reactor centerline. Access to the tubes is from the reactor trench around the top of the reactor tank. At this chamber position no temperature problem should exist.

The drive system to control the positions of these chambers can be much more simple than that for the fission chambers, since the chamber tubes are essentially vertical. The adjustment of chamber position is not as drastic as in the case of the fission chambers which involves position changes during reactor operation. After the location of the ion chambers has been made originally it is seldom necessary to move them more than 12 in. compared to the 3 to 5 ft necessary for the fission chambers. In addition, gravity can be used to allow insertion and withdrawal of the chamber by a manual drive actuated at the top of the tube connected by a steel cable to the chamber proper and its shielding.

7.172 Fuel Monitoring. Three fuel element coolant variables are monitored intermittently in the reactor. These are temperature, flow, and organic composition (drawing off samples for laboratory analysis). This monitoring is accomplished by the use of monitor tubes which are installed in the reactor vessel top head and which extend down into the upper end-box of the individual fuel elements. The tips of the monitor tubes extend through the orifice plate mounted in the fuel element upper end-box. (See Sections 7.123 and 7.125 for further description of the monitor tubes and fuel elements). The monitor tubes consist of a thermocouple well and a tube which may be used for either pressure-sensing or coolant-sampling. Reading of the monitors during reactor operation is accomplished by a technician standing on the reactor vessel top shielding head. No leads running to other parts of the reactor building are used.

Monitor tubes are initially supplied for the twenty driver fuel element positions, and provisions are incorporated

in the reactor top head for the future addition of other tubes in all fuel element positions. Seals are to be designed for minimum leakage and easy replacement. The monitor tubes are to be constructed to withstand the upward force of the fuel element during reactor operation, and also the lateral force of the coolant flowing horizontally across the vessel to the exit pipe.

7.180 Biological Shielding. The biological shield is designed to attenuate the gamma and neutron radiations produced during reactor operation at full design power of 220 Mw to safe reasonable levels. In areas where continuous personnel occupancy is necessary, sufficient shielding is provided to attenuate the radiations to less than one-half the permissible occupational exposure level[1] at the outer surface of the biological shield.

Two different types of concrete were investigated for use in the biological shield surrounding the sides of the cylindrical reactor tank--ordinary concrete having a density 2.3 g/cc and high density concrete having a density 3.5 g/cc. Using the gamma flux at the inner surface of the biological shield determined in the gamma heat derivations in Section 5.340, calculations were made to determine the thickness of concrete required to attenuate the radiation to 0.75 mrem/hr on the outside surface of the shield. Using ordinary concrete, 9 ft are required. Using high density concrete, 6 ft are required. High density concrete was chosen for the biological shield because (1) there is no significant difference of in-place cost between 6 ft of high density concrete and 9 ft of ordinary concrete, (2) a smaller floor area would be required, and (3) there are better heat transfer characteristics with the thinner shield.

The ETR biological shield is constructed of 8 ft of magnetite concrete. However, the basic shielding calculations gave a thickness of approximately six feet. The additional 2 ft were added to provide for the radiations produced by experimental loops which pass through 1-ft diameter vertical sleeves in the biological shield; thus, the EOCR shield thickness compares with the ETR calculations.

The top and bottom of the EOCR tank is shielded by 2 ft of steel. The top head is removable to permit refueling of the reactor and to permit insertion and removal of experiments during shutdowns. The bottom head has a number of penetrations for entry of experimental loops, fission chamber thimbles, etc. When the penetrations are not in use, they are plugged with material of equivalent density and thickness to prevent streaming of radiation into the subpile room.

7.181 Power. During operation of the reactor the top head will be in place. This allows personnel to work on the reactor top without time restrictions.

---

1. "Maximum Permissible Radiation Exposures to Man", Addendum to National Bureau of Standards Handbook 59; April 15, 1958.

Entry into the subpile room, the primary coolant valve cubicle, and the reactor coolant pipe tunnel will be prohibited by the high radiation fields which exist while the reactor is in operation. All other areas are accessible to personnel.

7.182 Shutdown. The reactor is shut down for refueling and for inserting and removing experiments. Sufficient shielding is necessary to attenuate the residual activity emanating from the core region to permit as much working time as possible on the reactor top and in the subpile room.

The spent fuel will be removed from the reactor and transferred to the storage canal to reduce the radiation source in the reactor tank. Shielding for fuel transfer is provided by flooding the reactor pit above the reactor tank with water to the level of the canal. Removal of the bulkhead then permits direct transfer of the spent fuel to the canal with special handling tools. The reactor tank top is located 13 ft below the surface of the water. Careful handling during the transfer operations is necessary to prevent the fuel section of the fuel element from coming closer than 6 ft to the surface of the water; otherwise, the momentary radiation exposure dose-rate becomes prohibitive.

7.183 Experimental Tube Installation. Installation of an experimental in-pile tube requires considerable work in the subpile room, on the reactor top, and in the reactor tank. Before this work commences, the spent fuel elements are removed to the canal to reduce the radiation source in the tank.

To prevent streaming of radiation from the core through the in-pile tube to the subpile room and reactor top, removable lead plug shields will be placed in the tube. These plugs are removed after the tube has been installed and filled with water or organic.

In-tank work is accomplished by lowering the water level in the tank and limiting the worker's in-tank time as necessary to maintain his exposure within permissible limits.

7.190 Reactor and Canal Structures. Referring to Figs. 7.1A, 7.1B, 7.1C, 7.6B, 7.6E, and 7.6F, some of the main features of the reactor and canal structures may be seen. These structures are described in the following sections:

7.191 Reactor Structure. The reactor vessel is set at the bottom of the 14-ft deep reactor pit and is shielded by 6 ft of high (3.5) density concrete. High density concrete may use barytes, magnetite, or hematite as aggregate, but must meet the density requirements stated above. This biological shielding will extend from the top shielding head to the bottom shielding head of the reactor and will support the reactor vessel proper. The reactor pit, reactor vessel, and biological shielding are supported by a circular wall of concrete forming the reactor subpile room.

Figs. 7.1A and 7.1B show the two primary cooling lines through the west side of the structure and the eight nozzles which penetrate the reactor structure. The nozzle trench covers 180° near the top of the reactor vessel.

The inside surface of the biological shielding is lined with and may be formed from carbon steel plate. This steel lining extends from the bellows seal at the vessel top flange down to the reactor subpile room. Between the steel lining and the pressure vessel is a water-cooled lead shield. The lead shield is separated from and supported by the steel lining and is also separated from the vessel by an air gap.

7.192 Canal Structure. The circular reactor pit above the reactor vessel opens into the canal, but may be isolated from the canal by means of a removable bulkhead with inflatable seals. This canal is 8-ft wide, 18-ft deep, and 30-ft long, from the bulkhead to the end of the canal. The south end of the canal should be designed in a fashion which would permit southward extension of the canal in the future. Encompassing the canal and reactor pit is a 3-ft high parapet. The canal and reactor pit has a positive liner seal of stainless steel, fiberglass, or some other suitable substance. This seal restrains any demineralized water from coming into contact with or leaching out into the concrete structure, and must also resist radiation damage from spent fuel elements, etc. The biological shielding around the canal is also high density concrete. The thickness on the sides and bottom is 5 feet. The south end has a thinner, temporary wall to allow removal at a later date should it be desirable to expand the canal.

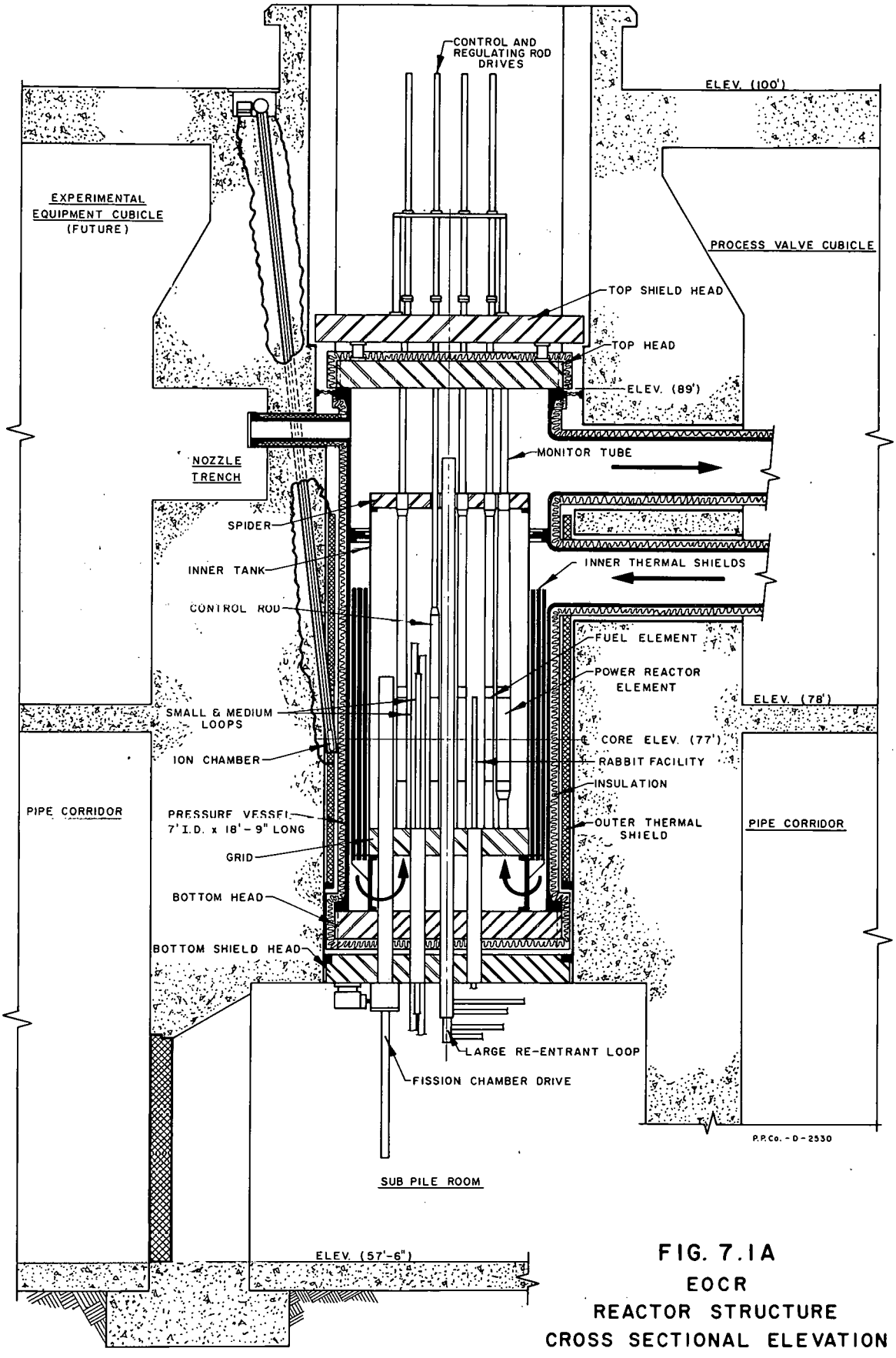

FIG. 7.1A
EOCR
REACTOR STRUCTURE
CROSS SECTIONAL ELEVATION

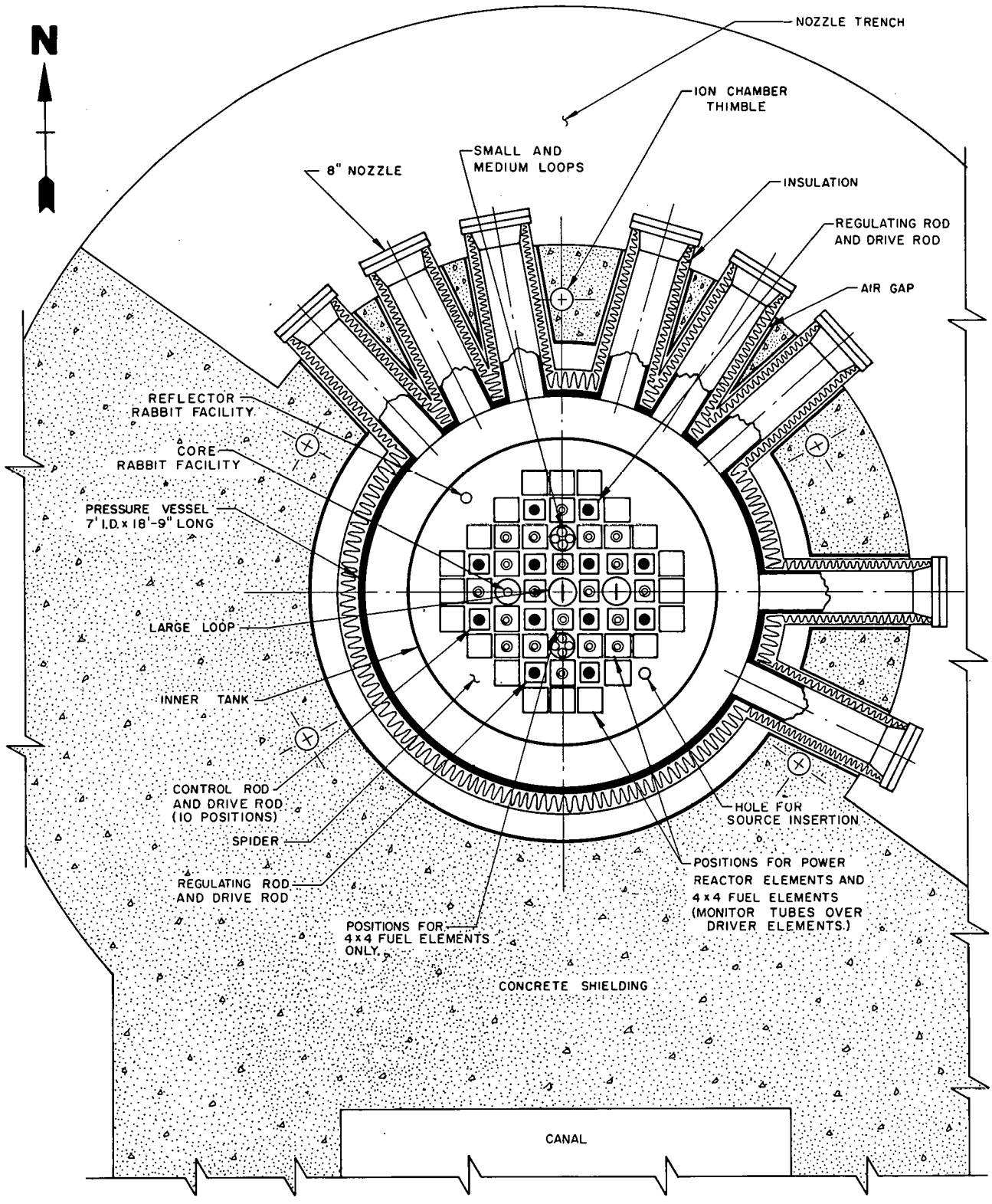

FIG 7.1 B

EOCR

REACTOR STRUCTURE

HORIZONTAL SECTION THROUGH NOZZLES

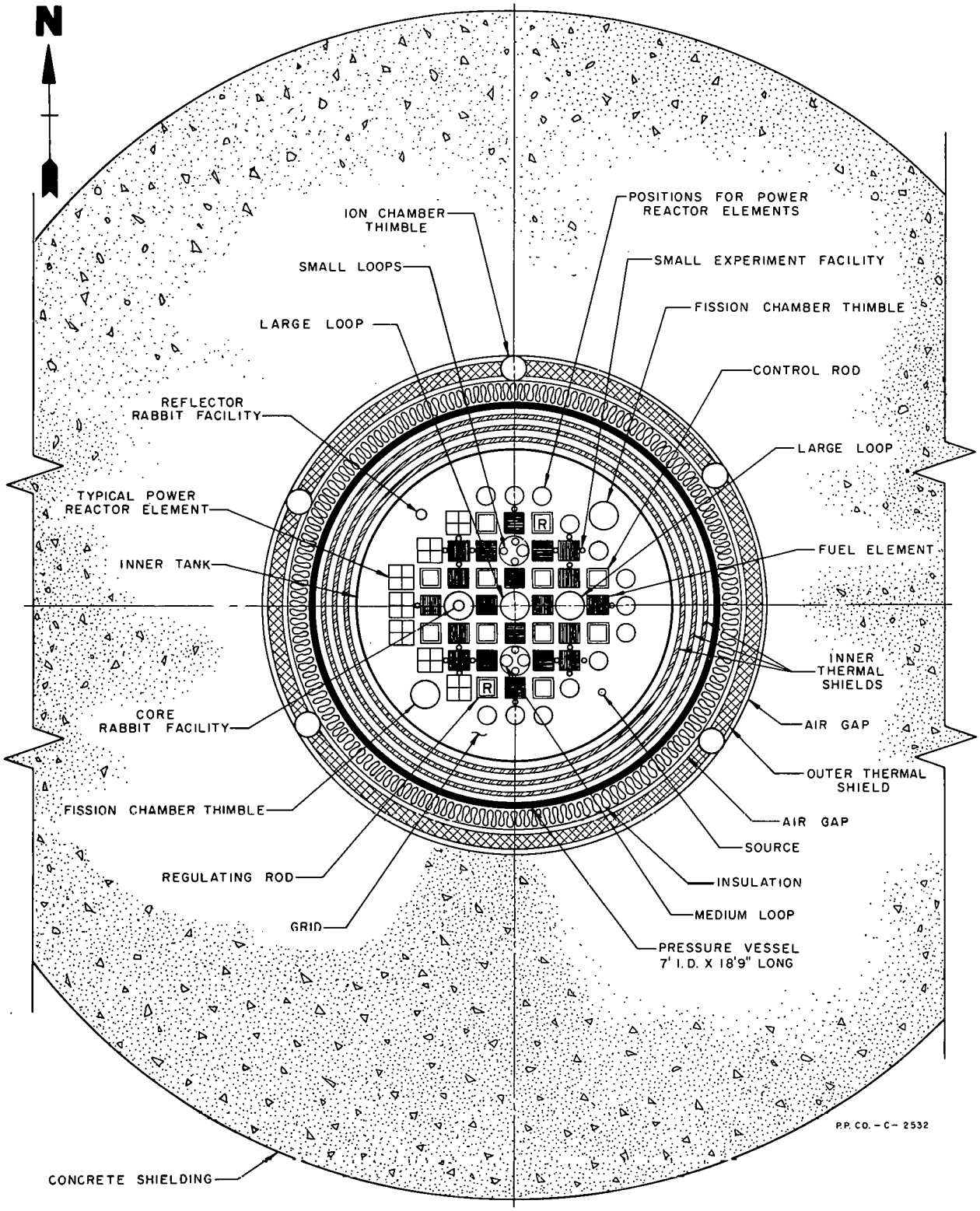

FIG. 7.1 C

E O C R

REACTOR STRUCTURE

HORIZONTAL SECTION THROUGH CORE CENTERLINE

7.200 Reactor Post-Shutdown, Handling, and Pre-Startup Procedures.

Since the EOCR reactor is cooled and moderated by organic coolant which is opaque and solidifies at elevated temperatures (approximately 300°F for Santowax R or OMP), considerable effort has been expended in an attempt to eliminate or simplify the blind handling procedures and elevated temperature conditions now contemplated for some proposed organic power reactors. As a direct result of this effort, it appears feasible to purge the organic from the reactor tank with hot (350°F) demineralized water, displace the hot water with ambient temperature high-pressure demineralized water, and conduct all in-tank handling and other operations under water which is at room temperature. The term "water-flooding" is applied to this procedure. Tests performed to demonstrate water flooding feasibility are discussed in Section 12.000. The following sections will discuss the reactor shutdown, flushing, and handling procedures involved in the operation of the EOCR.

7.210 Reactor Post-Shutdown Procedures. After the reactor has been shut down, the organic coolant will continue to be circulated while the coolant and tank temperatures are reduced at controlled rates to a temperature of approximately 350°F. The reactor tank and a small section of primary coolant piping are then isolated by closing the main primary coolant-loop block valves. The next operation is to displace the organic in the reactor tank with water. Fig. 7.4E shows the equipment associated with the water-flooding operation. Valves at the top and bottom of the reactor are opened, and hot demineralized water will force the organic from the reactor tank to the degassing tank. After the organic in the reactor tank has been displaced by hot water, cold high-pressure demineralized water is pumped into the bottom of the reactor tank at controlled rates, displacing the hot water back to the water-flooding storage tank and reducing the temperature to 180°F or less. The water-flooding valves are then closed, the water level in the reactor tank is dropped 6 to 8 inches, and the reactor top head is removed to dry dock.

7.220 Reactor Handling Procedures. Those experimental loops in which fuel elements, samples, or capsules are scheduled for changeout during the reactor shutdown will also be purged with hot water and then filled with cold demineralized water at the same time or after completion of water-flooding of the reactor tank. After the reactor top head is removed to dry dock, the loop top closures will be opened, instrumentation leads broken, etc., preparatory to removal of the experimental samples.

After completion of the above operations, the 14-ft deep reactor pit located immediately above the reactor tank is filled with demineralized water. (See Section 7.190 for description of the reactor pit.) The isolation bulkhead between reactor pit and water-filled canal may then be removed, allowing direct transfer of fuel elements, control rods, experimental samples, etc., from the reactor to storage racks located in the canal. Hot samples stored in the canal,

but scheduled for reinsertion in the reactor, would be transferred to the reactor and inserted into their respective sample positions.

Since all reactor handling is to be conducted through demineralized water, it is not expected that handling problems connected with the EOCR will be any more severe than those connected with any test reactor. As in any reactor, special allowances must be made for in-pile tube insertion and removal, but it is expected that these in-pile tubes will be installed on a semi-permanent basis, and that experimental equipment will be designed to adapt to the in-pile tubes available. Section 8.111 discusses insertion and removal of in-pile tubes.

After all "hot" transfers have been effected between the reactor and canal, the bulkhead is replaced in the canal and the reactor pit is drained to the plant sump. Cold fuel and experiments may now be placed in their respective positions, experiment loop top closures re-installed, and experimental instrumentation leads routed out of the reactor vessel via the nozzles located near the top of the reactor tank. In the case where the experimental instrumentation lead drawbar penetrates the reactor top head, the instrumentation lead would be connected after the top head is replaced on the reactor.

7.230 Reactor Pre-Startup Procedures. After the reactor top head has been installed and experimental instrumentation connected, hot demineralized water from the water-flooding storage tank is again admitted at the top of the reactor vessel at controlled rates. The cold water in the reactor tank is drained to the plant sump for disposal.

After the reactor tank and bulk coolant reach a temperature of approximately 350°F, the degasifier-pressurizer system pump is started. This pumps organic at 350°F into the reactor tank and displaces the hot water back to the water-flooding storage tank. After the hot water has been displaced and the reactor tank is again full of organic, the degassing system processes the organic in the reactor tank to remove any water that has been trapped in the vessel and piping. (For detailed descriptions and flow diagrams of the water-flooding system and degasifying system, refer to Sections 7.470 and 7.430 of this report).

After completion of the above procedures, the main coolant loop block valves may be reopened, and the reactor may be brought to temperature and begin nuclear operation.

7.300 Reactor Controls and Instrumentation.

The instrumentation system may be divided into three main categories for purposes of discussion: the control system which utilizes three modes of shim rod actuation to allow automatic operation of the reactor under pre-set conditions; the safety system which functions to protect the reactor throughout all conceivable operating situations, intended or accidental; and auxiliary instrumentation which provides control on peripheral functions necessary for continuous pre-set operation of the reactor. The above mentioned functions are discussed in Sections 7.310 through 7.330.

7.310 Control System. The control system provides a means for continuously measuring the power level and indicating the neutron flux level in the reactor and a means of controlling both their long and short time variations.

7.311 Power Level Instrumentation. The ultimate measurement of reactor power is, of course, a calorimetric measurement. The reactor power may be determined continuously by the multiplication of the main coolant flow rate by its temperature rise across the core and the appropriate constant. Measurement of the flow rate is accomplished by the placement of a Gentile tube or orifice plate in the main coolant line. The differential pressure across the orifice plate is converted by a transmitter to an electrical signal which is directly proportional to the flow rate. Such a device is non-linear and is specially designed for the purpose. These transmitters are in common use and are available commercially. The temperature rise (ΔT) is measured by standard means, with either thermocouples or resistance bulbs being used. The output signals from the flow and ΔT are then multiplied analogically by electronic instrumentation. A periodic check on the power level may be obtained by reading both variables from strip-chart recorders, accurate to $\pm 0.25\%$. The resulting hand calculation thus may be computed to $\pm 0.50\%$. In this reactor several resistance bulbs are used in order to allow better averaging of the inlet and outlet temperatures, thereby reducing the effect of stratification of the coolant in the piping. The block diagram for this system is shown in Fig. 7.3A.

The other indications of reactor power level come from neutron-sensitive ionization chambers. These are relative indications and vary as the neutron flux distribution changes throughout the reactor for a constant integrated reactor power. This flux distribution may change for various changes in control rod position as the control rods are withdrawn to compensate for fuel burnup and for changes in experimental loading. Two of these chambers indicate the neutron flux on a six-decade logarithmic scale and the other three indicate on a linear scale reading from 0 to 150% of full reactor power. These are the same ionization chambers shown in the reactor safety instrumentation in Fig. 7.3B.

A sixth ionization chamber connected to a differential galvanometer as shown in Fig. 7.3C allows a more sensitive indication of the drift of power level than can be obtained by normal full scale indication. A carefully controlled zero offset allows a very sensitive measurement. In addition, with batteries as the high voltage supply, the system is also used as a failure-free power level indication independent of ac power generation.

7.312 Power Regulating System. The reactor is controlled by the use of the 12 control rods distributed through the reactor core as shown in Fig. 7.1B. The coarse control is accomplished by adjusting 11 of these rods while the one remaining rod is used to automatically control the power level. These control rods are the fuel-follower type where a neutron absorbing material is gradually replaced by a fuel section as the rod is pulled out of the reactor core. This is accomplished by operator demand on the 11 coarse control rods as the reactor control system allows.

The one remaining control rod, which can be chosen as desired, is connected to a servo control system such as that shown in Fig. 7.3D. The rod inserts and withdraws from the reactor core to damp small reactor power fluctuations as dictated by the servo control system. The ionization caused by neutrons in the compensated ion chamber allows current proportional to the neutron flux to flow through the motor-operated rheostat. The rheostat acts as a set point to produce a voltage from the ion current that is balanced against a fixed voltage in the servo amplifier. As the rheostat is varied a different power level is determined and the motor drives the control rod in a manner to allow a correction to be made to bring the voltage in balance. Two decades of power level are controlled by the servo system.

This type servo system, where a relatively large slow-moving control rod is used as the servo rod, is not a high performance system. This requires that sufficient analysis of the heat generation in the system be made to assure that under any conceivable experimental condition, the low performance servo control is sufficient to protect the reactor against any potentially destructive incident up to the point where the safety system takes over that responsibility. For a system such as that described in this conceptual design, the most satisfactory arrangement is to simulate the reactor, the control system, the reactivity effects such as rod movement, temperature coefficient, and external disturbance, and response times on an electronic analogue device. The kinetic behavior can then be evaluated and adjusted such that this overlap in control protection is obtained. This will be accomplished in the detailed design.

The motor drive on the one control rod used in the servo system merits special discussion. The servo system may be one of two types. It may be a proportional controller or an on-off controller. The proportional controller requires a motor which varies

in speed proportional to the error derived at the input to the servo system. The on-off controller uses a fixed speed motor which turns on at a constant speed at a given amount of error in the servo network, continues at that constant speed until the error returns below the given amount then turns off. The proportional controller usually allows more constant control of the reactor power. However, a carefully designed on-off controller will allow control of the reactor power to better than 0.5%.

In the case of the EOCR the choice of one of the twelve control rods for the servo system will probably be one of the outside eight rods. Since these are worth about 1.25% in reactivity, approximately the upper one-third of the rod will be used as the operating region of the servo control. This rod will move with a rate that will give it an over-riding rate of change of reactivity per unit time compared to any of the other control rods. This will allow a continuous withdrawal or insertion of a control rod with the servo control rod maintaining the servo error at essentially zero. Otherwise, the servo rod cannot catch up until withdrawal or insertion has stopped which is an undesirable operating characteristic.

For operational convenience the motor must be considered carefully in the detailed design. The motors chosen for all rods may be of the type that will allow changing of the number of poles (and thus the speed) on the stator by merely rearranging the windings with a relay switching arrangement. This will allow the one rod chosen as the control rod to be, say, doubled in speed by a mere switching choice. A second technique is the use of a wound rotor ac motor whose speed can be changed by inserting a resistor in series with the armature. Thus all rods except the one servo rod can be cut to half-normal speed. A third technique is to switch motors mechanically for the control rod chosen to be the servo rod. This, perhaps, is not as operationally desirable as the other two prospects. The desired operating characteristics of motor speed, however, can easily be attained.

7.320 Safety System. The safety system receives its activation from fission chambers and gamma-compensated ionization chambers which, either separately or in combination, provide a continuous indication of the neutron level in the reactor from the cold clean reactor (with neutron source) to greater, for example, than 150% of full power rating. These channels are adjusted to initiate shutdown of the reactor for unsafe operating conditions in whatever region of neutron level the reactor is operating.

7.321 Startup Instrumentation. The startup instrumentation consists of two channels of counting rate instruments to count the fissions in two fission chambers. The output from the log-count-rate meters as shown in the block diagram in Fig. 7.3E is recorded. On the recorder there are microswitches set so that the

control system will not allow the reactor to start up without having at least one of the count rate channels reading on-scale. These channels allow observation of the neutron flux in the cold clean reactor region with a reasonable size neutron source from which to multiply.

7.322 Mechanical Safety Rods. The same rods referred to as "Control Rods" in other portions of this report are also the safety rods, any of which render the reactor subcritical upon being inserted. Rapid insertion of these rods is called a "scram". An appropriate signal from the reactor safety instrument discussed in Section 7.323 will modify the rod-holding characteristics of the suspending mechanism sufficiently to cause a rapid insertion (scram) into the core. The means for allowing this to occur depends on the particular control rod drive design.

7.323 Safety Instrumentation. The safety instrumentation for the reactor makes use of many of the desirable features in the MTR. The block diagram of the safety instrumentation is shown in Fig. 7.3B. The signals from three level channels and two period channels originating from five separate neutron sensitive ionization chambers are tied to a common sigma bus. This sigma bus acts as an input signal to the nonlinear rod release amplifiers. The rod release amplifiers have characteristics such that as the input from the sigma bus goes either up above a certain voltage or down below a certain voltage, the output signal to the rod holding or latching mechanism goes down. Thus, for reactor power increasing and the resulting sigma bus voltage increase, or for shorting of the sigma bus resulting in a voltage decrease, the output signal decreases sufficiently to release the safety rods into the reactor. This system is commonly referred to as the "Fast Scram" or "Electronic Scram" instrumentation since it can occur in the millisecond range and does not require any mechanical relay operation. The "Slow Scram" and "Reverse", discussed in the following paragraphs, are usually initiated by recorder level switches using relays.

It is necessary to emphasize reasons for the application of either the reverse or scram in a reactor of this type. If the reactor core were to be only of one type, and further, if this type is not modified substantially, a set of non-variable limits could be established for such parameters as coolant pressure, temperature and flow rate and, as a back-up, the neutron flux level. There should be adequate flexibility for the operators to set these limitations according to each individual core, after detailed engineering calculations have substantiated these numbers. The same considerations should govern the use of these power reductions as dictated by the conditions under which the various experimental loops will be operated. The method by which an experiment can shut down the reactor is discussed in Section 7.335. There are, however, some corrections which must take place (if necessary) in the routine startup of any reactor. Among these are startup period limitation, and interlocks to assure the core adequate startup source strength. Table 7.3A contains some parameters and suggested set points.

Table 7.3A

CORRECTIVE SIGNALS

Corrective Action	Parameter
REVERSE	Neutron Level > ~ 1.3 N_F*
	Thermal Power Level > ~ 1.3 N_F
	Coolant Temperature
	Coolant Flow
	Coolant Pressure
	Manual Operation above $3N_L$ **
	High Radiation Level at Coolant Outlet
	Experiment Interlocks
	Reactor Period < 5 Seconds
SCRAM	Neutron Level > ~ 1.5 N_F
	Reactor Period < 1 Second
	Thermal Power Level > ~ 1.5 N_F
	Coolant Temp. < 350°F, > 1.5 N_F
	Coolant Pressure
	Coolant Δ P
	Coolant Flow
	Loss of Instrument Voltage
	Loss of Purchased Power
	Loss of Relay Bus Voltage
	Experimental Interlocks

* $N_F \triangleq$ Full Power

** $N_L \triangleq$ 1% Full Power

The Reverse is an action, the purpose of which is reduce power by running the rods in by their drive motors. Reactivity is reduced approximately uniformly until the actuating condition is relieved. When the trouble condition has been relieved the rods will stop driving in, but the reactor will then be subcritical, perhaps by a per cent or two, and the reactor power after a typical incident will be down by two or three decades depending, of course, on how long the rods have been reversed. The reactor is left in a condition from which it is easy to recover and the original operating conditions can be reached with minimum difficulty and time.

The Scram is the final and most drastic corrective action which may be taken by the control system and results in complete shutdown. The ultimate safety of the reactor depends on the existence of numerous independent means for achieving the scram so that the probability of simultaneous failure of all is made vanishingly small.

In the Table 7.3A an experimental interlock allows the choice of any of the two corrective signals desired.

Thus, calculations are made of possible incidents that may occur for each individual experiment inserted in the reactor. The same criteria are used as are used in the evaluation of the servo system and its overlap with the scram system discussed in Section 7.312. The choice of the corrective signal required is made and when the experiment reaches that particular limit of temperature, pressure, etc., the corrective action is taken.

7.330 Auxiliary Instrumentation.

7.331 Process Instrumentation. All important process variables are recorded and displayed in the appropriate locations. Since this instrumentation is fairly standard and straightforward as related to reactor operation and control, it is not detailed here.

7.332 Fission Break Monitoring Instrumentation. There are two fission break detectors, one on the vapor outlet on the degassing tank and one on the stack. The degassing tank monitor will see direct radiation increase from degassing of the organic coolant within approximately a minute after the coolant has passed through the reactor. It is expected that a direct radiation technique is satisfactory for this measurement as compared to the integrating technique used on the stack. The stack has this same gas plus 16,000 cfm of air from the cubicles passing through it. Scintillation counters with totalizers are used for both gas and particulate monitors. The instantaneous level of each is recorded in the control room.

7.333 Health Physics Instrumentation. Both direct radiation and/or air monitoring is performed in each unit area of the EOCR layout and all indications are remotely indicated and some recorded in the Health Physics office. These monitor types are standard in reactor areas and need not be considered in detail in this report.

Adequate protection is provided for personnel monitoring including hand and foot counters and friskers for direct radiation detection at entrances to the reactor building.

7.334 Auxiliary Thermocouples. With the temperatures encountered in the organic coolant, the structure temperatures for the reactor can be high. Thermocouples will be located at many points in the container vessel, thermal shields, lead shield, concrete biological shield, etc., in order to allow monitoring of pertinent points. These will be recorded on multi-point recorders.

7.335 Experiment Interlocks. Near each experiment cubicle is located a panel with a switch and multiconductor plug for access to the reactor supervisory safety system (scram, reverse). The conduit carrying these wires will connect each cubicle to the instrument room.

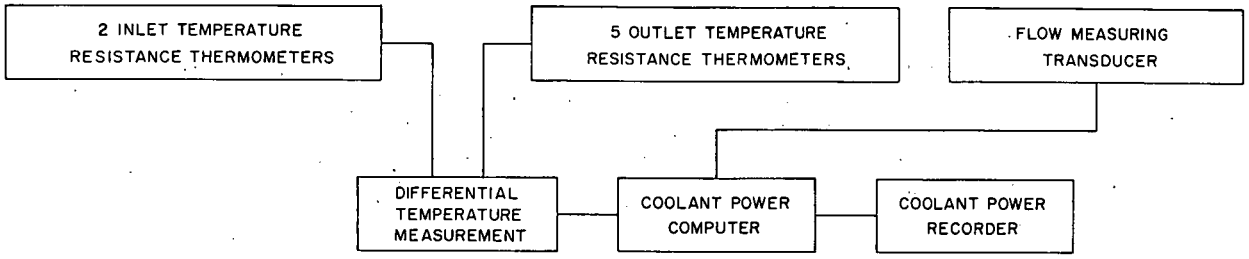

FIG 7.3A

POWER LEVEL INSTRUMENTATION

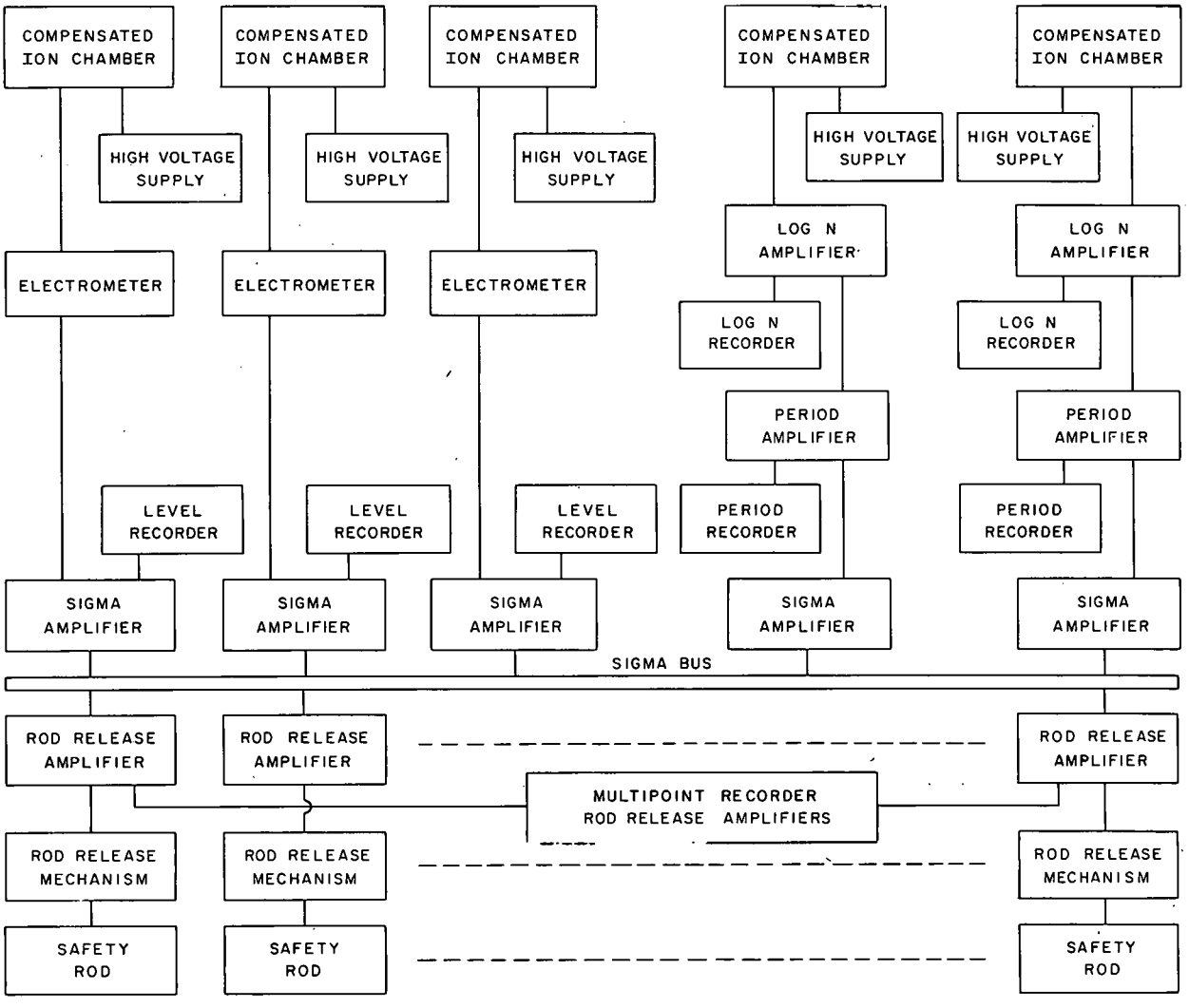

P.P.CO-C-2515

FIG. 7.3B

REACTOR SAFETY INSTRUMENTATION

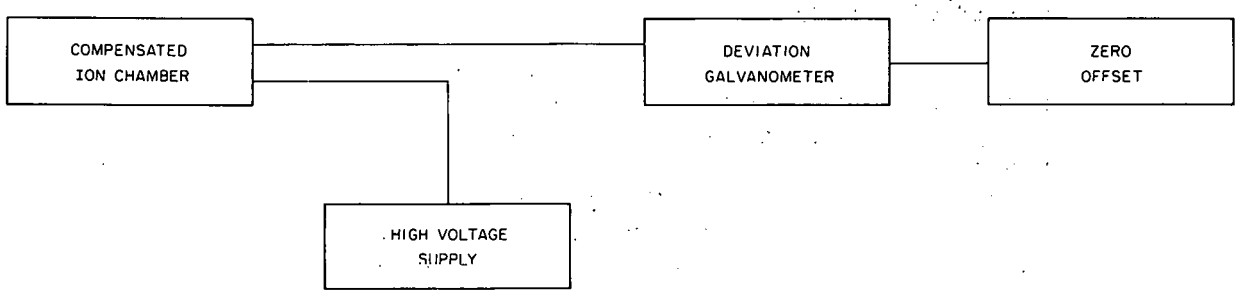

FIG. 7.3C

DIFFERENTIAL GALVANOMETER

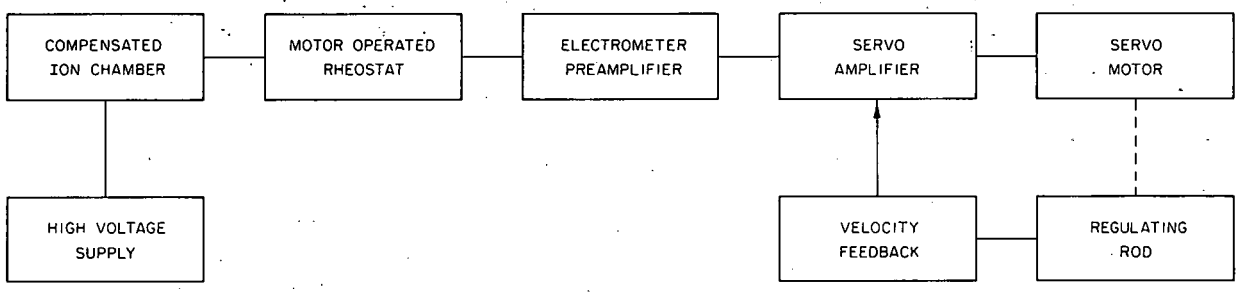

FIG. 7.3D

POWER REGULATING SYSTEM

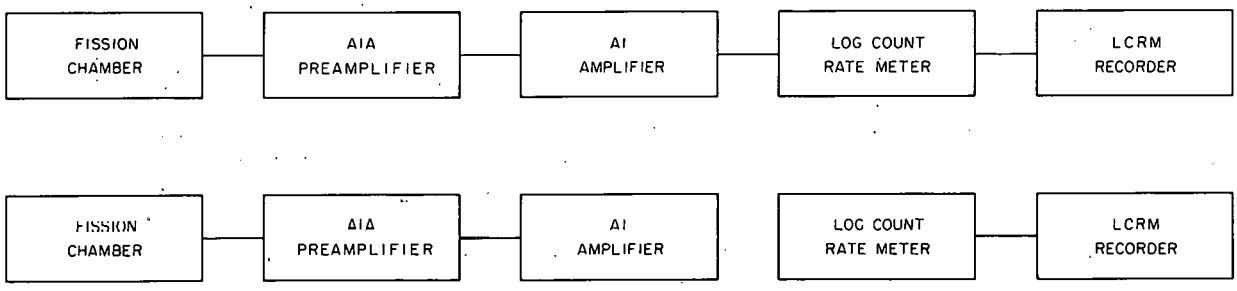

P.P. CO.-C-2516

FIG. 7.3E

STARTUP INSTRUMENTATION

7.400 Primary Coolant System

The reactor coolant system components are designed to provide sufficient organic coolant flow to adequately cool the reactor core as well as to dissipate the thermal energy of the reactor to the atmosphere in a safe and efficient manner. The primary loop is designed to remove 45 Mw of heat at a flow rate of 25,000 gpm with a reactor inlet temperature of 500°F and an outlet temperature of 526°F. Systems for maintenance of coolant gas, HB, and water content are included in this section as well as the pressurizing system for the primary coolant system.

7.410 Primary Coolant Loop (Fig. 7.4A). The primary coolant system provides the necessary facilities to remove the heat generated in the reactor core. The system is designed for a maximum heat load of 45 Mw at the normal operating conditions of 500°F reactor inlet temperature, 526°F outlet temperature, 25,000 gpm flow and 150 psig pressure, and the system is designed for a maximum pressure of 300 psig at a temperature of 850°F.

The system includes one main circulating pump, a liquid-to-forced-air heat exchanger, a pressurizing and degassing system, a purification system, valves, and instrumentation necessary to safely cool the reactor fuel elements under normal and emergency operating conditions.

The primary pump (25,000 gpm, 170 ft tdh, 1250 hp) discharges coolant through the main 24-in. loop piping, through a butterfly control valve and a main inlet block valve into the reactor vessel. The coolant flows down through the internal thermal shield, up through the reactor core, and out of the 24-in. outlet pipe. The coolant then flows through the main outlet block valve and the Gentile flow tube to a finned-tube forced-draft air heat exchanger where the reactor thermal heat is dissipated to the atmosphere. The coolant, after being cooled in the heat exchanger, returns to the suction side of the main coolant pump.

A 500-gal capacity surge tank is connected to the main 24-in. coolant piping on the pump discharge to dampen pressure transients which could result due to rapid coolant temperature fluctuations, when the reactor is scrammed.

The system is pressurized by means of two pressurizing and degassing pumps (200 gpm, 550 ft tdh, 40 hp), one of which is a spare. The pumps take suction from a 10,000-gal capacity degassing tank, and discharge coolant into the main system near the suction side of the main coolant pump. The flow from the two degassing and pressurizing pumps is measured by means of an orifice which, via a flow recorder-controller, positions a flow control valve to maintain a constant flow from the degassing system into the main 24-in. coolant loop. Organic is bled from the main loop system via a 3-in. pressure control valve

positioned by means of a pressure recorder-controller which senses the reactor coolant inlet pressure. The volume of coolant flowing through the back pressure control valve to the degassing tank is equal to the volume of liquid being pumped into the main system continuously by the pressurizing pump, so that a constant primary coolant pressure is maintained. More details of pressurizing system are given in Section 7.430.

7.411 Heat Exchangers. Three finned-tube heat ex-exchangers, mounted on structural steel supports west of the reactor building at an elevation of approximately 60 ft above the reactor core center are connected in parallel to the 24-in. reactor outlet line; Coolant from the three heat exchangers discharges into the 24-in. pump suction piping. Coolant from the reactor flows through the tubes of the heat exchanger and is cooled by forced-draft fans which blow air across the finned tubes. Specifications for the heat exchangers are as listed in Table 7.4A. Since future reactor operation may be at higher than design temperature, the performance of these exchangers was calculated for several outlet organic temperatures at a 25,000 gpm organic flow rate and the results are summarized in Table 7.4B.

The reactor coolant temperature is controlled by a temperature recorder-controller which automatically positions the heat exchanger top shutters to vary the air flow as required. Commercial power failure, or low reactor coolant flow, automatically completely opens the top shutters for maximum cooling at this time. An override to this feature is provided so that the shutters can be manually closed after the coolant temperature has decreased sufficiently. The reactor is scrammed by low coolant flow and loss of commercial power; Shutdown cooling is provided by thermal circulation since no emergency cooling pumps are provided. A manual by-pass valve is installed around the heat exchangers so that the coolant can be circulated through the primary system with the heat exchangers shut off.

An oil-fired heater equipped with a blower is mounted below the heat exchangers so that the coolant in the exchangers can be melted if it has solidified while the reactor is down.

7.412 Primary Pump. The primary coolant pump is a four-stage vertical in-tank unit which pumps the coolant from the heat exchangers into the reactor tank. The pump is mounted outside the reactor building in a pump pit connected to the primary pump tunnel.

Specifications for the pump are given in Table 7.4C.

Table 7.4A

HEAT EXCHANGER SPECIFICATIONS

Liquid Data	
Specific gravity at 500°F	0.95
Specific heat, Btu/lb-°F	0.50
Flow, lbs/hr	11.9×10^6
Inlet temperature, °F	526
Outlet temperature, °F	500
Heat exchanged, Btu/hr	154×10^6
Air Data	
Elevation, ft	5400
Air temperature, maximum ambient, °F	100
Flow, lbs/hr	2.74×10^6
Materials and Construction	
Tubes	Seamless Steel
Heat transfer area, ft^2	1.295×10^5
Overall heat transfer coefficient, Btu/hr-ft^2-°F	4.18
Log mean temperature difference, °F	290
Design pressure, psig	300
Design temperature, °F	1000

Table 7.4B

ORGANIC TEMPERATURE VS HEAT EXCHANGER CAPACITY*

Organic Temperature Leaving Heat Exchangers, °F	Organic Temperature Difference, °F	Heat Removal Capacity, Mw
500	26	45
600	33	57
700	39	68
800	46	80

* The assumptions used are: (1) the air and organic mass flow rates are constant, (2) the specific heat of the organic and air are constant at 0.5 and 0.25 Btu/lb-°F respectively, and (3) the overall heat transfer coefficient is constant.

Table 7.4C

PRIMARY PUMP SPECIFICATIONS

Type	Vertical Turbine
Stages	Four
Design Pressure	300 psig
Head, ft	170
Flow	25,000 gpm
Temperature, °F	1000
Material	Stainless Steel
Connections	Flanged, 300 psig
Seals	Double-Mechanical Non-Leaking
Motor, hp	1250
volts	2400
phase	3

Although the use of only one pump for pumping the primary coolant may result in some reactor down time, proper preventative maintenance during scheduled reactor shutdowns will reduce this down time to a minimum; however, some unplanned shutdowns are anticipated from pump component failures. One pump is most economical and, because it eliminates pump headers and isolation and check valves, it results in a simpler system.

7.413 Valves. The two main 24-in. block valves on the main loop piping are constructed of stainless steel because these valves must be corrosion resistant to the hot demineralized water used in the flooding operations. The valves are located in a valve pit in the reactor building and are accessible for servicing by removing a hatch cover. The valves are motor-operated from the process control room and are also equipped with hand wheels for manual manipulation. Position interlocks on these valves, connected to reactor instrumentation, prevent closing the valves while the reactor is at power or starting the reactor if either of the two valves is closed.

The flow-control valve is a butterfly valve which is motor-operated and manually controlled. This valve is also equipped with reactor instrumentation interlocks to prevent closing the valve while the reactor is at power or starting the reactor while the valve is closed. This valve is capable of withstanding total pump head so that the pump can be started with this valve closed, after which the valve is slowly opened until the required flow is established.

7.414 Instrumentation. The primary coolant system instrumentation is designed to measure and control flow, pressures, and temperatures which are necessary for safe operation of the reactor.

The required coolant flow is controlled by adjustment of the main process butterfly valve. The position of this valve is set prior to reactor startup with minor adjustments being made as the reactor is brought to operating power and the coolant temperature increases. The coolant flow is measured by means of a Gentile tube, and the flow is recorded in the process control room and the reactor control room. Reactor power reductions are initiated by low flow as measured by the flow tube.

Four resistance bulbs, located in the main inlet piping upstream of the butterfly valve, monitor the reactor coolant inlet temperature. This temperature is recorded in both control rooms, and the temperature recorder-controller positions the heat exchanger shutters to automatically maintain the required coolant inlet temperature. Loss of commercial power and low coolant flow overrides temperature control of the shutters so that maximum cooling is obtained under conditions of low flow or loss of commercial power.

Four additional resistance bulbs installed in the reactor coolant outlet line measure the coolant outlet temperature. Signals from the coolant-inlet and -outlet temperature recorders are transmitted to a temperature difference recorder whose signal is combined with one from the flow recorder, and the integrated flow and temperature difference is recorded on a power recorder. Reactor power reductions are initiated by high ΔT, high inlet or outlet coolant temperature, and by high reactor power. These parameters are recorded in both the reactor control room and the process control room.

The reactor coolant-inlet and -outlet pressures are also recorded in both control rooms. The inlet pressure recorder-controller positions the back pressure valve which is controlling the reactor coolant pressure. Loss of commercial electric power or low inlet coolant pressure closes the back pressure valve completely so that in an emergency coolant pressure is maintained.

The pressure drop through the reactor is measured and recorded and also initiates reactor power reductions when the pressure drop decreases to a preset level. This device serves as backup instrumentation for the flow recorder.

The pressure drop across the heat exchangers and the outlet temperature from each heat exchanger nozzle are recorded so that fouling or plugging of the heat exchanger tubes can be detected. No reactor power reductions are associated with these instruments.

Direct radiation instruments record the activity of the reactor inlet and outlet coolant, and high outlet radiation results in a reactor power reduction.

7.415 Surge Tank. A 500-gal surge tank located in the main coolant valve pit and connected to the 24-in. reactor-coolant inlet

line serves to dampen pressure surges in the coolant system. Nitrogen pressure is maintained above the coolant contained in this tank by means of a pressure-controlled nitrogen header. The nitrogen is supplied from six cylinders. Under normal operating conditions, the tank is two-thirds full of organic while the other third is nitrogen at system pressure at the discharge of the primary coolant pump. The surge tank is equipped with a level indicator, high- and low-level alarms, a pressure recorder, high- and low-pressure alarms, and a pressure-relief valve to prevent excessive tank pressures.

7.416 Miscellaneous Mechanical Design. The thermal expansion problem is a major consideration in this system because the piping and equipment will vary from ambient to 850°F. To eliminate large expansion loops in the system, expansion joints are installed as required with pipe guides, anchors, and hangers which are also designed to handle thermal expansion and contraction.

Four pressure relief valves are installed in the main process piping. Two of the four valves are located between the reactor vessel and the reactor main outlet block valve. The other two relief valves are located on the discharge side of the main coolant pump. These valves relieve into the coolant dump tank.

Drain valves, installed throughout the system at low points on the piping, permit draining the organic to the dump tank. Vent valves at all high points in the system piping provide a means of venting gases trapped in the system. Vents and drains are manually operated with no automatic features.

7.420 Emergency Shutdown Cooling. Cooling of the reactor under emergency conditions, i.e., loss of commercial power, is accomplished by natural circulation of the coolant in the main coolant loop. The heat exchangers, being mounted 60 ft above the core, provide the necessary hot and cold legs to effect natural circulation of the coolant on loss of the main coolant pump.

A difference of 25°F between the temperature of the coolant to and from the heat exchanger results in a density difference equivalent to a driving force of about 0.6 ft. This head is calculated to produce an initial natural circulation flow rate of 1100 gpm, (refer to Section 6.500) providing the pump does not add any resistance to flow when shutdown. The pump characteristics should be studied prior to establishing the final design of the system and provisions made to by-pass the pump if necessary for adequate natural circulation cooling after a commercial power failure.

7.430 Degasification and Reactor Pressurization (Fig. 7.4B and 7.4C). The degasification and reactor pressurization system is provided to (1) remove gaseous decomposition products which result from radiolytic and pyrolytic damage to the organic coolant, (2) remove water from the coolant which is introduced as a result of reactor water-flooding

operations, (3) maintain uniform pressure in the reactor and main heat transfer loop system and, (4) provide for thermal expansion of the coolant. The degasification vessel also serves as a reservoir for the displaced coolant during reactor water-flooding operations. (See Section 7.470).

7.431 Design Bases. The design bases for the degasification and pressurizing system are given below.

1. Pressurization. The system is designed to maintain reactor inlet pressures up to 300 psi.

2. Coolant Dewatering. The degassing system is designed to reduce the water content of the reactor vessel coolant from 4000 ppm to 600 ppm in a period of two hours prior to reactor startup while the system is maintained at a temperature of 350°F.

3. Coolant Degassing. The degassing system is designed to remove water remaining after the dewatering operation and up to 3.5 scfm of coolant decomposition gases by flashing 2 gpm of coolant and recovering the vaporized organic by partial condensation. Calculated soluble gas concentrations in the main coolant loop at 525°F and 850°F, as maintained by the degassing system, are shown in Table 7.4D.

Table 7.4D

CALCULATED DEGASIFIER OPERATING PRESSURES
AND MAIN LOOP GAS CONCENTRATIONS
AS A FUNCTION OF REACTOR OUTLET TEMPERATURE

Basis: 200 gpm flow to degassing system with 1% flashed.
Total Gas Generation: 0.5 scfm at 525°F and 3.5 scfm at 850°F

	Reactor Outlet Temperature	
	525°F	850°F
Degasifier Operating Pressure, psia*	1.2	53
Gas Concentration Maintained in Main Coolant Loop, cc(STP)/g Coolant	0.03	0.4
Saturation Gas Concentration at 50 psi Reactor Operating Pressure, cc(STP)/g Coolant	0.3	0.2
Saturation Gas Concentration at 150 psi Reactor Operating Pressure, cc(STP)/g Coolant	0.8	1.3
Saturation Gas Concentration at 300 psi Reactor Operating Pressure, cc(STP)/g Coolant	1.7	2.6

* Approximate only as pressure is varied as necessary to flash 1% of the feed flow. Actual operating pressure will vary depending on coolant composition, actual gas generation rates and coolant water content.

4. Coolant Expansion. The coolant system volume expands by about 4000 gal as the system temperature is increased from 350°F to 850°F. The degassing vessel is sized to hold this volume and still leave adequate free space for coolant degassing.

5. Filtration. Very few data are available on coolant filtration requirements for organic-cooled reactor systems at this time. It has been assumed for this design that filtration of the 200-gpm side stream flow to the degasifier through a 50-mesh screen filter will maintain the solids concentration in the reactor and main coolant loop system at an acceptable level. Finer filter media can be installed after reactor startup, if necessary.

7.432 System Description. The degasification and reactor pressurization system is a complete circuit originating in the reactor outlet piping and terminating in the reactor inlet piping. The flow of coolant from the degasifier is regulated to the desired flow rate by a flow controller located downstream of the pressurizing pumps. The pressurizing pumps discharge upstream of the main-loop coolant pump during normal operation and downstream of the main-loop reactor inlet block valve during the dewatering operation. Flow of coolant to the degasifier is regulated by a pressure control valve to maintain the desired operating pressure in the reactor core. When the bulk coolant temperature changes, the flow automatically varies to compensate for the volume change. Under steady-state operating conditions, the flows to and from the degasifier are equal. Two horizontal centrifugal pressurizing pumps are provided. Each pump is capable of delivering the design flow of 200 gpm.

The degasifier is a 10,000-gal horizontal carbon-steel tank fitted with spray headers, to facilitate diffusion of gases out of the organic feed stream, and a small steam heater provided to maintain a 350°F temperature during dewatering operations. The degasifier operates at pressures varying from about 1 psia to 60 psia, as required to flash 1% of the feed stream; its operating pressure depends on the composition and temperature of the entering coolant and is regulated by a pressure controller operating a control valve on the vapor outlet of the after condenser.

Vapors leaving the degasifier pass through a condenser, after-condenser, freeze trap, and water-vapor condenser to remove condensible vapors and are then discharged to the cubicle exhaust system through either of two 10-scfm sliding-vane vacuum pumps. The condenser and after-condenser are operated at exit temperatures approximately 75°F to 150°F and 200°F to 250°F lower than the degasifier operating temperature, respectively, and at the same pressure as the degasifier to condense the bulk of the organic from the vapor stream and return it to the degasifier. The freeze trap is operated at approximately 1-psia pressure with a 150°F outlet temperature. Under these conditions the organic vapors remaining in the vapor stream freeze out on the heat transfer surfaces, and the water vapor

passes on to the water vapor condenser where it is condensed at approximately 70°F. Two freeze traps are provided, each with a 150-lb organic capacity. The capacity of one trap is sufficient for the entire dewatering operation or for 24 hours of normal operation. When a trap is loaded, as indicated by inability to maintain the 150°F outlet temperature, the alternate trap is placed in service, and the organic in the loaded trap is melted and returned to the degasifier. Only one water vapor trap is provided because it will not be necessary to remove water vapors from the gas stream after the removal of water from the coolant following system startup. (The 50-gal water capacity is adequate for the entire dewatering operation).

Temperatures and pressures maintained by the control instruments when the degassing system is operating with the normal 525°F inlet temperature are indicated in Fig. 7.4B. The heat loads indicated in this figure are the maximum loads anticipated for the degassing or dewatering operations. Maximum ratings of the dewatering heater, freeze traps, and water-vapor condenser are determined by the requirements of the dewatering operation. Maximum ratings of the degasifier condenser and after-condenser are determined by the requirements of the degassing operation.

The coolant for the degasifier condenser and after-condenser must be at a temperature which is high enough to prevent freezing of the organic liquid. A 250 psi pressurized water system is used to supply high-temperature water for use as coolant. This system is also used to cool the purification still condenser and is shown in Fig. 7.4C.

Particulate matter (which may be present in the circulating coolant as a result of coolant decomposition, corrosion or debris remaining from construction) is removed in 50-mesh cartridge-type filters located upstream of the degasifier vessel. Provisions are made to allow the substitution of other filter media, such as sintered stainless steel cartridges, if filtration through a finer media proves necessary in the future.

7.440 Purification System (Fig. 7.4D). The radiolytic and pyrolytic decomposition of the organic coolant produces high-molecular-weight compounds (high boilers or HB) which must be removed from the coolant. The coolant purification system continuously removes these compounds by a vacuum distillation process. The system also removes particulate matter and decontaminates the coolant, as all solids and most of the radioactivity in the coolant remain in the still-bottom stream. In addition, all new coolant is processed through the purification unit before addition to the coolant system to insure that it is free from impurities.

7.441 Design Bases. The purification system is designed to separate 2000 lbs/hr of coolant feed containing 10% HB into a distilled product stream containing 1.5-wt% HB and a residue stream

containing 99.5-wt% HB. This design rate is adequate to maintain a 10% HB content in the coolant system at the maximum anticipated reactor operating temperature of 850°F. At normal reactor operating temperatures and higher coolant HB concentrations, the excess purification unit capacity is used to build up and maintain a 15,000-gal inventory of distilled coolant to allow rapid replacement of the entire coolant system inventory, if necessary.

7.442 System Description. Coolant is withdrawn from the main coolant loop, blended with the new coolant makeup stream, and fed at a controlled rate to the 130 kw electrically-heated still preheater. The preheater supplies the heat necessary to vaporize most of the feed stream. The heated feed enters the upper section of the vacuum distillation column where about 70% of it flashes to vapor. Both the preheat temperature and still operating pressure are controlled to give the desired exit vapor stream composition. Unflashed feed flows down through a packed stripping section where a countercurrent vapor stream rising from the reboiler strips the terphenyl concentration down to about 0.5 wt%. Reboiler heat is supplied by a 20-kw heater controlled from the still-bottom temperature. The flash section of the distillation column is 30 in. in diameter by 5 ft high with a tangential feed entry nozzle. The stripping section is 16 in. in diameter by about 12 ft high with an 8-ft-high packed section of 1-in.-by-1-in. Raschig rings.

The HB residue stream leaving the bottom of the distillation column flows to the 100-gal HB receiver vessel. From this vessel it is pumped to the HB storage tank where radioactivity is allowed to decay before it is ultimately discharged to drums for burial.

Vapors from the top of the distillation column are condensed in the still condenser and flow to the distillate receiver, from which the distillate is pumped to the distilled-coolant storage tank. Distilled coolant from this tank is pumped back to the coolant system via the degassing tank as necessary to maintain the desired coolant system inventory.

Temperatures and pressures shown in Fig. 7.4D correspond to the operating requirements for the normal entering coolant temperature of 525°F. At entering feed temperatures above 700°F, the still operating pressure must be increased in order to keep more than the desired quantity of coolant from flashing and thus increasing the HB content of the distillate. At an entering feed temperature of 850°F, the still operating pressure will be maintained at about 5 psia.

The degassing-system vacuum pumps are the vacuum source for the purification unit. The distillate condenser is cooled by high-temperature pressurized water from the system described in Section 7.430.

7.450 Receiving, Storage and Makeup Systems (Fig. 7.4D). New coolant is received from the manufacturer at a rate of about 7500 gallons per month in tank trucks. The coolant is melted within the truck by means of a contained steam coil and discharged to the new-coolant storage tank. The capacity of this tank (15,000 gal) is equivalent to a two-month supply. The new coolant is pumped to the purification unit from the storage tank via a 5-gpm pump as required to maintain the distilled-coolant storage-tank inventory at the desired level.

A 15,000-gal distilled-coolant storage tank is provided to receive purified coolant from the purification unit. This tank maintains a distilled coolant inventory large enough to completely displace all coolant from the reactor and main coolant loop. Coolant from this vessel is normally pumped via either of two 5-gpm makeup pumps to the degasifier tank at rates controlled to maintain the degasifier tank at the desired operating level. Coolant from this vessel can also be pumped directly into the system via the 100-gpm coolant fill-pump. This routing is used during initial filling operations or when it is desired to displace contaminated coolant from the system. The distilled coolant tank is blanketed with dry nitrogen to prevent the coolant from absorbing water during storage.

High-boiler wastes from the coolant purification system are stored in a compartmented 10,000 gal storage tank to allow time for the decay of the radioactive components of this stream before it is loaded into drums for disposal by burial. Average holdup time for the wastes in this tank is about 30 days. Drum loading is accomplished via a 5-gpm positive-displacement pump.

A 15,000-gal system dump tank is provided to contain the entire reactor and main coolant loop coolant inventory should it become necessary to drain the system for maintenance or to displace contaminated coolant. Coolant from this tank may be routed back to the main coolant loop via the 100-gpm system fill pump or to the purification unit via a 5-gpm feed pump.

The new-coolant and distilled-coolant storage tanks are located above ground outside of the reactor building. The high-boiler-residue storage tank is located underground in the same area outside the building. The system dump tank is located underground next to the subpile room under the reactor building. All of these vessels and their connecting lines are steam-traced and insulated to keep the contents above the 310°F freezing temperature of Santowax R.

7.460 Insulation and Steam-Tracing. The piping and equipment in the process system (except for heat exchangers) is insulated to minimize heat losses so that air temperatures in cubicles and pits do not become excessive, and thermal heat in the equipment is conserved when the reactor is not operating. An additional function of insulation is to permit melting the organic with a minimum steam load to the steam tracing.

Piping with a nominal diameter of 2 in. or larger is insulated with a high-temperature insulation made from calcined diatomaceous earth, magnesium carbonate and binders. This insulation material is covered with eighty-five per cent magnesia. Piping with a nominal diameter of less than 2 in. is insulated with high-temperature insulation only, and no eighty-five per cent magnesia covering is used to cover the high temperature insulation. Tanks and vessels are insulated in a manner similar to that used to insulate large piping.

Steam-tracing is installed on all organic piping and equipment so that the organic does not freeze during reactor shutdowns and can be melted in piping and equipment in case it solidifies.

The steam-tracing is banded to the piping and equipment and the tracers are covered with a heat-conducting cement to increase the effective heat transfer area between the tracing and the piping and equipment. Steam to the tracing is manually controlled as needed. Traps are installed to adequately drain the condensate from the tracing, and pressure relief valves are installed on the tracing to prevent excessive steam pressures if water is trapped in the tracing lines when the coolant temperature increases above 350°F.

7.470 Water-Flooding (Fig. 7.4E). When the reactor is shutdown for in-tank work, the primary coolant will continue to be circulated until the temperature of the organic coolant is reduced to 350°F. The reactor tank is then isolated from the primary coolant system by closing the 24-in. main block valves. The water-flooding valve at the top of the tank is opened, and the remotely operated motor valve at the bottom of the reactor tank is slowly opened. Hot demineralized water at 350°F to 375°F flows from the water-flooding storage tank into the top of the reactor, displacing organic from the reactor tank into the degassing tank. The organic continues to flow out the bottom of the tank while 350°F demineralized water flows in the top. Flow is maintained at about 200 gpm until all of the organic has been transferred from the reactor tank to the degassing tank. When hot water begins to flow out the bottom of the tank, a pressure increase on the pressure gauge down stream of the motor valve is noted due to flashing of the hot water down stream of the water valve. Flow to the degassing tank increases as the 350°F water flashes down stream of the motor valve. At this time, the bottom drain valve is closed to prevent water from entering the degassing tank. The 2-in. drain line containing organic and some hot water is now isolated from the 3-in. degassing line and drained to the system dump tank. The two 24-in. primary coolant lines between the main 24-in. block valves and the tank are also drained to the system dump tank until water appears in the sight glasses, and then the drain valves are closed.

The reactor tank and 24-in. coolant piping to the block valves now contain 350°F water. The water flooding pump is now started, and the cold demineralized water is admitted to the 2-in. tank

drain line at 100 to 200 gpm as indicated by the high-pressure demineralized water flow indicator. The hot water in the reactor tank is displaced into the water-flooding storage tank, until the reactor-tank water temperature has been reduced to 180°F or less. At this time, the top and bottom flooding valves are closed, the high pressure demineralized water pump is shut off, the tank water level is lowered 6 to 8 inches, and the top head is removed to dry dock. That section of the canal over the reactor vessel is filled with demineralized water at a flow rate of 1000 gpm. When this section of the canal is full, the bulkhead is removed, and fuel transfer and in-tank work are started.

When all in-tank work is completed, the bulkhead is replaced in the canal, the canal section over the reactor is drained, and the top tank closure is replaced. Hot demineralized water from the water-flooding storage tank is again admitted to the top of the reactor vessel, and the cold water is drained to warm waste. When the water in the vessel reaches a temperature of about 350°F (a steam injector is provided to supply additional heat to the water), the hot water flow is shut off, and a pressurizing pump is started which pumps organic at 350°F into the reactor tank, pressurizing the hot water back into the water-flooding storage tank. Four 2-in. check valves spaced around the top of the inner tank open by gravity when there is no flow in the reactor. When the main flow is raised to 25,000 gpm, the pressure drop across these checks will be equal to the core pressure drop which will close these valves. These valves are needed only when the organic is returned to the tank after water flooding so that the water between the outer tank and the inner tank can be purged out by organic. When the reactor vessel is full of organic, and all the hot water has been displaced, the degassing system processes the coolant in the reactor tank to remove any water that has been trapped in the vessel and piping.

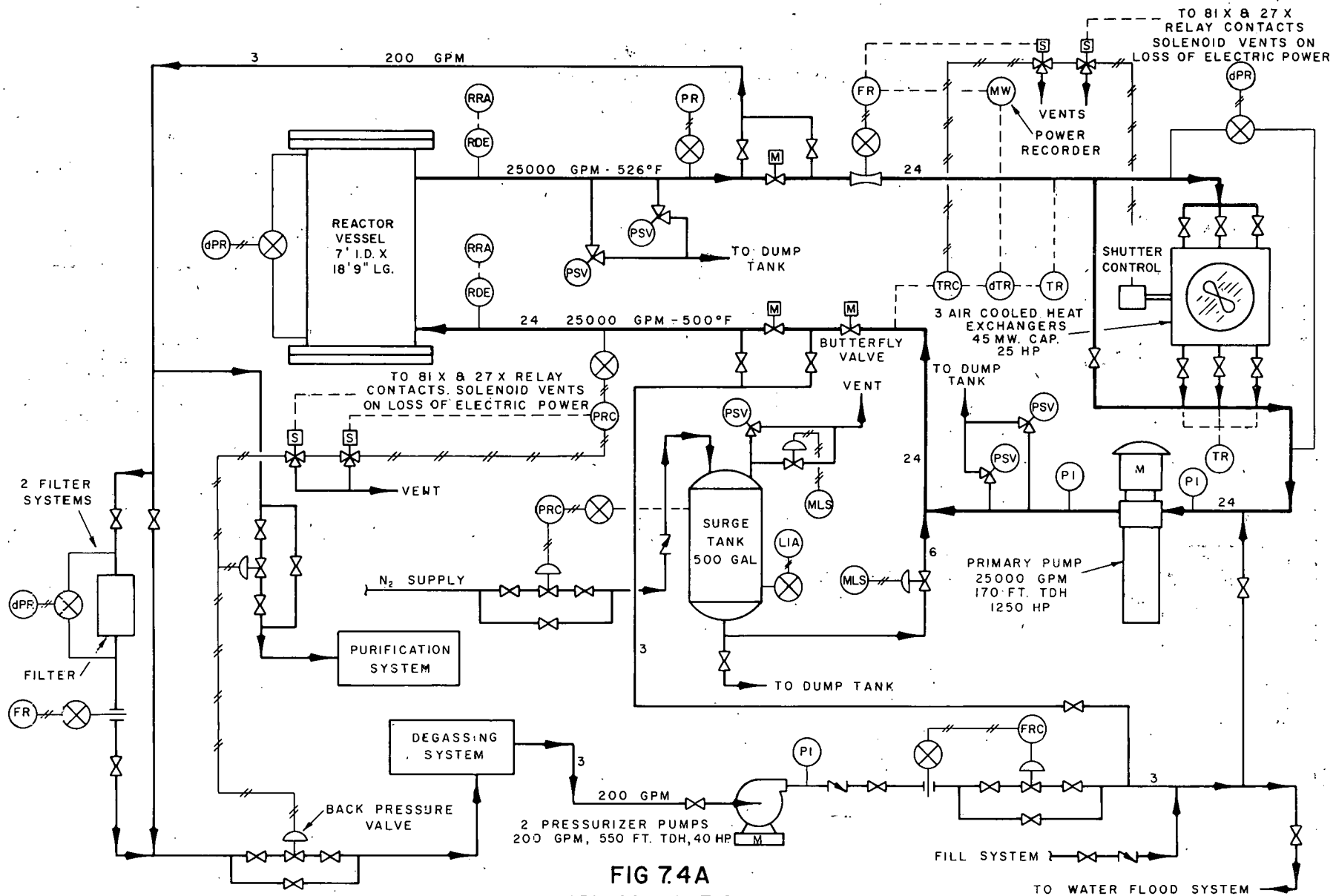

FIG 7.4A
PRIMARY COOLANT SYSTEM
FLOW DIAGRAM

P.P.CO.-C-2517

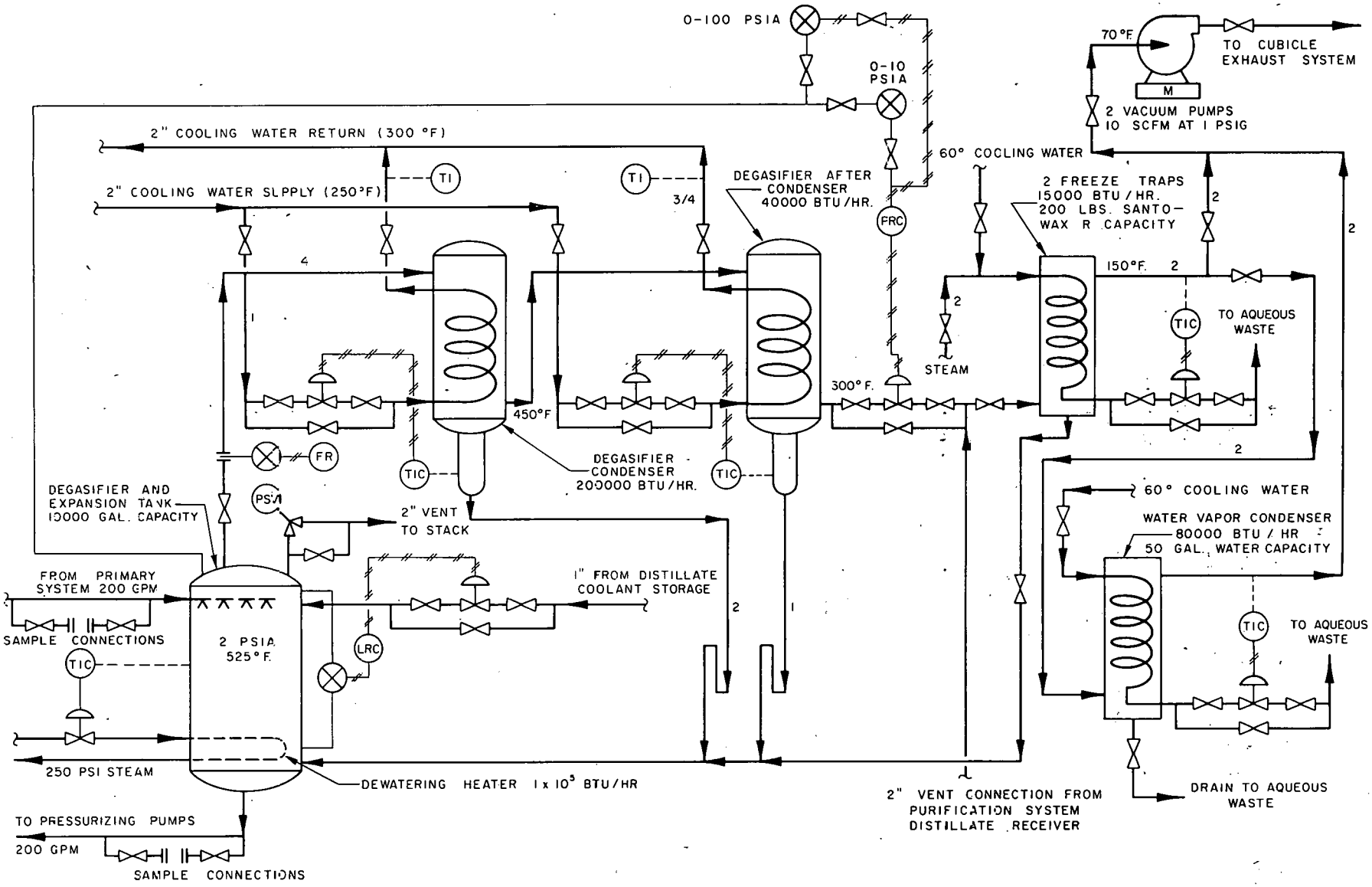

FIG. 7.4B

COOLANT DEGASSING AND DEWATERING SYSTEM FLOW DIAGRAM

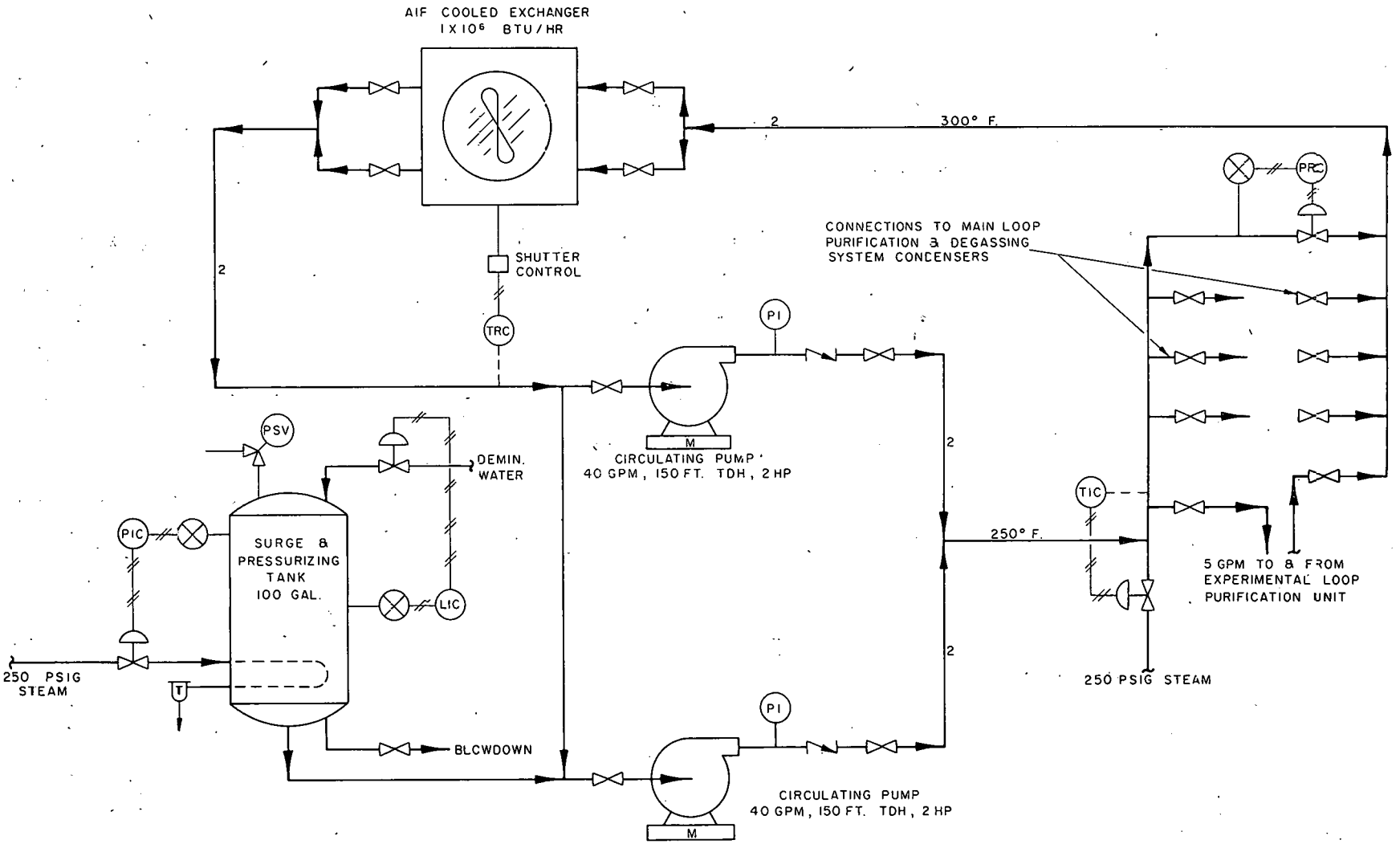

FIG. 7.4C

PRESSURIZED-WATER CONDENSER COOLING SYSTEM FLOW DIAGRAM

P.P. CO.- C-2519

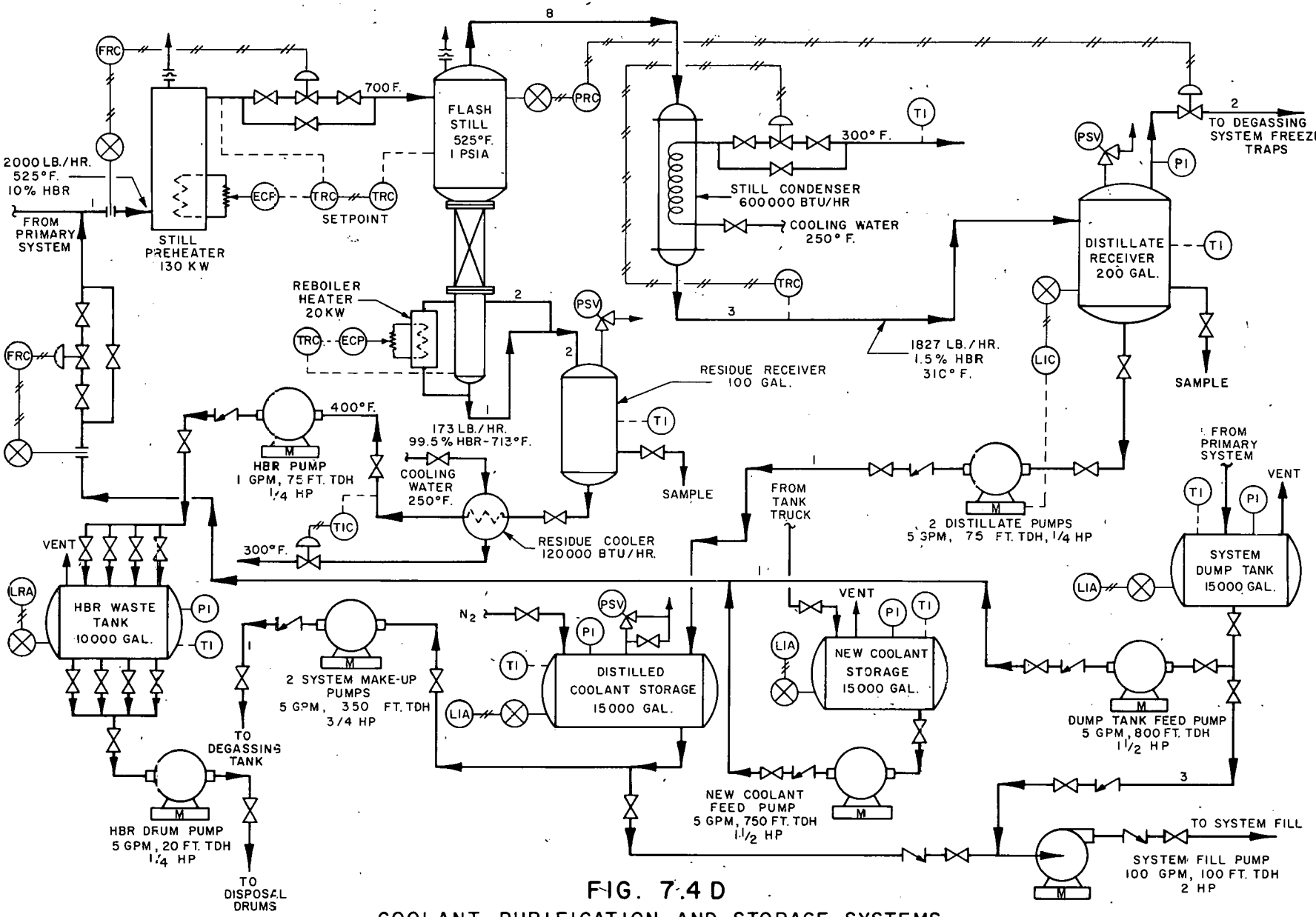

FIG. 7.4 D

COOLANT PURIFICATION AND STORAGE SYSTEMS

FLOW DIAGRAM

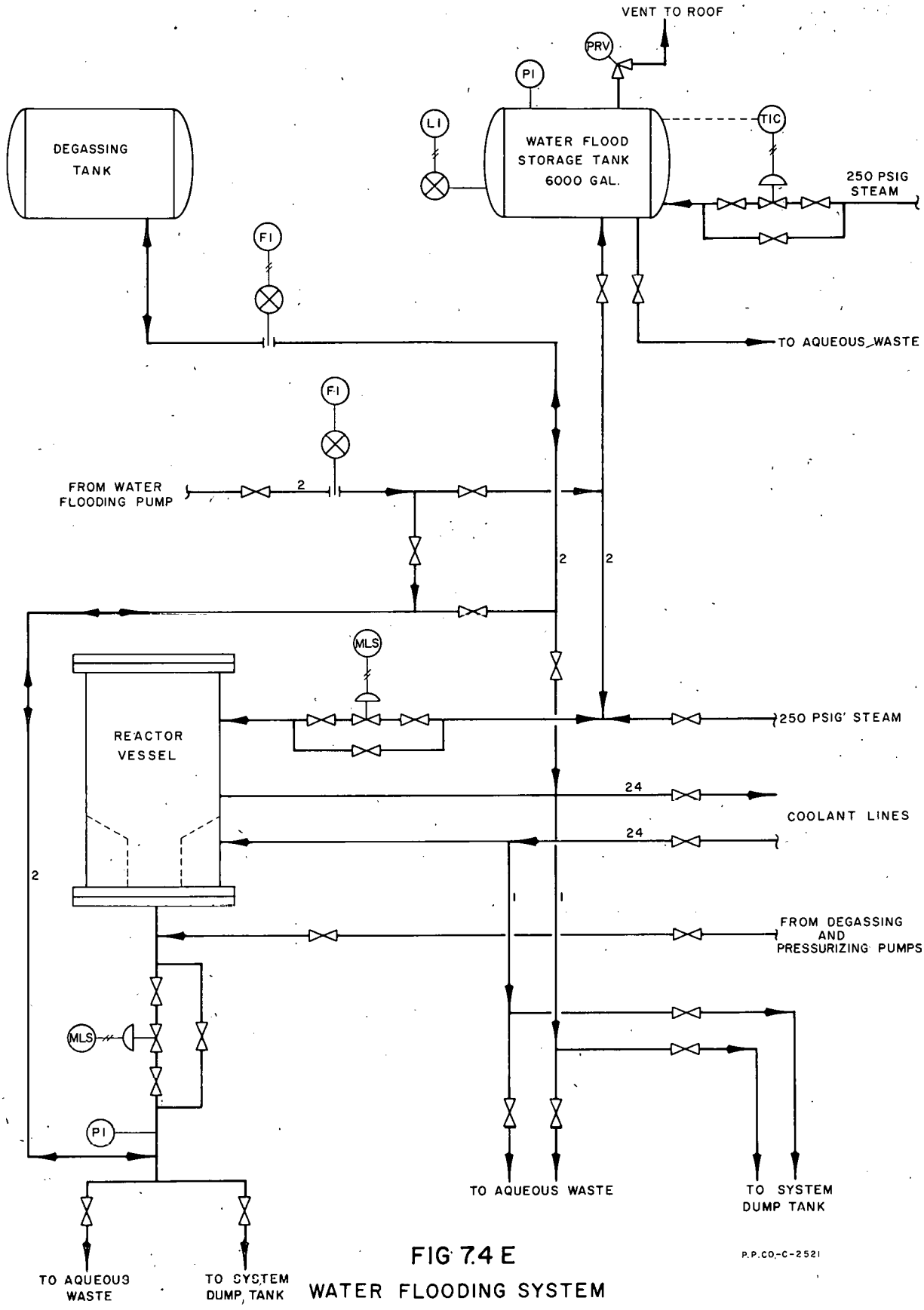

FIG 7.4 E

WATER FLOODING SYSTEM FLOW DIAGRAM

P.P.CO.-C-2521

7.500 Utilities (Summary given in Table 7.5A at end of section)

The EOCR site (except for commercial electrical power, organic coolant, fuel oil, and chemicals) is essentially self-sufficient. Water is pumped and treated at the site, air is furnished by motor-driven air compressors, heat is furnished by oil-fired boilers, aqueous wastes are disposed of in a leaching pond, and gaseous wastes are discharged to the atmosphere.

Commercial electric power is furnished from SPERT substation via a two mile 13.8 kva feeder; organic coolant, fuel oil, and chemicals are transported to the site by commercial carriers; telephone service is furnished by commercially installed and serviced telephones; and mobile fire protection is furnished by the NRTS fire department. Hot waste burial is provided at the existing NRTS burial ground.

7.510 Electrical Power (Fig. 7.5A). Electric power for the EOCR is provided by commercial NRTS power from SPERT substation and by a plant-installed motor-generator-battery unit, which provides failure-free power for 20 to 30 minutes after power failure.

7.511 Commercial Power. The total connected plant load is about 3400 kva. These loads are summarized in Fig. 7.5A.

7.512 Failure-Free Power. One 125 kw-generator, driven by a 200 hp electric motor, supplies the total failure-free power requirements for the plant and experiments. One 15-hp dc motor-driven 10-kw ac generator set supplies reactor instrumentation power. The batteries for this unit are charged by the 125 kw-generator set.

7.520 Water Systems.

7.521 Raw Water (Fig. 7.5B). Water from the deep well is pumped from 400 to 500 ft below grade by one deep well pump (500 gpm, 600 ft tdh, 100 hp). The water is chlorinated by means of an automatic chlorinator before it enters the storage tank. The water is stored in a 200,000-gal ground-level steel storage tank. The storage tank is equipped with a level indicator, high- and low-level alarms, and high- and low-level well pump starting switches. A bypass around the storage tank permits operation of the water systems when the storage tank is cleaned or repaired.

Two service water pumps (150 gpm, 175 ft tdh, 10 hp), one of which serves as a standby, furnish raw water for the sanitary requirements, demineralizer feed, air compressor cooling, air conditioner cooling, experimental requirements, and the purification system freeze traps.

Firewater to the building sprinkler system and the firewater loop which encircles the building is furnished by either of two 2000-gpm, 175 ft-head firewater pumps. The normal firewater pump is driven by a 125-hp electric motor and is started automatically whenever the firewater pressure decreases to 50 psig. A small line between the

service water system and the firewater system maintains pressure in the firewater system until a fire hydrant is opened or until the sprinkler system is actuated. The standby firewater pump is powered by a diesel engine and is started manually in the event of a power failure or failure of the normal firewater pump. Additional fire protection is provided by dry chemical systems for the experimental cubicles, the purification and degassing cubicle, and the pipe tunnel and pump pit.

7.522 Demineralized Water (Fig. 7.5C). Demineralized water for the canal, for the water flooding operation, for experimental heat exchangers, and for boiler makeup is provided by treating raw water in a conventional two-bed demineralizer. The demineralized water produced has a specific resistance of 200,000 to 500,000 ohms and a total solid content of one to two ppm. Two sulfuric acid regenerated cation units, one degasifier equipped with a blower, two degasified water pumps (60 gpm, 140 ft tdh, 2.5 hp)--one of which is a spare--and two caustic regenerated anion units produce 60 gpm of demineralized water. The demineralized water is stored in a 50,000-gal stainless-steel ground-level storage tank. The tank is equipped with an overflow, a water level indicator, and high-and low-level alarms.

Water for the laboratory, canal, experiments and boilers is furnished by either of two demineralized water pumps (75 gpm, 400 ft tdh, 10 hp). A third pump (200 gpm, 400 ft tdh, 25 hp) is used intermittently to supply demineralized water for the water flooding operation.

The canal purge is estimated to be 10 gpm, but, in case fast fill of a section of the canal is required, an 8-in. stainless-steel line from the demineralized water storage tank to the canal provides for filling at a rate of 1000 gpm or more by gravity.

One 1000-gal concentrated-sulfuric-acid-storage tank and one 1000-gal 50%-caustic storage tank, located outside the utilities section of the building, store sufficient demineralizer chemicals for a month or more of operation at a maximum flow rate. No acid or caustic transfer pumps are provided since the chemical proportioning pumps for anion and cation regeneration take suction from the bottoms of the storage tanks. The caustic tank is heated to 85°F by means of an internal steam heater to facilitate pumping.

7.530 Plant and Instrument Air (Fig. 7.5D). Two 200-scfm two-stage reciprocating air compressors, one of which is a standby, deliver air at 150 psig to a 1000-cu-ft air receiver. The two-inch plant air header is supplied directly from the receiver through a two-inch motor valve which automatically closes if the receiver pressure drops to 100 psig so that an adequate air supply is reserved in the receiver to operate instruments and motor valves. The instrument air is dried in one of two steam-regenerated silica-gel driers. The instrument air, after leaving the driers, is reduced to 100 psig by means of a pressure-controlled motor valve. Instrument air at 100 psig is delivered to the two-inch instrument

air header. Instrument air is further reduced to 15 or 30 psig by small locally mounted pressure reducing valves.

No emergency or failure-free power is supplied to the air compressors, because the air receiver is large enough to supply instrument air requirements for thirty to sixty minutes after power failure. This is estimated to be sufficient time to permit an orderly shutdown of the plant before all instrument air pressure is lost.

7.540 Steam Plant (Fig. 7.5E). Two 5000-pound-per-hour water tube boilers, one of which is a standby, are located in the utilities area. These boilers supply saturated steam to the plant facilities and the experiments via a 2.5-inch steam header. The boilers are packaged type, equipped with the conventional safeties and controls, and burn steam-atomized No. 6 fuel oil. Demineralized water is supplied for make-up.

Auxiliary equipment includes a 12,500-pound-per-hour deaerating feed water heater, two motor-driven feed water pumps (25 gpm, 700 ft tdh, 7.5 hp) and a 500-gal blowdown tank. Chemical feed systems are also provided to treat the boiler water with disodium phosphates for pH control and to treat the feed water with sodium sulfite for residual oxygen removal.

A 500-gal condensate surge tank located in the basement area serves as a collection and surge tank for the condensate return from the various facilities. Two motor-driven condensate pumps (25 gpm, 125 ft tdh, 1 hp) return the condensate from the tank to the feed water heater.

One motor-driven fuel oil unloading pump (50 gpm, 5 hp), two motor-driven fuel oil transfer pumps (2.5 gpm, 200 ft tdh, 0.5 hp), two duplex fuel oil strainers, and two fuel oil heaters are located in the oil pumphouse adjacent to the fuel oil storage tank.

The fuel oil storage tank has a storage capacity of 50,000 gallons. This storage volume is sufficient to fire one boiler at a maximum rate for a period of 30 to 40 days. The storage tank is insulated and equipped with a suction heater. The oil pumped to the boilers in excess of that burned is recirculated to the storage tank. Two displacement type meters, installed in fuel oil supply and return lines, measure the quantity of oil burned.

7.550 Utilities for Experiments. Raw water, demineralized water, pressurized water, instrument air, steam, cubicle exhaust air, failure-free and commercial power are supplied to the experiments by plant-installed utilities. The experimental utility requirements have been included in the estimates made in sizing the plant equipment. The quantities required for experiments are given in Section 8.500.

7.560 Heating and Ventilating System (Fig. 7.5F). For heating and ventilating purposes the building is divided into four general areas: (1) the reactor first floor and basement, (2) the reactor control and instrument rooms, (3) the office building, and (4) the utilities building. All areas, except the utilities area, are heated and ventilated by individual systems consisting of intake air filters, steam heating coils, blowers, and supply and return ducts. The utilities area is heated by wall-mounted unit heaters. Air conditioning is provided in the reactor control and instrument rooms; all other areas have summer ventilation only.

7.561 Reactor First Floor and Basement Areas. The heating and ventilating equipment for the reactor first floor and basement areas is located in the heating and ventilating room, which is in the basement below the office area. The equipment consists of an outside screened intake and intake plenum (common to three heating and ventilating systems), washable filters, steam heating coils (equipped with temperature-controlled dampers and by-pass dampers), two 16,000-cfm 15-hp blowers, and a supply duct to the reactor area first floor where the air is distributed through outlet grills.

The blowers are sized for six air changes per hour, three of which are return air during winter operation when 16,000 cfm of air is returned to the blower room from the reactor first floor area. For summer operation, no air is returned from the first floor area and 16,000 cfm of air is exhausted by two 30-inch roof-mounted exhaust fans (8000 cfm, 3 hp each).

Half of the 32,000-cfm supply air to the first floor passes into the reactor area basement through openings through first floor provided around the periphery of the area. All of the supply air to the basement is exhausted to the stack via the cubicle exhaust header and blowers. Since the experimental cubicles are located in the basement and are potential sources of air contamination, no air is returned from the basement area.

7.562 Reactor Control and Instrument Rooms. Six air changes per hour are supplied to the control and instrument rooms by one blower (1000 cfm, 1 hp). Supply air for the blower is taken from the intake air plenum through washable filters and steam heating coils which are provided with temperature-controlled dampers and by-pass dampers. The blower discharges through grilled openings in the supply duct in the reactor control and instrument rooms. The system for these rooms is a once-through system, and the inlet air is discharged through louvered openings in the doors.

Refrigeration coils in the inlet air duct cool the air for summertime operation. One 7.5-ton packaged refrigeration unit supplies the necessary cooling requirements of these two rooms.

7.563 Office Area. The office area heating and ventilating equipment consists of washable filters, steam heating coils (which are equipped with temperature-controlled dampers and by-pass dampers), and one supply blower (3000 cfm, 2.5 hp). Four air changes per hour, two of which are return air during the winter, are provided. For summer operation, all of the supply air leaves the building through windows and doors.

7.564 Utilities Area. The utilities area is heated by two wall-mounted unit heaters. The units are equipped with inlet and recirculating dampers that are manually controlled. The two blowers (2400 cfm, 1 hp) provide for two air changes per hour. Two roof-mounted exhaust fans (4500 cfm, 1.5 hp) provide six air changes per hour for summer ventilation purposes.

7.570. Waste Disposal. All aqueous wastes are disposed of at the EOCR site using plant installed facilities. Solid wastes and HB are disposed of by transporting them to the NRTS burial ground. Gaseous wastes are exhausted to the atmosphere through a stack for dilution with atmospheric air.

7.571 Gaseous Waste. (Fig. 7.5G). The total volume of air supplied to the reactor basement area is exhausted by means of two cubicle exhaust blowers (8000 cfm, 15 hp) which discharge to a 30-inch diameter steel stack mounted on the building roof. A suction header, consisting of 24-in. and 36-in. diameter pipe, is installed near the basement ceiling and along the basement walls. Six 12-inch nozzles with adjustable dampers are connected to the experimental cubicles and the one experimental purification cubicle, and exhaust 1000 cfm from each of these cubicles. These volumes of air enter the cubicles from the general basement area. Four 12-inch nozzles with adjustable dampers exhaust the basement area directly. One 20-inch nozzle exhausts 4000 cfm from the primary coolant pipe tunnel and the pump pit.

A 14-inch nozzle is provided to exhaust 1500 cfm of air from the purification and degassing cubicle. Another 14-inch nozzle which terminates on the reactor area first floor is provided to exhaust the reactor pit when the top closure is removed. An estimated 1000 cfm of air is exhausted from the subpile room. The building sump is also vented to this header, but the volume exhausted from this source is small.

The total quantity of gas discharged to the stack is measured and recorded in the process control room. Gaseous and particulate activities are also measured and recorded in the process control room.

7.572 Aqueous Waste (Fig. 7.5H). The aqueous plant wastes (from the utilities area, the reactor area, the laboratory, and the canal overflow and drains) flow by gravity to a 3000-gal concrete sump located below the basement floor. The sump is vented to the cubicle exhaust header to eliminate the possibility that gaseous activity might contaminate the basement air. Two sump pumps (250 gpm, 100 ft tdh, 10 hp), one of which is a spare, pump the aqueous wastes from the sump to a 6-inch vitrified clay line through which the waste flows to the leaching pond. A level indicator controller automatically stops and starts the sump pumps. When a sump pump starts, a small sampling pump also starts and continuously samples the waste being discharged to the leaching pond so that a representative waste sample is collected and is analyzed for radioactivity. Elapsed time meters actuated by the pump motor starters indicate the pump running time so that the gallons of waste discharged from the sump can be calculated.

The demineralizer wastes, being highly corrosive, are discharged directly to the vitrified clay line and are not discharged to the building sump. Waste piping within the building is constructed of cast iron. Demineralizer sump drain lines are Duriron, and yard piping is vitrified clay.

The sanitary wastes drain to a 6-inch concrete sewer main and flow by gravity to a concrete lift sump at the west end of the site. Either one of two level-controlled sewage lift pumps (50 gpm, 50 ft tdh, 1 hp) discharges the sewage to a fenced stabilization pond located west of the main plant area. The sewage pond is constructed above grade and has an area of about one acre. The dikes and bottom are compacted to minimize percolation. The stabilization pond effluent flows through a 4-inch concrete pipe to the leaching pond. The overflow is controlled by means of a shear gate installed in the overflow line so that the depth of the pond can be varied.

7.573 HB Disposal. HB, after sufficient decay time in the HB storage tank, is pumped to 55-gal used oil drums and shipped to the NRTS burial ground. At this time it does not appear economically sound to install a boiler for burning HB.

7.574 Radioactive Solid Wastes. The disposal of all solid radioactive wastes is made by transporting the wastes by truck to the NRTS burial ground.

7.580 Communications. The communication system consists of four main parts. Two-way intercom units with call buzzers are located in all normal working areas and at all experimental control panels, and are connected to a master station in the reactor control room. The paging system utilizes the intercom system with additional paging horns.

Two sound-powered circuits are also installed to provide communications from the experimental control panels and remote areas to the reactor control room.

A manual automatic-coding fire alarm system is installed and consists of alarm boxes connected to a centralized relay and terminal strip unit. Low firewater pressure, low raw-water-storage-tank level, starting of the fire pump, activation of a dry chemical system or the sprinkler system, is coded and annunciates at the NRTS central fire station as well as at the plant area.

The above communication systems supplement a commercially installed and serviced telephone system which is connected to the existing NRTS commercial system.

7.590 Nitrogen Blanketing. The primary-coolant surge tank is blanketed with nitrogen supplied from a nitrogen header which is supplied by six nitrogen bottles. The header pressure is reduced from cylinder pressure to required pressure by means of a reducing valve. The surge tank is protected from overpressure by means of a suitable pressure relief valve installed on top of the surge tank. High- and low-pressure alarms are also installed on the nitrogen header.

A dry nitrogen blanket, at two-inch water gauge, is provided on the distilled-coolant storage tank to prevent the absorption of atmospheric moisture. Twenty nitrogen cylinders, connected to a header, furnish the nitrogen through a pressure-reducing valve to the storage tank. A pressure relief valve and a high-pressure alarm, installed on the nitrogen header, protect the storage tank from over pressure. No nitrogen blanketing has been provided for the other storage tanks. These tanks are vented to the atmosphere. The fire and explosion hazards associated with this type of venting system should be further investigated.

Table 7.5A - SUMMARY OF UTILITIES

Electric Power	
Commercial, 13.8/2.4 kv	3,400 kva
Failure-Free, 480 volts	125 kva
Raw Water	500 gpm
Demineralized Water	60 gpm
Plant and Instrument Air	200 cfm
Steam, 250 psig	5,000 lb/hr
Gaseous Waste	250 gpm
Leaching Pond	10,000 ft^2
Sewage Stabilization Pond	1 acre

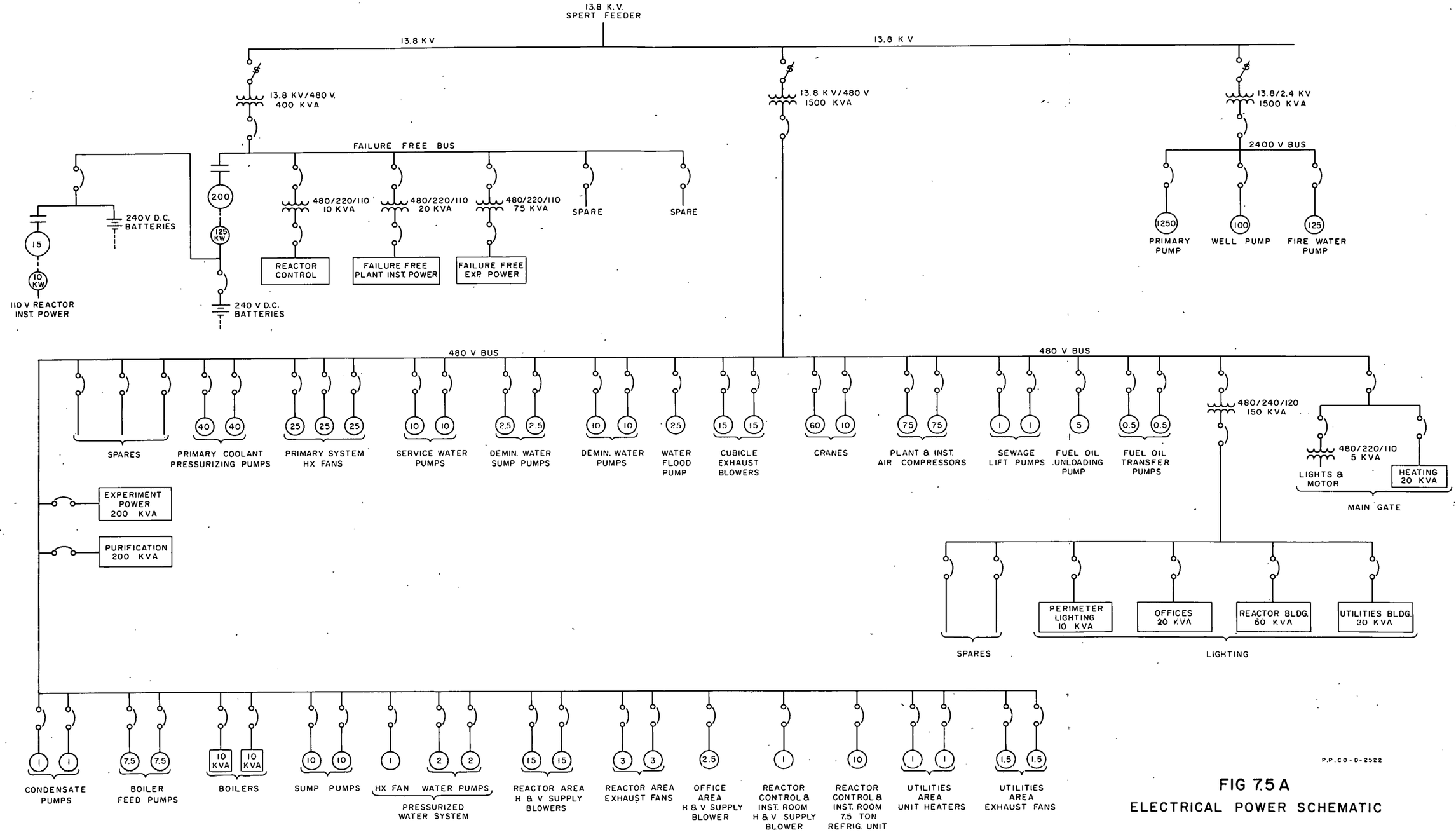

P.P.CO-D-2522

FIG 7.5 A

ELECTRICAL POWER SCHEMATIC

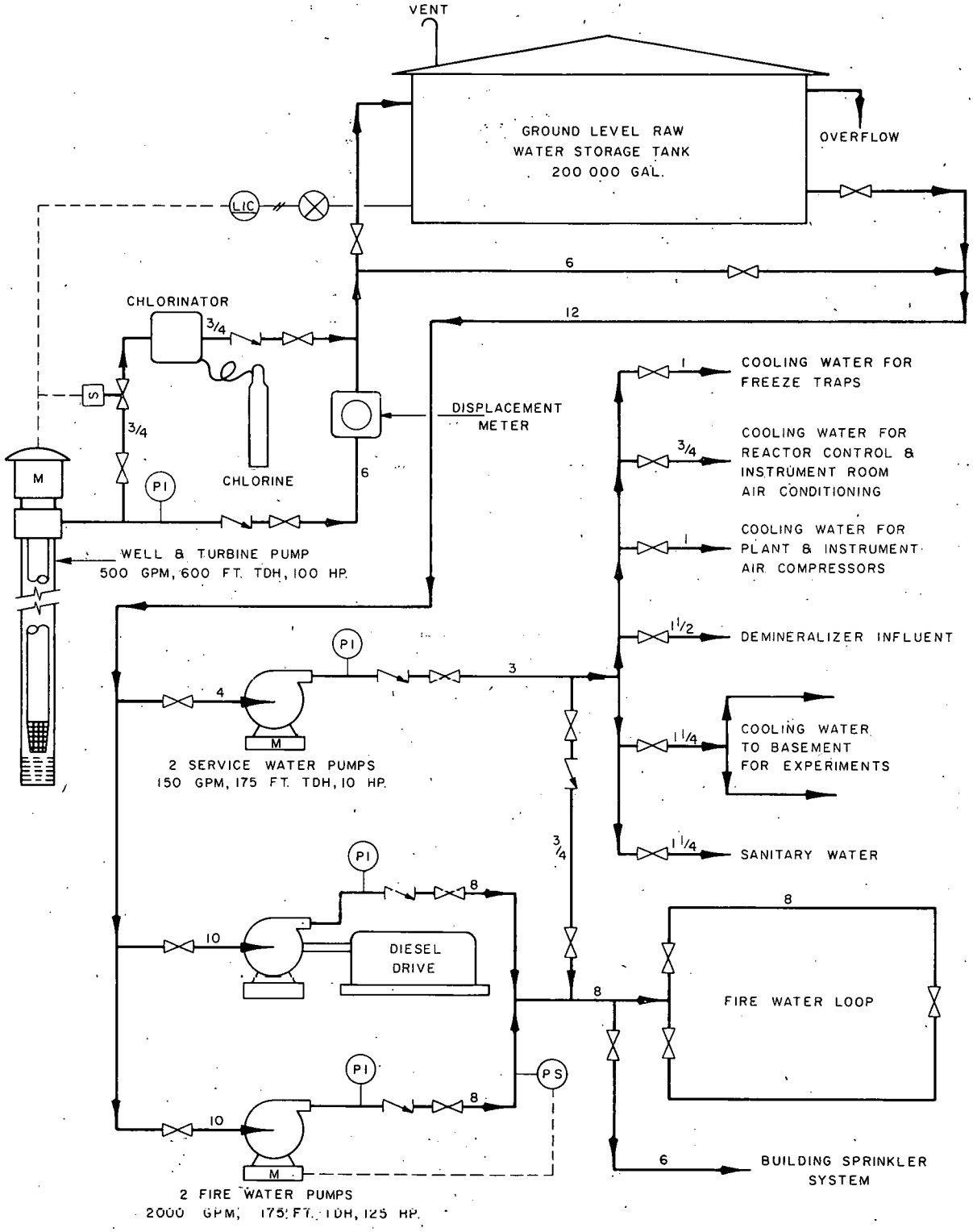

P.P.CO.-C-2523

FIG 7.5B

RAW AND FIRE WATER SYSTEMS

FLOW DIAGRAM

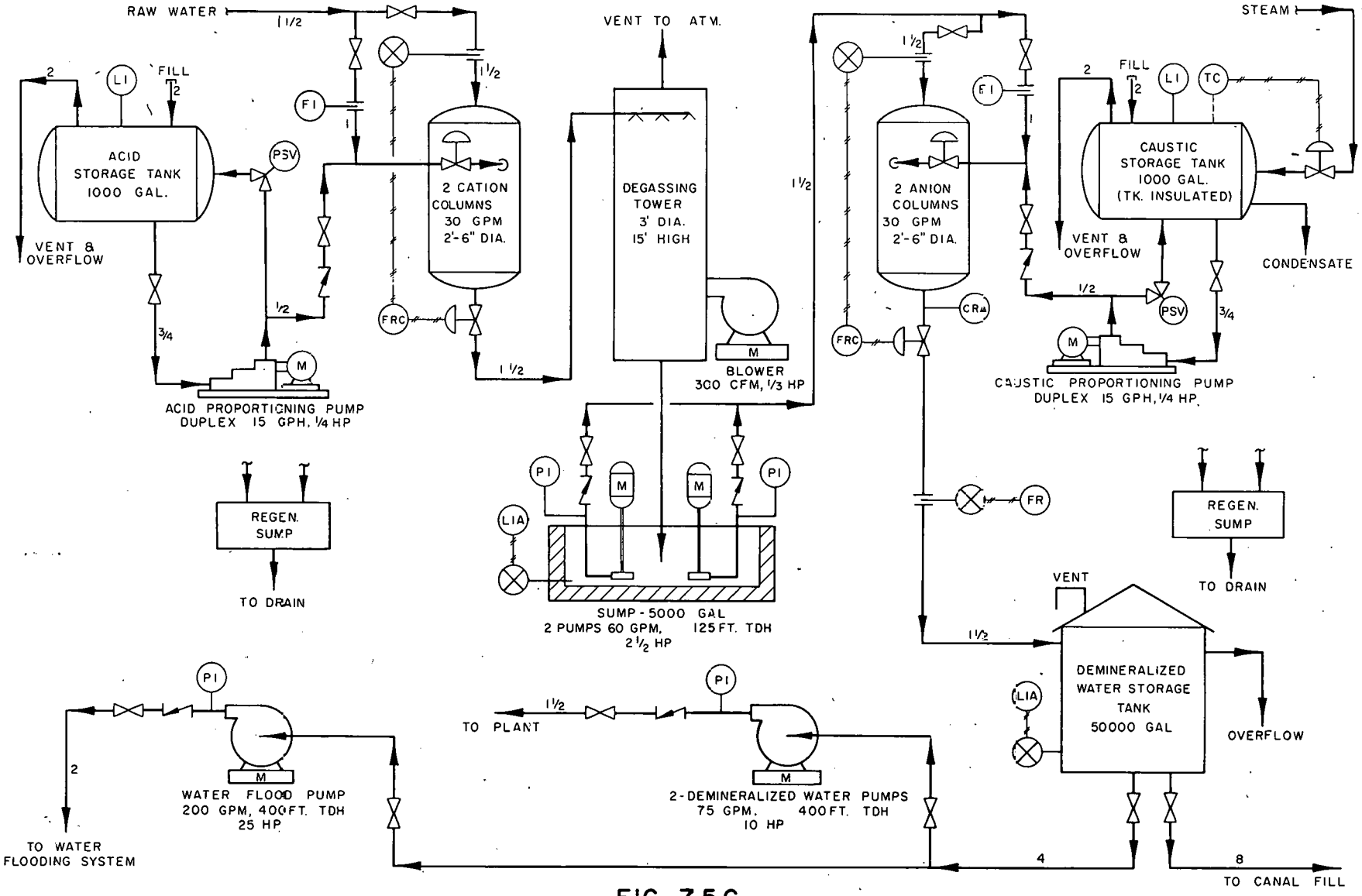

FIG. 7.5C

DEMINERALIZED WATER SYSTEM

FLOW DIAGRAM

P.P. CO.-C - 2524

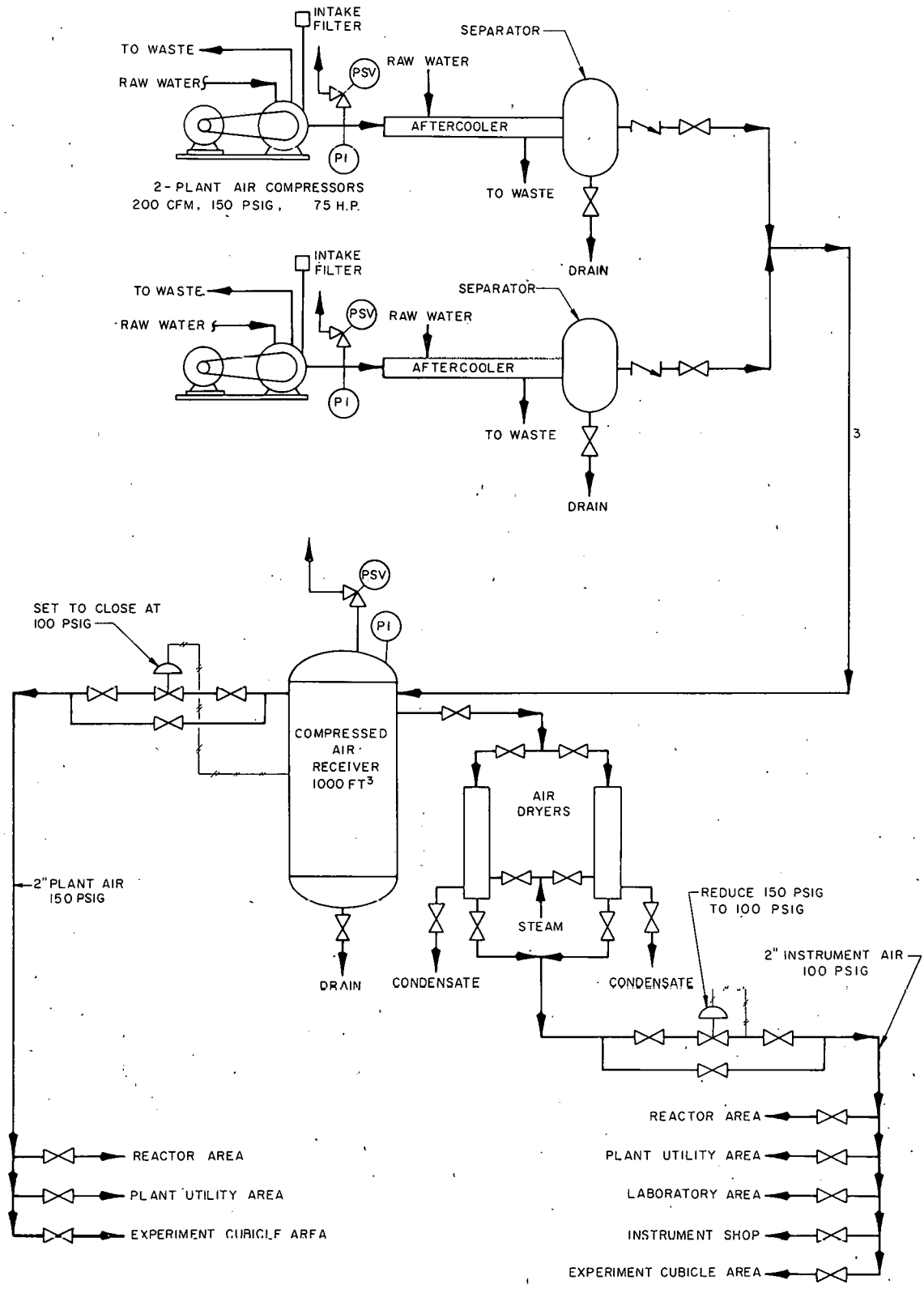

FIG 7.5D

PLANT AND INSTRUMENT AIR SYSTEM FLOW DIAGRAM

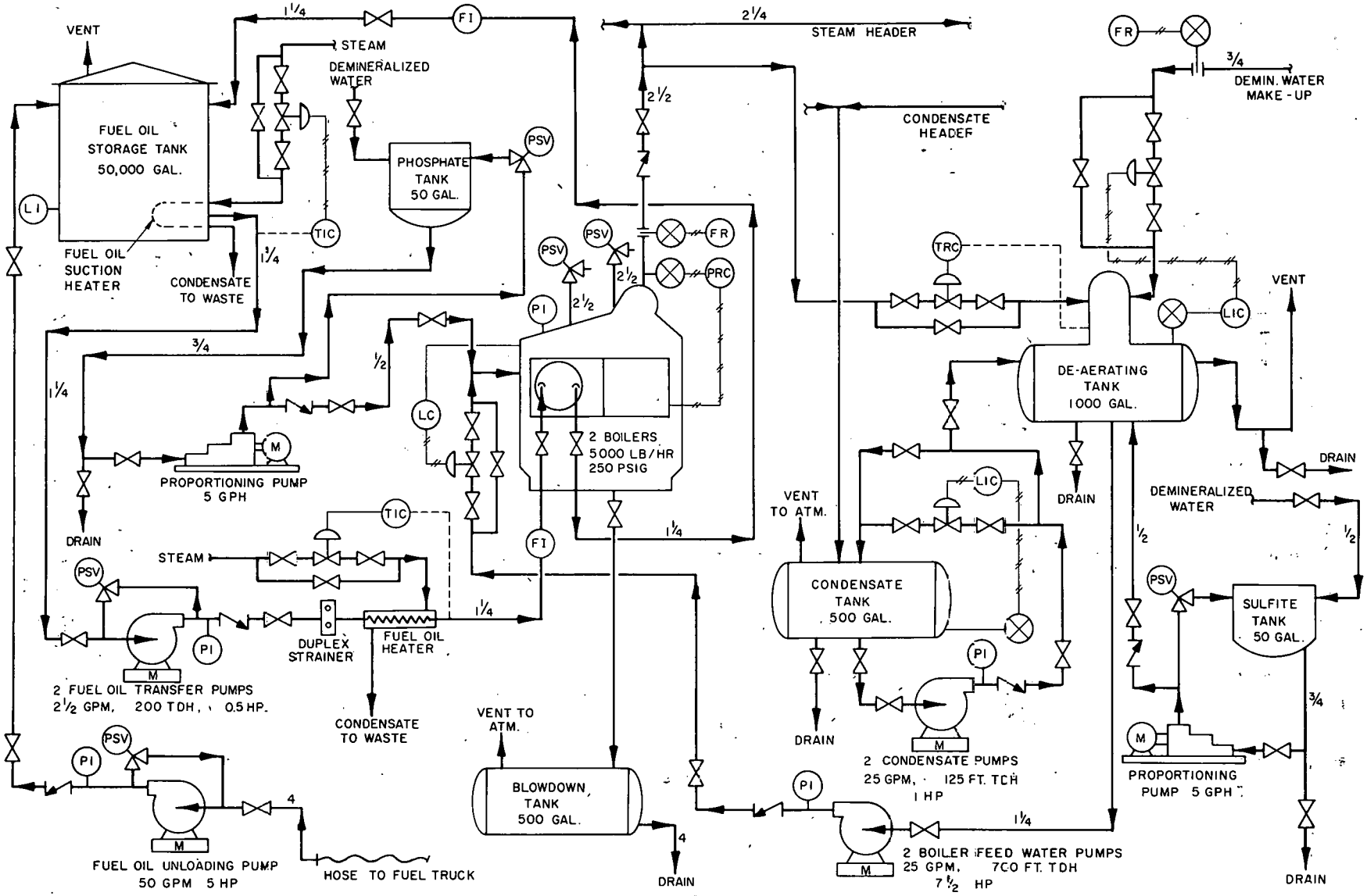

FIG 7.5 E

PLANT STEAM SYSTEM
FLOW DIAGRAM

P.P.CO.-C-2526

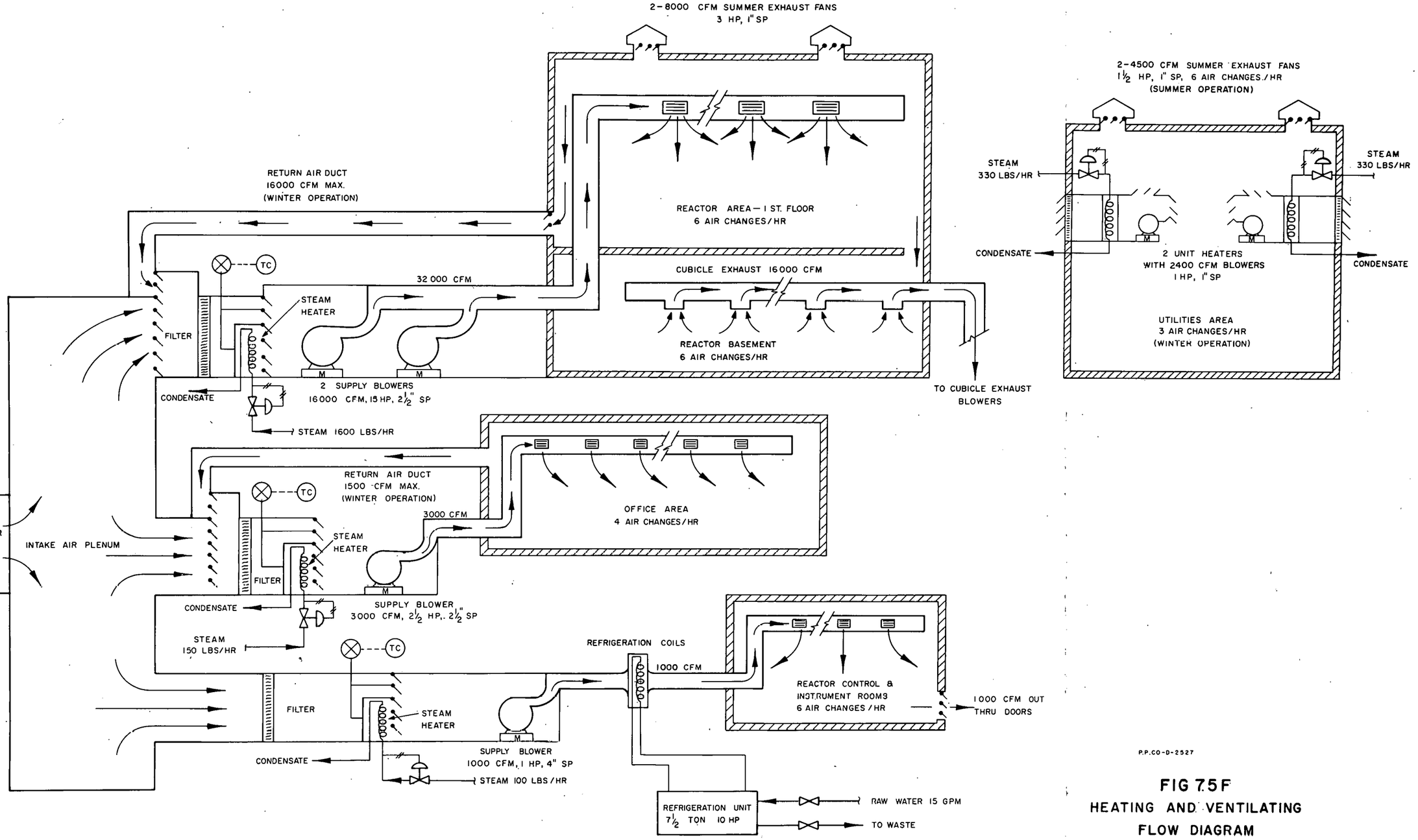

P.P.CO-D-2527

FIG 7.5F

HEATING AND VENTILATING

FLOW DIAGRAM

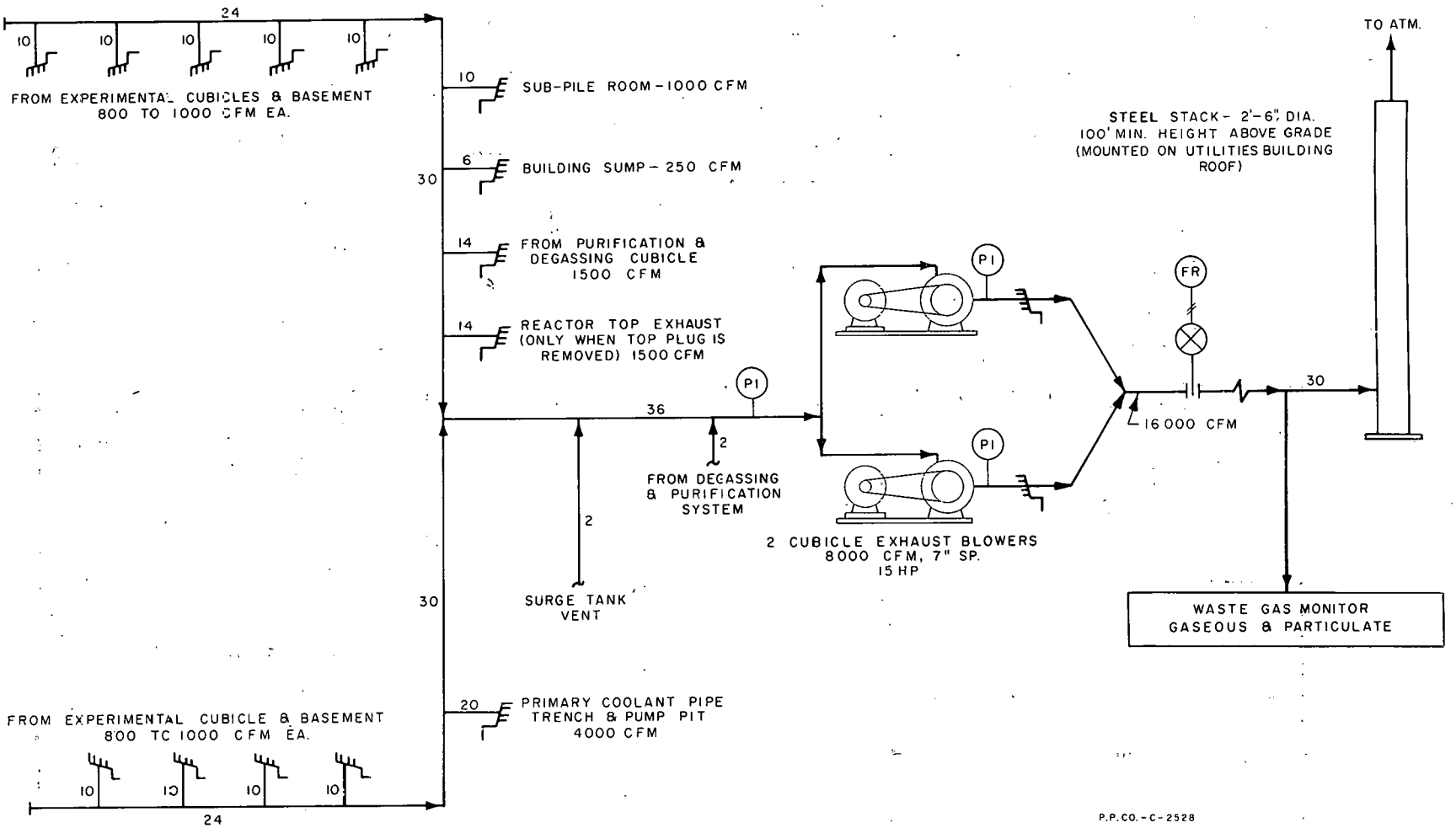

FIG 7.5 G

GASEOUS WASTE SYSTEM
FLOW DIAGRAM

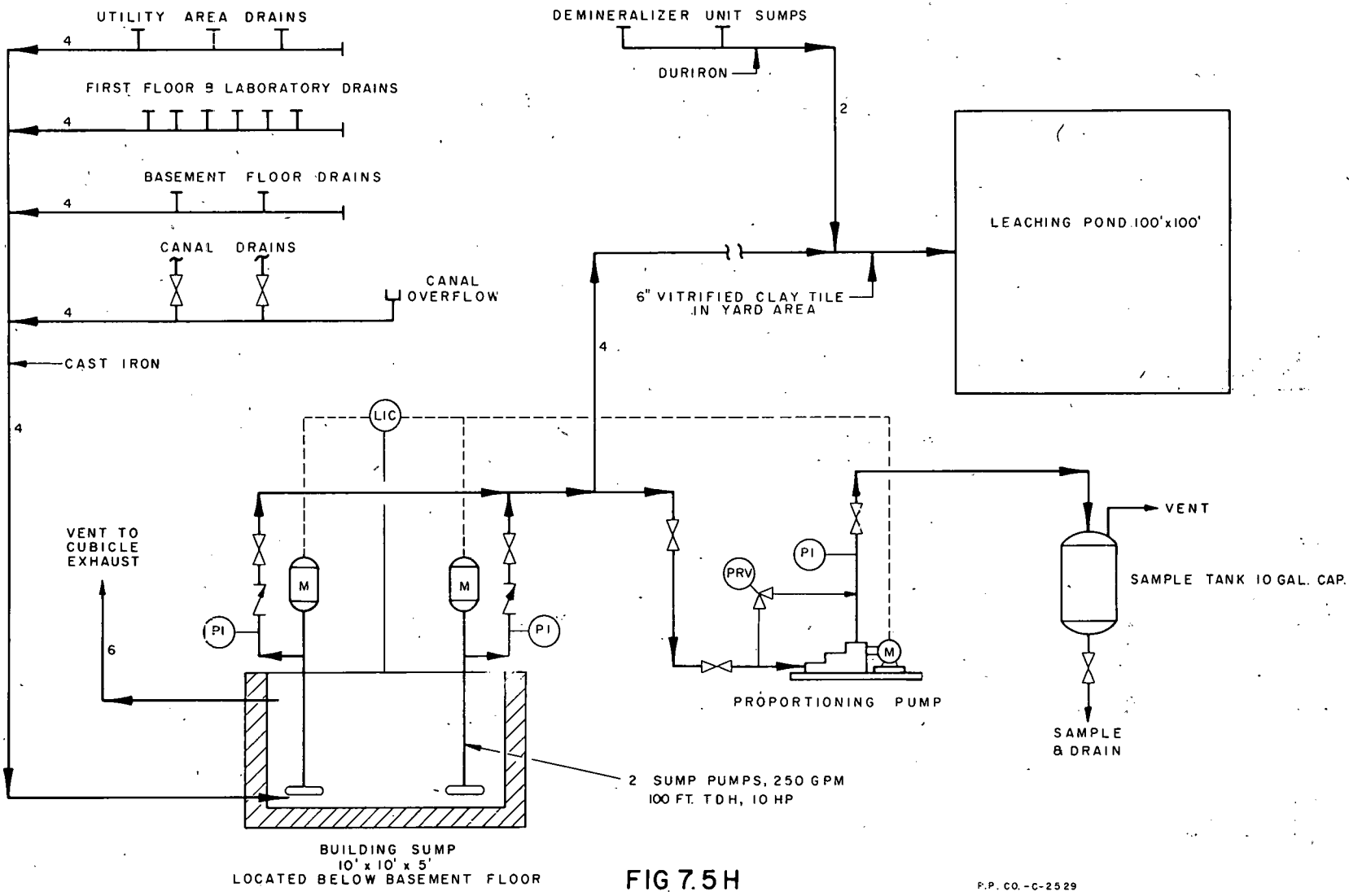

FIG 7.5H

AQUEOUS WASTE SYSTEM
FLOW DIAGRAM

P.P. CO. -C-2529

PAGES 129 to 130

WERE INTENTIONALLY

LEFT BLANK

7.600 Site, Buildings and Facilities

The following sections include a brief engineering description of the EOCR site, buildings, structures and facilities. For purposes of this report, it is assumed that the EOCR site is located in or closely adjacent to the SPERT - OMRE complex at the National Reactor Testing Station located west of Idaho Falls, Idaho.

7.610 Site Plan. The proposed plot plan for the EOCR site is shown on Fig. 7.6A - EOCR Site Plan. The more important assumptions used in the layout of the proposed area include the following:

1. Reactor containment shells will not be necessary.

2. Reactor primary coolant systems will be shielded or isolated from areas normally occupied by personnel.

3. Prevailing wind direction will be as shown on the plot.

4. An adequate supply of ground water will be available.

5. Liquid and gaseous wastes may be returned to the environment under controlled conditions through a leaching bed and stack.

6. Reasonable space will be provided for future expansion.

7. The EOCR complex is dependent upon other areas for administrative, engineering, maintenance, finance, cafeteria, warehousing, and other functions.

The EOCR site is 400 ft wide in an east-west direction by 370 ft-long in a north-south direction, not including the leaching pond and sewage stabilization pond located west of the plant, or the parking area located east of the plant. The site proper will be enclosed by 7-ft high chain link fence topped by three strands of barbed wire. Access to the site will be via the guard house and truck gate located near the southeast corner of the site. Yard lights, located on poles inside the fence, will provide perimeter lighting around the entire EOCR site. Adequate roadways and sidewalks are provided to serve various buildings and facilities as necessary.

Final location of the leaching pond and sewage stabilization pond will be dependent upon sub-surface drainage. These ponds will be fenced with net or barbed wire as specified by the IDO Engineering Standards Manual. The sewage stabilization pond is to be located at least 800 ft from the nearest occupied building.

An asphalt-paved parking area approximately 100 ft wide by 150 ft-long is provided east of the EOCR site and north of the plant guard house for bus and other vehicle parking.

Buildings and facilities associated with the EOCR complex should be located and designed to allow for reasonable future expansions, such as lengthening the reactor canal and reactor area. Future additions (such as maintenance shops, office and laboratory areas, etc.) can be placed south or southwest of the reactor building.

7.620 Reactor Building. The reactor building is the only large building structure to be located at the EOCR site. The reactor, operating area, office area, health physics lab, experimental equipment and consoles, reactor process equipment, and the majority of the plant utilities are all located in this building. The following sections include a brief description of the reactor building as shown on figures:

Fig.	7.6B	EOCR	Reactor Building	First Floor Plan
Fig.	7.6C	EOCR	Reactor Building	Basement Plan
Fig.	7.6D	EOCR	Reactor Building	Sub-Basement Plan
Fig.	7.6E	EOCR	Reactor Building	Sectional Elevation "A-A"
Fig.	7.6F	EOCR	Reactor Building	Sectional Elevation "B-B"
Fig.	7.6G	EOCR	Reactor Building	East Elevation
Fig.	7.6H	EOCR	Reactor Building	North Elevation

7.621 Reactor Area First Floor. The first floor plan, shown on Fig. 7.6B, includes the reactor area and office area; most of the functions associated with these areas consist of housing and operating the reactor.

The reactor area is located on the west side of the south end of the reactor building and is 76 ft long by 55 ft wide. The reactor vessel is located at the bottom of a 14-ft deep reactor pit at the north end of an 8-ft wide by 30-ft long water-filled storage canal, but is isolated from the canal by means of a removable bulkhead with inflatable seals.

During reactor operation, the reactor pit will be dry, and the reactor top head, including drives, will be located there. When the reactor is shut down, the top head will be removed, and the reactor pit will be flooded with water so that fuel assemblies, control rods, etc., may be transferred directly to the canal without utilizing shielded casks. (See Section 7.200 for handling facilities and procedures).

Truck access to the reactor area is provided by a truck door located in the south end of the building. Personnel access from outside of the reactor building or from other areas of the reactor building is provided as indicated on the above figure. Experimental equipment, fork lift, or other items to be located or used in the reactor area basement will be dropped through hatches located in the first floor by a 30-ton bridge crane operating over the reactor area and running in a north-south direction. This crane should have a 25-ft hook clearance above the canal parapet. A 2-ton handling crane is located above the bridge crane and operates over the reactor pit and canal.

Other items located on the first floor of the reactor area are a dry dock for the reactor top head and two spiral stairways for personnel access to the reactor area basement level.

The office area is located east of the reactor area and is 76 ft long by 57 ft wide. This area includes the reactor control room, reactor instrument room, instrument repair room, health physics office, change room, shift supervisor's office, reactor superintendent's office, rest rooms, main entryway to the EOCR reactor building, and a stairwell leading to the reactor area basement level.

7.622 Reactor Area Basement. The reactor area basement is located directly beneath the reactor area and the office area and provides a net area approximately 75 ft-long by 110 ft-wide. (See Fig. 7.6C). The reactor and canal structures extend downward through this area. Surrounding these structures are future shielded experimental-equipment cubicles and the primary-coolant valve cubicle. Piping or instrumentation-lead access from in-pile experiments is provided by means of nozzles radiating from the reactor vessel below the top head and by means of piping corridors around the reactor sub-pile room located below the basement level. The experimental consoles would be located east of the equipment cubicles. Net usable height above the basement floor is approximately 20 ft, and experimental consoles could be installed on two levels by the future addition of a balcony in the console area, if required.

The reactor area basement also contains the reactor-building heating and ventilating equipment, access stairway to the sub-basement areas, and three stairways for access to the first floor level. Equipment to be installed or used in the basement areas would be dropped through hatches in the reactor area first floor by means of the 30-ton bridge crane.

7.623 Reactor Area Sub-Basement. (See Fig. 7.6D). The reactor sub-pile room, piping corridors for experimental piping to the experimental equipment cubicles located on the basement floor, reactor building sump and sump pumps, system dump tank (organic), system fill pump, and dump tank feed pump are located in the sub-basement areas. A 6-ft wide stairway beginning near the east side of the basement area extends directly down and west to the reactor sub-pile room. The experimental piping from in-pile tubes would extend through the reactor vessel bottom head into the sub-pile room, out through radial holes in the sub-pile room walls to the piping corridors around the sub-pile room, and up to the experimental equipment cubicles located in the basement area. Two fission chamber drives also operate in the reactor sub-pile room.

Access to all other sub-basement areas is provided from the corridor leading to the sub-pile room. Immediately outside of the sub-pile room shielding wall and on both sides of the corridor,

access doors lead to the piping corridors encircling the reactor sub-pile room structure. Immediately east of these doors are doorways leading to the plant sump and system dump tank. The plant sump (aqueous) is 10 ft wide by 10 ft long by 5 ft deep, and is located below the sub-pile room floor level on the north side of the corridor. Two sump pumps pump aqueous plant wastes to the leaching pond. The system dump tank, system fill pump, and dump tank feed pump are located south of the stairway leading to the sub-pile room, and should be below the level of the reactor vessel bottom head. The reactor dump tank is a horizontal pressure vessel resting on reinforced concrete saddles, is insulated and coated since it contains high temperature organic (approx. 375°F) and is buried, and has a skirt on the north end which is attached to the south side of the pump room. The pressure vessel attachment to the pump room should be water tight.

7.624 Reactor Area Construction Details. The foundations, curtain walls, basement floor, and first floor of the reactor and office areas are of reinforced concrete construction as shown on Figs. 7.6E and 7.6F. Representative floor loadings for various areas should have approximately the following values:

Reactor Area First Floor	3000 lb/ft^2
Reactor Area Basement	3000 lb/ft^2
Control Room, Instrument Room, and Health Physics Office	300-500 lb/ft^2
Other Office Areas	150 lb/ft^2
Canal	3000 lb/ft^2 plus Water Load

The high bay section of the reactor building over the reactor area is of insulated panel or equivalent construction, and will extend approximately 50 ft above grade. Means are provided for isolating this area from the office area and from the utilities area.

The office area section of the reactor building is of concrete or pumice block construction with prestressed concrete roof slabs and built-up gravel-covered roofing. This section will be approximately 11 ft high.

7.625 Utilities and Process Areas. The process area is located in the north end of the reactor building, and is approximately 49 ft long by 112 ft wide as illustrated by Fig. 7.6B. The process control room, laboratory, two failure-free power motor-generator sets, two boilers, two fire pumps, two plant air compressors, service pumps, water flood pump, demineralizer unit and demineralized water pumps, and the primary coolant degassing, purification, and distillation systems are all located in the utilities area. In addition, the electrical switchgear is located over the process control room and the battery room is located over the laboratory. The primary coolant, degassing, and purification systems are located in a high bay reinforced concrete cubicle located in the southwest corner of the utilities area.

This cubicle will shield these process systems and will also support the 30-inch diameter stack whose top is a minimum of 100 ft above grade level. The experimental equipment cubicles, process degassing system, and other areas which might discharge or release contamination will be vented to atmosphere via this stack. The experimental equipment cubicle exhaust blowers are also located in a pumice block cubicle located on the roof of the utilities area, and the cubicle exhaust duct is brought from the basement via a duct extending up through the southwest corner of the process control room. Descriptions of process and utility systems are given in Sections 7.400 and 7.500 of this report.

The utilities area section of the reactor building is of concrete or pumice block construction with prestressed concrete roof slabs and built-up gravel-covered roofing, except that the degassing, purification, and filtration cubicle will be of reinforced concrete construction. The utilities area of the reactor building will be approximately 21-ft-high, except that the above cubicle and cubicle housing the experimental equipment exhaust blowers will extend above the roof line.

Access to the utilities area is provided by access doors from the reactor area, office area, and by a truck and personnel door located in the north wall of the area.

Significant portions of the primary coolant system are shown on Figs. 7.6B, 7.6E, and 7.6H, and will be discussed here. The 24-inch diameter process lines extend westward from the reactor vessel, through the primary coolant valve cubicle located in the reactor area basement, and enter the primary coolant pump pit located west of and just outside of the reactor building. After leaving the primary coolant pump pit, the process lines extend westward through a concrete pipe trench approximately 50 ft where they rise to the air-cooled primary coolant heat exchangers. These heat exchangers are located approximately 36 ft above grade on fireproofed steel columns with reinforced concrete foundations.

All portions of the primary coolant piping and other organic process piping will be insulated and steam traced, and will be shielded by high density or reinforced concrete walls, except the risers to the heat exchangers are not shielded. The area around the heat exchangers will be fenced to control personnel access. In the event of a fission break, it may be necessary to closely control personnel access to that area west of the reactor building where the primary pump and heat exchangers are located.

7.630 Miscellaneous Buildings and Structures. Usage of other buildings and structures shown on Fig. 7.6A-EOCR Site Plan is self explanatory. The 50,000-gallon fuel oil storage tank is located in a diked area in the northwest sector of the site. Outside of the dike and south of this storage tank is the fuel oil pump house. Immediately east of the fuel oil storage tanks are the water well, caustic and acid

storage tanks, raw water storage tank, demineralized water storage tank, and transformer yard. Power will be brought to the transformer yard from the SPERT substation via a high line, and the capacity of the SPERT substation will be expanded to include the power requirements for the EOCR site.

The air receiver is located just north of the utilities area of the reactor building and west of the truck access door leading to that area. West of the utilities area and north of the primary coolant heat exchangers are three organic storage tanks. The westernmost tank is buried with a small pump pit over or near it. This tank will be used for HB storage, and HB will be pumped from this tank into drums for disposal as required. The other two organic storage tanks are located above grade and will be used for new organic and distilled organic storage.

The guard house is located near the southeast corner of the EOCR site. This building will be of pumice block or equivalent construction, and will be sized to meet the needs of the facility.

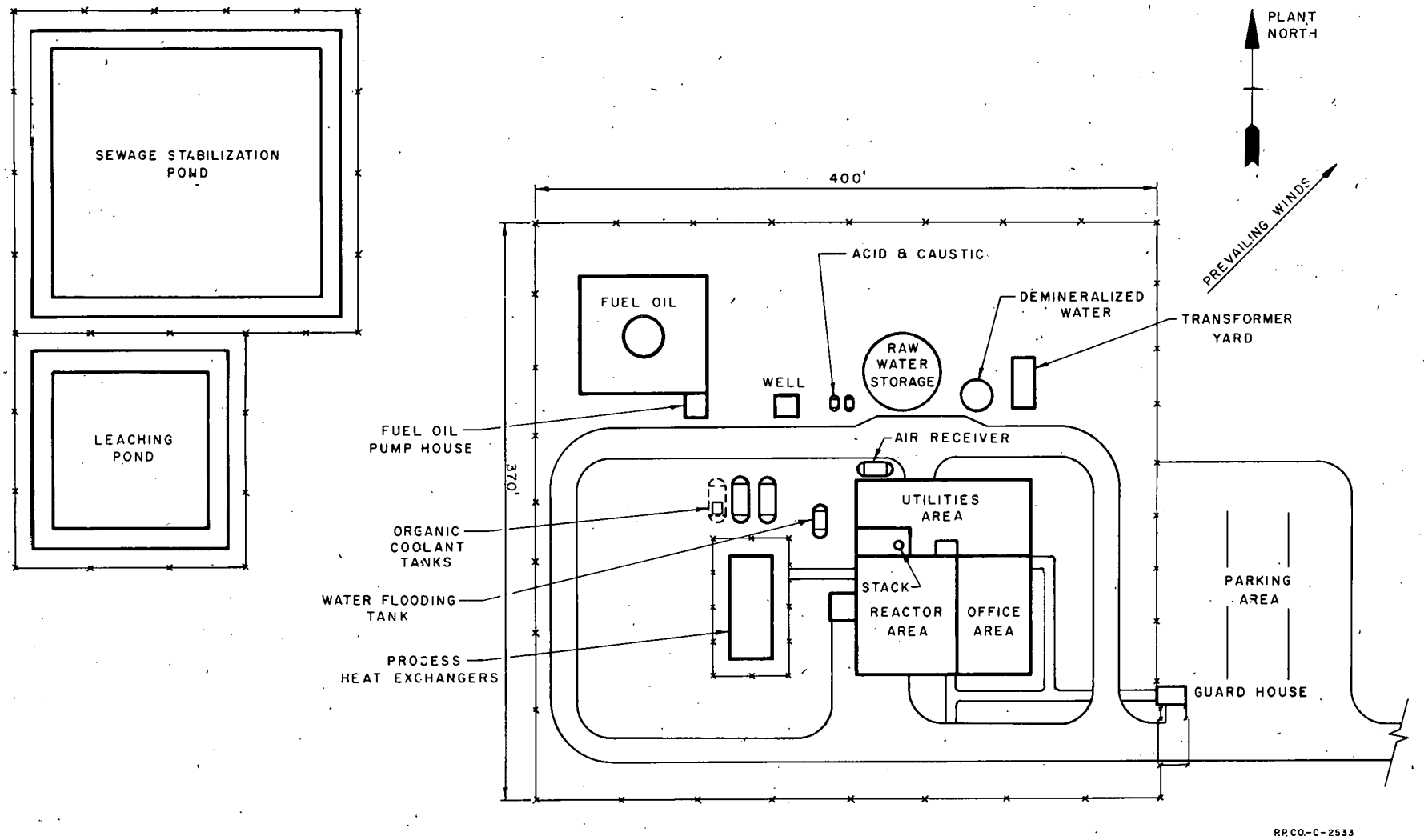

FIG 7.6A

EOCR SITE PLAN

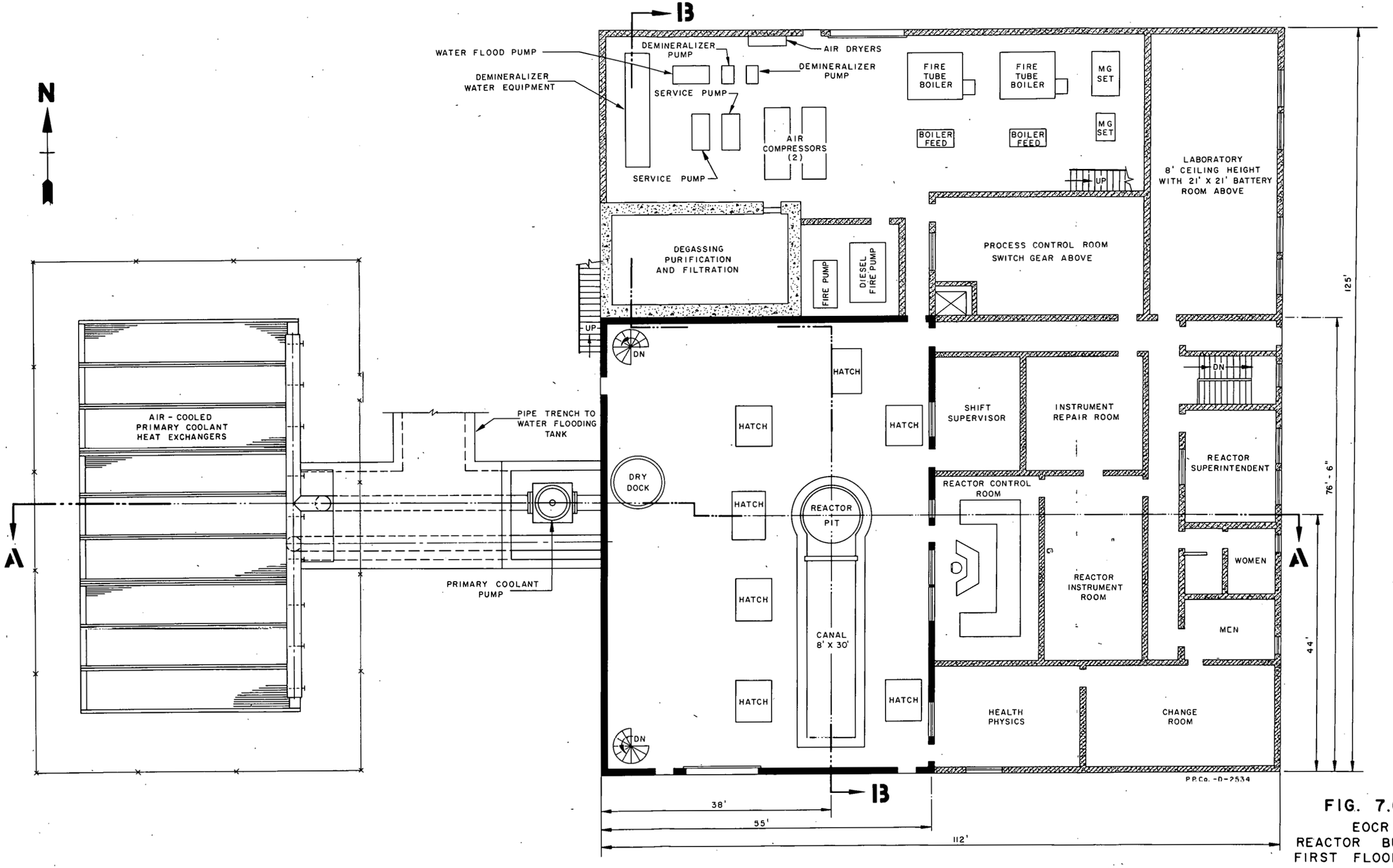

FIG. 7.6B
EOCR
REACTOR BUILDING
FIRST FLOOR PLAN

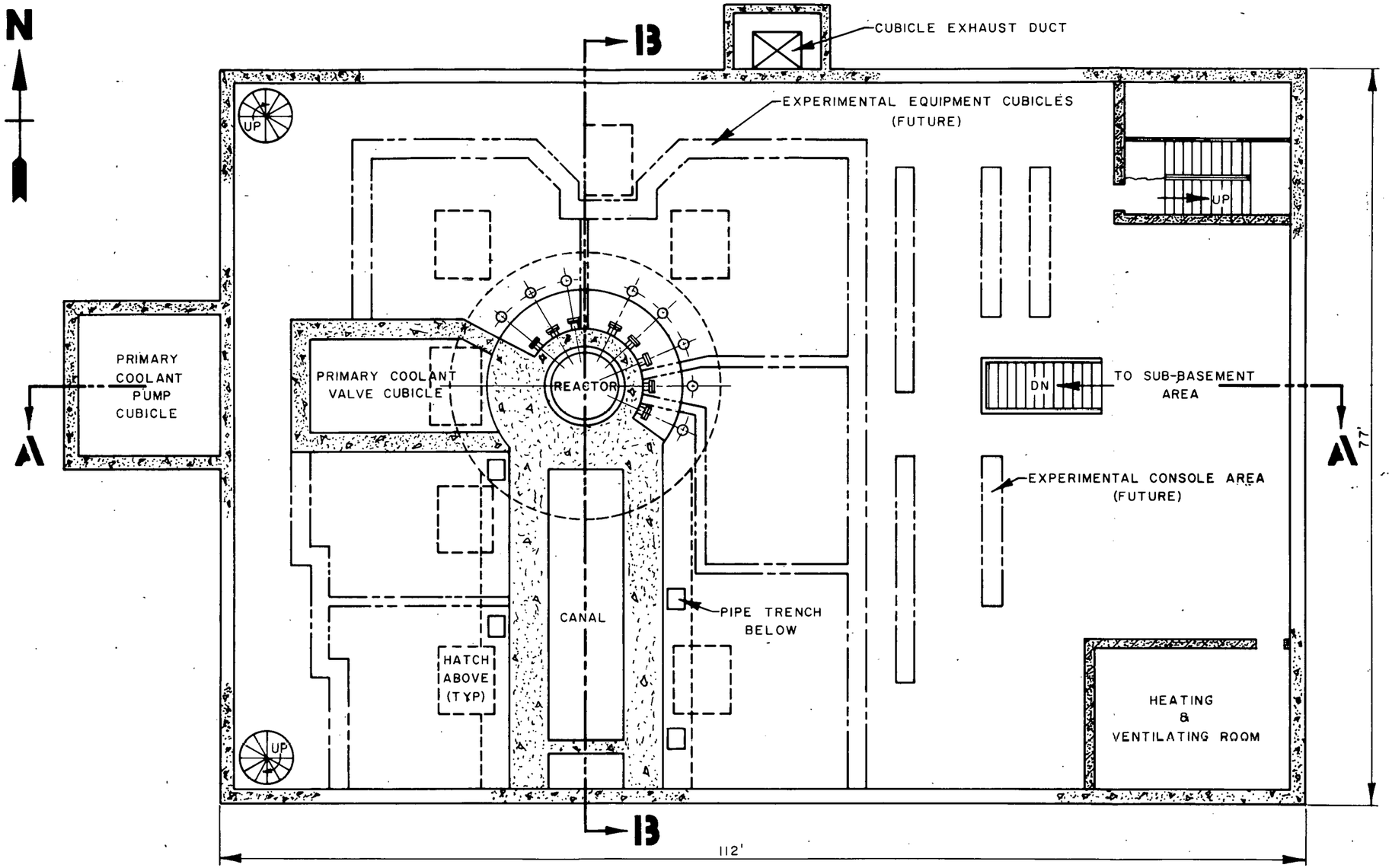

PPCO-D-2535

FIG. 7.6C
EOCR
REACTOR BUILDING
BASEMENT PLAN

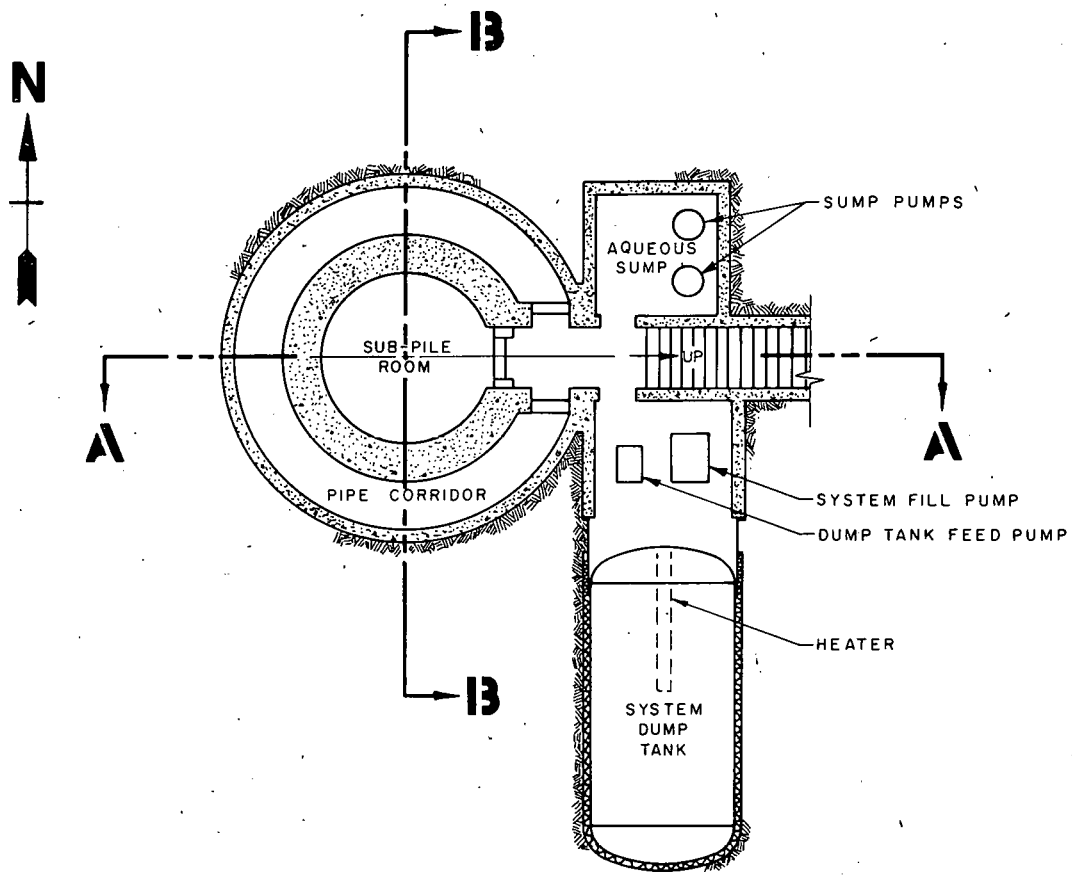

PPCO-C-2536

FIG. 7.6D

EOCR
REACTOR BUILDING
SUB-BASEMENT PLAN

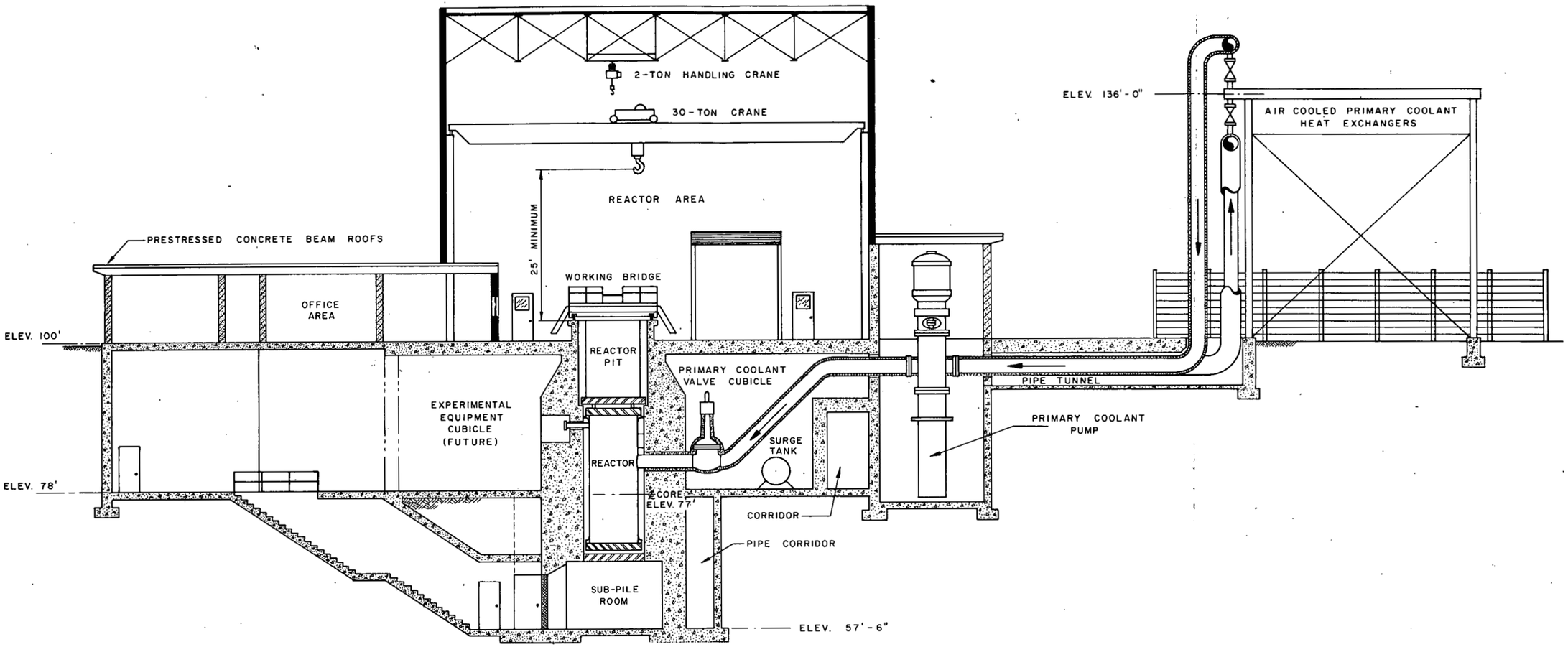

PPCO-D-2537

FIG. 7.6E

EOCR
REACTOR BUILDING
SECTIONAL ELEVATION "A-A"

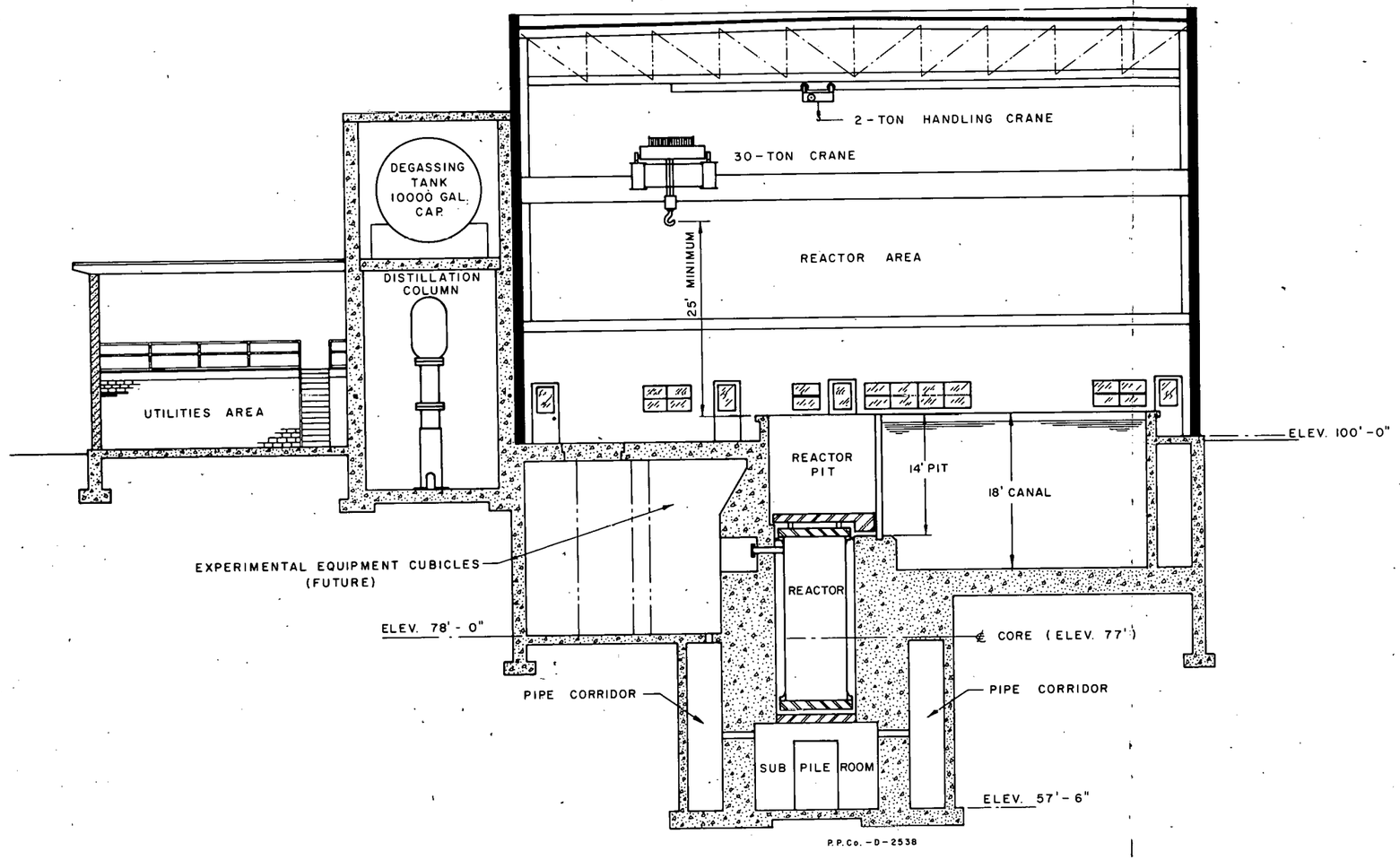

FIG. 7.6F

EOCR
REACTOR BUILDING
SECTIONAL ELEVATION "B - B"

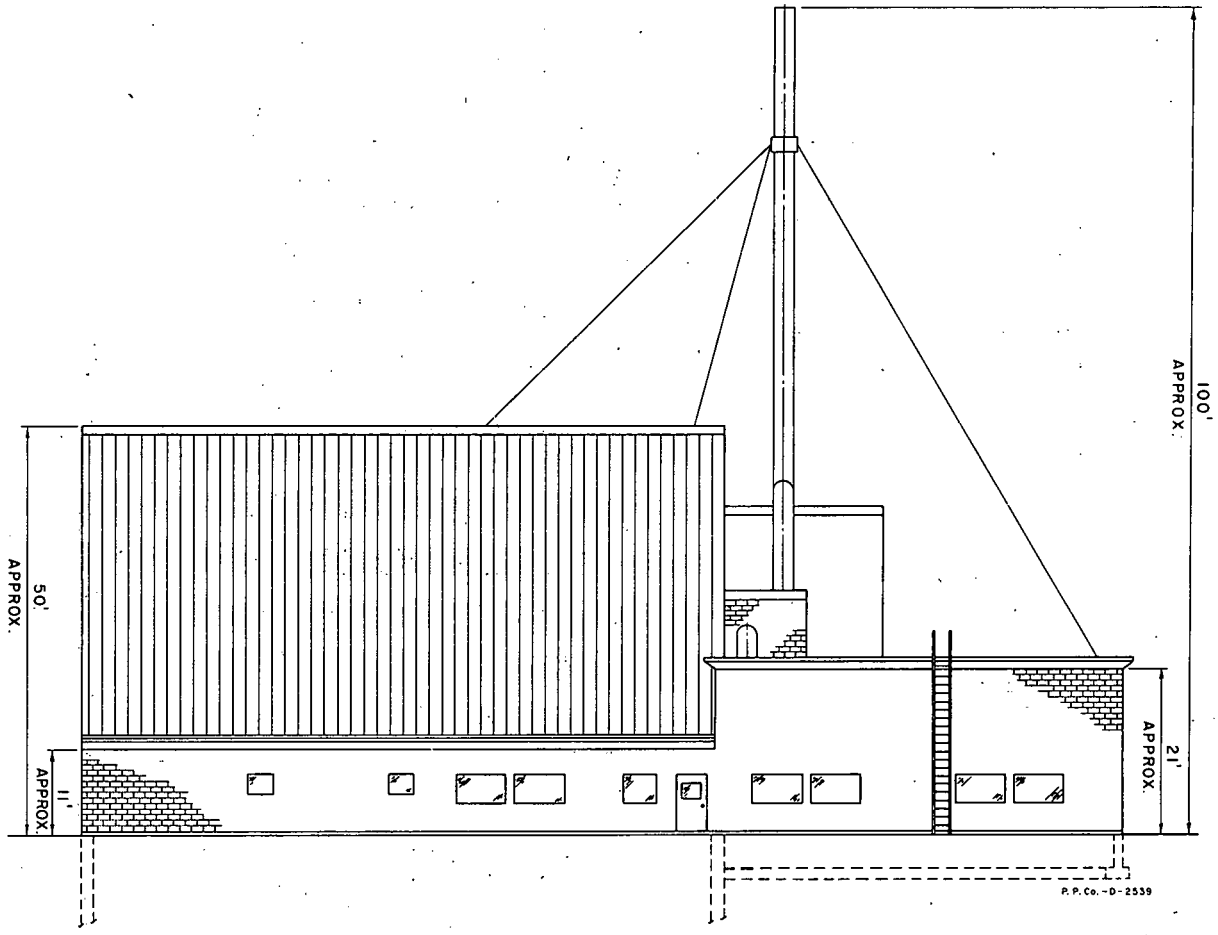

FIG. 7.6G

EOCR REACTOR BUILDING EAST ELEVATION

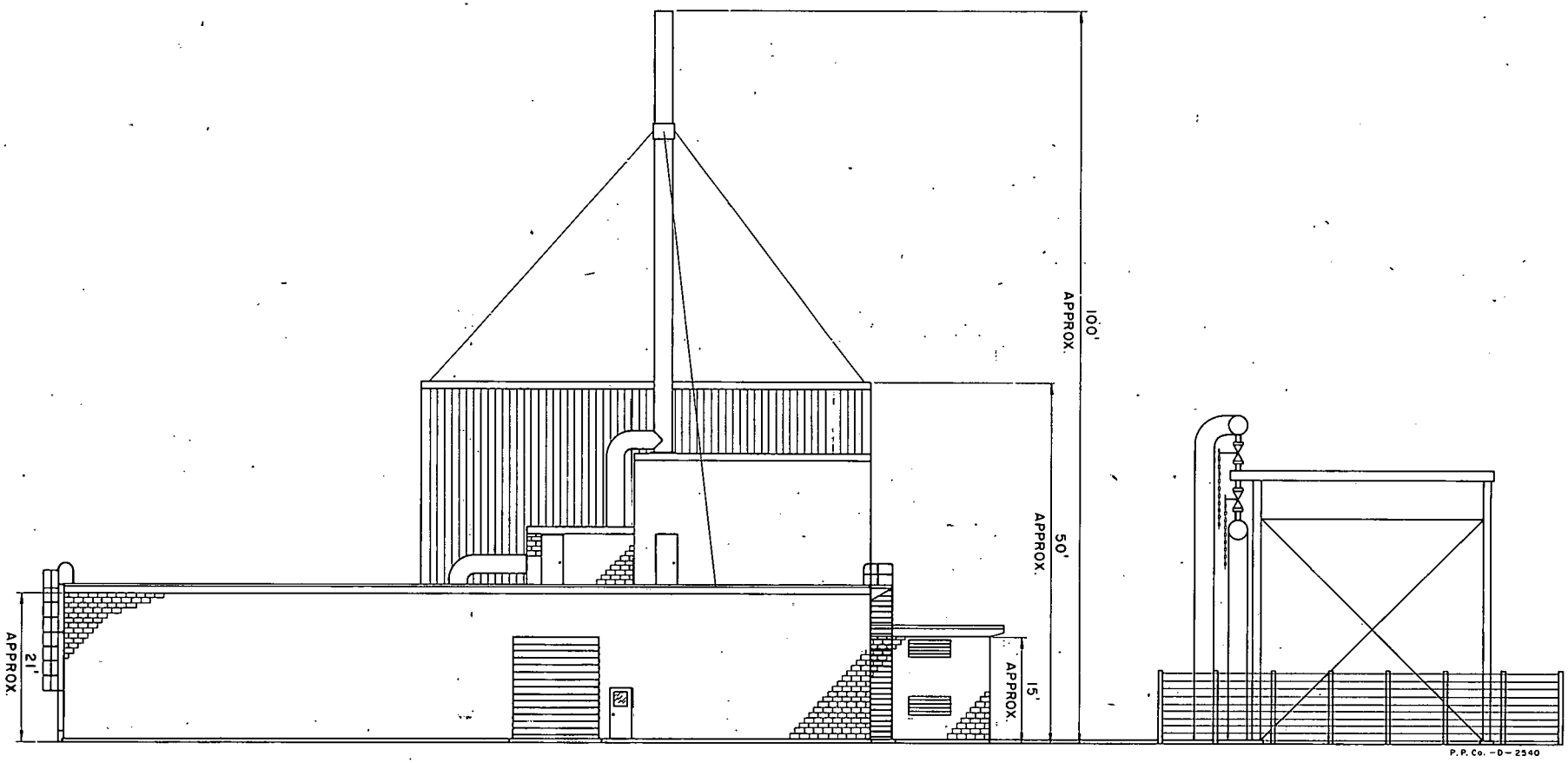

FIG. 7.6H

EOCR REACTOR BUILDING NORTH ELEVATION

PAGES 145 to 150

WERE INTENTIONALLY

LEFT BLANK

8.000 LOOP AND EXPERIMENT FACILITIES

The standard core has two large experimental loops and three small experimental loops located in the core as shown in Fig. 4.1A. In addition, the core contains two rabbit facilities and space for numerous lead-type experiments. Operation of these experiments will require space in the reactor building, equipment both in-pile and out-of-pile, and auxiliary utilities. A conceptual design of one typical large loop and the equipment and utility needs for all of the experiments that are recommended for the initial EOCR loading are described in this section.

8.100 Design of a Typical Loop Experiment

A preliminary design of a typical large loop is presented to illustrate the type of facility that the EOCR will accommodate. The re-entrant type loop described is designed to test a fuel element similar to that proposed for the 300 Mwe forced convection power reactor,[1] except that the inner-most ring of fuel pins in the test element is removed to provide space for the coolant return. The basis of the design, established from the objectives outlined in Section 3.000, is as follows:

Maximum Coolant Flow	500 gpm
Loop Coolant Temperature	900°F
Maximum Pressure in Loop	300 psi
Reactor Pressure	100 psi
Maximum Reactor Temperature	700°F
Maximum Gamma Heating	10 watts/gm

The preliminary loop design was completed prior to establishing the final reactor operating parameters; hence, the reactor operating pressure is 150 psi instead of 100 psi, which was used as the design basis for the loop. This change will probably result in some minor changes in the wall thickness of the external tube of the in-pile tube assembly.

8.110 In-Pile Equipment. The in-pile equipment required for a test loop consists of an in-pile tube and associated instrumentation. The loop is a re-entrant type, in which the coolant enters and returns from the experiment via a single pipe penetrating the reactor bottom head. A cross-section of the in-pile tube is shown in Fig. 8.1A, and the coolant path is shown in Fig. 8.1B. The fuel element is cooled by coolant flowing upward past the fuel, which reverses direction above the test element and returns through the center hole in the fuel element. Two concentric pipes are used to allow the flow to enter and return from the reactor vessel through a single bottom head penetration. The in-pile

---

1. Bechtel Corporation and Atomics International, "Organic Cooled Power Reactor Study - 300 Mw Power Plant Conceptual Design", Supplement No. 2, Report BCPI-1, June 26, 1959.

tube is designed to operate at 900°F with pressures up to 300 psi inside the tube and 100 psi outside the tube. An air gap is provided to insulate the loop coolant from the reactor coolant.

The top of the in-pile tube extends to within about 2.5 ft of the top head[1] and is flanged to permit easy access to remove and insert test fuel elements. The bottom of the tube penetrates the reactor bottom head and is sealed to the bottom head as shown in Fig. 8.1C. The inner and outer pipes, shown in Fig. 8.1C, are permitted to move independently and the entire in-pile tube is allowed to move upward to allow for thermal expansion. The in-pile tube is supported laterally by the reactor lower head, lower grid plate, and upper spider, and the load is supported in the subpile room.

Since the outer pressure tube is isolated from the loop coolant by an air gap, the gamma heat (10 w/g maximum) produced in the outer pressure tube must be removed by the reactor coolant. The organic in the region between fuel elements flows at velocities between 0.2 and 0.5 ft/sec, which will not be adequate to cool the pressure tube which will generate a heat flux of about 90,000 Btu/hr-ft^2. Provision is made to allow reactor coolant to pass the outer loop pressure tube at velocities of about 5 ft/sec through a shroud around the in-pile tube like that shown in Fig. 8.1A.

8.111 Insertion and Removal of Loops and Test Pieces. Although fuel can be removed directly into a cask if desired, the handling of in-pile tubes and fuel elements in loops is normally done when the reactor vessel and in-pile tubes are filled with water. In-pile tubes are inserted into the reactor through the top head and lowered through the bottom head. The bottom end of the tube is equipped with mating surfaces that fit and line up with the bottom head seal plug. The seal plug is supported by hydraulic jacks and as the tube mates the plug, the plug is lowered to allow the tube to enter and pass through the bottom head.

Fuel pieces are removed after the loop coolant in the experiment tube has been replaced with water using a technique similar to that described for flooding the reactor vessel. A draw bar attached to the top of the fuel element, used to hold the fuel and return tube in position during operation, is used as a handle to permit easy removal of the fuel piece after the top access flange is removed from the loop (refer to Fig. 8.1D).

8.120 Out-of-Pile Equipment. The out-of-pile equipment for a large loop consists of pumps, heat exchangers, degassing system, purification system, make-up tank, dump tank and associated valves, piping and instrumentation. Except for size the equipment is similar to the reactor primary loop. A flow diagram for the loop equipment is shown in Fig. 8.1E.

---

1. Refer to Fig. 7.1A.

Two 250-gpm pumps supply forced flow for cooling of the experiment. Failure-free power is provided for one of the pumps to provide shutdown heat removal for the first 15 minutes after loss of commercial power. After this time heat will be removed from the experiment by forcing coolant from the make-up tank to the dump tank by pressurizing the make-up tank. If additional cooling time is required the dump tank may be pressurized and the coolant forced back to the make-up tank.

The heat exchangers are organic-to-boiling-water type with temperature control provided by controlling the water side pressure and by-passing part of the main stream around the exchanger.

A batch purification system capable of handling 60 lb/hr is provided to control HB content. This system size is sufficient to service the second large loop.

Pressure control is accomplished by maintaining a nitrogen blanket (from bottles) on the pressurizing tank which also acts as a surge to provide for expansion and contraction of the coolant.

The degasifying system removes radiolytic gases from the coolant by continuously flashing a portion of the coolant into a 30-gal vacuum tank. The overhead vapors from the tank are fed to the primary condenser which is cooled by 300°F demineralized water; non-condensibles from the primary condenser are fed to a secondary condenser cooled by cold water. Nitrogen is maintained on the system to reduce explosive hazards.

8.121 Instrumentation. Loop instrumentation is provided to allow automatic operation and provide a centrally located control center. This instrumentation is tied into the reactor control system to provide reactor power reduction in case of experiment failure or loss of loop control. The instrumentation is designed to measure and control flow, temperature, and pressure of the loop continuously. In addition, instrumentation may in some cases be attached to the test sections and removed from the top or bottom of the reactor as indicated in Fig. 8.1C.

The purification equipment used to remove HB from coolant for the loops will be operated on a batch basis and will not require any automatic instrumentation.

Safety circuits are provided on all measurements in the loop that pertain to parameters vital to the safety of personnel, the reactor, or loop equipment. An alarm will advise the operator of any abnormal conditions and automatic corrections will be provided wherever practical.

Radiation instrumentation will be provided to monitor activity in the equipment cubicles.

8.200 Equipment and Space Requirements for all Experiment Loops in Standard Core

The previous section discusses the design of a typical large loop. Provision is made in the design for a purification system that will also distill coolant from the other large loop. Small loop purification will be accomplished in the laboratory or by continuous purge. In addition to purification of the coolant, provision is made for equipment and space for operation of the other loops. These provisions, as well as the auxiliary utility and supporting services for all loops, are discussed below.

8.210 Equipment Requirements. The equipment required for the second large loop will be similar to the equipment shown for a typical loop except for the purification system which is common to both large loops. The heat exchanger used with the large loop not in the center position of the core will be smaller than the heat exchanger for the typical loop, which is sized for the center position.

The equipment required for the small loops will be much simpler than that used in the large loops since it will be possible to maintain HB content and gas content of the coolant in the small loop by addition of fresh coolant or laboratory batch distillation. Heat exchangers for the small loops must be sized according to the loop. The type of heat exchangers probably will be similar to the boiling water type used in the typical loop design.

Out-of-pile equipment is required for two rabbit facilities to permit insertion and removal of tests while the reactor is operating. This equipment will have to be shielded so the operator can remove radioactive samples of organic from the facility.

8.220 Space Requirements. The five experimental loops that are recommended for the standard EOCR core require shielded cubicle space for process equipment and floor space for control panels. It is estimated that about 3800 square feet of floor space will be required for these loops. Fig. 7.6C shows a typical floor plan with space allocated for cubicles and panels.

8.230 Utilities. The five loops will require power, water, steam, and air to operate. A summary of the total utility requirements is given in Table 8.2A.

Table 8.2A

LOOP UTILITY REQUIREMENTS

Commercial Power	190 kw
Failure-Free Power	66 kw
Demineralized Water	38 gpm
Instrument Air	7.2 scfm
Steam	35 - 200 lb/hr
Utility Water	8 - 26 gpm

8.240 Supporting Services. To get the desired information from the operation of tests in loops, the organics being tested must be analyzed to determine changes in properties and heat transfer characteristics. A hot chemistry laboratory is necessary to permit chemical analysis and distillation of organics being tested. A heat transfer facility is necessary to determine what changes in heat transfer properties occur to the coolant as a result of irradiation and HB buildup. In addition, hot-cell services must be available to permit examination of test specimens and fuel elements after completion of the tests.

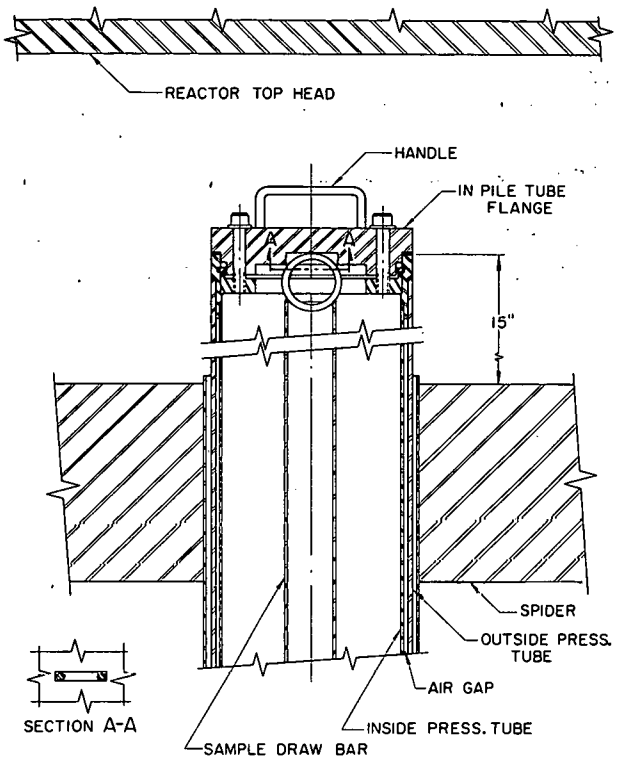

FIG 8.1 D
TYPICAL EOCR LARGE LOOP
IN-PILE TUBE

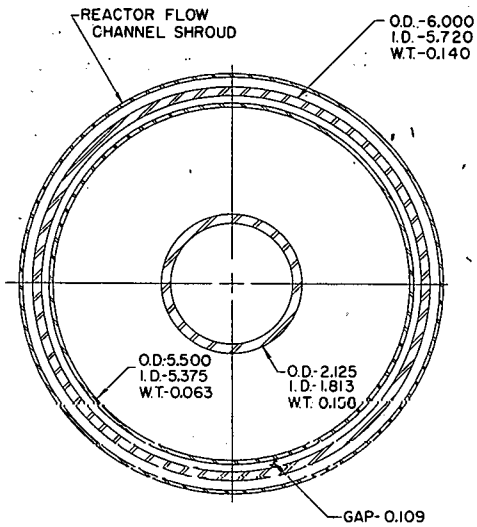

FIG 8.1 A
TYPICAL EOCR LARGE LOOP
CROSS SECTION OF IN-PILE TUBE

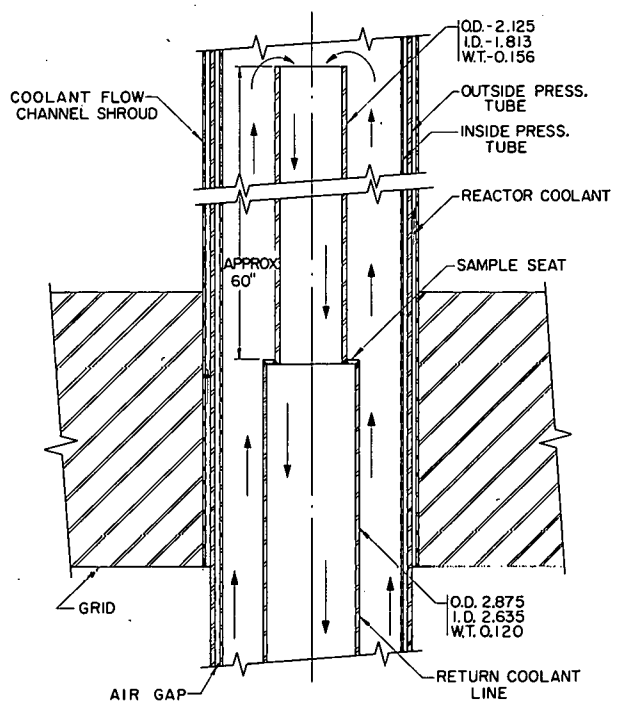

FIG 8.1 B
TYPICAL EOCR LARGE LOOP
CORE SECTION IN-PILE TUBE

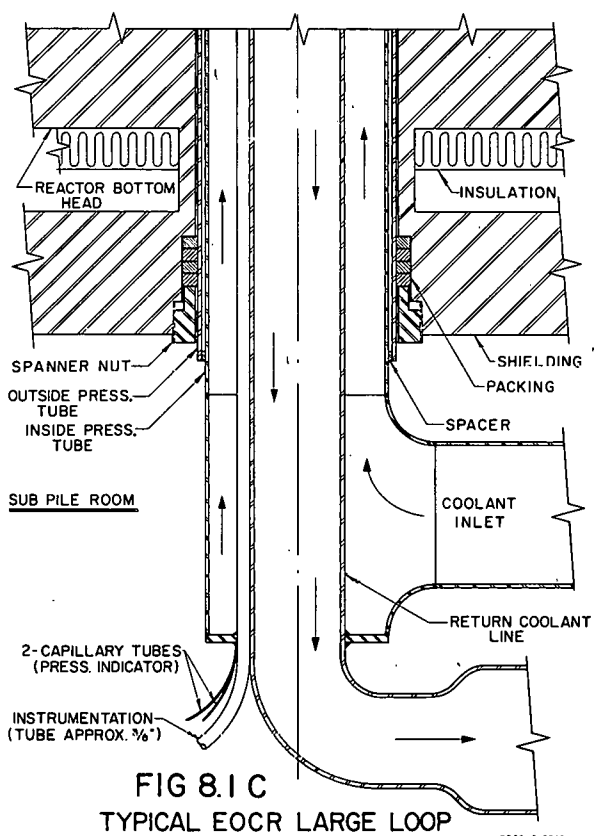

FIG 8.1 C
TYPICAL EOCR LARGE LOOP
BOTTOM HEAD DETAIL

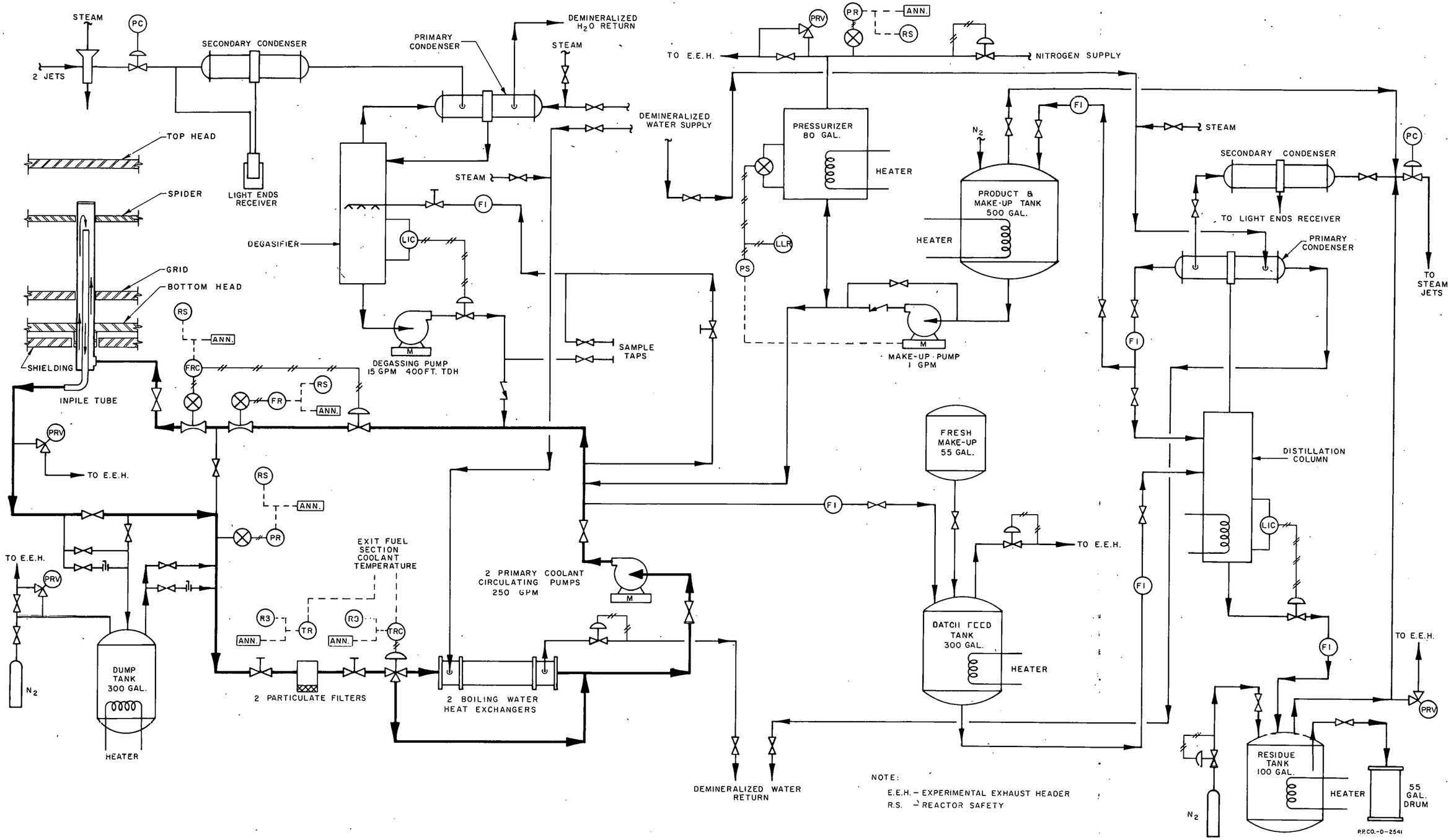

NOTE:
E.E.H. – EXPERIMENTAL EXHAUST HEADER
R.S. – REACTOR SAFETY

FIG. 8.1E
TYPICAL ORGANIC LOOP FLOW DIAGRAM

THIS PAGE

WAS INTENTIONALLY

LEFT BLANK

9.000 COSTS AND PERSONNEL

Estimates of the capital costs, operating costs and personnel requirements are given in this section. It is assumed, for both capital cost estimates and operating cost estimates, that the reactor will be located at the NRTS at a site removed from existing facilities.

9.100 Capital Costs

The estimated cost for the EOCR site, buildings, and systems (excluding loops) is $6,310,000. A typical, very basic, large loop experiment is estimated to cost $484,000. The five loops recommended for the initial experiment loading in the EOCR are estimated to cost approximately $1,800,000. The estimated cost breakdown for the EOCR site, buildings, and systems is presented in Table 9.1A. The cost breakdown for a basic large loop experiment is given in Table 9.1B. Due to the conceptual nature and lack of detailed design on this project, the cost estimates must be considered to be approximate.

The exact location of the EOCR site is not known. For purposes of this report, the EOCR site is assumed to be in, or adjacent to, the SPERT-OMRE complex at the National Reactor Testing Station located west of Idaho Falls, Idaho.

The SPERT electrical substation is scheduled for expansion in connection with other reactor programs at the NRTS. It is assumed that this substation will be further expanded to cover the power requirements for the EOCR site. A proportional share of this expansion cost and the cost of two miles of power transmission lines are included in this estimate.

The cost estimate of $6,310,000 includes experiment utilities such as demineralized water, air, commercial and failure-free power, aqueous and gaseous waste disposal, etc., but does not include the cost of experimental in-pile tubes or out-of-pile equipment. In order to accommodate the experimental program approximately $200,000 has been included in the cost estimate for the initial installation of utility systems greater than those required for actual reactor operation.

Items such as handling tools, fuel transfer cask, canal saw, initial fuel charge, initial control rods, initial organic charge, etc. are considered to be operating costs and are not included in this cost estimate. Other items that will affect the overall project cost that are not covered by this cost estimate include land acquisition, communication lines and access road to the EOCR site, land exploration and core drilling, and developmental work necessary to accomplish the actual design of this reactor and its systems.

Table 9.1A

COST ESTIMATE-EOCR SITE, BUILDINGS, AND SYSTEMS

Site Development		
General Clearing and Grading	$ 500	
Security Fencing	6,800	
Perimeter Lighting	4,800	
Sanitary Sewage Pond and Yard Lines	15,900	
Leaching Pond and Yard Lines	9,500	
Site Roads, Sidewalks and Parking Area	13,500	
Yard Electrical	67,200	
Fire Water Loop	20,500	
Steam and Condensate Lines	1,000	
Raw Water System	75,600	
Fuel Oil Storage and Piping	16,000	
Storage Tanks-Demineralized Water, Acid and Caustic	69,000	
Organic Storage Tanks	29,000	
Water Flooding Storage Tank	34,000	
Sub-Total Site Development		$363,300
Buildings		
Guard House		
Architectural and Structural	5,000	
Electrical	1,000	
Piping, Heating and Ventilating	1,000	
Mechanical Equipment	500	
Communication and Alarms	5,000	
Sub-Total Guard House		12,500
Reactor Building		
Architectural and Structural	750,000	
Electrical	110,200	
Piping, Heating and Ventilating	95,900	
Communication and Alarms	16,000	
Mechanical		
Reactor and Reactor Structure	683,500	
Reactor Instrumentation	200,000	
Nitrogen System	2,000	
Primary Coolant System	389,000	
Pressurized Water Condenser Cooling	8,300	
Degassing System	52,000	
Purification and Storage System	77,800	
Water Flooding System	12,500	
Radiation Monitoring Equipment	25,000	
Chemistry Laboratory Furniture	4,000	
Cranes	65,000	
Aqueous Waste System	8,000	

Table 9.1A (Cont'd)

COST ESTIMATE-EOCR SITE, BUILDINGS, AND SYSTEMS

Plant and Instrument Air System	$ 23,000	
Gaseous Waste System	41,100	
Demineralized Water System	81,000	
Fuel Oil System	1,000	
Fire Protection Systems	40,000	
Fire Water System	28,500	
Steam and Condensate System	52,900	
Raw and Domestic Water Systems	4,400	
Electrical System	177,600	
Sub-Total Reactor Building		$2,948,700
Acceptance Testing		40,000
Direct Costs		$3,364,500
Indirect Costs (25%)		841,100
Total Construction Costs		$4,205,600
Engineering Design and Inspection (20%)		841,100
Sub-Total		$5,046,700
Contingency (25%)		1,263,300
Grand Total-EOCR Site, Buildings, and Systems		$6,310,000

Table 9.1B

COST ESTIMATE-EOCR BASIC LARGE LOOP EXPERIMENT

Instrument and Electrical		
Instrument Panel (Complete)	$35,000	
Transmitter Cubicle	16,000	
Electrical Equipment	29,000	
Labor- Instrument	7,200	
Labor- Electrical	12,500	
Sub-Total Instrument and Electrical		$99,700
Piping		
Pipe	11,800	
Valves	17,500	
Insulation	2,000	
Labor--Pipefitter and Welder	37,200	
Sub-Total Piping		68,500
Equipment and Tanks		
Pumps	14,000	
Condensers	3,600	
In-Pile Tube	50,000	
Tanks	3,000	
Miscellaneous Equipment	2,200	
Insulation	2,500	
Labor	8,400	
Sub-Total Equipment and Tanks		83,700
Cubicle and Sample Station		
Walls (High Density)	2,400	
Shielded Dock	1,200	
Miscellaneous	1,100	
Labor	1,500	
Sub-Total Cubicle and Sample Station		6,200
Direct Costs		$258,100
Indirect Costs (25%)		64,500
Total Construction Costs		$322,600
Engineering Design and Inspection (20%)		64,500
Sub-Total		$387,100
Contingency (25%)		96,900
Grand Total--Large Loop		$484,000

9.200 Personnel Requirements ($403,000)

Table 9.2A contains the estimated personnel requirements for the direct on-site functions. Administrative services and indirect-site services are provided for in Table 9.3B. Wage and salary rates currently in effect at the MTR-ETR were used to estimate the cost of personal services. This estimate includes five per cent for employee benefits and payroll taxes.

Table 9.2A

PERSONNEL REQUIREMENTS

Superintendent	1
Operations Supervisor	1
Operations:	
Shift Supervisors	4
Senior Reactor Technicians	4
Reactor Technicians	8
Utility Operator	4
Utility Helpers	8
Services:	
Health Physics and Safety Supervisor	1
Health Physicists	4
Instrument and Electrical Supervisor	1
Senior Instrument Technician	1
Instrument Technicians	4
Electricians	2
Special Maintenance Supervisor	1
Mechanics	2
Mechanic Helpers	3
Janitor	1
Control Chemist	1
Lab Technician	1
Secretaries	3
Security Guards	4
EOCR Operating Staff	59

9.300 Operating Costs (Other Than Labor)

9.310 Fuel and Control Rods ($369,000). The estimate of nuclear fuel cost is based on the following design criteria: (a) the reactor operates 10,000 Mwd/yr utilizing three fuel cores per year; (b) a core loading consists of twenty-five fuel assemblies and twelve control fuel assemblies; and (c) each fuel assembly and control fuel assembly contains 1.625 kg U-235.

Table 9.3A

COMPUTATION OF ANNUAL FUEL COST

Fabrication of Fuel

25 core fuel assemblies x 3 loadings = 75 x $3,000	$225,000
12 control fuel assemblies x 3 loadings = 36 x $4,000	144,000
Total Fabrication Cost	$369,000

(Note: In addition to the above it is estimated that burnup, fuel reprocessing and reconversion will amount to $880,200 per year. These costs are nonprogram and for this reason are not included in this report.)

9.320 Organic Coolants ($120,000). The cooling system capacity is 135,000 pounds of organic liquid (15,000 gal); at an estimated price of $0.20/lb the cost of the initial charge of coolant is $27,000. It is estimated that make-up of coolant while the reactor is operating at full power will amount to 2,400 lb/day or $480/day. The estimated annual cost for make-up is $120,000.

9.330 Materials and Services ($618,000).

Table 9.3B

OTHER EXPENSE

	Annual Cost
Materials and Supplies	$ 80,000
Chemicals	3,000
Fuel Oil	7,000
Electricity	85,000
Telephone and Telegraph	10,000
Administrative and Site Services	433,000
	$618,000

9.400 Annual Cost ($1,510,000)

Table 9.4A

ESTIMATED ANNUAL OPERATING COST*

	Annual Cost
Direct Personnel	$ 403,000
Nuclear Fuel Fabrication	369,000
Organic Coolant	120,000
Materials and Services	618,000
Total	$1,510,000

*. Does not include depreciation costs which are non-program for this type of operation.

THIS PAGE

WAS INTENTIONALLY

LEFT BLANK

10.000 ACKNOWLEDGEMENTS

To Operations Division of AEC Idaho Operations Office for their assistance in developing the research program on which the conceptual design was based and for their aid in obtaining materials for the water flooding tests.

To the Engineering and Construction Division of AEC Idaho Operations Office for their assistance in the development of the cost estimates contained in this report.

To the Civilian Power Reactors Branch of the AEC Division of Reactor Development for their helpful comments during the September, 1959, review of several preliminary reactor concepts.

To the Atomics International staff at OMRE for their discussion of OMRE operational experience and for their assistance in obtaining coolant for the water flooding tests.

To the Atomics International staff at Canoga Park for the many helpful discussions on physics, heat transfer, fuel element technology, coolant chemistry, and auxiliary process systems.

Many of the Phillips staff, in addition to those listed on the title page, participated in various phases of the conceptual design and test program, and their contributions are gratefully acknowledged.

THIS PAGE

WAS INTENTIONALLY

LEFT BLANK

S U P P O R T I N G I N V E S T I G A T I O N S

SECTIONS 11.000 THROUGH 20.000

THIS PAGE

WAS INTENTIONALLY

LEFT BLANK

11.000 SELECTION OF EOCR CORE

The standard core, discussed in Sections 4.000 and 5.000, was selected after studying a number of designs. The other cores, one using cylindrical fuel elements, two using OMRE fuel elements, and one flux trap core using both EOCR and OMRE type fuel elements, are presented in Figs. 11.1A through 11.1D. A brief description of the cores, summary of the physics calculations, and the basis for selection of the EOCR core are given below.

11.100 Description of Cores

Drawings of the four core arrangements used for physics calculations are given in this section along with a summary of results. All of the physics results presented in Tables 11.1A through 11.1D correspond to rod positions at the end of the cycle. Thus, the power densities shown for experiments and maximum-to-average flux ratios in both the driver elements and the central loop are not the maximum that can be attained by selective control rod programming.

Precise comparisons cannot be made between Tables 11.1A through 11.1D because experiment calculational models and fuel loadings were different. Table 11.1D is based on 7.5% enriched fuel in the experiments whereas the other tables are for 2.5% enriched fuel in the experiments. In Section 5.000 the power density in experiments with 7.5% enriched fuel is shown to be about 1.9 times that of experiments with 2.5% enriched fuel.

11.110 Cylindrical Fuel Element Core. A core arrangement using 6.375 in. cylindrical fuel elements, spaced in a 7.375 in. triangular lattice, was considered for the EOCR because removal of one large fuel element provided space for a large experimental loop. Physics calculations were made for this core, arranged as shown in Fig. 11.1A with test fuel elements in each position containing 2.5% enriched fuel.[1] A summary of the results of the calculations is given in Table 11.1A. The calculated k_{eff} for this core with 32 kg of U-235 was 1.13.

---

1. Bechtel Corporation and Atomics International, "Organic Cooled Power Reactor Study - 300 Mw Power Plant Conceptual Design", Supplement No. 2, Report BCPI-1, June 26, 1959.

Table 11.1A

SUMMARY OF PHYSICS CALCULATIONS FOR INVOLUTE PLATE FUEL ELEMENT CORE WITH 40 MW GENERATED IN DRIVER FUEL ELEMENTS

			Driver Assemblies	Large Center Loop	Small Off Center Loop	Peripheral Power Reactor Element
Flux x 10^{-14}	Fast	Avg	2.21	2.50	2.90	0.78
		Max/Avg	1.88	1.40	1.40	2.69
	Thermal	Avg	0.45	0.88	0.42	0.41
		Max/Avg	3.45	1.57	2.23	3.07
Power Density* watts/cc		Avg	---	105	59	45
		Max	---	165	133	154

* Power density based on 2.5 per cent enriched fuel in tests.

11.120 OMRE Fuel Element Cores. Two core arrangements using OMRE fuel elements were studied because OMRE fuel elements have been proven for organic reactor use. One core, shown in Fig. 11.1B, has fuel elements spaced on 4.5-in. square centers. This core does not allow space for loops larger than about 5.5 in. in diameter. A flux trap variation of the OMRE core, shown in Fig. 11.1C, was designed to provide space for a larger center loop. The physics calculations for these cores are summarized in Tables 11.1B and 11.1C. All fuel elements in test positions were 2.5%[1] enriched for these calculations and arranged as shown in the figures. The calculated k_{eff} for the OMRE-type core is 1.19 with 42.6 kg of U-235 and k_{eff} for the flux trap core is 1.23 with 46 kg of U-235.

1. Bechtel Corporation and Atomics International, "Organic Cooled Power Reactor Study - 300 Mw Power Plant Conceptual Design", Report BCPI-1, Supplement No. 2, June 26, 1959.

Table 11.1B

SUMMARY OF PHYSICS CALCULATIONS FOR OMRE TYPE CORE
WITH 40 MW GENERATED IN DRIVER FUEL ELEMENTS

		Driver Assemblies	Large Center Loop	Small Off Center Loop	Peripheral Power Reactor Element
Flux $\times 10^{-14}$	Fast Avg	1.52	2.0	1.70	0.77
	Max/Avg	2.04	1.40	1.48	2.36
	Thermal Avg	0.41	0.45	1.10	0.26
	Max/Avg	3.59	1.74	1.65	3.18
Power Density* watts/cc	Avg	---	57	124	31
	Max	---	97	199	94

* Power density based on 2.5 per cent enriched fuel in tests.

Table 11.1C

SUMMARY OF PHYSICS CALCULATIONS FOR OMRE TYPE FLUX-TRAP CORE
WITH 40 MW GENERATED IN DRIVER FUEL ELEMENTS

		Driver Assemblies	Large Center Loop	Small Off Center Loop	Peripheral Power Reactor Element
Flux $\times 10^{-14}$	Fast Avg	1.59	2.10	1.60	0.53
	Max/Avg	2.08	1.47	1.49	1.77
	Thermal Avg	0.39	0.99	1.10	0.20
	Max/Avg	3.48	2.12	1.65	2.87
Power Density* watts/cc	Avg	---	113	118	24
	Max	---	230	196	63

* Power density based on 2.5 per cent enriched fuel in tests.

11.130 EOCR Flux Trap Core. A flux trap variation of the standard core is shown in Fig. 11.1D and a brief summary of physics calculations is given in Table 11.1D. This core was made up of both EOCR and OMRE type fuel elements. All test fuel elements used for these calculations contained 7.5% enriched fuel, and k_{eff} is 1.167 with 45 kg of fuel in the core.

Table 11.1D

SUMMARY OF PHYSICS CALCULATIONS FOR EOCR FLUS TRAP CORE WITH 40 MW GENERATED IN DRIVER FUEL ELEMENTS

		Driver Assemblies	Large Center Loop	Small Off Center Loop	Large Off Center Loop
Flux x 10^{-14}	Fast Avg	1.70	2.58	1.97	1.97
	Fast Max/Avg	2.20	1.43	1.52	1.64
	Thermal Avg	0.36	0.57	0.43	0.36
	Thermal Max/Avg	3.33	2.22	1.63	2.08
Power Density* watts/cc	Avg	---	177	134	116
	Max	---	368	215	227

* Power density based on 7.5 per cent enriched fuel in tests.

11.200 Basis for Selection of the EOCR Core.

A comparison of some of the features of the cores studied with the design requirements is presented in Table 11.2A. The maximum power densities listed for a loop in the center of each of the cores are those at the start of each reactor cycle with the central control rods pulled and with the loops containing 7.5% enriched fuel elements. These values are not on the same basis as the tables in Section 11.100. The numbers shown for the cylindrical element core and the OMRE cores are obtained by correcting the values shown in Tables 11.1A through 11.1C to apply to 7.5% enriched fuel and the different rod configurations. The coolant flow rates shown for all of the cores are based on total reactor flows that are about 5000 gpm higher than the flow required to cool only the core components. This flow is necessary to cool the moderator and experimental fuel elements in core positions and allow for leakage between components. The EOCR core coolant requirements are less than the requirements for the other cores because the fuel elements for this core were designed to make the most efficient possible use of the coolant for heat transfer.

---

1. Bechtel Corporation and Atomics International, "Organic Cooled Power Reactor Study - 300 Mw Power Plant Conceptual Design", Report BCPI-1, Supplement No. 2, June 26, 1959.

Table 11.2A

COMPARISON OF EOCR DESIGN REQUIREMENTS
WITH CALCULATED PERFORMANCE OF CORES AT 40 MW*

Design Feature	Design Requirements for Initial Tests	EOCR Standard Core	Cylindrical Element Core	OMRE Element Core
Number of Test Positions	13 0.5" to 1.5" OD 3 2.5" OD 2 6.5" OD	26 1.0 to 1.5" OD 4 2.5" OD 2 6.5" OD	6 1.0" OD 3 2.3" OD 1 6.5" OD	4 2.5" OD 1 6.0" OD
Number of Incore Positions	10 5.38" sq or larger	20 5.5" sq	12 7.2" OD	40 4.4" sq
Maximum** Power Density in Large Loops, w/cc	300	495	405	338
Heat Flux Driver Elements Btu/hr-ft^2	----	650,000	560,000	700,000
Reactor*** Coolant Flow Required	25,000	25,000	28,000	31,000

* Based on control rod positions corresponding to start of cycle.

** Power density based on 7.5% enriched fuel elements.

*** The total flow shown allows 5000 gpm for experiment coolant flow, leakage flow past the core components, and for cooling the moderator.

Table 11.2A shows that the peak power density in the test positions for the EOCR core are higher than for the other cores at the start of the cycle. The average values for the EOCR and cylindrical element core at the start of the cycle are about the same. At the end of the cycle the cylindrical element core gives power densities in the central test loop about 15% greater than in the EOCR. However, the EOCR core will compare favorably with the cylindrical core at all times if (1) the outer loops in EOCR are replaced with fuel as in the cylindrical element core and (2) the loadings are adjusted to give the same k_{eff}.

The OMRE element core is inferior to the standard core because the smaller lattice does not permit adequate moderator around a large loop. This results in the OMRE element core having about 45 per cent lower maximum power density in a large loop than the standard core.

The flux trap variation of the standard core provided higher flux in a central loop than the standard core; however, the standard core configuration was selected because it met the design objectives and involved fewer complications in mechanical design. The standard core also allows more flexibility in arrangement because all of the core components are uniformly spaced.

In summary, the reasons for selection of the EOCR core, with 4 in. square fuel elements spaced on 5.75 in. centers in a square lattice, are as follows:

1. The core has adequate experimental space to accommodate the initial test requirements outlined in Section 3.000, and the core contains enough fuel elements to permit changes in the core arrangement and addition of more experiments without significantly changing the reactor operation.

2. Any or all of the driver fuel elements, except those in positions adjacent to large loops, can be replaced by large power reactor fuel elements without making any mechanical changes within the reactor vessel.

3. The maximum power density available in a large center loop meets the maximum design objectives with the EOCR operating at 40 Mw, and other core positions provide power densities suitable for testing organics and fuels at conditions corresponding to proposed power reactor operation.

4. The flat-plate fuel elements and control rod assemblies used as drivers can be fabricated without major development work.

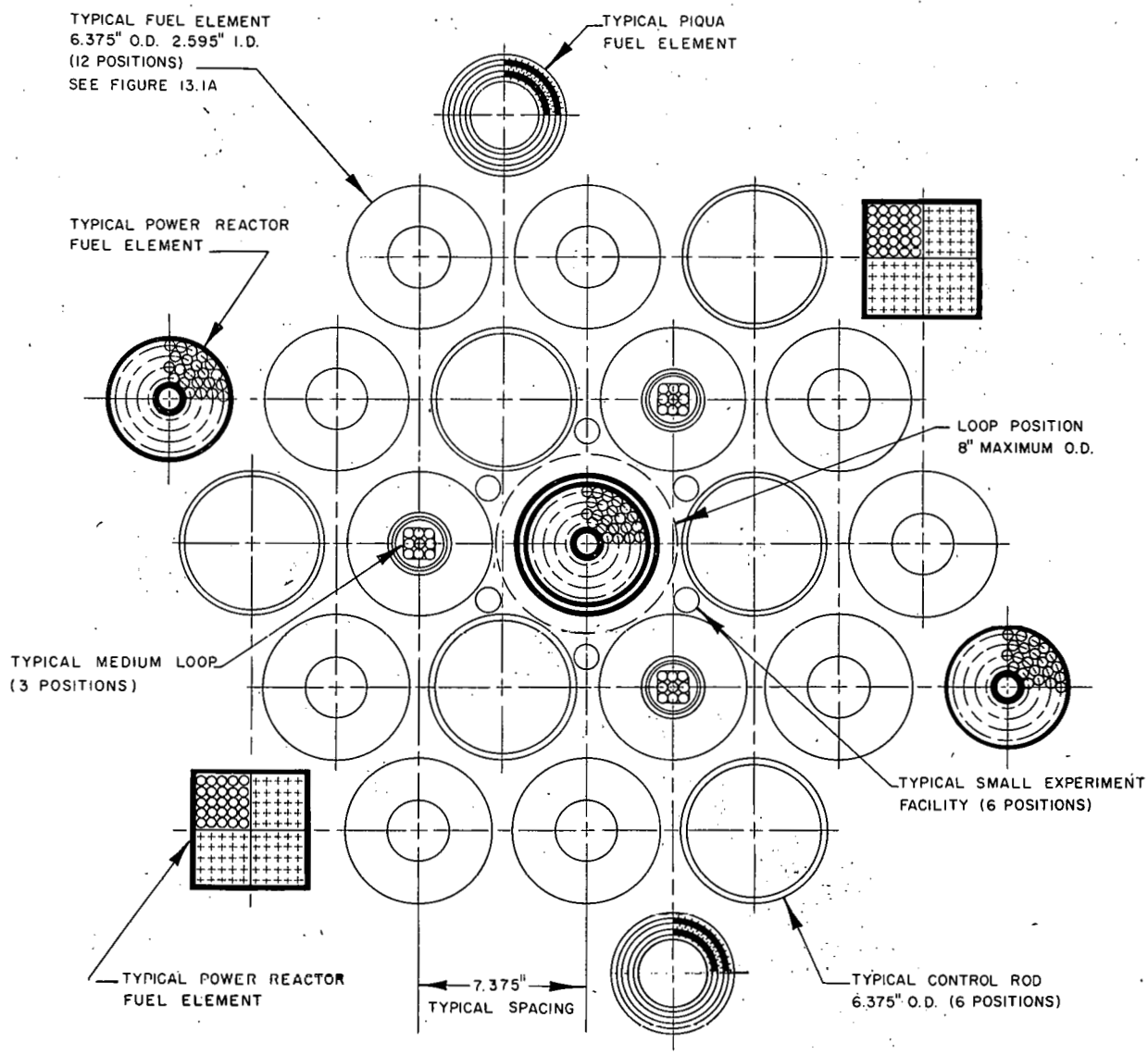

FIG. II.1A
EOCR CORE WITH CYLINDRICAL FUEL ELEMENTS

P.P. CO. - C - 2543

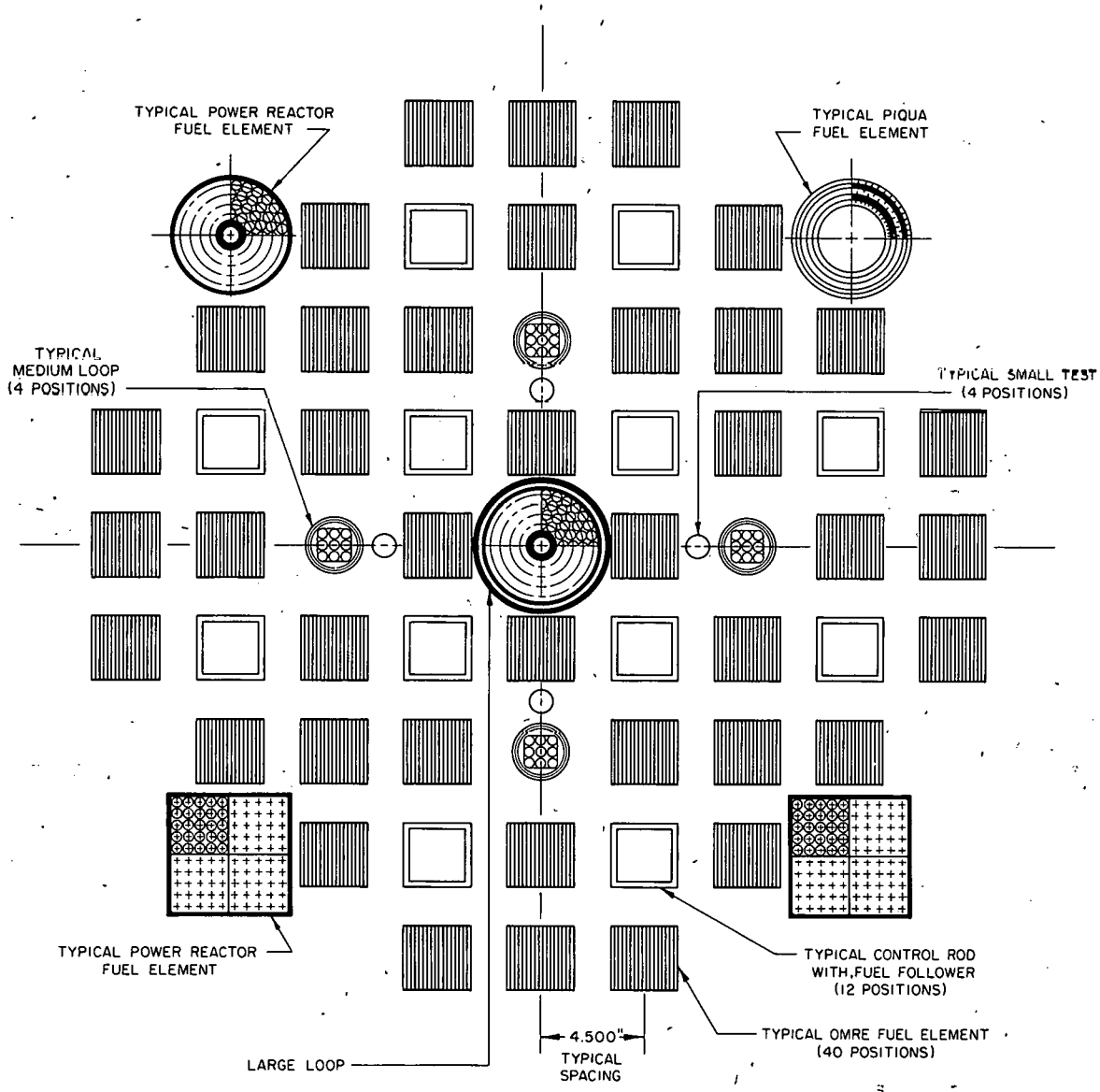

FIG. II.IB

EOCR CORE WITH OMRE TYPE FUEL ELEMENTS

P.P. CO. - C - 2544

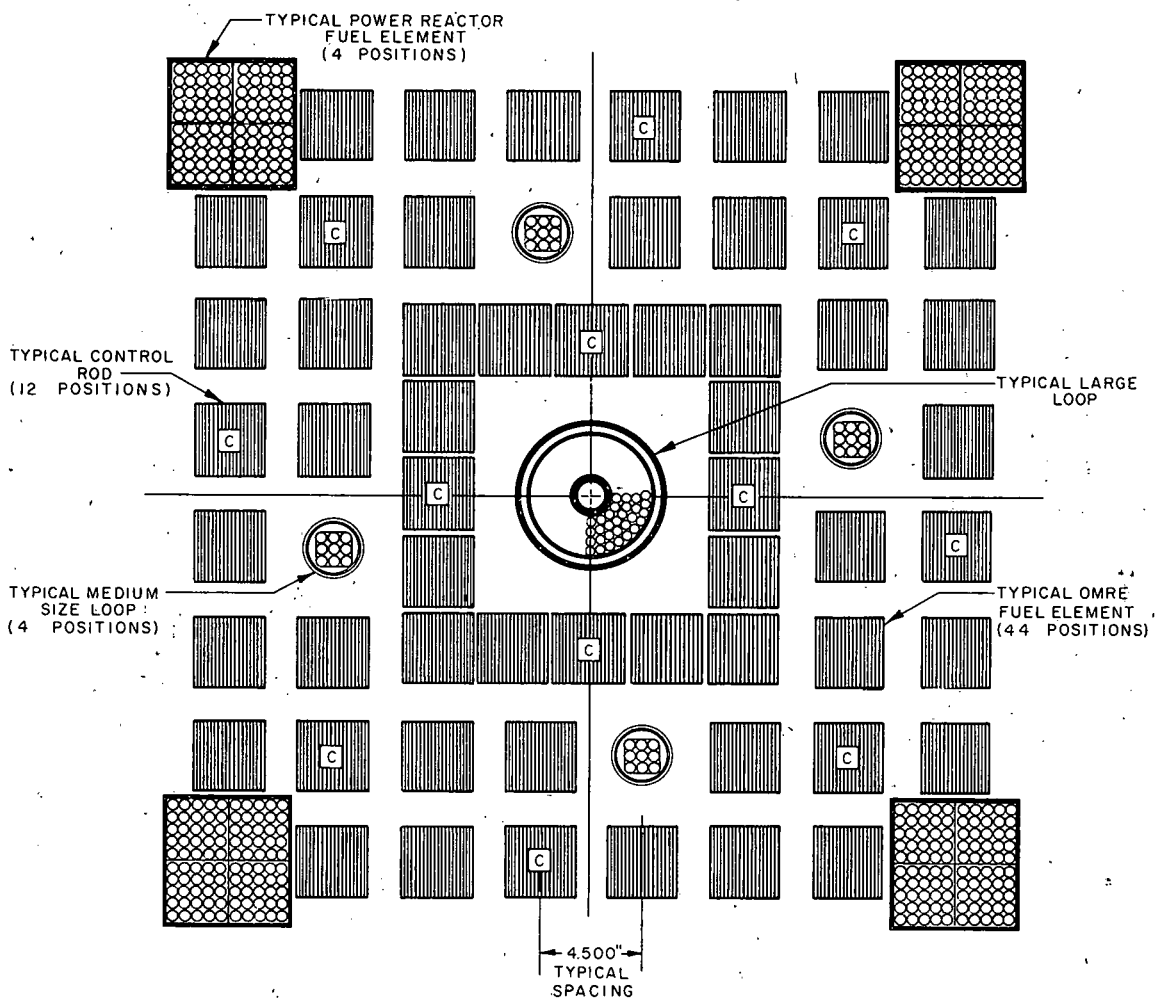

FIG. II.IC

EOCR FLUX TRAP CORE
WITH OMRE FUEL ELEMENTS

P.P. CO.—C—2545

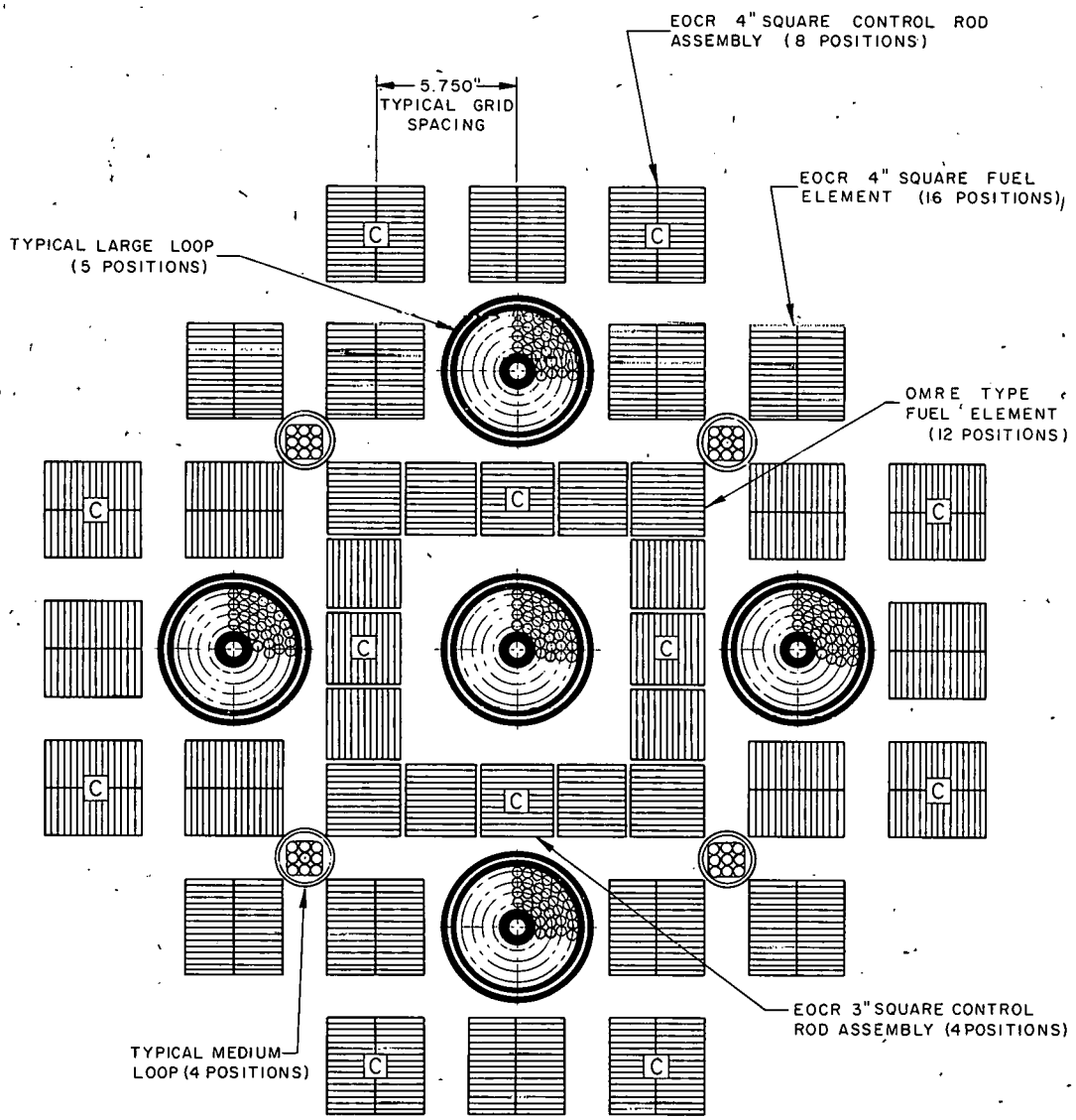

FIG. 11.1D

EOCR FLUX. TRAP CORE

PP. CO.-C-2546

12.000 WATER FLOODING EXPERIMENTS

The method of handling fuel elements and in-pile equipment described in Section 7.200 was chosen after several tests were performed to demonstrate experimentally that hot organic could be replaced with hot water and the water cooled or flushed until clear. Six tests were conducted in a 40-gal vessel with different Santowax compositions to determine: (1) how much organic remained on components after completion of the flushing operation, (2) how much mixing would occur between the water and organic during flushing, (3) whether or not fuel elements would stick to other components as a result of buildup of frozen Santowax, and (4) how many flushings are required before the water becomes clear.

These tests, as described in the subsections that follow, demonstrated conclusively that hot organic can be replaced with hot water, that 3 to 5 cold water flushes clarify the water so the core components are visible, and that the core components will remain free of residue organic if the water temperature during the first flush is kept well above the freezing point of the organic. In test No. 6, Santowax R was replaced with hot water that remained above 343°F during the first flush and the dummy fuel element was nearly as clean after completion of the test as it was before the test, as shown in Fig. 12.3E.

12.100 Organic Materials

Four organic compositions were used in the six tests. Unirradiated Santowax OMP was used for two tests, a mixture of Santowax OMP and Santowax R was used for one test, irradiated OMRE coolant with 27 per cent HB was used for two tests, and Santowax R was used for one test.

The water content of the Santowax in the as-received-condition was approximately 250 ppm. The maximum impurities present were chlorine, 2 ppm; iron, 1 ppm; sodium, 0.7 ppm; and silicon, 0.5 ppm. The water content of the irradiated OMRE coolant was approximately 400 ppm.

The melting point of Santowax R and OMP is about 300°F. The irradiated OMRE coolant was liquid (though quite viscous) at room temperature.

The density difference between liquid Santowax (both unirradiated and irradiated) and water at various temperatures is approximately constant (see Fig. 12.1A).

The solubility[1] of water in unirradiated Santowax R at 350°F is approximately 8000 ppm.

---

1. R. H. F. Gercke, F. C. Silvey and G. Asanovich, "The Properties of Santowax R (Mixed Terphenyl Isomers) as Organic Moderator-Coolant", Report NAA-SR-Memo-3223.

12.200 Test Apparatus and Procedures

The apparatus used for the tests consisted of a 40-gal pressure vessel, which held organic to start the tests; a 66-gal tank, into which the organic was transferred; and a 100-gal water tank, which supplied hot water for the replacement and flush. The flow system is illustrated in Fig. 12.2A.

An ETR fuel element was inserted into the pressure vessel to determine how much organic would remain between the fuel plates and if the fuel element would stick in simulated grid plates. The fuel-element assembly, Fig. 12.2B, consisted of a dummy fuel element held upright by plates and guide plate with clearances between the fuel element and the bottom grid plate of 0.002 inch. The clearance between the top square guide plate and face element was 0.004 inch, and the fuel element rested in a tapered grid plate. The assembly and fuel element was constructed of aluminum alloy 6061.

12.210 Replacement of Organic. The Santowax and water for tests 1, 2, 3, and 6 were heated to 350°F. A globe valve in the exit line from the pressure vessel was set to control the rate of flow, and an attempt to maintain a constant pressure difference, and hence flow rate, was made by applying nitrogen pressure on the water tank and by venting the organic receiving tank. The OMRE irradiated coolant and water were heated to 200°F in one replacement and 300°F in the last replacement.

The organic replacement rate was measured by diverting the stream for a short period of time and also by establishing the time for the total replacement to occur.

12.220 Sampling. Samples of organic were taken at intervals through a sampling line (Fig. 12.2A) on the downstream side of the flow control valve. Samples of flush water were taken through the same sampling line. The completion of organic replacement could be detected by steam or water coming from the sampling line as well as by rapid rise of pressure in the organic receiving tank.

12.230 Measurement of Clarity of the Water. The top of the pressure vessel was removed after three flushes in the first two replacements, after five flushes in the next three replacements, and after four in the last. The depth of visibility of the fuel element assembly and tank was noted both by spot light above and in two replacements by use of a 1000-watt underwater lamp.

12.240 Organic and Water Analyses. The organic and water analyses were performed by the Chemical Processing Plant staff of Phillips Petroleum Company. The analysis of organic for water content was made by a modification of the Karl Fisher method using Karl Fisher's reagent, water-methanol standard, and chloroform as the dissolution medium. The precision of the organic analyses to be associated with the average (water content of most samples 1,000-3,000 ppm) was a standard deviation of ± 260 ppm.

The analysis of the water for organic content was made by extracting the organic into carbon tetrachloride and measuring the absorption of the aromatic carbon-hydrogen bond on an infra-red spectrometer. The precision was ± 15% of the amount present with an approximate lower limit of 2 ppm.

12.250 Organic Holdup on Fuel Element Surfaces. The organic holdup on the fuel-element surfaces was examined visually and by estimating the force to manually remove the fuel element from the grid plate assembly.

12.300 Results

Six tests were run as indicated in Table 12.3A which shows the temperature conditions before and after transfer of the organic and the flow rates of the organic-water interface. The tests with high melting Santowax R and Santowax OMP demonstrated the importance of keeping the Santowax from freezing during transfer. In test No. 6, where the flush water was kept above 343°F, little film remained on the fuel element after the flush. In test numbers 1 to 3, where the water cooled to near the freezing points of the mixtures, Santowax remained on the surfaces of the fuel element. Table 12.3B gives the water content of the organic and the organic content of the water. The samples indicated in the table as number 1 were taken shortly after the organic flow started, samples number 2 approximately in the middle of the replacement, and samples number 3 at the end, but before the organic-water interface was detected.

Table 12.3A

ORGANIC FLOW RATES AND TEMPERATURE CONDITIONS

Test Number and Organic Used	Organic Temperature, °F		Water Temperature, °F		Water Pressure (lb/in^2)	Water Temp., °F at Removal	Flow Rate Through Vessel (ft/min)
	Before Transfer	After Transfer	Before Transfer	After Transfer			
1 Santowax OMP	372	285	336	320	140	160	3.3
2 Santowax OMP	383	300	350	315	148	150	Initial 0.5 Avg. 0.2
3 Santowax OMP + Santowax R	385	300	350	305	134	90	Initial 0.5 Avg. 0.2
4 Irradiated OMRE Coolant	197	125	200	---	0	80	1.1
5 Irradiated OMRE Coolant	300	---	300	287	58	80	1.4
6 Santowax R	390	230	350	343	121	137	2.5

Table 12.3B

WATER CONTENT OF ORGANIC AND ORGANIC CONTENT OF WATER

Test	Water Content Of Organic (ppm) Sample Number			Organic Content of Water (ppm) Volume of Flush Water				
	1	2	3	2***	3	3.5	5	5.5
1	3,750	115	25,000*	45	10	--	--	---
2	3,590	1,520	32,400*	65	3	---	---	---
3	1,340	2,000	31,600*	---	7	---	Not Detectable	---
4	1,385	382	200	1,200**	8,500**	---	3	---
5	2,095	2,020	1,256	140	--	4	---	3
6	1,125	510	1,275	7	3	1	---	---

* Two phases present after sample cooled made sampling for analysis uncertain.

** Globules of organic in sample bottle (globules may have let go from pipe surfaces).

*** Numbers refer to volumes of flush water per volume of organic.

12.310 Flow Measurement and Uniformity of Samples. The flow measurement at the start of the test was used to predict the sampling times and the time for completion of transfer. The estimated time for completion of transfer agreed well with the completion time except in test 2 and 3, wherein two values are given for the flow rate (Table 12.3A).

Most of the water present in the discharge line from the pressure vessel was removed by heating at the start of each test (after draining under nitrogen pressure). The quantity of organic (1-5 gal) used for flow measurement was used to purge the line before the first organic sample was taken, however, sample 1 in tests 1 and 2 evidently contain water from the piping system.

Difficulty was also experienced for the first flush water samples in which the organic phase would come through in globules, and the size of the globule caught in the sample caused large deviations in the organic content of the flush water sample. It is to be noted, however, that no difficulty was experienced in determining the completion of the replacement. The passing of the organic-water interface down the fuel element and through the pipes was reasonably sharp.

12.320 Drainage and Sticking of the Fuel Element. After the desired number of flushes with water had been completed, the pressure vessel was opened and the fuel element manually lifted out. In the first two tests with Santowax OMP the force required to lift the fuel element was estimated as less than 50 pounds, with that for test 2 less than for test 1. In test 3 the force required to lift the fuel element was estimated as greater than 100 pounds (the element was pried loose before lifting). In this test there was solid organic between the fuel element and the guide plates and grid plates and although the channels were not closed solid, there was some bridging of organic between the fuel plates.

Fig. 12.3A shows the fuel element after completion of test 2 which used Santowax OMP at 350°F. (The fuel element looked about the same after test 1). An organic film can be seen on the surfaces with the heaviest film on the surface which is located between the guide plate and top of the fuel element. It is noted that the organic has drained from the slots on the bottom end box leaving a thin overall film. Fig. 12.3B shows the film on the fuel element after test 5 with irradiated OMRE coolant. The drainage is good, and the film appears to be of even thickness.

Fig. 12.3C(1) shows a view of the fuel plates and coolant channels of the same fuel element shown in Fig. 12.3A. The thickness of the film is greater in some places, but a maximum of less than half of the channel is filled. Fig. 12.3C(2) shows that for test 5 with irradiated OMRE coolant, there is less film buildup. Fig. 12.3E shows that for test 6 there is little Santowax R remaining on the surfaces or channels. The force required to lift the fuel element was estimated at less than 100 pounds. It should be mentioned that the force to remove an element in the ETR varies, sometimes being as high as 100 pounds.

The force required to lift the fuel element in tests 4 and 5 using irradiated OMRE coolant was very low (not much greater than with no organic).

12.330 Water Clarity Evaluation. In Fig. 12.3D the clarity of the water after flushing is shown to be poor, after three flushes, in test 2. The light from the underwater lamp almost reached extinction when the lamp was at 7.5 feet (compare views (1), (2), and (3) for test 2). It should be noted that the temperature of the water was 150°F, hence steam bubbles contributed to the extinction. Table 12.3B also shows that after three flushes in all tests, the organic content of the water is greater than three ppm, and this is detectable by sight as a colloidal dispersant in the water. View (4) of Fig. 12.3D shows that in test 5, after five flushes, the bottom of the vessel can be detected along with some organic that was left from test 3. The light spots are the result of reflections from scum on the top of the water. Table 12.3B indicates that the organic content of the water is three ppm or less after five flushes. The temperature of the water at the time the picture was taken was 70°F.

The clarity of the water after four flushes (test 6) at 137°F was such that the bottom grid could be seen through 5 ft of water.

The important variables affecting visibility through the water were the temperature of the water, the colloidal organic in the water, time for coalescence, and the removal of scum on top of the water.

12.400 Discussion.

The effect of difference in the rate of the organic-water interface (though it varied from 0.2 to 3.3 ft/min) moving past the fuel element could not be detected in the six replacements conducted. The drainage of organic at 3.3 ft/min in test 1 was not much different than at 0.2-0.5 ft/min. A rupture disc broke in test 1 (disc was downstream from the flow control valve) necessitating stopping the flow to replace the disc. An organic ring was noticed on the fuel element after removal at a position that would just about correspond to the interface at the time of stoppage; however, the organic film on the surface and in the channels was not much different from that shown in Fig. 12.3A and Fig. 12.3C view (1) for test 2.

In test 3, in which the fuel element was difficult to remove, there were two variables that may have caused more organic to hold up in the clearances, in the coolant channels, and on the fuel element surfaces. These variables are: (1) lower organic temperature during replacement, and (2) reuse of Santowax OMP from test 1 and 2 which had picked up a small amount of rust particles. From Table 12.3A it is seen that the water temperature in the pressure vessel after replacement of the organic was lower than in test 2. This correlates with the lower water pressure before transfer. Because of baffling in the water tank it was possible to have and to retain higher temperature water in the top of the tank, hence the reason for the higher water pressure indicated in Table 12.3A for the same water temperatures. The pressure vessel also had an appreciable heat capacity, and further modification of the heating system before test 6 was necessary to get a fairly uniform temperature throughout the vessel and organic. Therefore, although the organic in test 3 was at a higher temperature before transfer and after transfer than test 1 the replacement water (producing the organic-water interface) was at a lower temperature. The higher temperature of organic after transfer in test 3 as compared to test 1 (while the organic-water interface was at a lower temperature) can be explained by the heat obtained from the piping system during the rather long transfer time (50 minutes). This conclusion that holdup of the organic on the surfaces was due to low interface temperature is borne out by the organic which solidified in the bottom of the pressure vessel after test 3 (see Fig. 12.3D view (4), and by test 6 using Santowax R. The water after transfer was at 343°F and very little Santowax remained on the surfaces, Fig. 12.3E.

Any dirt on the surfaces (especially horizontal surfaces) does increase the holdup of organic, but this effect will decrease with increase in temperature or decrease in melting point of organic; e.g., as with test 4 and 5.

The replacement rate of the organic over the range studied was not found to affect the organic content of the water nor the water content of the organic as seen in Table 12.3B. It is believed that the prevention of boiling during replacement and also the method of steam blowoff which was used in order to flush with hot water is of much greater importance to the problem of mixing of organic and water than the flow rate.

The volume of flush water used to give clear water at the bottom of the 10 foot vessel was approximately 5 times the volume of organic. The clarity of the water apparently depends upon the extent of boiling during replacement and flushing, in addition to the volume of flush, and upon the temperature of the water and time of standing. The colloidal organic had a tendency to coalesce and settle out on standing.

The completion of replacement of the organic was not difficult to detect, especially at the small bleed stream from the sampling line. Completion could also be detected on the pressure gage on the organic tank. From the manner in which the water at the sampling line cleared, it is believed the organic-water interface passed fairly sharply through the line. As is seen in Table 12.3B trouble was experienced with only two samples from globules breaking lose and passing into the water samples. Results shown in Table 12.3B show, however, that there is water above the saturation value passing with the organic before the interface was detected, however the amount of this high-water-content organic is estimated to be low.

When the organic became super-saturated with water and heat was applied some frothing of the organic was noted as steam was released. This tendency was not serious although noted with both unirradiated and irradiated organic.

The number of contacts between organic and water before saturation is reached was greater than one (see Table 12.3B). It is realized that some water went into the organic tank at the end of the replacement and was boiled off so that one run represents more than one organic-water contact.

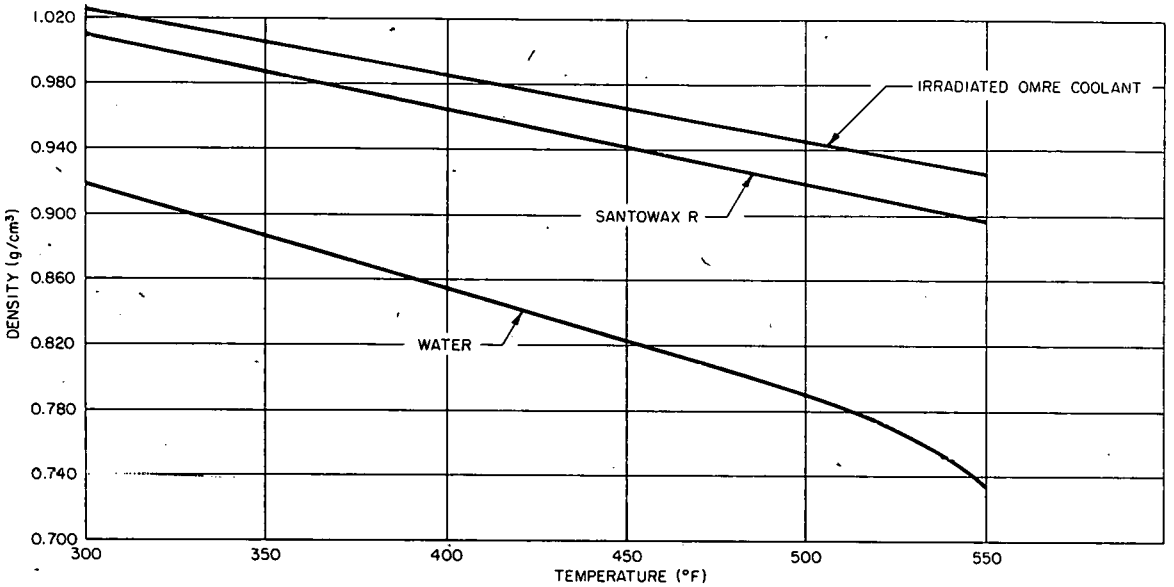

FIG. 12.1 A

DENSITY OF ORGANIC AND WATER AT VARIOUS TEMPERATURES

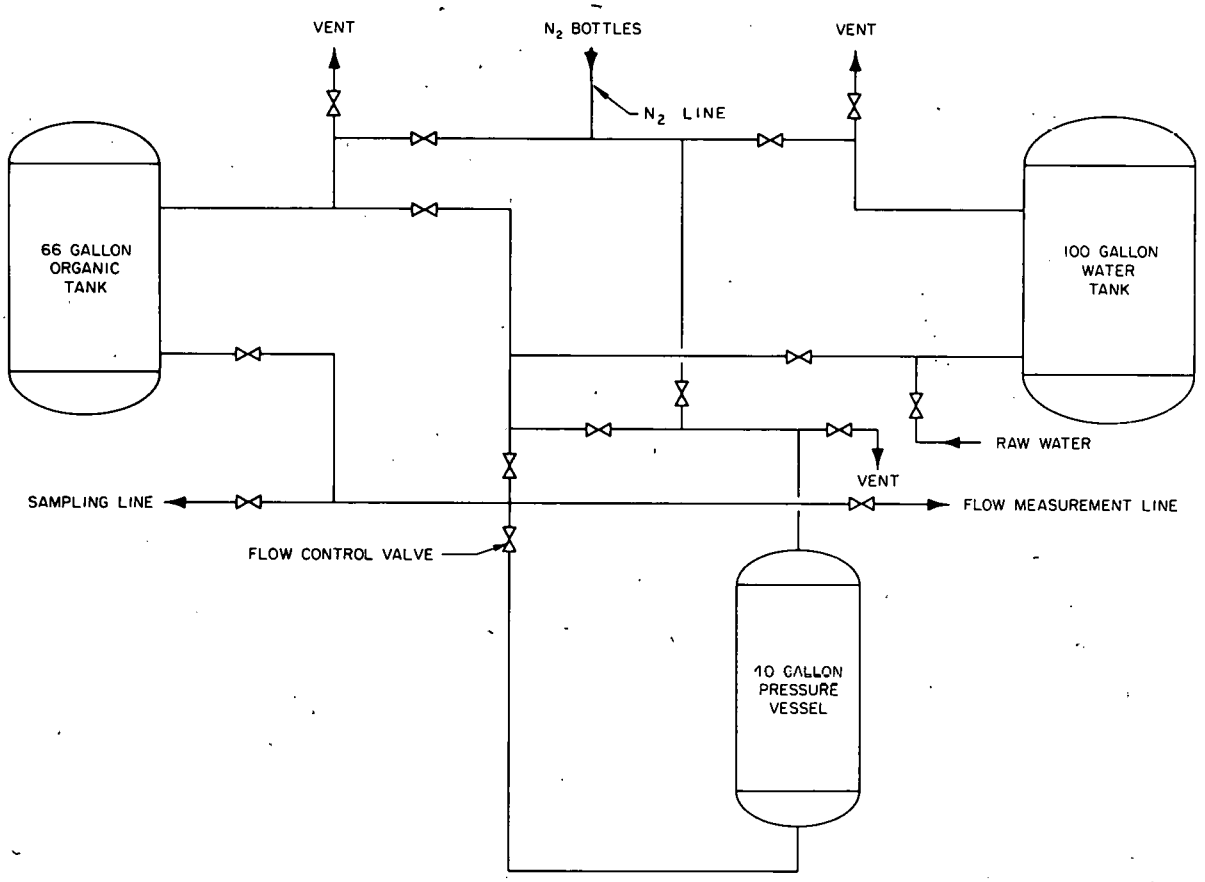

FIG. 12.2 A

FLOW DIAGRAM FOR WATER FLOODING EXPERIMENTS

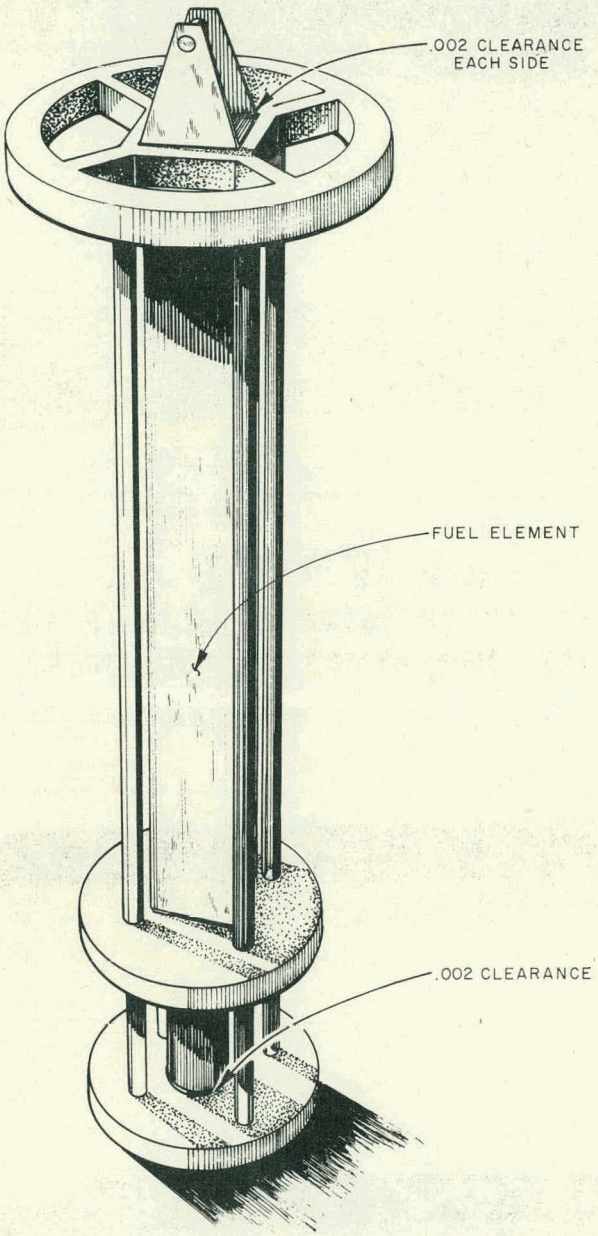

PRCO.— C — 2548

FIG. 12.2B

FIXTURE FOR HOLDING ETR FUEL ELEMENT
IN WATER FLOODING TESTS

FIG. 12.3A
FUEL ELEMENT AFTER WATER FLOODING USING
SANTOWAX OMP AT 350 °F. RUN No. 2

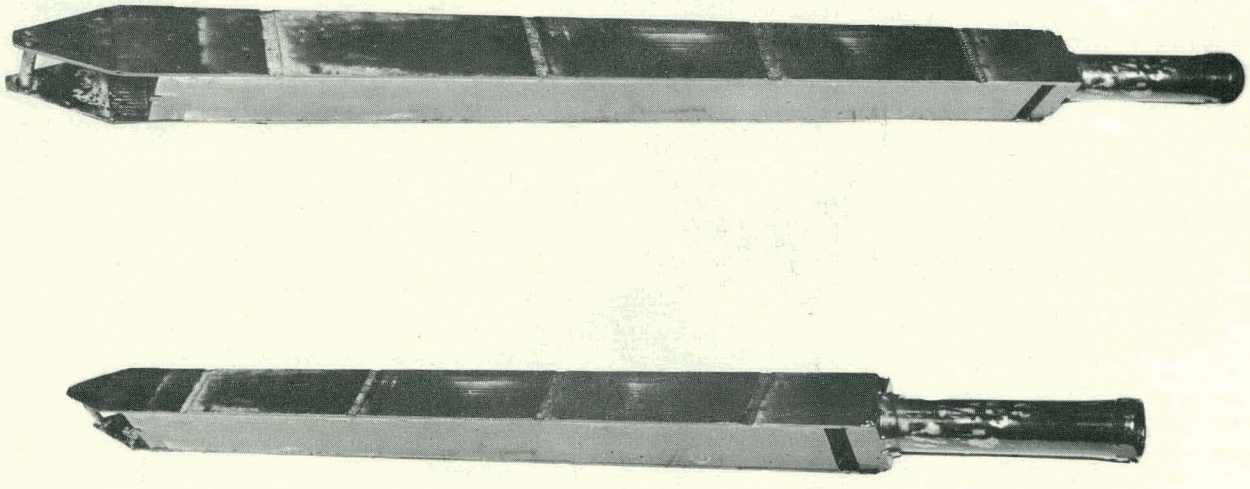

FIG. 12.3B
FUEL ELEMENT AFTER WATER FLOODING USING IRRADIATED
OMRE COOLANT AT 300 °F. RUN No. 5

P.P. Co.

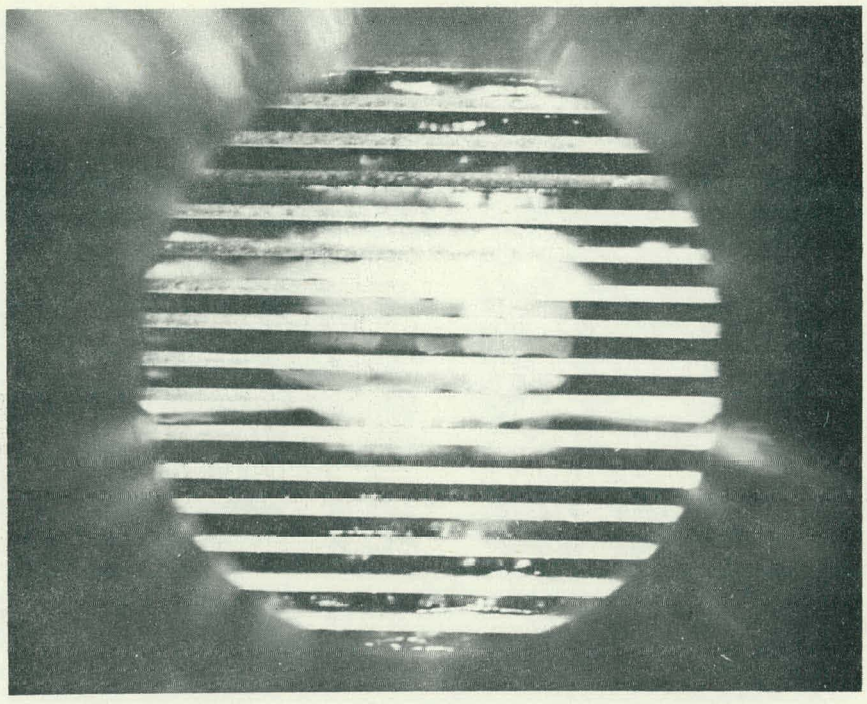

(1)
AFTER USING SANTOWAX OMP AT 350 °F. RUN No. 2

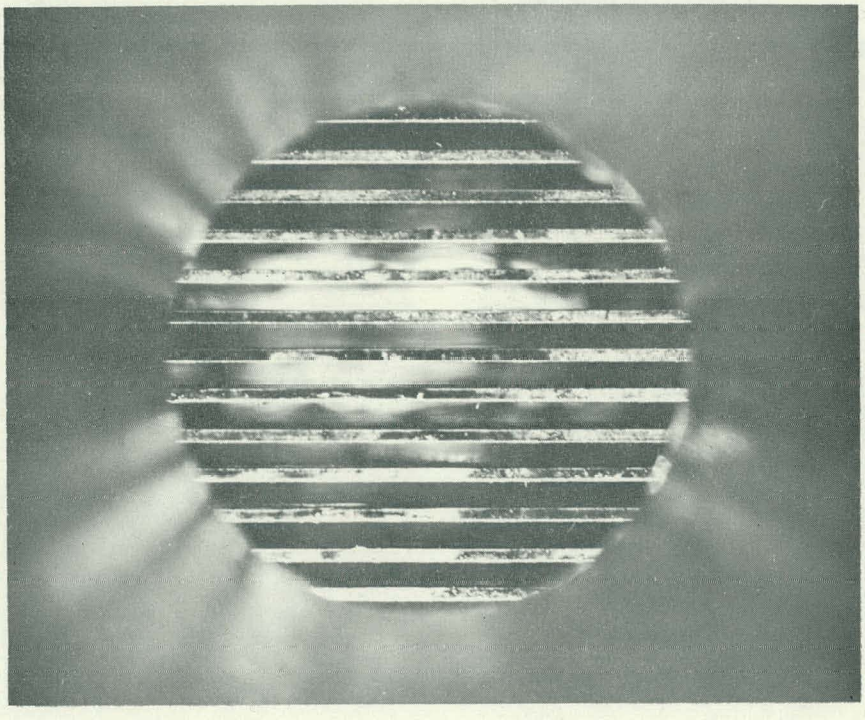

(2)
AFTER USING IRRADIATED OMRE COOLANT AT 300 °F. RUN No. 5

FIG. 12.3C
VIEW OF FUEL ELEMENT PLATES THROUGH THE BOTTOM END BOX

P.P.Co.

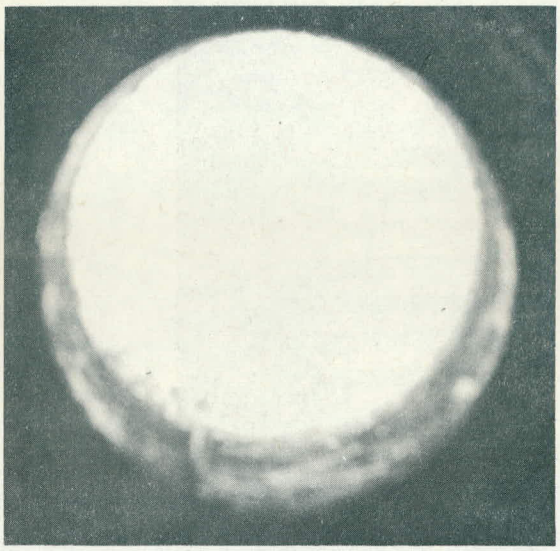

(1)
UNDERWATER LAMP (1000 WATT) FACE-UP THROUGH 3 FEET OF WATER (3 FLUSHES, WATER AT 150°F.) PRODUCES DIFFUSE LIGHT ACROSS DIAMETER OF VESSEL, RUN No. 2

(2)
UNDERWATER LAMP FACE-UP THROUGH 6 FEET OF WATER (SAME CONDITIONS AS (1)

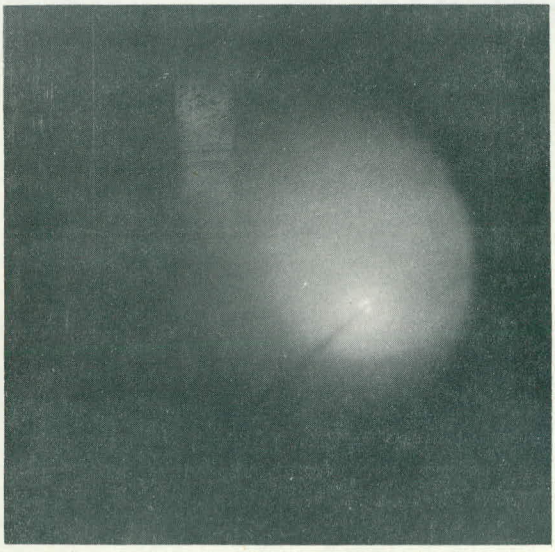

(3)
UNDERWATER LAMP FACE-UP THROUGH 7 1/2 FEET OF WATER (SAME CONDITIONS AS (1)

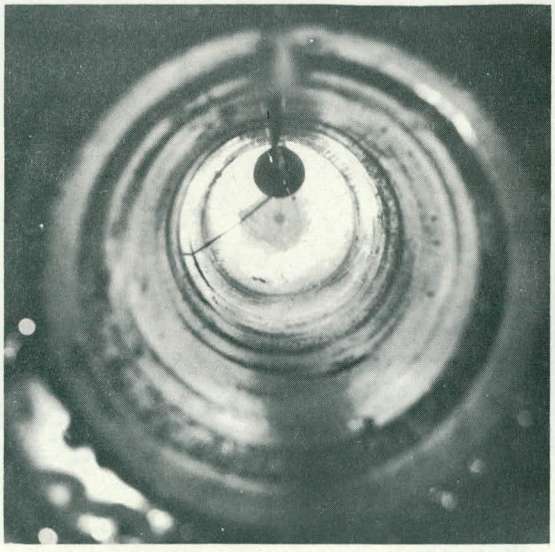

(4)
UNDERWATER LAMP (1000 WATT) FACE-DOWN THROUGH 10 FEET OF WATER (5 FLUSHES WITH WATER TEMPERATURE 70 °F.), RUN No. 5

FIG. 12.3D
CLARITY OF WATER AFTER FLUSHING

P.P.Co.

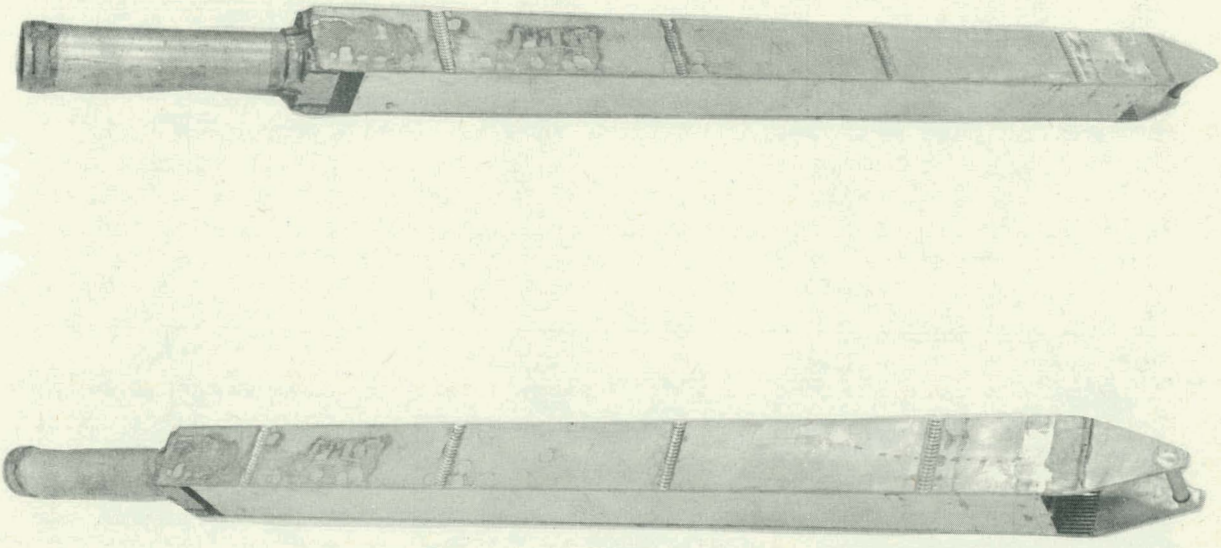

FIG. 12.3 E
FUEL ELEMENT AFTER ORGANIC - WATER CONTACT
IN TEST 6

13.000 FUEL ELEMENTS AND CONTROL RODS FOR EOCR

The selection of the type of fuel elements for the EOCR was based on a study of published information on the present technology of organic-reactor fuel elements, discussions with personnel at Atomics International who developed the OMRE fuel element, and discussions of fuel element manufacture and cost with representatives of some of the prominent fuel fabricators. As a result of this study, the driver fuel element design was established as described in Section 4.000. Some of the materials that might be used in organic-reactor fuel elements, the fuel element designs that were considered, and their fabricating costs are discussed below.

13.100 Fuel Elements

Stainless-steel-clad UO_2-SS plate type fuel elements have been proven to operate in organic reactors;[1] whereas, as pointed out in Section 1.000, the acceptability of other proposed elements, such as those employing aluminum cladding, has not been demonstrated. Consequently, use of UO_2-SS in the driver fuel elements is desirable for at least the first reactor core loading. The use of stainless steel rules out the possibility of using extended-surface fuel elements because little improvement in heat transfer can be obtained with fins and other types of extended surface due to the relatively poor conductivity of stainless steel. Fuel element geometries studied were based on either flat or curved fuel plates, and the final fuel element selected for use as the driver fuel element is a flat plate fuel element.

13.110 Materials. Several materials are compatible with organic coolants and can be used as fuel and cladding materials for fuel elements. The temperature of operation, however, eliminates the use of aluminum alloys and other materials when the fuel element design depends upon the strength properties. Although work is under way to develop powdered aluminum materials as fuel element cladding,[2,3] these materials have not yet been proven for reactor use and were not considered as driver elements for the initial loading.

13.120 Design. Four different fuel elements were considered during development of the conceptual design. Two of these elements were cylindrical in cross section and two rectangular with flat fuel plates, as shown in Fig. 13.1A.

---

1. C. A. Trilling, "The OMRE - A Test of Organic Moderator Coolant Concept", Proceedings of 1958 Geneva Conference, 9, Paper A/Conf.15/P-421 (1958).
2. General Nuclear Engineering Corporation, Power Reactor Technology, 2, No. 4 (1959).
3. Civilian Reactor Fuel Element Review Group, "Report on Civilian Reactor Fuel Elements", June 1959.

Cylindrical fuel elements of the size proposed for EOCR use have never been fabricated. The feasibility and cost of fabricating the two possible plate configurations shown, i.e., with concentric fuel tubes and involute fuel plates, were investigated by several fabricators. The concentric tubular element would require fuel plates of several widths, whereas the involute plates could be fabricated with all the fuel plates having the same width. Consequently, the cost of concentric tubular elements was estimated to be about twice the cost of involute-plate fuel elements. Both types of elements require development before acceptance for EOCR use.

Flat-plate-type fuel elements of the OMRE design and proposed EOCR design are also shown in Fig. 13.1A. Although the fabrication technique is well established, either type of fuel element would require some development and testing at coolant velocities proposed in EOCR. Since the 4-by-4-in. fuel element selected for the EOCR core consists of two 2-by-4-in. segments, the fuel plates have a span of two inches. Thus, the fuel element will be strong mechanically, but it is possible that thermal stresses developed in the element during reactor operation may be excessive. Thermal stresses will require further study before a final design is established.

Three possible modified fuel elements are shown in Fig. 13.1B that might be developed for use as driver fuel elements for the EOCR. The 4-in. square fuel element shown in Fig. 13.1B(1) is similar to the driver element except the stainless steel center support plate has been removed and two additional fuel plates added to the assembly. This design change does not significantly change the amount of metal in the fuel element. The fuel core area per plate is also increased since the non-fuel regions adjacent to the center support plate are no longer required. The addition of two fuel plates and the wider fuel core alloys increases the total heat transfer area in the fuel element by about 20% and would significantly reduce the required reactor coolant flow.

A tube bundle arranged as shown in Fig. 13.1B(2) could provide more efficient cooling in the region of severe flux peaking in the fuel element. Larger diameter tubes in the high flux outer ring of the 4-by-4-in. element would receive more coolant flow than the smaller diameter tubes in the center of the fuel element. Fabrication of such a tube bundle would be possible but would probably cost more than flat plate elements of similar size.

The concentric square tube design shown in Fig. 13.1B(3), or a similar concentric round tube element, would provide an efficient means of controlling the flow within a fuel element by spacing the coolant channels to match the flux peaking. Fuel elements of this type of construction have been fabricated but at a high development cost. It may be practical to procure a few of these elements for the high flux region of the EOCR and obtain a higher reactor power level with the same primary coolant flow.

13.200 Control Rods

Control rods of both the fuel-follower type and cruciform type were considered for use in the EOCR. The fuel-follower type is preferred because this type does not interfere with test space between fuel elements and it provides more reactivity control with a smaller number of rods.

The poison materials considered for use in the control rods included those proposed for use in organic power reactors, which are boron stainless, boron carbide, and europium oxide. For high temperature operation of the EOCR any of these poison materials would have to be clad with steel, and the cladding would provide the required strength to support the poison section. Europium oxide is too expensive to be used for the relatively short lifetime expected of any control rod in EOCR use, where it may be necessary to change the control rods for power core tests like those proposed in Section 3.500. Therefore, at the present time boron carbide or boron stainless steel, in rod or powder form, clad with stainless steel, appears to be the best choice of poison material. Some development and test work[1] may be required to prove the final design of any control rod assembly.

---

1. Refer to Section 19.000.

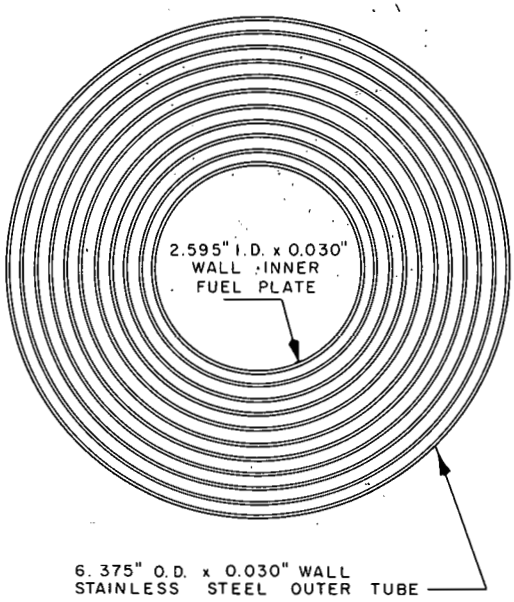

(1)
CYLINDRICAL CONCENTRIC TUBES

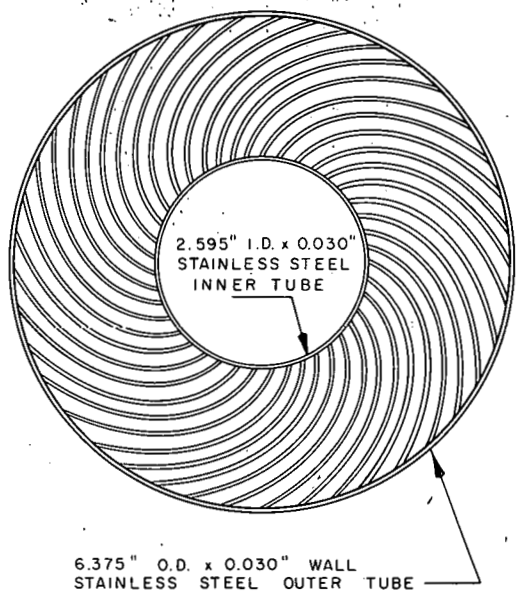

(2)
CYLINDRICAL INVOLUTE PLATES

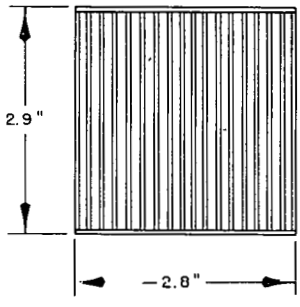

(3)
OMRE

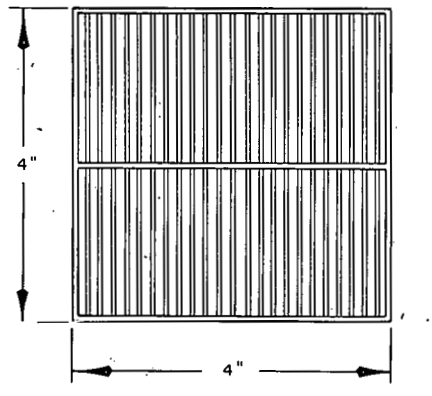

(4)
EOCR

P.P. CO. - C - 2549

FIG. 13.1A
CROSS SECTIONS OF FUEL ELEMENTS CONSIDERED FOR EOCR

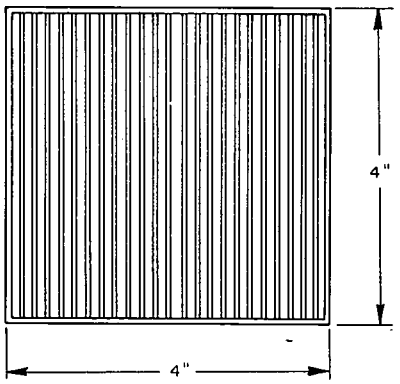

(1)
FLAT PLATES

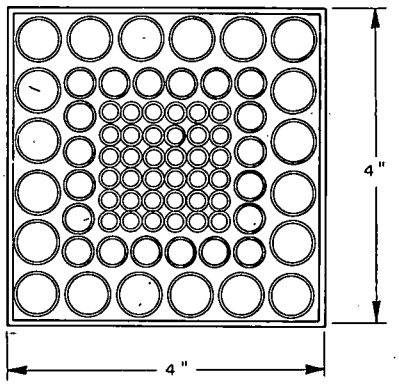

(2)
TUBE BUNDLE

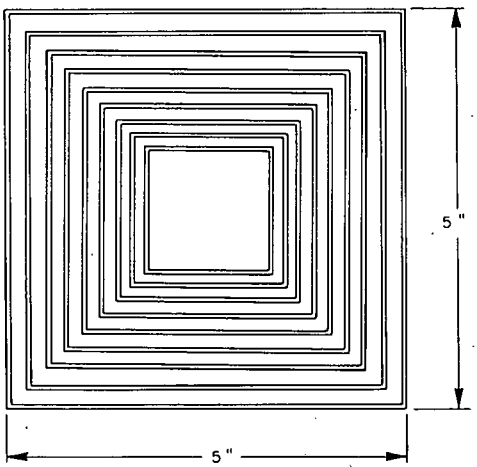

(3)
CONCENTRIC SQUARE TUBES

nn co. c 8550

FIG. 13.1B
CROSS SECTIONS OF POSSIBLE MODIFIED FUEL ELEMENTS FOR EOCR

14.000 REACTOR PHYSICS SUPPLEMENT

14.100 Calculational Methods and Constants

14.110 Calculational Methods. Precise calculations of k_{eff} and of the flux distributions in reactors such as the EOCR and the OMRE are difficult for a number of reasons. The spaced lattice introduces a heterogeneity that produces serious errors when uncorrected diffusion theory is used. The relatively small size of the core casts some doubt on the validity of conventional methods of treating heterogeneous reactors as these methods have been developed for reactors large enough to be considered essentially infinite in size. The constants for organic moderators and organic--stainless steel mixtures have not been measured over the range of temperatures required for calculation of reactivity effects in the EOCR. Even in water-moderated reactors it is still customary to make empirical corrections to the constants in order to obtain satisfactory agreement between calculations and experiments. These empirical corrections are not available for organic-moderated reactors.

The methods for the calculations on the EOCR have been chosen to be satisfactory for the purposes of a conceptual design without being inordinately time consuming or expensive. Time restrictions have permitted only a very limited amount of investigation and development of methods and constants. The EOCR with its numerous test facilities cannot be adequately represented by a one-dimensional model. The heterogeneous core makes it desirable to use two-dimensional transport theory approximations. However, such methods require excessive time on large computers and have not been considered feasible for this project. To at least partially circumvent the difficulties resulting from the combination of a heterogeneous core and the lack of one-dimensional symmetry two sets of calculations have been made. The flux and power distributions are determined by two-dimensional diffusion theory. Reactivity effects are studied using a one-dimensional model and applying cell theory for heterogeneous reactors. Spherical harmonic approximations to transport theory are used to calculate the flux distributions in a cell and thus determine corrections for a diffusion-theory calculation of reactivity. The reference core of Fig. 5.2A is investigated by both methods to provide the necessary correlation. Two neutron groups are used for all calculations of k_{eff}. Since Santowax R with no high boiler residue is used as moderator, the calculations apply to conditions at startup.

An attempt has been made to be realistic without being unduly conservative. Calculations of the OMRE reactivity, described in Section 14.200, have been made and compared with measured values to provide corrections for the calculated EOCR reactivities. The fuel loading has been determined at temperature and with a typical array of loops and experiments in the core. In the calculations of fuel burnup and fission product formation allowances have been made for the non-uniform flux distribution.

To reduce the number of calculations a fuel loading equivalent to 45 kg of U-235 for a core of 32 driver fuel elements is used in most of the work. The final fuel loading is determined from a study of the variation of k_{eff} with fuel loading and from the estimates of the reactivity requirements for an operational core. Flux and power distributions are given for the 45 kg loading.

14.111 One-Dimensional Calculations. Prior to the one-dimensional diffusion theory calculations of reactivity, corrections to the thermal-absorption, Σ_{2a}, and fission cross sections, Σ_{2f}, are determined using spherical harmonic approximations to transport theory. Separate corrections are determined for the flux depressions from the coolant channels into the fuel plates and for the depression from the surrounding organic into the fuel element. For each correction two thermal absorption cross sections are found. These are the homogeneous cross section, $\bar{\Sigma}_{2a}^{hom}$, and the heterogeneous cross section, Σ_{2a}^{het}, which are defined by the following equations.

$$\Sigma_{2a}^{hom} = \frac{V^1\Sigma_{2a}^1 + V^2\Sigma_{2a}^2 + V^3\Sigma_{2a}^3}{V^1 + V^2 + V^3}$$

$$\Sigma_{2a}^{het} = \frac{\bar{\phi}_2^1 V^1\Sigma_{2a}^1 + \bar{\phi}_2^2 V^2\Sigma_{2a}^2 + \bar{\phi}_2^3 V^3\Sigma_{2a}^3}{\bar{\phi}_2^1 V^1 + \bar{\phi}_2^2 V^2 + \bar{\phi}_2^3 V^3}$$

Where:

the superscripts designate the region.

V is the volume of the region.

$\bar{\phi}_2$ is the average thermal flux.

The correction factor, C_{2a}, is then determined from the ratio of Σ_{2a}^{het} to Σ_{2a}^{hom}

$$C_{2a} = \Sigma_{2a}^{het} \Big/ \Sigma_{2a}^{hom}$$

A similar treatment is used to find the correction factor for the thermal fission cross section.

A double P_1 spherical harmonics approximation is used to find the average thermal fluxes required to make the corrections for the fuel plate flux depressions. The computations are made using an IBM-650 program developed at the Atomic Energy Division of Phillips Petroleum Company.[1]

---

1. D. R. Metcalf and G. A. Cazier, "Double P_1 Spherical Harmonics Approximation in Slab Geometry", IDO-16572, to be published.

An infinite slab model is used, and three regions are considered: the fuel matrix, the cladding and the organic. The source is assumed to be constant in the organic and zero in the other regions. Maxwellian cross sections are taken from a tabulation. These are used because a more pronounced flux depression occurs than with Wigner-Wilkins cross sections and better agreement with experiment is attained for k_{eff}.

The correction factors resulting from the double P_1 computations are designated C^1_{2a} and C^1_{2f} for the absorption and fission cross sections respectively. These corrections are relatively small, and the effect on the thermal utilization is negligible except where small changes in reactivity are important such as in finding the temperature coefficient.

The flux distributions within a cell, required in obtaining the correction for flux depression from the surrounding organic into the fuel element, are computed by a P_3 spherical harmonics approximation; the IBM-650 program was developed by Weil.[1] An equal area cylindrical model is used to represent the square cell in order to make a one-dimensional calculation. The cell is divided into three regions, the homogenized fuel plates and coolant channels, the stainless steel box which forms the exterior portion of the fuel element and the organic between the fuel elements. The sources for each region are obtained using two-neutron-group diffusion theory with MUFT III and DONATE constants to determine the average fast flux in each region. The source for a region is the product of the average fast flux and removal cross section for the region. The input data for the P_3 program are taken from the tabulation of Maxwellian cross sections used with the double P_1 program.

The P_3 correction factors are designated C^3_{2a} and C^3_{2f}. These factors are significant and cannot be neglected. The P_3 approximation introduces an unknown amount of error into the determination of the flux depression. The one-dimensional model and the assumption of zero leakage between cells introduce further errors. These effects may be significant in determining reactivity coefficients. However, it is doubtful if the use of two-dimensional higher order approximations to transport theory is justified until the cross sections and their variation with temperature are better known.

The one-dimensional calculations of the effective multiplication factor are made by two-neutron-group diffusion theory. The DMM code for the IBM-650 is used to obtain the eigenvalue and flux distributions.[2] It is assumed that in the axial direction a reflector savings can be added and the reactor represented by an equivalent bare core. The actual core for the EOCR is represented by an equal-area cylindrical model so that the actual three-dimensional problem is reduced to one dimension.

---

1. J. Weil and P. Cabral, "P_3 Flux Distribution", 650 Program Library, File Number 8.2.014.

2. E. J. Leshan, et al., "Diffusion Multigroup Multiregion, DMM", 650 Program Library, File Number 8.2.015.

The constants required are obtained from the MUFT III and DONATE programs for the IBM-650. The thermal absorption, Σ_{2a}, from DONATE is multiplied by the product of C_{2a}^{1} and C_{2a}^{3} before being put into DMM. A similar correction is used for Σ_{2f}. The value of the removal cross section, Σ_R, as obtained from MUFT III is modified by using the age as determined in Section 14.121 in place of the age from MUFT III. The relative flux distributions from the DMM program are normalized using the relationship between power and flux shown below:

$$P = (\overline{\phi}_1 \Sigma_{f1} + \overline{\phi}_2 \Sigma_{f2}) \frac{V}{C}$$

P is the total power produced in the core.

V is the volume of the core.

C is the fissions per second to produce a unit of power. A value of 3.15×10^{16} fissions per second to produce one megawatt is used.

The entire core is homogenized and represented by a single region. An essentially infinite reflector of organic is placed beyond the core.

14.112 Two-Dimensional Calculations. The two-dimensional flux distributions are obtained from the PDQ program for the IBM-704.[1] Two-neutron-group diffusion theory is used without transport theory corrections. MUFT III and DONATE constants are used without modification of the thermal-absorption or fission cross sections. The removal cross section from MUFT III is adjusted by the same method as used for the one-dimensional calculations. The core is represented in rectangular geometry with equal area approximations for the circular test facilities. Each fuel element including the fuel plates, organic in the coolant channels and the box is individually homogenized. The same axial reflector savings is used as for the one-dimensional calculations, and an infinite organic reflector is placed outside of the core.

14.120 Constants

14.121 Age In Hydrocarbons. The Fermi age in hydrocarbons has not been measured to date at high temperatures. In particular no experimental data exist at any temperature for the ages in Santowax O-M and Santowax R. The Fermi ages for pure diphenyl and a stainless steel - diphenyl mixture with a volume ratio of 0.2 at 185°F have been measured.[2] The terphenyl compounds Santowax O-M and Santowax R are quite similar to diphenyl in slowing down neutrons.

The following equation was used to obtain the Fermi ages for pure diphenyl and for a stainless steel - diphenyl volume ratio of 0.2 as a function of temperature (see Fig. 14.1A).

---

1. G. G. Bilodeau, et al., "PDQ an IBM-704 Code to Solve the Two-Dimensional Few-Group Neutron Diffusion Equations", WAPD-TM-70, August 1957.

2. R. O. Williams, Jr., et al., "Reactor Analysis of the Organic Moderated Reactor Experiment and Comparison with Experimental Results", Paper No. 630, Second United Nations International Conference on the Peaceful Uses of Atomic Energy, 12, 518-524, 1958.

$$\tau(T) = \tau_o \left(\frac{1 + V}{\frac{\rho(T)}{\rho_o} + \beta V} \right)^2 \qquad (1)$$

$\tau(T)$ = age in mixture at temperature T.

τ_o = age in pure diphenyl at experimental temperature T_o.

V = metal-to-diphenyl volume ratio.

ρ_o = diphenyl density at temperature T_o.

$\rho(T)$ = diphenyl density at temperature T.

β = a constant, independent of temperature.

The quantity β was determined by normalizing to the experimental age values for pure diphenyl and for the stainless steel - diphenyl volume ratio of 0.2 at 185°F.

The variation of age with temperature for Santowax R and Santowax O-M was obtained by multiplying the age of diphenyl by the square of the ratio of the hydrogen atom density of diphenyl to that of the terphenyl. The calculated age curves are shown in Fig. 14.1A.

When the age for a mixture of Santowax and metal is desired at a particular temperature, the ages for pure diphenyl and stainless steel - diphenyl are used to determine the effect of the stainless steel in the Santowax. The effect of adding stainless steel to the Santowax compounds is assumed as being the same as adding stainless steel to diphenyl.

The MUFT III program for fast group constants gives a lower age than determined from these curves especially at high temperature. As discussed in Section 14.200 and shown in Fig. 14.2A, the calculated k_{eff} values for OMRE using Fermi ages based on Fig. 14.1A appear at present to be too high. Thus, if we were to use the MUFT III ages directly the calculations would be even further in disagreement with experiment.

14.122 Reflector Savings. A total axial reflector savings of 14 cm has been used in all calculations of EOCR and OMRE reactivity. This value is consistent with that determined for a highly enriched reactor with stainless-steel fuel elements but with light-water moderation and reflection. The axial leakage is sufficiently small that any reasonable value for the reflector savings used is satisfactory for determining k_{eff}. However, the change of reflector savings with temperature may be significant in the calculation of reactivity coefficients. The calculation of the reflector savings involves an iterative comparison of bare and reflected cores, and time has not permitted a determination of it as a function of temperature.

14.123 Vertical Maximum-to-Average Flux Ratio. A vertical maximum-to-average ratio of 1.4 is used in determining maximum fast- and thermal-flux values from the average values. This ratio is computed assuming a cosine vertical flux distribution extending from the center of the core and becoming zero 7 cm, half of the total reflector savings, beyond the core. The average flux is found by integrating the cosine from the center to the edge of the core and the maximum-to-average ratio found from the following equation.

$$\text{Maximum-to-Average} = \frac{1}{\frac{1}{L}\int_0^L \cos\frac{\pi x}{2(L+R)}\,dx}$$

where: L is 1/2 the length of the active core.

R is 1/2 the total axial reflector savings.

A value of 1.39 is found and rounded to 1.4.

14.124 Discussion and Tabulation of Constants. The fast-group constants are obtained exclusively from MUFT III program for the IBM-650.[1] with the removal cross section modified as described in Section 14.110. For all diffusion-theory calculations the thermal-group constants are obtained from the DONATE program for the IBM-650.[2] This program averages the cross sections over a Wigner-Wilkins Spectrum. The Wigner-Wilkins spectrum is known to be quite satisfactory for water-moderated systems but may not be as applicable with organic because of the different chemical bonding and molecular mass. However, for this study it is considered satisfactory to assume that a hydrogen atom in organic is equivalent to one in water. The cross sections required as input data for MUFT III and DONATE are taken from Westinghouse decks. The Maxwellian cross sections used in calculating the transport-theory corrections are taken from a tabulation.[3] A value of 2.47 is used for ν in the thermal group.

Table 14.1A contains the constants for the homogenized EOCR core. The correction factors are described in Section 14.110. Table 14.1B lists the constants for Santowax R used as the reflector in calculations on the EOCR. Table 14.1C contains the constants for the homogenized fuel element including the organic in the coolant channels. For computations such as the temperature coefficient the differences in the constants are important and more significant figures are carried in Tables 14.1A and 14.1B than justified by the accuracy of the measurements from which the constants are obtained.

---

1. R. L. Hellens, et al., "Multigroup Fourier Transform Calculation of MUFT III Code", WAPD-TM-4.

2. H. Amster and R. Suarez, "DONATE", 650 Program Library, File Number 8.2.005.

3. AlW Physics Tables of Maxwellian Averaged Thermal Cross Sections, Second Issue, September 1958.

Table 14.1A

HOMOGENIZED CORE CONSTANTS

Temperature	300°F	350°F	400°F	500°F	600°F
M/O Ratio	0.12377	0.12377	0.12377	0.12377	0.12377
	Atom Densities x 10^{-24} atoms/cm^3				
H	0.32778	0.031996	0.031344	0.029911	0.028542
C	0.042144	0.041137	0.040300	0.038456	0.036698
U^{235}	0.00018736	0.00018736	0.00018736	0.00018736	0.00018736
U^{238}	0.00001303	0.00001303	0.00001303	0.00001303	0.00001303
Oxy	0.00040077	0.00040077	0.00040077	0.00040077	0.00040077
Fe	0.0059639	0.0059639	0.0059639	0.0059639	0.0059639
Cr	0.0016537	0.0016537	0.0016537	0.0016537	0.0016537
Ni	0.00088059	0.00088059	0.00088059	0.00088059	0.00088059
Mn	0.00014295	0.00014295	0.00014295	0.00014295	0.00014295
	Diffusion Code Constants				
$\nu\Sigma_{1f}$	0.004441	0.004440	0.004439	0.004438	0.004436
D_1	1.5282	1.5572	1.5822	1.6402	1.6998
Σ_R	0.02283	0.02246	0.02197	0.02082	0.01983
Σ_{1a}	0.003074	0.003069	0.003065	0.003055	0.003045
$\nu\Sigma_{2f}$ Uncorrected	0.1541	0.1497	0.1497	0.1383	0.1318
$\nu\Sigma_{2f}$ P-3 Corr.	0.06658	0.06688	0.06697	0.06701	0.06707
$\nu\Sigma_{2f}$ P-3 & DP-1 Corr.	0.06231	0.06284	0.06315	0.06358	0.06395
D_2	0.3271	0.3384	0.3487	0.3716	0.3952
Σ_{2a} Uncorrected	0.09766	0.09485	0.09238	0.08778	0.08388
Σ_{2a} P-3 Corr.	0.04825	0.04807	0.04786	0.04735	0.04700
Σ_{2a} P-3 & DP-1 Corr.	0.04528	0.04528	0.04523	0.04503	0.04491
	P-3 Transport Correction Factors				
C^3_{2f}	0.43206	0.44673	0.45966	0.48450	0.50884
C^3_{2a}	0.49408	0.50675	0.51803	0.53941	0.56038
	Double P1 Transport Correction Factors				
C^1_{2f}	0.93579	0.93959	0.94286	0.94885	0.95362
C^1_{2a}	0.93849	0.94210	0.94522	0.95092	0.95544

Table 14.1B

SANTOWAX "R" CONSTANTS

Temperature	300°F	350°F	400°F	500°F	600°F
	Atom Densities x 10^{-24} atoms/cm^3				
H	0.036835	0.035956	0.035224	0.033613	0.032075
C	0.047360	0.046229	0.045288	0.043216	0.041240
	Diffusion Code Constants				
D_1	1.7513	1.7941	1.8314	1.9191	2.0112
Σ_R	0.02971	0.02919	0.02858	0.02718	0.02576
Σ_{1a}	0.000176	0.000171	0.000168	0.000160	0.000153
D_2	0.2901	0.3045	0.3179	0.3473	0.3896
Σ_{2a}	0.009007	0.008526	0.008112	0.007341	0.006598

Table 14.1C

CONSTANTS FOR HOMOGENIZED FUEL ELEMENT AT 500°F

Atom	Atom Density x 10^{-24} Atoms/cm^3	Diffusion Code Constants	
H	0.02596	$\nu\Sigma_{1f}$	0.008996
C	0.03338	D_1	1.434
U-235	0.0003872	Σ_R	0.01532
U-238	0.00002692	Σ_{1a}	0.006084
Oxy	0.0008281		
Fe	0.01232	$\nu\Sigma_{2f}$	0.2464
Cr	0.003417	D_2	0.4618
Ni	0.001820	Σ_{2a}	0.1527
Mn	0.0002954		

14.200 OMRE Calculations

Calculations have been made of k_{eff} at four temperatures for the OMRE 31-element core and compared with measured values.[1] The results have been used to provide an experimental basis for the EOCR calculations. As nearly as possible, identical methods have been used for the EOCR and OMRE determinations of k_{eff}. Fig. 14.2A shows calculated and measured curves of k_{eff} versus temperature for the OMRE and indicates that the measured k_{eff} is slightly lower than the calculated value throughout the range considered. In comparing them it should be kept in mind that there is some uncertainty in the measured curve because it depends on control rod calibrations and was plotted from three points given in Table 7-11 of reference 1.

The agreement is such that the methods appear adequate for determining the EOCR fuel loading. However, the difference in shape of the calculated and measured curves casts some doubt on calculated temperature coefficients because these depend on the slope of the curve. Indications are that the actual temperature coefficient is more positive than calculated. The reported value of the measured OMRE temperature coefficient is approximately 0.0025% $\Delta k/k$ per ^{o}F[2] at 500°F. The value taken from the measured curve of Fig. 14.2A is approximately half of this. Thus, any conclusion from comparison of actual and calculated values of the temperature coefficient is somewhat doubtful.

14.300 Supplementary EOCR Calculations

14.310 Effect of Moderator Annulus on Flux in Test. The thermal flux in a test can be markedly increased above that in the core by surrounding the test with an annulus of moderator. Since this flux-trap principle has been extensively investigated for light- and heavy-water moderators, the following description is brief.[3,4,5]

---

1. J. R. Dietrich and W. H. Zinn, "Solid Fuel Reactors", 696-727, Addision Wesley, 1958.
2. R. O. Williams, Jr., et al., "Reactor Analysis of the Organic Moderated Reactor Experiment and Comparison with Experimental Results", Paper 630, Second United Nations International Conference on the Peaceful Uses of Atomic Energy.
3. R. J. Howerton, et al., "Parameters of High Flux Testing Reactors", IDO-16406.
4. C. F. Leyse, et al., "An Advanced Engineering Test Reactor", AECU-3775.
5. S. M. Feinberg, et al., "An Intermediate Reactor for Obtaining High Intensity Neutron Fluxes", Paper 2142, Second United Nations International Conference on the Peaceful Uses of Atomic Energy.

Consider first a case in which the core is packed tightly around a test. The thermal neutrons in the test come from leakage out of the core and thermalization in the test. Thus for loops such as are used in the EOCR the thermal flux in the test is depressed below that in the core. When an annulus of moderator is placed around the test, the thermal flux in the annulus rises above that in the core because of thermalization of fast neutrons. This effect increases the source of thermal neutrons flowing into the test. As the thickness of the moderator annulus is increased, the ratio of the test flux to the core flux increases, goes through a maximum and then decreases as the loss to absorption in the moderator becomes excessive.

The neutrons coming into the moderator annulus or flux trap arise to a large extent from the fuel in an annulus of limited thickness nearest the flux trap. Thus, as the thickness of the moderator annulus is increased, the volume of the core contributing neutrons to the test is also increased, and at constant core power density the core power rises. Therefore two optimizations are possible. First, the attainment of the maximum thermal flux in the test per megawatt of core power and second, the attainment of the maximum ratio of test flux to core flux. In general, the second type of optimization, which produces the highest test flux, requires a considerably thicker moderator annulus and higher amount of core power ascribed to the test than for the first type of optimization. The optimization depends upon the properties of the core, flux-trap moderator and the test and for highest fluxes must consider the problem of heat removal. The situation in a multi-loop core such as the EOCR is complex, but in general the EOCR core corresponds to the optimization for maximum test flux per megawatt of core power. The alternate flux-trap arrangement of the EOCR core represents more nearly the second type of optimization for the central loop. Provision of the large annulus for the other loops would greatly increase the core size.

Limited studies have been made of the variation of test flux with thickness of the moderator annulus using a one-dimensional model with Santowax R as the moderator. For a large central loop the maximum test flux per megawatt of core power occurs with a flux trap thickness of about 2.5 cm and the maximum ratio of test to core flux at approximately 8 cm. For the small loop these thicknesses are about 6 cm and 12 cm, respectively.

The equivalent equal-area moderator thickness in the EOCR core is 2.5 cm for a large loop and 7.5 cm for a small loop. The thermal flux with a large loop is increased approximately 30% above that which would exist if no flux trap were used. That in the small loop is increased about 300%. The power densities of Section 5.320 computed on a more exact model of the core show the ratio of the thermal fluxes in the small and large loops to be about 1.6 instead of 2.3 as determined from these flux trap calculations.

The alternate flux-trap arrangement has an equivalent moderator annulus of 6 cm with a large loop, and the test thermal flux is increased about 25% above that in the EOCR core. This factor is reasonably consistent with the results of Section 5.320.

In general slowing down power is the most important property of a moderator, provided the neutron absorption is reasonably low, for use in a flux trap. Thus cold water is more efficient in the flux-trap region around the test. The advantage from using water must be weighed against the neutron loss in the structural material required to separate the water from the organic moderator of the core. If in the future an alternative arrangement such as the flux-trap core of Section 11.000 is used, this method of increasing the thermal flux in the test should be considered.

14.320 Effect of Fuel Element Spacing. The properties of the EOCR are quite dependent on the lattice structure, that is the size of fuel element, the amount of stainless steel in the elements and the spacing between the fuel elements. Limited studies have been made on one method of changing the lattice structure. The variation of k_{eff} with fuel element spacing has been determined for a one-dimensional representation of the EOCR reference core. The results are shown in Fig. 14.3A.

It is apparent that the 1.75 in. spacing between fuel elements in the EOCR is considerably larger than that at which the maximum k_{eff} occurs. A change in the fuel element spacing produces a number of effects, and a compromise is necessary in selecting the spacing which best meets the EOCR objectives. Reduction of the spacing to the point where k_{eff} is maximized minimizes the required fuel loading and thus maximizes the thermal flux in the driver elements. The decreased spacing makes the temperature coefficient more negative, and this may be desirable. However, decrease of the spacing reduces the size of the loops and test elements which can be placed in the core and thus reduces the flexibility. In addition for the same size tests the moderator annulus around them is decreased and this reduces the thermal flux in them as discussed in Section 14.310.

An alternate approach for modifying the lattice structure is to hold the cell size constant while the size of the fuel element is increased. If the metal-organic ratio and U-235 content of the fuel element are held constant as its size is increased the k_{eff} of the reactor will decrease. The temperature coefficient becomes more negative, but the change is smaller than for the method of placing elements closer together because the leakage does not increase. This method does not reduce the flexibility to the extent that decreasing the spacing does, but it still produces the harmful effect of removing moderator from around the test.

In general, the most desirable lattice structure for the EOCR is the one that produces maximum thermal test fluxes per megawatt of core power while maintaining an acceptable temperature

coefficient. It is probably desirable to have the temperature coefficient negative with the smallest absolute value that permits safe operation. This allows the moderator channel between elements to be as large as practical which improves the test fluxes.

14.400 Gamma Heating Calculations

The results and general remarks concerning the gamma and neutron-heating calculations are given in Sections 5.330 and 5.340 for the standard core and a 220-Mw power reactor core, respectively. The following discussions of the gamma-heating calculations are also divided into these two major subdivisions.

14.410 Gamma Heating and Shielding Calculations for a Power Reactor Core. As stated in Section 5.340, the shield design was based on a 220-Mw power reactor core with the following dimensions and properties.

Height	4.5 ft
Diameter	4.0 ft
Volume	1.6×10^6 cc
Enrichment of Uranium	1.85% U-235
Mass of U-235	118 kg
Power Level	220 Mw
Average Power	138 watts/cc
Moderator	Santowax R
Moderator Temperature	600°F

The macroscopic thermal-absorption neutron cross sections for the fuel elements were obtained by using the volume fractions for the 330-Mw Nucleate-Boiling Fuel Element.[1]

14.411 Heating From Core Sources. In order to determine the average gamma source density in the core, it is necessary to determine the approximate neutron balance among thermal-neutron captures in core materials. The neutron balance is determined on a per-fission basis in order that all gamma ray source densities may be simply ratioed to core power. The absorption cross sections were Maxwellian-averaged at a temperature of 600°F. The following equations determine the average thermal-neutron balance among core materials.

$$\frac{\text{Average Leakage Neutrons}}{\text{Fission}} = \frac{\nu\Sigma_f\epsilon P - \Sigma_a}{\Sigma_f} = .41 \frac{\text{Neutrons}}{\text{Fission}}$$

$$\Sigma_a = 0.1056 \text{ cm}^{-1}$$
$$\Sigma_f = 0.0676 \text{ cm}^{-1}$$
$$\epsilon P = 0.80$$

---

1. Bechtel Corporation and Atomics International, "Organic Cooled Power Reactor Study - 300 Mw Power Plant Conceptual Design", Report TID-8501 (Part 2), July 1959.

Thus on the average there are 2.47-1.41=1.06 neutrons per fission available for fast-neutron capture in U^{238} and thermal radiative capture among core materials. With an ϵ_p of 0.80, 0.50 neutrons per fission are captured by U^{238} resonances, leaving 0.56 neutrons available for radiative capture among core materials. The total radiative capture cross section of the core materials including U^{235} is 0.038 cm^{-1}. The distribution of the 0.56 neutrons per fission among core materials is given by the following equation.

$$\text{Events per fission in element i} = 0.56 \frac{\Sigma_{ai}}{0.038\ cm^{-1}}$$

where Σ_a is the thermal radiative capture cross section of the i^{th} element. The gamma energy produced by the i^{th} element in the core is given by

$$\frac{\text{Mev}}{\text{fission}} = \text{Binding energy of neutron} \times \frac{\text{events.}}{\text{fission}}$$

Three average gamma-ray energies were chosen as representative of the gamma sources in the core due to both fission and radiative capture processes. The sources per fission are detailed in Table 14.4A, and the volume sources of the three energies for a mid-plane power density of 180 watts/cc are given in Table 14.4B.

Table 14.4A

DETAILED POWER REACTOR CORE GAMMA SOURCES

Element	Σ_a, cm^{-1}	Binding Energy, Mev	Event per Fission	Total Gamma Energy Mev/ Fission	Energy Group, Mev
Hydrogen	0.00414	2.20	0.06	0.134	3
Carbon	0.00051	4.95	0.0074	0.0037	3
Iron	0.0035	10.16	0.051	0.52	7
Aluminum	0.00089	7.72	0.013	0.10	3
U^{238} (Thermal)	0.017	5.50	0.25	1.37	3
U^{238} (Fast)		6.00	0.50	3.0	3
U^{235}	0.0124	6.80	0.182	1.24	3
Fission	0.0676		1.0	13.0	1
Leakage			0.41		

Table 14.4B

SUMMARY POWER REACTOR CORE GAMMA SOURCES

Photon Energy, Mev	Mev/fission	Core Gamma Power, watts/cc
1	13.0	19.9
3	5.85	5.3
7	0.52	0.48

The core was assumed to be a fairly homogeneous source of gamma rays with the gamma-ray power density listed above. The following equation[1] will give the gamma-ray flux at points outside of the core for various shielding thicknesses, for each gamma photon energy arising in the core.

$$\phi = \frac{B\, Sv\, R_o^2}{2\,(a+z)} \qquad F\,(\theta,\, b_2)$$

The gamma-ray flux has the dimensions watts/cm^2 when the core source density has the dimensions watts/cm^3. The gamma-ray flux from core sources was calculated at the inner tank, pressure vessel and concrete, and the results are listed in Table 5.3.

The mass absorption coefficient for the homogeneous mixture of core materials is given by

$$\frac{\mu'}{\rho'} \cong \frac{\sum_i A_i N_i \left(\frac{\mu_o}{\rho}\right)_i}{\sum_i A_i N_i}$$

$$\mu' = \left(\frac{\mu'}{\rho}\right)\rho'$$

$$\rho' = \sum_i \frac{A_i N_i}{6.025 \times 10^{23}}$$

A_i = Atomic weight of element i

N_i = Atom density of element i homogenized over the core

$\left(\frac{\mu_o}{\rho}\right)$ = Mass absorption coefficient of element i for one photon energy

$\left(\frac{\mu'}{\rho'}\right)$ = Mass absorption coefficient for the mixture for one photon energy

μ' = Linear absorption coefficient for the mixture for one photon energy

ρ' = Homogenized density of the mixture

14.412 Heating From Reflector and Shield Sources. For the three gamma photon energies considered above, the core diameter is many mean-free paths and, thus can be effectively approximated by an infinite slab geometry. This approximation is useful in considering the gamma-ray flux due to thermal-neutron capture in the reflector and the shield regions. To obtain an upper-limit estimate of the gamma heating at the inner reactor tank, reactor pressure vessel, and concrete, the reflector was considered to be a homogeneous source of 2.20-Mev gamma photons due to a fairly uniform thermal-nuetron flux throughout the 9-in. reflector. The 0.41 neutrons per fission leaking from the core give an average leakage current from the core of 3.6×10^{13}

1. Theodore Rockwell III, "Reactor Shielding Design Manual", 1st Edition, Von Nostrand Company, Ch. 9, Section I-6, 360.

neutrons/cm^2. These are essentially all fast neutrons because the net thermal-neutron current at the core interface has a negative gradient. At the inner reactor tank vessel most of the fast leakage current from the core has been thermalized in the 9-in. hydrogen reflector so that the thermal neutron source throughout the shielding region can be neglected. The thermal neutron flux throughout the shielding region will therefore be considered to be that due to diffusion of an infinite-plane thermal source at the inner reactor tank. The value of the thermal flux at the inner reactor tank was taken to be 2.5×10^{13} n/cm^2-sec. The average value of the thermal flux throughout the 9-in. reflector was estimated at 8×10^{13} n/cm^2-sec. These flux values have been compared with those for the Piqua OMR[1] and have been found to be reasonable for the assumed operating power and reflector thickness.

The above approximations are admittedly a simplification of the problem, however they are close enough to actual conditions to give a good estimate of the shielding which will be required. The gamma flux throughout the shielding region due to the 2.2-Mev gamma photons originating in the homogeneous reflector will then be given by[2]

$$\phi = \frac{B\, S_v}{2\mu_s} \left[1 - E_2 \left(\mu_s d \right) \right]$$

and the gamma flux throughout the shielding region from the contribution arising in the homogenized shielding region due to exponential attenuation of the thermal flux in the iron and moderator will be given by[3]

$$\phi = \frac{B}{2\mu_s} S_o e^{k_i d} F_1 \left(\mu_s d, \frac{-k_i}{\mu_s} \right)$$

The gamma-flux and -heating were determined at the inner reactor tank, the reactor pressure vessel, and the concrete biological shield for a number of thermal- and lead-shield thicknesses, and the final values arrived at were three 1 in. steel thermal shields and 3 in. of lead between the pressure vessel and biological concrete. The gamma-fluxes and -heating are listed in Section 5.000, Table 5.3H. The gamma heating in the biological concrete without the 3 in. of lead shielding is far in excess of permissible limits. The fast-neutron heating in the structural members is not listed because it was determined to be negligible in comparison to the gamma heating. Because of the scarcity of buildup-factor data for organic-moderated heterogeneous mixtures, the buildup factors were estimated from curves for infinite-plane sources in water and iron.[4] For the reflector, the buildup factors were obtained from the curves for water; for the shielding region and the core buildup factors were obtained from the curves for iron.

---

1. D. S. Duncan, "Results of Preliminary Shield Analysis for the 45.5-Mw OMR", Report NAA-SR-2234.
2. Theodore Rockwell III, "Reactor Shielding Design Manual", 1st Edition, Von Nostrand Company, Ch. 9, Section I-4.2, 353.
3. Theodore Rockwell III, "Reactor Shielding Design Manual", 1st Edition, Von Nostrand Company, Ch. 9, Section II-4.2, 397.
4. Price Horton and Spinney, "Radiation Shielding", 1st Edition, Pergamon Press, Ch. 2, 48.

14.420 Gamma Heating Calculatins for the Standard Core. Limited calculations were made to determine whether the heating rates stated in the design objectives could be met. By inspection of the data shown in Sections 5.000 and 6.000 it was determined that the power density averaged over about two relaxation lengths from the center of the core is about 200 watts/cc at the start of the cycle. This average power density was assumed in calculating the source and methods similar to those in Section 14.410 used to calculate the heating rate near the core center. The source densities of 1, 3 and 7 Mev gammas for an average power density of 200 watts/cc and the standard core composition are shown in Table 14.4C.

Table 14.4C

GAMMA SOURCES IN CORE CENTER

Photon Energy, Mev	Mev/Fission	Core Gamma Power, watts/cc
1	13.0	13.5
3	2.2	2.3
7	2.9	3.1

Using these sources the values shown in Section 5.000, Table 5.3F, were computed for the core center. The core boundary value shown in the source table was computed by assuming a power density of 95 watts/cc in elements on the edge of the core.

Some local values of gamma heat may be higher than those shown in Table 5.3F due to the very high local power density (up to 600 watts/cc) in the inner plates of the driver assemblies; however, the values presented are considered sufficient for the conceptual design.

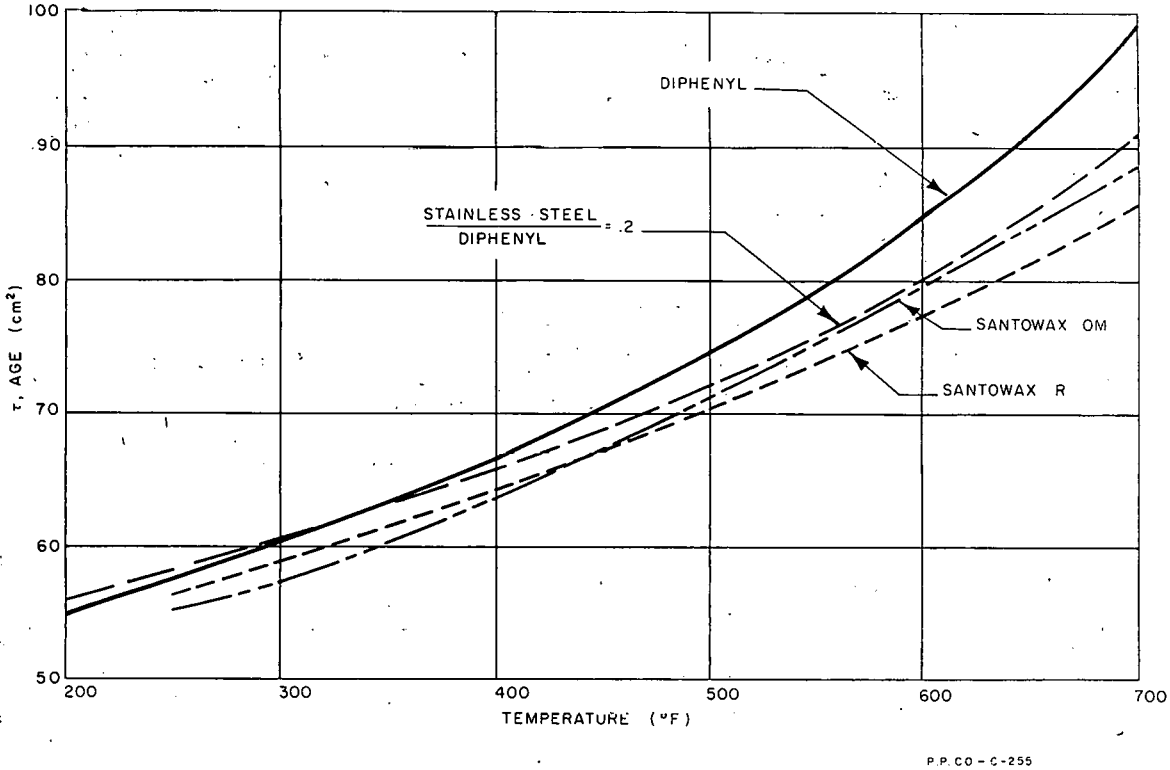

FIG. 14.1A

AGE OF PURE HYDROCARBONS AND STAINLESS STEEL - HYDROCARBON MIXTURES VERSUS TEMPERATURE

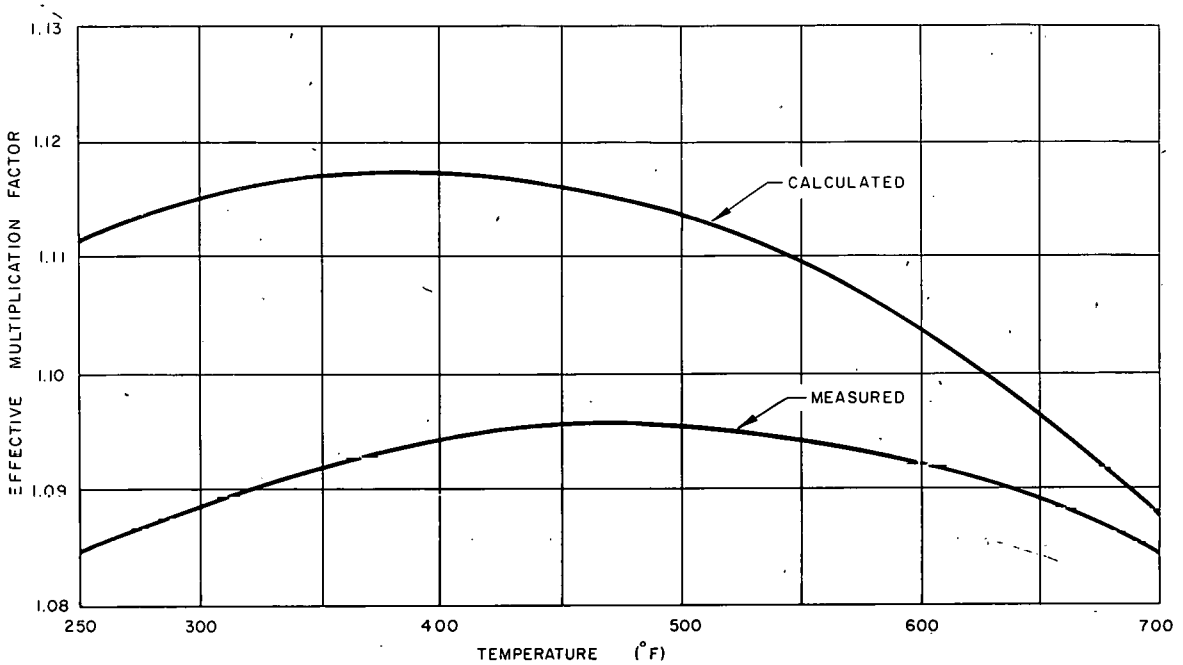

FIG. 14.2 A

EFFECTIVE MULTIPLICATION FACTOR VERSUS TEMPERATURE
OMRE 31-ELEMENT CORE

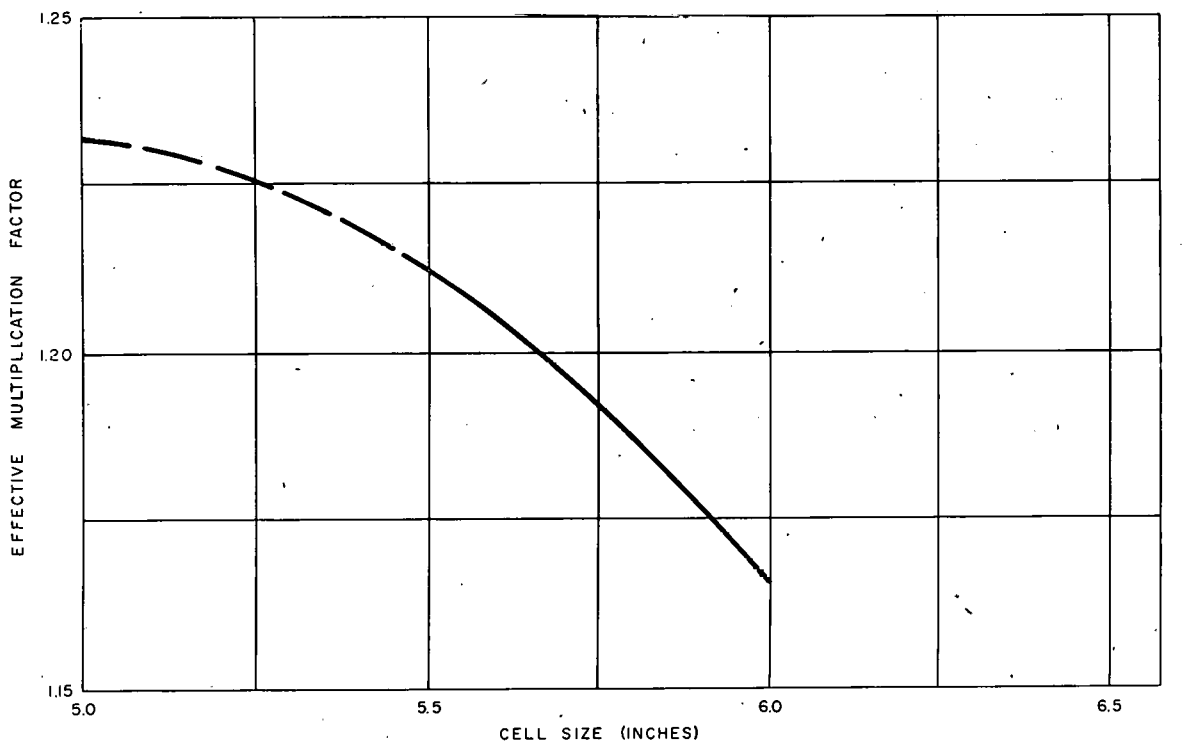

P.P.CO.-C-2552

FIG. 14.3 A

EFFECTIVE MULTIPLICATION FACTOR VERSUS CELL SIZE
EOCR REFERENCE CORE

15.000 HEAT-TRANSFER SUPPLEMENT

A summary of the results of the heat transfer calculations using fuel elements with non-uniform plate spacing is presented in Section 6.000. A more detailed discussion of the calculations and results for an alternate fuel element design are presented in this section along with a discussion of the heat transfer correlations used in this study. The traditional hot-spot hot-channel analysis used in water-cooled reactor design was omitted in the EOCR heat-transfer calculations for reasons given in Section 15.400.

15.100 Study Bases and Objectives

The EOCR is designed to provide experimental facilities to test fuel in power density regions in excess of those expected in organic-cooled power reactors. Thus, the driver fuel elements operate at higher power densities than normally encountered in organic reactor designs and the driver fuel element coolant requirements are relatively high. Flux peaking in driver fuel elements is severe because of the open lattice core design. This flux peaking also increases the driver fuel element coolant requirements. In order to keep the reactor coolant requirements (and also the size of processing equipment) to a minimum, driver fuel element cooling was optimized by: (1) optimizing the inlet temperature of the coolant, (2) orificing the fuel elements so that elements in all positions operate at the same maximum surface temperature, and (3) spacing fuel plates to adjust cooling in each channel to permit each plate to operate near the maximum allowable surface temperature.

15.200 Heat Transfer Correlations

15.210 Forced Convection Correlation. The most extensive work on heat transfer with polyphenyl coolants was done by Silberberg and Huber[1] with unirradiated diphenyl, a 2 to 1 mixture of ortho- and meta-terphenyl, and Santowax R. They obtained the correlation:

$$Nu = 0.015\ Re^{0.85}\ Pr^{0.3}$$

Their correlation was based on fluid properties which have since been superseded.[2] A revision of their work was made by Martini, who prepared

---

1. M. Silberberg and D. A. Huber, "Forced Convection Heat Transfer Characteristics of Polyphenyl Reactor Coolants", Report NAA-SR-2796, January 15, 1959.

2. W. R. Martini, "Summary of Organic Coolant Heat Transfer", Report NAA-SR-MEMO-4183, July 23, 1959.

a graphical correlation for unirradiated Santowax R and for Santowax R containing 30% HB, which is shown in Fig. 15.2A. Since irradiated Santowax R was not available for performing heat transfer tests, the coefficient for Santowax R with 30% HB was obtained by assuming HB to affect Santowax R similarly to OMRE coolant, for which this effect was measured. This correlation, which is given in terms of coolant bulk temperature, is independent of coolant property values, since it is merely a plot of the data based on the exponents of V and D_e obtained by Huber and Silberberg. Film coefficients at bulk coolant temperatures less than 500°F were obtained by extrapolation of this curve. All forced convection calculations given in this report are based on the correlation given in Fig. 15.2A.

15.220 Burnout Correlation. Core and Sato have measured burnout heat fluxes with diphenyl, Santowax R,[1] and Santowax OMP.[2] The correlation for Santowax R, based on ten experiments, was

$$Q/A_c = 552\ \Delta T_{sub}\ V^{2/3} + 152{,}000$$

and for Santowax OMP,

$$Q/A_c = 407\ \Delta T_{sub}\ V^{2/3} + 100{,}000$$

where Q/A_c = the critical or burnout heat flux.

The Santowax OMP used in the tests contains 12.6, 58.6, and 27.9 weight per cent ortho-, meta-, and para-terphenyl respectively, and differs from Santowax R primarily in that the OMP is free of pyrolytic polymers which commercial Santowax R contains to a varying degree. Both correlations were based on properties of Santowax R. The discrepancy in the two correlations, up to 35%, is not explained in the references. The more conservative OMP correlation was used to determine burnout heat flux for this report.

15.300 Reactor Coolant Flow Requirements

The first fuel element studied for the selected core was similar to the final elements except that the fuel plates were equally spaced.

---

1. T. C. Core and K. Sato, "Determination of Burnout Limits of Polyphenyl Coolants", Report IDO-28007, Azusa, California, February 14, 1958.

2. T. C. Core and K. Sato, "Determination of Burnout Limits of Santowax OMP", Report No. 1672, Space Technology Division, Aerojet General Corporation, Azusa, California, September 15, 1959.

This arrangement results in velocities in excess of those required in all but one channel of each element. A varied spacing arrangement was then chosen which reduced excessive velocities and total flow significantly.

15.310 Flow Requirements of Equispaced Plate EOCR Element. Operation of EOCR fuel elements with equispaced fuel plates was based on orificing of the elements so that the velocity in all channels of each element was that required to remove the maximum heat flux in the element. Since peaking of heat fluxes within the elements is high, this condition results in flows in excess of the minimum required to maintain all fuel plates below the maximum surface temperature. The flow requirements are given in Table 15.3A. Fuel element numbers refer to Fig. 6.2A. Total flow requirements for the driver elements are 24,500 gpm.

Table 15.3A

COOLANT VELOCITIES AND FLOW RATES
IN EQUISPACED PLATE EOCR FUEL ELEMENTS

Element (Refer to Fig. 6.2A)	1	2	3	4	5	6
Required Coolant Velocity, ft/sec	33	30.5	24.4	12	13.7	12
Required Coolant Flow per Element, gpm	1270	1270	1180	940	530	502
Total Flow Requirements 24,500 gpm						

15.320 Flow Required in Core with Fuel Elements with Non-Uniform Plate Spacing. The simplest method of improving cooling efficiency, within the limitations imposed by physics and mechanical design of the element, is to space the plates to provide high coolant velocities in coolant channels adjacent to fuel plates having high heat fluxes relative to the other fuel plates in the element. Since the highest flux peaking occurs at one end of the element in all positions, the first three channels in the high flux region were widened. Thus the hottest fuel plate may occur in one or all of the first four channels or in the last, unspaced channel, depending upon the flux distribution in the core position in which the element is used. The arbitrary plate spacing given in Table 6.2A was chosen, based on one of the highest-heat-flux core positions. Flow rates in the element were based on the flow required by the hottest channel. Heat transfer calculations were made for all channels operating near 850°F, and the required flows per element given in Fig. 6.3A, are based on the velocity required by the channel found to be the hottest. No attempt was made to achieve a compromise spacing better adapted to all core positions. Such a spacing should reduce core flow further. The present driver element flow, 20,500 gpm, is considered satisfactory from the standpoint of process system economics.

15.400 Boiling and Burnout

The common practice of designing water-cooled reactors on the basis of "hot-spot hot-channel" temperatures has been abandoned in this study. The objective of hot-spot analyses is generally to preclude to a high probability the danger of operating conditions or fuel failures seriously affecting the plant or its operation or resulting in a catastrophe. The conditions to be avoided are generally extensive boiling, which can affect reactor control seriously, fuel element failures resulting in fission product release and requiring plant shutdown, and metal-water reactions resulting in the destruction of large parts of the core.

In EOCR, nucleate boiling may occur on limited areas of fuel element surfaces if all of the conditions generally postulated in a hot-spot hot-channel analyses should occur in the same place. Because of the large subcooling (about 500°F) nucleate boiling void-fractions are insignificant and bulk boiling is extremely improbable unless blockage of a coolant channel occurs. Thus boiling should have no effect on EOCR operation. Extensive fuel plate burnout has occurred in OMRE without detection for long periods of operation, emphasizing the minor effect upon plant operation. The danger of core meltdown is extremely small in this reactor since excessive transients are obviated by the control system and no exothermic reactions occur between fuel element materials and coolant.

The heat flux factors given in Table 15.4A were applied to the maximum heat flux to determine the hot-spot heat flux, which is estimated to be the maximum heat flux that might occur at any spot on a fuel plate providing all the factors of Table 15.4A occur simultaneously. This hot-spot heat flux was compared to the burnout heat flux in Table 6.4A, and the comparison indicated an adequate margin of safety between the hot-spot and burnout heat fluxes.

Table 15.4A

HEAT FLUX FACTORS

Power Measurement and Control	1.05
Heat Transfer Area per Plate	1.04
Fuel Content per Plate	1.03
Local Fuel Core Thickness	1.05
Local U-Density of Fuel Core	1.05
Error in Flux Calculations	1.15
Total Heat Flux Factor	1.43

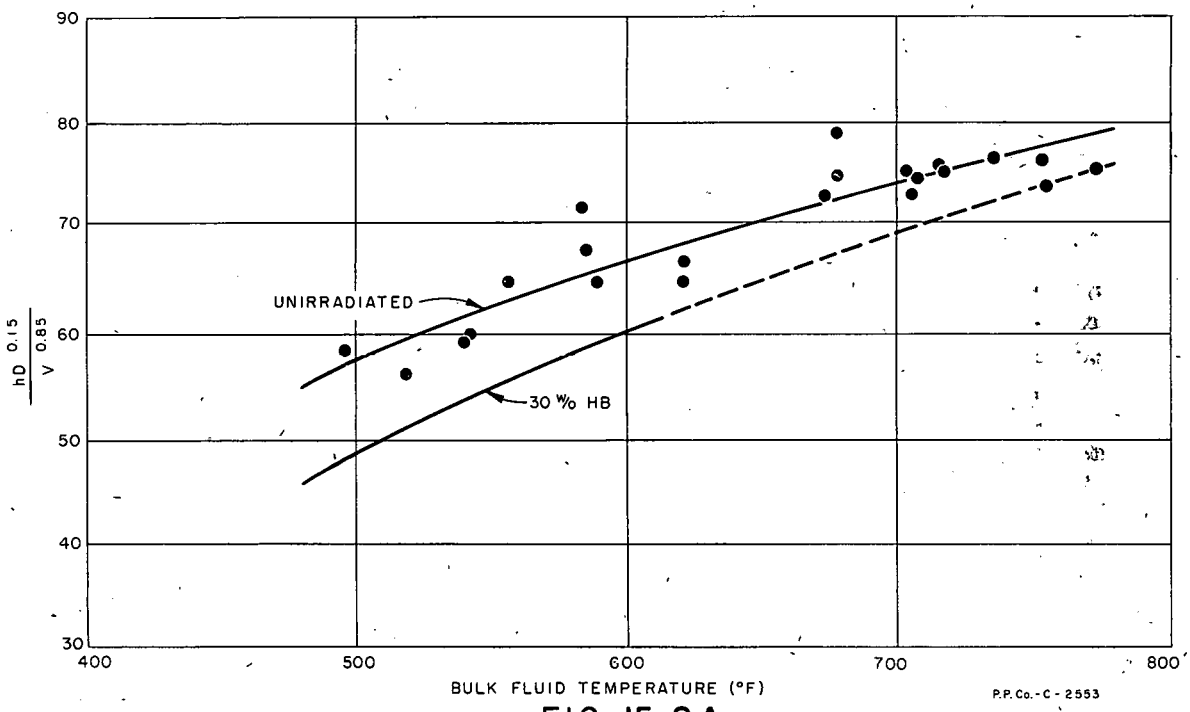

FIG. 15.2A

FORCED CONVECTION HEAT TRANSFER
COEFFICIENTS FOR HEATING SANTOWAX-R

16.000 ALTERNATE REACTOR ARRANGEMENT WITH CASK HANDLING

During the early studies conducted in an attempt to find a rapid and economical fuel handling scheme, a cask handling method was investigated. Since that time tests have been made of the water flooding technique, and it appears that water flooding is acceptable for this reactor. Water flooding is described in the main body of this report, but a short description of a cask handling method is presented in this section as supplementary information.

Figure 16.0A shows a vertical cross section of the reactor vessel utilizing cask handling techniques. The vessel is mounted approximately flush with the building main floor with provisions for placing the lead-filled cask over the reactor. Thus, the elevation of the reactor vessel in the building and the cask with associated equipment are the only major differences between the two reactor arrangements. The vessel internals remain basically the same. Some tanks, pumps, etc., associated with the water flooding may be eliminated with the cask handling alternate.

The cask and its shielded indexing head are patterned after the Piqua OMR power reactor fuel handling method. The prime difference is that, by maintaining hot organic in the reactor vessel at a level just below the fuel element upper end-box, handling tools are kept out of the organic. This minimizes fouling and contamination problems associated with submerging the tools in the organic. By means of a slotted shielding head and a traveling shielding cover plate, the cask is positioned over any required point. The cask is transported to the unloading station in the canal by the overhead crane, a trolley, or other means. The unloading station consists of a shielding ring that serves as a shield to personnel while the fuel element is being discharged into the canal receiver. The element is then moved to its canal storage rack.

The cask handling alternate does not appear as attractive as water flooding for the following reasons:

1. The EOCR is primarily a test reactor, and, as such, should have maximum simplicity and flexibility built into all phases of its operation, handling equipment and procedures, capacity to accept varied types of experiments, etc. It is anticipated that the majority of reactor shutdown time will be expended on the installation and removal of in-pile experimental facilities and experiments. Under these conditions, visual handling is more acceptable and is probably less expensive since it requires a minimum of indexing devices, casks, etc., to precisely position or contain experiments prior to insertion or removal. Also, tools, bolts, nuts, or other miscellaneous items will be unintentionally dropped into the reactor in the course of this in-tank work. This material would be very hard to locate and remove from the opaque organic coolant with remote handling methods.

2. With the reactor pit located over the reactor vessel, flooding of this pit and water flooding of the reactor are compatible. It is anticipated that most fuel, experiment, and other transfers to the

water-filled reactor canal can be effected under water without utilizing cask handling. Direct visual handling is more satisfactory since operations personnel can see what is happening in the reactor and can control movement of components by feel rather than by the more purely mechanical remote handling methods.

3. The remote handling arrangement shown on Fig. 16.0A would make it necessary to insert handling tools through a cask and then pull the component up into the cask. The cask, its locating, transfer and indexing mechanism, etc., is estimated to increase the cost of this project by $300,000 to $400,000. It might also be necessary to increase the building height above the reactor to compensate for increased tool length and travel.

4. The removal and replacement of large reactor vessel internal components introduces shielding problems when using the cask handling method. Either large shields are required or the building must be evacuated except for shielded crane personnel. In the water flooding method, all large components would be handled entirely under water.

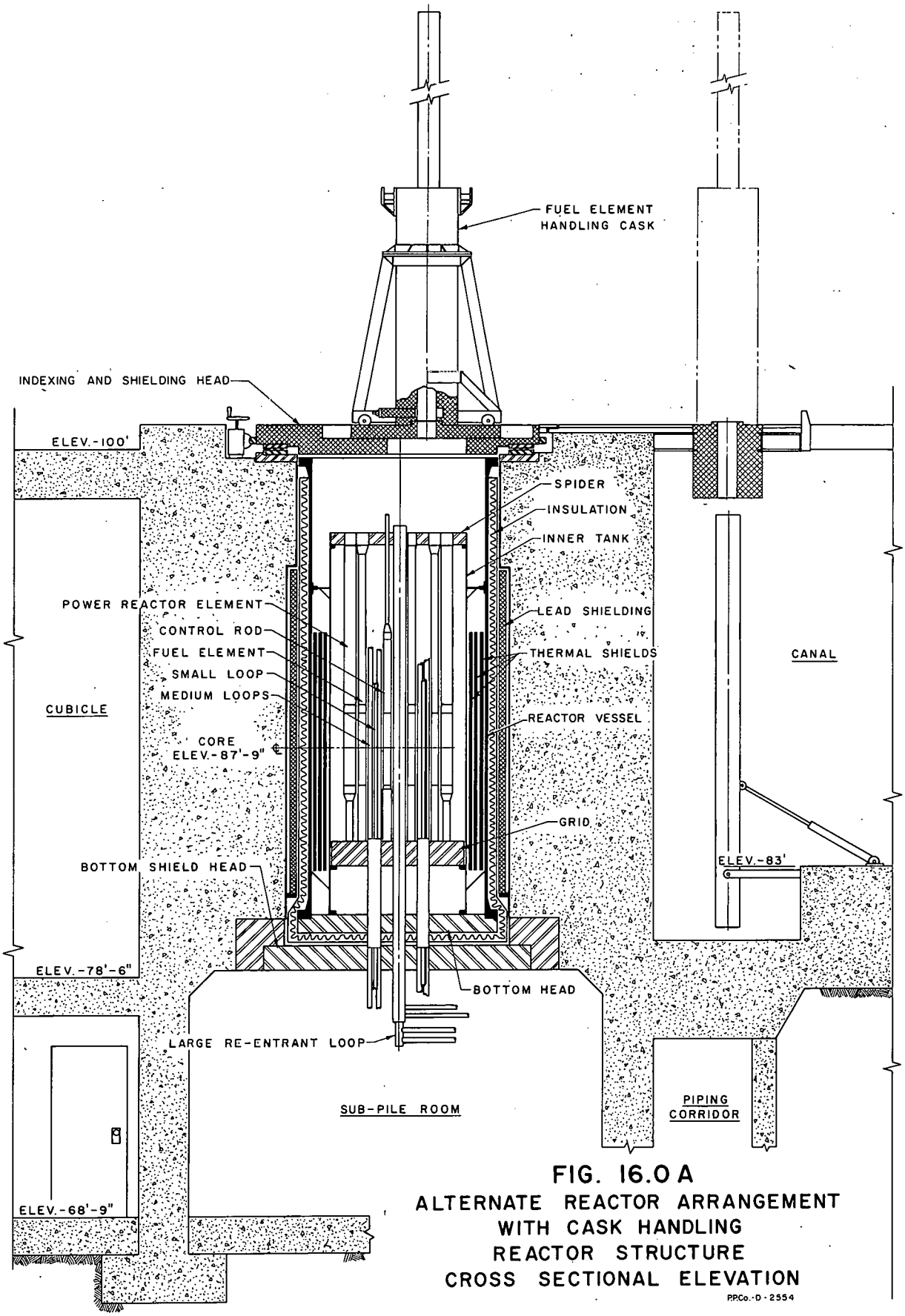

FIG. 16.0 A
ALTERNATE REACTOR ARRANGEMENT
WITH CASK HANDLING
REACTOR STRUCTURE
CROSS SECTIONAL ELEVATION

PPCo.-D-2554

17.000 MATERIALS OF CONSTRUCTION

The primary coolant loop and reactor vessel are the only portions of the reactor complex which require special consideration of nuclear and corrosion effects on materials. Standard industrial practice in selecting materials for the remainder of the installation suffices. AISI type 347 stainless steel is selected as the material composing the inner tank, internal thermal shields, reactor pressure vessel, and piping up to and including the block valves on the primary-coolant inlet and outlet lines. Preliminary corrosion tests with a few specimens and strength considerations, however, indicate the possibility of the use of a low alloy steel such as Croloy 1-1/4 for these structural parts.* The adherent protective film formed in the organic during the corrosion tests was not adversely affected during the replacement with water. Should further corrosion tests show no localized breakdown of the protective film, the use of a low alloy steel such as Croloy 1-1/4 could be recommended for the vessel, internal thermal shields, and piping.

Beyond the block valves, carbon steel is used throughout the remainder of the primary system; however, trim on valves and the pump is AISI 347 steel.

17.100 Reactor Vessels and Internal Thermal Shields

ASME designation SA-240 type 347 18-8Cb-stabilized stainless steel is selected as the material of construction for the inner tank, internal thermal shields, and pressure vessel. Corrosion resistance to alternate contact with organic coolant and water and the attendant need to guarantee vessel life are the main considerations in choosing stainless steel.

Stainless-clad carbon steel was rejected because the effect of the large temperature cycle, approximately 800°F, on the bond between base metal and cladding is unknown. In any case, the ASME Code, Section VIII, for Unfired Pressure Vessels specifically does not recommend this type construction for operating temperatures over 800°F.

The possibility of the use of mild steel as the structural material exists because the corrosion of conventional structural materials in irradiated organic fluids[1] is relatively minor. Stainless steel, aluminum, and mild steel[2] exhibited insignificant weight changes in dynamic corrosion tests. There was slight surface discoloration of

---

1. J. R. Dietrich and W. H. Zinn, Solid Fuel Reactors, Ch. 7, "Organic Cooled and Moderated Reactors", p. 695. Addison-Wesley Publishing Company (1958).
2. H. E. Kline, N. J. Gioseffi, W. N. Bley, "Dynamic Corrosion in Polyphenyls Under Irradiation", Report NAA-SR-2046, May 15, 1958.

* See Section 20.000.

the aluminum and stainless steel specimens and blackening of the surfaces of the mild steel. Very similar results were obtained (see Section 20.000) in alternate contact of Santowax R and water; however, the number of specimens tested and length of testing time was inadequate for a recommendation of Croloy 1-1/4 as the structural material. A further corrosion testing program may provide the basis for this recommendation.

A search through the literature was made to evaluate the carburization effect from the hydrocarbon coolant on Cb-stabilized AISI 347 steel. The theory generally advanced to explain carbide precipitation and the accompanying intergranular corrosion in austenitic steels of the 18-8 type is chromium depletion of grain boundary layers. Chromium carbide is believed to be precipitated along the grain boundaries and in the slip planes when these steels are heated to the sensitization range (900°F to 1400°F). The result of the loss of chromium from a grain periphery is to render this region susceptible to corrosion, and intergranular failure will then occur readily in service. Columbium, being a more active carbide-former than chromium, tends to prevent depletion of the corrosion-resistant chromium from 18-8 steels stabilized with this element. Type 18-8 steels have been used for years in high temperature-refining applications up to 1600°F maximum metal temperatures. However, service life versus operating temperature data is rather meager. Tests conducted by Republic Aviation Corporation in 1946 in evaluating steels for aircraft exhaust manifolds show that carburization is practically nil until metal temperatures reach the 1300°F-to-1400°F temperature range.[1] However, these were only 3-hour tests and were run at normal atmospheric pressure. It is known that carburization increases with increase in pressure of the carburizing gas. The carbon availability of the atmosphere (carburizing-decarburizing potential), the temperature, and time are the important variables affecting carburization of a particular steel. The temperature not only influences the diffusion rate but determines the equilibrium concentration of carbon in the steel.

Tests conducted by Timken at 1680°F show maximum carbon penetration of .025 in. These tests had a duration of 36 hours, and each specimen was subjected to 20 cycles.[2]

The design temperatures of the EOCR results in metal surface temperatures in the 850°F-to-900°F temperature range, or just under the 900°F lower limit of the sensitization range (900°F to 1400°F). Therefore, in view of the above data the EOCR vessel should have a satisfactory life-span. A metallurgical evaluation program, with emphasis on weld samples, can be carried out in conjunction with the operation of the reactor.

---

1. W. Kahn, H. Oster, and R. Wachtell, "Investigation of a Type of Failure of 18-8 Stabilized Stainless Steel", Transactions of the American Society for Metals, 37, 567, (1946).

2. "Resume' of High Temperature Investigations Conducted During 1943-44, The Timken Roller Bearing Company, Steel and Tube Division, 1944.

17.200 Primary Loop

The primary loop external of the block valves next to the reactor vessel is composed of mild steel. Where trim is required, as in valves, 347 stainless steel is used. Since this part of the primary loop is never in direct contact with water during refueling operations as is the reactor vessel, there is no need for the corrosion resistance of stainless steel. Mild steel possesses satisfactory corrosion resistance to organic coolants. While it is true, that for short periods of time the primary coolant may be saturated with water, preliminary corrosion tests reveal this will not result in any significant metal loss. In any case indications are that the mild steel portion of the primary loop is satisfactory from a service-life standpoint.

18.000 DESIGN OF PRESSURE VESSELS AND THERMAL SHIELDS

18.100 Design Summary

Fig. 7.1A is a vertical cross-section view of the EOCR pressure vessels and thermal shields. The inner reactor tank immediately surrounding the core is 5 ft 11 in.-ID by 0.5-in. thick and the reactor pressure vessel is 7 ft 0 in.-ID by 1.25-in. thick. In the annulus between these shells are three 1-in. thick thermal shields. The diameters of the thermal shields are such that the coolant channels between them are of the same thickness. Table 18.1A summarizes the design features of each component except the magnetite-concrete biological shield. Section 7.180 gives the design basis for choosing 6 ft 0 in. of magnetite-concrete for the biological shield. As far as strength is concerned, the design parameters for the biological shield are less severe than those for the ETR biological shield; therefore, stress calculations were not made. The pressure vessels and internal thermal shields are calculated by ASME Code rules to be safe for operation at 220 Mw reactor power, 850°F primary coolant temperature, 300 psig maximum operating pressure and 40 psi core pressure drop. Calculations of the neutron and gamma internal heat generation rates are in Section 5.340.

18.200 Stresses and Temperatures

18.210 Pressure Vessel. The 1.25-in. pressure-vessel shell thickness is designed according to the ASME Code, Section VIII, Unfired Pressure Vessels, using the following design parameters.

Vessel ID	7 ft 0 in.
Material	SA-240 Type 347 SS
Maximum Operating Pressure	300 psig
Design Pressure	330 psig
Maximum Metal Temperature	900°F
Maximum Allowable Stress	14,100 psi at 900°F (Table UHA-23, ASME Code Section VIII)

The thermal stress is calculated using the following equation and assuming uniform internal heat generation of 0.05 w/g or 22.4 Btu/hr-cu in. and a flat plate not free to bend.

$$\sigma = \frac{E\alpha}{2(1-\mu)}\left[\frac{q_g t^2}{6k} + T_2 - T_1\right]$$

where:
- σ = thermal stress in the circumferential or longitudinal direction
- E = modulus of elasticity
- α = coefficient of thermal expansion
- μ = Poisson's ratio
- q_g = uniform internal heat generation rate
- t = plate thickness
- k = thermal conductivity
- $T_2 - T_1$ = difference in temperature of the two faces of the plate.

Table 18.1A

DESIGN OF VESSELS AND SHIELDS

	Inner Reactor Tank Shell	Internal Thermal Shields	Pressure Vessel Shell	External Thermal Shield	Biological Shield
Material	SA-240 Type 347	SA-240 Type 347	SA-240 Type 347	Lead	Magnetite Concrete
Maximum Oper. Pressure	----	----	300 psig	----	----
Design Pressure	48 psig external	0 psig	330 psig	0 psig	0 psig
Design Temperature	900°F	900°F	900°F	----	120°F inside 70°F outside
Wall Thickness	0.5 in.	3 shells each 1 in.	1.25 in.	3 in.	6 ft
Uniform Internal Heat Generation Rate	<0.5 w/g	<0.3 w/g	<.05 w/g	<.03 w/g	<.00046 w/g at inner face
Mechanical Stress	14,100 psi	0	14,100 psi	0	----
Thermal Stress	7,645 psi	4,580 psi	4,770 psi	----	----
Maximum Metal Temperature	900°F	900°F	900°F	----	----
Max. Allowable Stress	*21,150 psi	*21,150 psi	*21,150 psi	----	----
Minimum Film Coefficient h Inside	Assumed = 0	284 Btu/hr-ft^2-°F	120 Btu/hr-ft^2-°F	Cooled by water in SS tubes cast in the lead.	Cooled by air under forced convection at inner face; by air under natural convection at outer face.
Minimum Film Coefficient h Outside	685 Btu/hr-ft^2-°F	284 Btu/hr-ft^2-°F	Assumed = 0		
Available Film Coefficient h	840 Btu/hr-ft^2-°F	840 Btu/hr-ft^2-°F	$\frac{\text{Inside}}{840}$ Btu/hr-ft^2-°F		

* Maximum allowable stress = 1.5 times applicable value in Table UHA-23, Section VIII, ASME Code for Unfired Pressure Vessels (Case No. 1273-N).

The calculated maximum thermal stress is 4,770 psi tension which occurs at the inside surface of the shell. Since the mechanical stress is 14,100 psi, the total maximum stress is then 18,870 psi, which is less than the maximum allowable stress for nuclear vessels (ASME Case No. 1273N) of 1.5 times the s-value or 1.5 x 14,100 = 21,150 psi.

The calculated temperature difference from inner to outer surface is 16.5°F based on 0.05 w/g. Since the maximum bulk coolant temperature is 850°F, organic-film heat transfer coefficient, h, of 120 Btu/hr-ft^2-°F on the inner vessel surface is required to remove the heat generated and keep the maximum metal temperature below 900°F. A coefficient of 840 Btu/hr-ft^2-°F is calculated for the inner surface of the vessel which provides adequate cooling for the design conditions.

18.220 Internal Thermal Shields. The diameters of the three 1-in. thick internal thermal shields are based on equal coolant velocities in the four annuli. Equal coolant velocities on both sides of a shield tend to make metal skin temperatures equal on both sides, thus keeping thermal stress at a minimum. Since the outside diameter of the inner tank is 5 ft 11 in., the inside diameters of the internal thermal shields are 73.5 in., 77.0 in., and 80.5 in., respectively, a total flow rate of 25,000 gpm results in a coolant velocity of 11.0 ft/sec.

Assuming equal skin temperatures and no mechanical or pressure stress and with an internal heat generation rate of 0.3 w/g, the maximum stress is 4,580 psi and occurs at both surfaces. This is well within the maximum allowable stress of 21,150 psi at 900°F. An average film heat transfer coefficient of 284 Btu/hr-ft^2-°F is required to keep maximum metal temperatures below 900°F, and the calculated coefficient is 840 Btu/hr-ft^2-°F.

18.230 Inner Tank. The inner tank is subjected to an external operating pressure of 40 psig due to the pressure drop across the reactor core. A design external pressure of 48 psig was chosen, and the vessel wall thickness was calculated to be 0.5 in. per Paragraph UG.28, ASME Code for Unfired Pressure Vessels. Maximum metal temperature was assumed to be 900°F.

Assuming the inner wall to be insulated and with internal heat generation rate of 0.5 w/g, the thermal stress is 7,645 psi. Although the total stress shown is about 900 psi over the maximum allowable, it is still considered a safe design since no credit was taken for cooling on the inside surface in calculating thermal stress. Also, if the internal heat generation rate assumed in the calculation had been 0.43 w/g instead of 0.5 w/g, the total stress would be less than the allowable stress. Table 5.3G actually lists a value of 0.37 w/g for the heat generation rate in the inner tank vessel wall.

18.240 External Thermal Shield. An external thermal shield is required to reduce the heat generation rate in the biological shield to an acceptable value. A 3-in. thickness of lead is chosen, based on the

ETR design of 3-1/2 inches. Assuming that a hollow cylinder of lead 4-ft high and 3-in. thick with a mean diameter of 7 ft 6-1/2 in. has a uniform internal heat generation rate of .03 w/g, the cooling water requirement for cooling tubes in the lead is 258 gpm with a 50°F temperature rise. Design figures for the ETR are 50 gpm of cooling water with a 10.8°F rise. Actual ETR operating conditions at the present time are 150 gpm with a 2°F to 3°F rise.

18.250 Concrete Biological Shield. No attempt is made to calculate the thermal stress in the concrete biological shield because (1) the calculated gamma heating incident to the inside face is less than the value used in designing the ETR shield, and (2) the thickness for the EOCR shield is 6 ft 0 in. of magnetite concrete compared with 8 ft 0 in. of magnetite concrete for the ETR. Both of these factors reduce thermal stress in the concrete biological shield, especially the smaller thickness because stress is approximately proportional to thickness squared. Cooling is provided at the inner face of the concrete shield by forced convection to air flowing in the annulus between the lead and concrete. The reinforcing steel required in the concrete biological shield will be computed by the design engineer contractor.

19.000 DEVELOPMENT PROGRAM TO SUPPORT EOCR DESIGN

The EOCR design was based on known technology wherever possible; however, there are specific tests which will contribute markedly toward improving the final EOCR design. The objectives of this experimental work are to:

(1) study problems of water flooding unique to the EOCR mechanical design;

(2) experimentally determine certain heat transfer information for Santowax not presently available;

(3) test the driver fuel elements proposed;

(4) test the control rod assemblies and drives; and,

(5) perform additional corrosion tests on low alloy steels which might provide the basis for their selection as structural materials instead of stainless steel.

Exploratory water-flooding and corrosion tests have already been completed.

19.100 Water-Flooding Tests.

The tests performed to date to explore the feasibility of displacement of organic with water for fuel-handling operations have been discussed in Section 12.000. Since water flooding has such potential in expediting the introduction and removal of fuel and experiments, fullest development of this concept is planned. Tests should be performed with the simulated end fittings of the final design of various reactor internals such as control-rod dash pots and fuel-element end-fittings. These tests can be carried out in the facilities described in Section 12.000.

19.200 Experimental Heat Transfer Program to Support EOCR Concept.

The heat transfer studies with organic coolants conducted to date by several experimenters in out-of-pile tests have not answered all of the specific questions encountered in this design concept. Additional out-of-pile heat transfer tests are recommended before final design. These tests are required to (1) determine the rate of fouling of fuel elements exposed to EOCR shutdown heat fluxes with coolant velocities of 0.1 to 2.0 ft/sec, (2) determine the natural convection burnout heat flux with natural convection flow rates similar to those expected in the EOCR tank, and (3) determine the best heat transfer correlation that applies to irradiated Santowax R or OMP coolant at EOCR design conditions. The need for each of these tests is discussed below and conditions recommended for each of the tests are outlined in Table 19.2A.

Table 19.2A

RECOMMENDED TEST CONDITIONS FOR EOCR
EXPERIMENTAL HEAT TRANSFER STUDIES

Note: Irradiated Santowax R with 30% HB should be used for all tests if available

Test	1	2	3
Test Condition	Low Velocity Fouling Tests	Natural Circulation Burnout	Forced Convection
Test Cross Section	Tube 0.25" ID	0.134" x 1.9" Rectangular Channel	Tube 0.25" ID
Coolant Temperatures, ^{o}F	350 to 700	350 to 500	500 to 700
Coolant Velocity, ft/sec	0.1 to 2.0	Natural Circulation	10 to 35 ft/sec
Heat Flux, Btu/hr-ft^2	20,000 Max	Burnout 50,000 - 100,000	700,000 Max
Pressure, psi	Atmospheric	Atmospheric	150
Number of Tests Required	3 to 6 (130 Hours Max Duration)	2 to 6	10 Reproducible Data Points

19.210 Fouling at Reactor Shutdown Conditions. Heat flux of about 5000 Btu/hr-ft^2 is obtained in EOCR driver elements during extended shutdown periods. Fouling data are not available at the low velocity, temperatures, and heat flux which obtain during shutdown although some evidence of fouling has occurred in OMRE elements. It is recommended that the fouling rate on heated surfaces with heat fluxes up to 10,000 Btu/hr-ft^2 be determined with EOCR coolant containing 30% HB at coolant velocities between 0.1 and 2.0 ft/sec and coolant inlet temperatures to the test section between 350^{o}F and 700^{o}F. These data are also needed for the overall organic reactor program. The results of these tests will be used to determine whether or not provision for forced convection shutdown cooling will be necessary for the EOCR.

19.220 Natural-Convection Burnout Tests. There is no published information on burnout with natural circulation cooling using organic coolants under conditions similar to those encountered in a shutdown reactor with the tank isolated from the process system. These values are available for water-cooled systems and are useful in determining the time at which forced flow is no longer required. Experiments are proposed to measure the burnout heat flux in a loop that permits natural convection cooling.

The most extreme shutdown conditions expected in the EOCR are those encountered when the reactor is at atmospheric pressure with the coolant at 500°F. Burnout tests should be conducted with test sections 0.12 in. by 2.0 in. in cross section and 36 in. in height. The test section could be connected in parallel to an unheated leg and heated to burnout, thus allowing natural convection cooling of the burnout test section. Santowax R or OMP with 30% HB should be used as coolant for these tests with coolant temperatures between 350°F and 500°F.

19.230 Forced-Convection Heat Transfer. The forced-convection heat transfer correlation recommended by Atomics International[1] is based on data obtained with unirradiated Santowax R coolant and data obtained with irradiated Santowax OM in the OMRE heat transfer loop. Tests were conducted with a maximum coolant velocity of 15 ft/sec and maximum heat flux of about 300,000 Btu/hr-ft^2. Fuel elements in the EOCR operate at heat fluxes up to 660,000 Btu/hr-ft^2 and are cooled with Santowax R containing 30% HB at coolant velocities up to 35 ft/sec. It is recommended that forced-convection heat transfer tests be performed with Santowax R coolant containing 30% HB at coolant velocities of 10 to 35 ft/sec at heat fluxes up to 700,000 Btu/hr-ft^2. These data will also be useful to the overall organic-cooled-reactor program, specifically the D_2O-moderated organic-cooled system.

19.300 Fuel Element Testing and Development.

The fuel element shown in Fig. 4.2A was designed so that very little development work would be necessary for fabrication and use of the element in the EOCR. However, extensive hydraulic testing of this fuel element is recommended (1) to determine whether the element is strong enough to resist the hydraulic forces developed with unequal thicknesses of coolant channels and the pressure differences between fuel and moderator and (2) to obtain proper orificing for the different regions of the core. Additional hydraulic tests are recommended to prove the design of flow monitors (and possibly temperature monitors) that will be used in the EOCR.

---

1. M. Silberberg and D. A. Huber, "Forced-Convection Heat Transfer Characteristics of Polyphenyl Reactor Coolants", Report NAA-SR-2796, January 15, 1959.

Several fuel elements have been proposed to improve the heat removal efficiency in the EOCR; these fuel elements are discussed in Section 13.000. One of them, using flat fuel plates without the center support plate, may be developed for use in the initial EOCR core. Fabrication of this element is less expensive than the proposed element because of fewer fuel plates, and some development work is recommended to determine the feasibility of this design. Calculations indicate that the box required with a 4 in. unsupported span would have to be about 0.150-in. thick to withstand the lateral pressure differences between fuel and moderator. Because of the complexity of this type of calculation, there is some uncertainty in the results; therefore, it is recommended that a fuel element of this design be fabricated and tested.

The problem of thermal stress in the fuel elements may make it necessary to provide for expansion of the fuel plates. Methods of fabrication may have to be developed (e.g., adaptation of the proven OMRE fabrication technique) and tests performed to evaluate the performance of the fuel elements.

19.400 Control Rods and Drives.

The test program for the control rods and drives is very dependent upon the final design. If a drive is chosen which has been tested, no testing should be required except pre-operational checking in the reactor to determine drop-time characteristics and to establish operability of components such as mechanical disconnects.

If an untried control rod design is used, a test facility should be built to prove the mechanical reliability of the control-rod-and-drive combination, determine the drop-time of the rod, and establish its hydraulic characteristics. Two control-rod-drive test facilities are available at NRTS which might be adapted to this testing.

19.500 Corrosion Tests on Low Alloy Steels.

Preliminary corrosion tests on several structural materials (Section 20.000) with alternate Santowax R and water contact showed the formation of a protective film and low corrosion rate. The possibility of the use of a low alloy steel such as Croloy 1 1/4 as structural material for the reactor exists. Since the number of specimens tested was small (only two), it was not deemed advisable to recommend this material without further corrosion tests; therefore, additional corrosion tests are recommended to determine the probability of localized attack of low carbon steels.

20.000 CORROSION EXPERIMENTS

In the EOCR design it is advantageous in the handling of experiments and the changing of fuel elements to replace the Santowax with water. The behavior of conventional structural materials in alternate contact with Santowax and water was unknown. There is some corrosion of structural parts of the OMRE that are exposed to organic and then to the atmosphere. It was therefore desirable to place samples of some structural materials in a corrosion environment such that they would be subjected to contact with organic and then water.

Two specimens of each of several conventional structural materials were placed in an autoclave and subjected to alternate contact with organic and water. The good corrosion resistance of conventional structural materials in Santowax R or OMRE-irradiated coolant was not adversely affected by replacement of the organic with water at 330°F to 350°F for periods of time up to 55 hours. It is well known that the initial film formation affects the subsequent corrosion rate and, in addition, an organic film remains which at least partially protects the metal. Some corrosion of exposed areas of the OMRE carbon steel structural parts has been observed, so that some breakdown of the film apparently does occur in localized areas; however, with the small number of specimens tested in the autoclave no breakdown of the film occurred.

The replacement water does increase in chloride ion concentration upon contact with the organic. For approximately equal volumes of organic and water the chloride ion content in the replacement water was between 1.5 and 2.2 ppm.

The corrosion of the structural materials tested in ten Santowax R-water replacement cycles was low with a weight gain of 1.4 mdd for 336 hours of testing occurring for APM alloy M-257.

One U-bend specimen of sensitized type 304 stainless steel and one galvanic couple of type 304 stainless steel and APM alloy M-257 were also subjected to the alternate contact with organic and water with no evidence of stress corrosion and little galvanic attack.

The corrosion of the structural materials tested in one OMRE coolant-water replacement cycle was also low.

20.100 Introduction

Austenitic stainless steel (as well as some other structural materials) is susceptible to stress corrosion cracking in high-temperature chloride water environments. Intermittent wetting (wherein the chloride ion concentrates on the specimen) with steam and water produced cracks[1] with water containing as little as 1 ppm chloride ion.

---

1. D. J. DePaul, ed., "Corrosion and Wear Handbook", AEC, 187-223, McGraw Hill Book Company, N.Y., 1957.

Oxygen appears to be a strong accelerator[1] of stress corrosion of austenitic stainless steels in hot-water environments. Some corrosion tests on stainless steels[1] with plain chloride-bearing water (degassed) show no stress corrosion cracks after 14 days in 300 ppm chloride ion and after 25 days in 80 ppm chloride ion with type 310 and 347 stainless steel.

The possibility for the replacement water in organic-water replacement cycles picking up chloride ion does exist as the organic (Santowax R and OMRE coolant[2]) contains 2 ppm chloride ion.

The corrosion resistance of APM aluminum alloy M-257 is reported[3] to be as good as 1100 and 3003, and superior to 2014-T4 and 6061-T6.

20.200 Test Procedures.

Samples of APM alloy M-257, stainless steel types 304 and 347, and mild steel types A-201 and Croloy 1-1/4 were prepared by machining and rough polishing through 3/0 emery paper (see Table 20.2A). A galvanic couple of type 304 stainless steel and M-257, and U-bend specimens from sensitized type 304 stainless steel were also prepared.

The samples were suspended with quartz hooks from a stainless steel rack (except the stainless steel specimens for which stainless steel wire was used). The U-bend specimen was placed in the bottom of the stainless steel autoclave. The organic was heated to 350°F and introduced by nitrogen pressure into the autoclave. The temperature was increased to above 750°F and held for 1/2 hour, then cooled to 330°F. The water (demineralized - 2.5 megohm resistivity) was heated to 350°F and used to replace the organic in the autoclave. The samples were left in contact with the water at 330°F to 350°F from 12 to 55 hours. The autoclave was then cooled and the samples removed.

The samples were cleaned in benzene and weighed and the cycle repeated.

---

1. D. J. DePaul, ed., "Corrosion and Wear Handbook", AEC, 187-223, McGraw Hill Book Company, N.Y., 1957.

2. J. R. Dietrich and W. H. Zinn, Solid Fuel Reactors, Ch. 7, "Organic Cooled and Moderated Reactors", Addison-Wesley Publishing Company, 1958.

3. J. P. Lyle, Jr., "Aluminum Powder Metallurgy Products" Materials and Methods, 106, April 1956.

Table 20.2A

MATERIALS TESTED

Material and Condition	Composition (per cent)
APM M-257 Strip, as Received	Al_2O_3-7.8, (nominal)
Stainless Steel Type 304 Annealed	C-.08 max.; Mn-2.0 max.; Si-1.0 max.; Cr-18; Ni-8 (nominal)
Stainless Steel Type 347 Annealed	C-.08 max.; Mn-2.0 max.; Cr-18; Ni-10 (nominal)
Low Alloy Steel, Croloy 1-1/4 Hot Rolled	C-.15; Cr-1.25; Mo-0.5; Si-0.75; Mn-0.45; Fe-bal. (nominal)
Mild Steel, A-201 Grade B Firebox, Hot Rolled	C-.17; Mn-.48; P-.017; S-.028; Si-.15; Bal. Fe
Galvanic Couple of Type 304, SS and APM M-257	
U-Bend Specimens, 1.5 in. Radius, 0.188-in. Thickness; Sensitized by Heating to 1225°F for 2 Hours	

20.300 Results.

All of the samples cycled at high temperature developed an adherent film which differed in color and thickness. The color of the film on the aluminum samples was brown (Fig. 20.3A View-1), and that on the stainless steel was thin and yellowish (Views-2 and -3) while that on the mild steel samples was bluish-black (Views-4 and -5). The film was removed with 4/0 emery paper and found to be very tenacious, which agrees with results of bend tests.[1]

The maximum weight addition occurred during the first cycle and over the remaining nine cycles increased but little, so that the calculated weight change (Table 20.3A) after the first cycle is much higher than the weight change calculated on the basis of the total weight gain for the total time.

---

1. H. E. Kline, N. J. Gioseffi, and W. N. Bley, "Dynamic Corrosion in Polyphenyls Under Irradiation", Report NAA-SR-2046, May 15, 1958.

Table 20.3A

CORROSION TEST RESULTS IN SANTOWAX R AND WATER

Material and Sample No.		Wt Change After First Cycle (mg)	Wt Change All Cycles (mg)	Corrosion Rate During First Cycle (mdd)[a]	Corrosion Rate During All Cycles (mdd)[a]	Total Time In Organic and Water Above 330°F (hours)
M257-	C	+3	+5	20.7	1.3	336*
-	D	+4	+6	24.7	1.4	336
Type 304-	G	+1	+1	5.3	0.2	336
SS -	H	+1	+1	5.3	0.2	336
Type 347-	M	0	+1	0.0	0.2	323**
SS -	N	+2	+2	2.8	0.4	323
Steel, A201-	K	+3	+6	9.6	0.7	336
-	L	+2	+6	6.5	0.8	336
Steel, Croloy 1-1/4-	O	+4	+5	9.8	1.1	205***
	27A	+1	+4	7.7	1.2	336

* Total time includes 141 hours in organic at 330°F - 350°F; 5 hours in organic at 750°F - 800°F; and 190 hours in water at 330°F - 350°F.

** Total time includes 135 hours in organic at 330°F - 350°F; 4.5 hours in organic at 750°F - 800°F; and 183.5 hours in water at 330°F - 350°F.

*** Total time includes 91.5 hours in organic at 330°F - 350°F; 2.5 hours at 750°F - 800°F; and 111 hours in water at 330°F - 350°F.

(a) See below.

Table 20.3B

CORROSION TEST RESULTS IN OMRE-IRRADIATED COOLANT AND WATER

Material and Sample		Wt Change After One Cycle (mg)	Corrosion Rate During One Cycle (mdd)[a]	Total Time in Organic and Water at 330°F - 350°F (hours)
M257-	A	+1	1.2	64*
-	B	+1	1.2	64
Type 304-	F	0	0.0	64
SS -				
Steel, Croloy 1-1/4-	P	+1	0.7	64
	26A	0	0.0	64

* Total time includes 18.5 hours in organic at 330°F - 350°F, and 45.5 hours in water at 330°F - 350°F.

(a) Corrosion "rate" as weight change for comparison purposes only. Weight losses after film was removed were comparable to weight gain.

The samples (Table 20.3B) cycled in OMRE-irradiated coolant and water at 330°F to 350°F for 64 hours showed very little film formation and insignificant weight changes. The APM alloy M-257 samples showed slight localized film formation and the mild steel a slight brown color. A U-bend specimen placed in the bottom of the autoclave as with the Santowax R test also showed insignificant corrosion.

The U-bend specimen in Santowax R showed negligible intergranular corrosion upon visual and metallographical examination at 100X after sectioning, polishing, and etching with an etchant of nitric and hydroflouric acids. The galvanic couple developed the same type of film as in the individual samples, except in the area under the bolt head and between the dissimilar metals, where slight pitting attack of the M-257 took place.

The water after contacting the organic and samples during a cycle was analyzed for chloride ion concentration and found to contain from 1.5 to 2.2 ppm chloride ion. The water after contacting the OMRE-irradiated coolant contained 1.7 ppm chloride ion.

20.400 Discussion.

The corrosion of conventional structural materials exposed first to Santowax R and then water at 330°F to 750°F (organic at higher temperature) is relatively low and not greatly different from results obtained in in-pile and out-of-pile tests with polyphenyls[1] at 550°F to 600°F. For example, the calculated corrosion rate over a 14-day period is given in Table 20.4D for comparison purposes only. These values are not significantly different from those given in Table 20.3A for somewhat similar materials for a comparable period of time, except in the case of aluminum alloys M-257 and 2S. These values differ by less than a factor of three.

Table 20.4D

CORROSION RATES FOR COMPARISON PURPOSES ONLY

Material	Corrosion Rates for 14-day Period (mdd)
Type 410 SS (in Santowax R)	0.4
Type 304 SS (in Diphenyl)	0.1
4130 Alloy Steel (in Terphenyl)	0.4
ASTM A7 Carbon Steel (in Terphenyl)	0.9
2S Aluminum (in Santowax R)	0.5

1. H. E. Kline, N. J. Gioseffi, and W. N. Bley, "Dynamic Corrosion in Polyphenyls Under Irradiation", Report NAA-SR-2046, May 15, 1958.

The initial rapid corrosion rate is normal for protective film formation. Comparison of these initial corrosion rates (Table 20.3A) with data in the literature reveals that these rates are low; e.g., in H_2O mild steel (0.15%C) at 195°F with negligible CO_2 and O_2 corrodes at a rate of 16.4 mdd.[1] The corrosion rate of 99.0% aluminum alloy[2] would be calculated as 22.9 mdd for 334.5 hours testing at 480°F in water. The weight gains given for the stainless steels in Table 20.3A are insignificant.

The chloride ion apparently does concentrate in the water, since approximately equal volumes of organic and water were used; but the resultant concentration would be expected to cause stress corrosion in stainless steels only in those areas alternately wet with steam and water.

20.500 Summary

The corrosion of the conventional structural materials tested in alternate organic-water autoclave tests was relatively low. The film formed on the carbon steels and aluminum was protective in that the overall corrosion rates were much lower than the initial corrosion rate. The film formed on the carbon steels was bluish black with no Fe_2O_3 formation observed.

The concentration of the chloride ion in the replacement water of 1.5 to 2.2 ppm did not produce any indication of stress corrosion in the sensitized type 304 stainless steel U-bend specimens tested. The galvanic couple of type 304 SS and M-257 showed slight pitting attack of the M-257 under the bolt head and between the metals where the film did not form.

The corrosion rates in this section are for comparison purposes only. The film was removed with 4/0 emery paper and the weight loss was comparable with weight gain (within a factor of 3).

---

1. H. H. Uhlig, "The Corrosion Handbook", 128, John Wiley and Sons, 1948.

2. P. O. Strom, L. M. Litz and M. H. Boyer, "Reproducibility of 480°F Static Aqueous Corrosion of Pure Aluminum", Report LRL-112, March 1954.

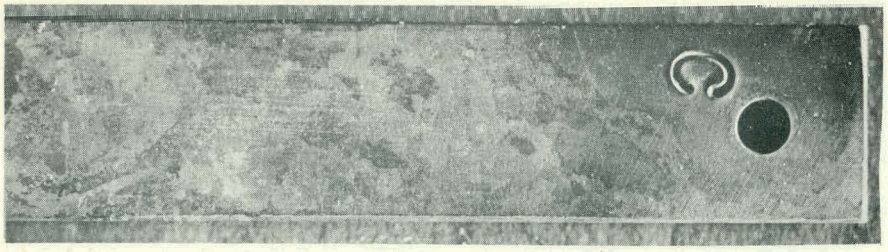

(1)
ALUMINUM ALLOY
M257

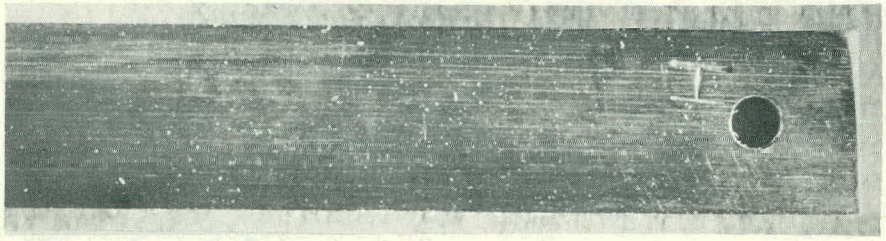

(2)
STAINLESS STEEL
TYPE 304

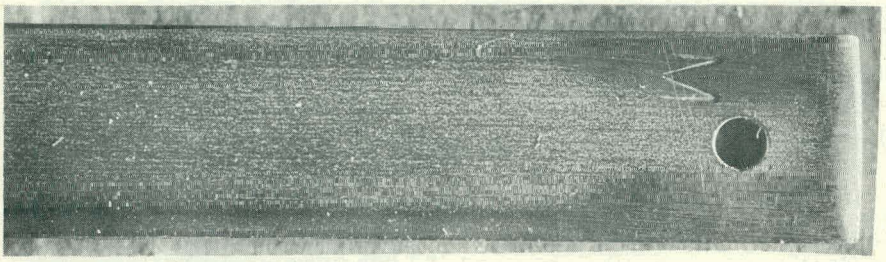

(3)
STAINLESS STEEL
TYPE 347

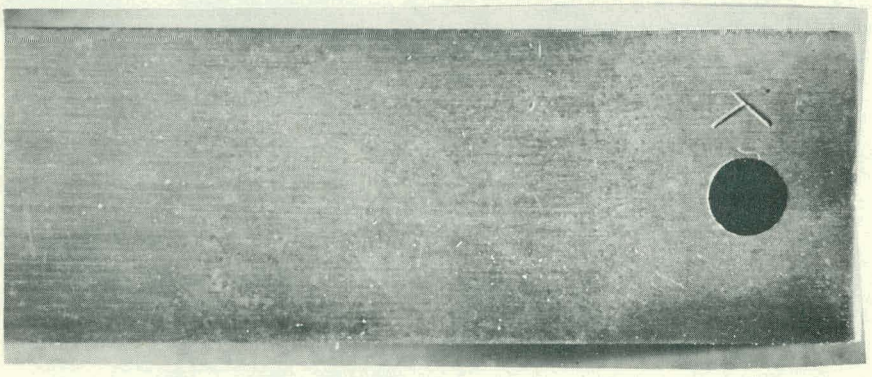

(4)
MILD STEEL
A201

(5)
MILD STEEL
CROLOY 1 1/4

FIG. 20.3A
CORROSION SPECIMENS FROM ORGANIC-WATER AUTOCLAVE TESTS

P.P.Co.

PHILLIPS
PETROLEUM
COMPANY

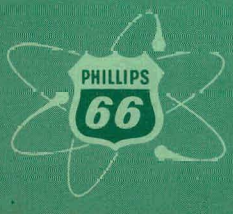

ATOMIC ENERGY DIVISION